The role of NRF2 in acute myeloid leukaemia (AML)

Thesis submitted in accordance with the requirements of the University of Liverpool for the degree of

Doctor in Philosophy

By

Niraj Mayank Shah

April 2018

Declaration

I declare that this thesis has been written solely by myself and that it has not been submitted, in whole or in part, in any previous application for a degree. Except where states otherwise the work presented is entirely my own. The work was carried out under the supervision of Prof. David MacEwan.

Niraj Shah

April 2018

Abstract

Acute Myeloid Leukaemia refers to the excess proliferation of myeloid progenitor cells. Whilst the 5-year survival rate is 40% in younger patients, this falls to 5% in patients over 65 and resistance to front-line chemotherapy agents remain a problem. We previously identified NRF2, a regulator of anti-oxidant genes, to be constitutively activated in AML and this correlated with resistance to chemotherapy. Recent studies have also suggested NRF2 also plays a more oncogenic role.

To further understand NRF2's role in both chemotherapy resistance and oncogenesis we looked at its ability to regulate miRNA in AML. Using a miRNA array, we identified several miRNAs, including miR-125b and miR-29b, whose expression correlated with that of NRF2 in both cell lines and AML patient samples.

Both miRNAs exist as paralogs, in that they contain the same miRNA sequence but exist in different genomic locations and we used qPCR to identify miR-125b1 and miR-29b1 as paralogs regulated by NRF2. Using a reporter assay we confirmed the activity of putative NRF2-ARE binding sites in both miRNA promoters. To understand the function of both in AML we manipulated their expression using miRNA "mimics" or antagomIRs. Individual manipulation of either miRNA resulted in a slight increase in apoptosis. However, the miRNAs appeared to act synergistically as when expressed simultaneously a significant increase in apoptosis was seen both in cell lines and patient blasts.

Manipulation of both miRNA also resulted in the increased sensitivity of AML cells to chemotherapy agents. BAK1, STAT3 and AKT2 were shown to be targets of both miRNAs providing a novel mechanism by which NRF2 expression can affect AML cells.

To further study the role of NRF2 in AML we used CRISPR-Cas9 to generate NRF2-deficient cells. CRISPR guide RNA were designed to target NRF2 Exons 1, 2 and genome editing validated in HEK293T cells. Leukaemic cell lines (K562 and THP-1) were virally transduced with guides targeting Exon 4 of NRF2. Once editing was verified clones were derived by growing selected cells in Methycellulose-containing medium.

Putative clones were initially screened using MG-132 (to stabilise NRF2) and further confirmed by treatment with the NRF2 inducers CDDO-Me and Sulforaphane. Verified clones were characterised by Sanger Sequencing. In addition to CRISPR-Cas9 we also validated a number of other gene-editing methodologies including CRISPR-Cpf-1 and TALENs.

Overall these methodologies represent powerful tools to further characterise the role of NRF2 in AML.

Some of the work in this thesis has been previously published in the following publications:

Shah NM, Bowles KM, Rushworth SA and MacEwan DJ (2015) "Understanding the role for miRNA in human leukemia" *RNA & Disease* 2:e540. [Review]

Shah NM, Zaitseva L, Bowles KM, MacEwan DJ and Rushworth SA (2015) "NRF2-driven miR-125B1 and miR-29B1 transcriptional regulation controls a novel anti-apoptotic miRNA regulatory network for AML survival" *Cell Death and Differentiation* 22, 654-664.

MacEwan DJ, Barrera LN, Keadsanti S, Rushworth SA, **Shah NM**, Yuan T, Zaitseva L. (2014) "Understanding life and death decisions in human leukaemias" *Biochem Soc Trans* 42(4):747-51. [Review]

Shah NM, Rushworth SA, Murray MY, Bowles KM and MacEwan DJ (2013) "Understanding the role of NRF2-regulated miRNAs in human malignancies" *Oncotarget* 4, 1130-1142. [Review]

Rushworth SA, Zaitseva L, Murray MY, **Shah NM**, Bowles KM and MacEwan DJ (2012) "The high Nrf2 expression in human acute myeloid leukemia is driven by NF-κB and underlies its chemo-resistance" *Blood* 120, 5188-5198.

Acknowledgements

I would first like to thank Prof David MacEwan for giving me the opportunity to study my doctorate under his tutelage. Dave, it has been a real journey from Norwich to Liverpool, thank you for bringing me along for the ride. I will never forget the first years when we it was just us two setting things up! Thank you for all the help and support these last few years!

I would like to thank Dr Nick Harper whose mentorship, friendship, (and beers) have kept me going these last few years! Thank you for all the help you have given me, from your invaluable CRISPR expertise (and general lab expertise) that made Chapter 5 possible, to putting up with me on my "itis days" ranging from Western Blot/PCR/T7(itis). Nick, I would like to especially thank you for helping me put everything together, and for tuning my "mad ramblings" into something more cohesive. You have also helped me develop as both a scientist and a person.

I would also like to say a special thanks to Dr Stuart Rushworth, whose support helped me keep going (especially in the early years) and was always a phone call away whenever I needed help. Thank you Stuart, for training me and helping me in my early lab days- I know it can't have been easy.

The past few years, from my PhD origins in Norwich to my end in Liverpool I have met lots of weird and wonderful people. There are too many to name here (and I will doubtlessly miss names out) but for those with the (mis)fortune to read this, it has been my pleasure to know you and you have improved my life for the better.

I would like to thank all members of the DJM lab past and present. From Norwich Lawrence, Megan, Lyuba, and Sally. From Liverpool John, Sujitra, Melanie, Vanessa, Taha, Amy R and Amy W. Also to Matt, Nas and Yasmina, you guys were good fun!

I next thank all the PhD students who have supported me these last few years. First my ex-housemate Rahul, and the "Beer trio" Matt, Emily and Stefan. From Liverpool I would like to thank Adam, Nicki, Laura, Georgia, Mateus, Govinda, Shankar, Lucy, Meirion, Fiona, Chris P, Paul Q, Tushar, and many more. Thank you for keeping me "sane" these past few years.

To all my Vine Court and Residential Advisor friends, thank you for making the move to Liverpool a much more enjoyable experience! In particular, I would like to thank Nikhil Gokani (and our chats till 3am!), Jordan and Michael (who kept me entertained through the tougher times).

Thank you to my family, who have done their best to understand my research (there have been flow charts and pop quizzes). Finally, I would like to thank my parents for always encouraging, believing in me and pushing me to improve myself. Without your support none of this would be possible! Ruchi, thank you for putting up with me all these years. Of course, I haven't forgotten my Ba, who has been patiently waiting for me to return to London.

Table of Contents

Declaration ii

Abstract iii

Some of the work in this thesis has been previously published in the following publications: iv

Acknowledgements v

Table of Contents vi

List of Figures xi

List of Tables xiv

Chapter 1 Introduction 1

Project overview and context 2

1.1 Overview of Leukaemia 2

1.1.1 Haematopoiesis 2

1.1.2 Subtypes of Leukaemia 5

1.2 Acute Myeloid Leukaemia 8

1.2.1 Overview of Acute Myeloid Leukaemia 8

1.2.2 Classification of AML 9

1.2.3 AML Translocations and Cytogenetics 12

1.2.4 AML Treatment 17

1.3 The redox-sensitive transcription factor - NRF2 18

1.3.1 Structure, activation and regulation by KEAP1 18

1.3.2 Pathological roles of NRF2 22

1.3.3 Oncogenic role of NRF2 in cancer 23

1.3.4 Oncogenic activation of NRF2 27

1.4 NRF2 regulation by NF-κB in AML 29

1.5 micro RNAs (miRNAs) 30

1.5.1 miRNA biosynthesis and physiological role 30

1.5.2 miRNA in haematopoiesis 32

1.5.3 miRNA dysregulation in cancer 34

1.5.4 Oncogenic role of miRNA 37

1.5.5 NRF2 and miRNAs 39

1.6 Gene Editing 41

1.6.1 Overview 41
1.6.2 Zinc Finger Nucleases 43
1.6.3 TALENs 43
1.6.4 CRISPR-Cas9 45
1.6.5 Other nucleases (i.e. CPF1) C2C2 FnCas9 Cas13 (RNA) 49
1.6.6 Research and Therapeutic Potentials 51
1.7 Aims 56

Chapter 2 Materials and Methods 57
2.1 Materials 58
2.2 Cell Biology Protocols 58
2.2.1 Cell Culture 58
2.2.2 Freezing cells 58
2.2.3 Assessment of cell viability using Cell Titer Glo™ 59
2.2.4 Annexin-V and Propidium Iodide staining 59
2.3 Primary cell culture 60
2.3.1 AML patient samples 60
2.4 Biochemical Techniques 60
2.4.1 Preparation of lysates for SDS-PAGE 60
2.4.2 SDS-PAGE 61
2.4.3 Western Blotting 62
2.4.4 Chromatin immunoprecipitation assay (CHiP) 63
2.4.5 Luciferase Reporter Assay 64
2.4.6 Site Directed Mutagenesis 64
2.5 Molecular Biology Techniques 65
2.5.1 Plasmids 65
2.5.2 Bacterial strains and Culture conditions 65
2.5.3 Preparation of Competent Cells 65
2.5.4 Transformation of *E.coli* 66
2.5.5 Isolation of Plasmid DNA 66
2.5.6 DNA Electrophoresis - Agarose and PAGE 67
2.5.7 Cloning of DNA 68
2.5.8 Polymerase chain reaction (PCR) 68
2.5.9 Restriction Digestion of Plasmid DNA 68
2.5.10 Ligation of digested DNA fragments 69

2.5.11 Colony PCR 70
2.5.12 Transfection of DNA into Mammalian Cells 70
2.5.13 Transfection of siRNA 70
2.5.14 Isolation of Genomic DNA 71
2.6 Real-time PCR 71
2.6.1 RNA extraction 71
2.6.2 Reverse Transcription 72
2.6.3 Quantitative real time-PCR (qPCR) 73
2.7 Lentivirus 74
2.7.1 Lentiviral vectors 74
2.7.2 Production of lentivirus 74
2.7.3 Transduction with Lentivirus 75
2.8 miRNA techniques 75
2.8.1 miRNA extraction 75
2.8.2 miRNA Reverse Transcription and real time PCR (miRNA) 76
2.8.3 miR-mimics and antagomir 76
2.8.4 Designing miRNA primers 76
2.9 qPCR primers 77
2.9 Statistical analysis 77

Chapter 3 Regulation of miRNAs by NRF2 78
3. 1 Introduction 79
3.1.1 Aims/Rational 80
3.2 Results 81
3.2.1 miRNA array methodology 81
3.2.2 Effect of NRF2 activation on miRNA expression array 82
3.2.3 miRNA profile following NRF2 knockdown 84
3.2.4 Analysis of miRNA array data: identification of NRF2-regulated miRNAs 86
3.2.5 Identification of NRF2-regulated miRNA promoters using bioinformatics 87
3.2.6 Validation of putative NRF2-regulated miRNA 89
3.2.7 Correlation between NRF2 and expression levels of miRs-125b and -29b in AML patient samples 90
3.3 Conclusions and Discussion 95

Chapter 4 Regulation of miR-125b and miR-29b by NRF2 98
4.1 Introduction 99

4.1.1 Aims and Rationale 101
4.2 Results 102
4.2.1 Genomic location of miRs-125b and miR-29b paralogs 102
4.2.2 NRF2 regulation of miRs-125b and miR-29b homologs and paralogs 103
4.2.3 NRF2 regulates miRs-125b and -29b through their individual promoters 105
4.2.4 Identification of potential ARE sites in the miRs-125b and -29b promoters 107
4.2.5 Identification of ARE binding sites using CHiP 108
4.2.6 Development of Luciferase p125b and p125bAREmut constructs 110
4.2.7 Validation of the miR-125b ARE site 111
4.2.8 Manipulation of miR-125b and miR-29b using antagomiRs and miR mimics 113
4.2.9 Modulation of miR-125b and miR-29b using antagomiRs and miRNA mimics induces apoptosis in AML cell lines 115
4.2.10 Cell death induction by antagomiRs and miRNA seen in primary AML blasts 118
4.2.11 AntagomiRs and miRNA mimics sensitise AML cells to chemotherapeutic agents 119
4.2.12 Increased sensitivity to chemotherapeutic agents in primary AML samples following treatment with antagomiRs and miRNA mimics 121
4.2.13 Identification of miRNA targets through manipulation of miR-125b / miR-29b 125
4.2.14 Confirmation of targets miRNA targets through NRF2 inhibition and KEAP1 knockdown 128
4.3 Conclusions and Discussion 130

Chapter 5 Modulating the NRF2 Pathway Through Gene Editing 133
5.1 Introduction 134
Aims and rationale 136
5.2 Results 137
5.2.1 Cloning guides into LentiCRISPR 137
5.2.2 Genotyping Primers 138
5.2.3 Determining CRISPR editing by T7 endonuclease assay 141
5.2.4 Guide efficiency in HEKs 143
5.2.5 Editing NRF2 Exon 4 with TALENs 147
5.2.6 Cpf1 guides targeting NRF2 Exon 4 152
5.2.7 Cloning KEAP1 guides and editing KEAP1 in HEK-293 cells 156
5.2.8 Generation of NRF2 and KEAP1 deficient HCT-116 159
5.2.9 Generation of NRF2-deficient K562 cells 165

5.2.10 Generation of NRF2 deficient THP-1 cells 172
5.3 Conclusions and Discussion 178

Chapter 6 General Discussion 183
6.1 Final Discussion 184
6.1.1 NRF2 regulation of miR-125b and miR-29b 184
6.1.2 Gene Editing NRF2 186
6.1.3 Future work 189

References 194

List of Figures

Chapter 1:

Figure 1.1: Schematic of the haematopoiesis process and the derivation of myeloid and lymphoid classes of blood cancers

Figure 1.2: Domain structure of NRF2 and KEAP1

Figure 1.3: NRF2 activation in cells following oxidative/chemical stress

Figure 1.4: Dysregulation of cancer cells by miRNAs

Figure 1.5: Overview of Gene editing with CRISPR-Cas9

Chapter 3:

Figure 3.1: miRNA Screening Array

Figure 3.2: Effect of Sulforaphane on miRNA expression in AML cells

Figure 3.3: miRNA expression changes following NRF2 knockdown

Figure 3.4: Schematic of miRNA promoter regions with putative NRF2 ARE binding sites

Figure 3.5: Confirmation of NRF2 dependent miRNA regulation

Figure 3.6: Expression of miRNA in AML blasts compared to normal CD34+ cells

Figure 3.7: miR-125b and miR-29b in primary AML

Chapter 4:

Figure 4.1: Schematic of genomic location of miR-125b and miR-29b and paralogs

Figure 4.2 Real time PCR detection of miRNA cluster members in THP-1 cells following NRF2 lentiviral knockdown

Figure 4.3: Schematic of the miR-125b-1 and miR-29b-1 promoter regions

Figure 4.4: Chromatin Immunoprecipitation assay (ChIP) was used to determine Transcription factor (TF) binding

Figure 4.5: miRNA promoter/reporter assay

Figure 4.6 Transcriptional activity of the putative NRF2 binding sites on the miR-125b1 promoter

Figure 4.7: Effect of a miR125b anatagomiR and a 29b mimic on miR125b and 29b

expression in THP-1 cells

Figure 4.8: Modulation of miR-125b/29b induces cell death in AML

Figure 4.9**:** miR-125b/29b modulation induces cell death in primary AML cells

Figure 4.10 Modulation of miR-125b and miR-29b increases daunorubicin sensitivity in AML blasts

Figure 4.11: Detection of miR-125b and miR-29b targets

Figure 4.12: miRNA targets confirmed through NRF2 modulation

Chapter 5:

Figure 5.1: Overview of CRISPR guide cloning

Figure 5.2: NRF2 Exon 1

Figure 5.3: NRF2 Exon 2

Figure 5.4: NRF2 Exon 4

Figure 5.5: DNA mismatch assay using a T7 Endonuclease

Figure 5.6: T7 endonuclease assay on Exon 1 guides

Figure 5.7: T7 endonuclease assay on Exon 2 guides

Figure 5.8: T7 endonuclease assay on Exon 4 guides

Figure 5.9: Construction of TALEN pair targeting NRF2 Exon 4

Figure 5.10: Construction of Left-Hand TALEN construct

Figure 5.11: Validation of TALEN pairs on NRF2 Exon 4

Figure 5.12: Cloning Cpf-1 guides

Figure 5.13: Validation of Cpf1 guides on NRF2 Exon 4

Figure 5.14: Keap1 guides

Figure 5.15: Generation of NRF2- and KEAP1-deficient HCT116 cells

Figure 5.16: Deriving NRF2-edited clones from puromycin selected HCT-116 cells

Figure 5.17: Confirmation of NRF2-deficient HCT-116 clones

Figure 5.18: Generation of NRF2-deficient K562 cells

Figure 5.19: Deriving an NRF2 edited clones from puromycin selected K562 cells

Figure 5.20: NRF2 inducers CDDO and Sulforaphane in NRF2-deficient K562 cells

Figure 5.21: Sanger sequencing of NRF2-edited K562 clones

Figure 5.22 Generation of NRF2-deficient THP-1 cells

Figure 5.23 Deriving an NRF2 edited clones from puromycin selected THP-1 cells

Figure 5.24: NRF2 inducers CDDO and Sulforaphane in NRF2-deficient THP-1 cells

Figure 5.25: Confirmation of NRF2 edited THP-1 cells by Sanger sequencing

List of Tables

Chapter 1:

Table 1.1: FAB classification of AML

Table 1.2: WHO classification of AML

Chapter 2:

Table 2.1: SDS-PAGE gel recipes

Table 2.2: Antibody sources and dilutions used for Western blotting or CHiP

Table 2.3: qPCR primers used for ChIP analysis on the ARE sites

Table 2.4 Example of typical PCR reaction with One Taq or Phusion

Table 2.5: Example of a typical Restriction Digest

Table 2.6: Example of a typical ligation reaction

Table 2.7: Example of a typical Reverse Transcription reaction using iSCRIPT

Table 2.8: Example of a typical 20µl qPCR reaction using SYBR Green

Table 2.9 Primer sequences used for qPCR

Chapter 3:

Table 3.1: Characterisation of the 27 primary AML samples used in this study

Chapter 4:

Table 4.1: Location and sequences of putative ARE sites in the miR-125b1 or miR-29b1 promoters

Table 4.2: Modulation of miR125b and miR-29b increases daunorubicin sensitivity in AML cell lines

Table 4.3: Daunorubicin sensitivity of AML blasts following miRNA manipulation

Table 4.4: List of putative miR-125b and miR-29b mRNA targets and their associated disorders.

Abbreviations

6-Thioguanine	6TG
Acute Lymphocytic Leukaemia	ALL
Acute Myeloid Leukaemia	AML
Acute Promyelocytic Leukaemia	APL
Ammonium Persulphate	APS
Antioxidant Response Element	ARE
All Trans Retinoic Acid	ATRA
Annexin V-Propidium Iodide	AV/PI
Asymmetrical Cell Division	AVD
Beta Beta Alpha	BBA
B Cell Receptor	BCR
Bric a' brac	BTB
Bruton's Tyrosine Kinase	BTK
Cas9 nickase	Cas9n
Core Binding Factor	CBF
Chronic Kidney Disease	CDK
1-chloro-2,4,dinitrobenzene	CDNB
Chromatin Immunoprecipitation	ChIP
Chronic Lymphocytic Leukaemia	CLL
Chronic Myeloid Leukaemia	CML
Chronic obstructive pulmonary disease	COPD
Clustered Regulatory Interspaced Short Palindromic Repeats	CRISPR
Threshold Cycle Value	CT
C terminal Region	CTR
Catalytically dead Cas9	dCas9
Diethylaminoethyl	DEAE
Double Glycine Repeats	DGR
Dulbecco Modified Eagle Medium	DMEM
Double Strand Break	DSB
Double Strand Break Repair	DSBR
Enhanced chemiluminescence	ECL
Ethylenediaminetetraacetic acid	EDTA
Epithelial- Mesenchymal Transition	EMT
Ethidium bromide	EtBr
French-American-British Classification	FAB
Fetal Bovine Serum	FBS
FMS like Tyrosine Kinase-3	FLT3
Glutathione Reductase	GR
Histone Deacetylase Inhibitor	HDAC
Homology Directed Repair	HDR

Higher Eukaryotes and Prokaryotes Nucleotide binding	HEPN
Haem Oxygenase 1	HO-1
Haematopoietic Stem Cells	HSC
Insertion Or Deletion Mutations	INDEL
Immunoprecipitation	IP
Internal Tandem Duplications	ITD
Kelch- like ECH associated protein 1	KEAP1
Loss Of Heterozygosity	LOH
Musculoaponeurotic Fibrosarcoma	MAF
National Center for Biotechnology Information	NCBI
Nuclear Export Signals	NES
Non-Homologous End Joining	NHEJ
Nuclear Localisation Signals	NLS
Nucleophosphin 1	NPM1
Nuclear factor (erythroid-derived-2) like 2	NRF2
Non-Small Cell Lung Cancer	NSCLC
N Terminal Region	NTR
Protospacer Adjacent Motif	PAM
Polymerase Chain Reaction	PCR
Precursor miRNA	pre-miRNA
Primary miRNA Transcript	pri-miRNA
Quantitative Real Time PCR	qPCR
Ribose 5-Phosphate	R5P
Retinoic Response Elements	RARE
Retinoic Acid Receptor Alpha	RARα
Rentinoblastoma	Rb
RNA Induced Silencing Complex	RISC
Reactive Oxygen Species	ROS
Roswell Park Memorial Institute	RPMI
Reverse Transcriptase	RT
Repeat Variable Di Residue	RVD
X linked Severe Combined Immunodeficiency	SCID-X1
Stem Cell Transplants	SCT
Single Nucleotide Polymorphism	SNP
Single Stranded RNA	ssRNA
Transcription Activator-Like Effectors	TALE
Transcription Activator Like Effector Nuclease	TALEN
Trypomysin 1	TPM1
World Health Organisation	WHO

Chapter 1

Introduction

Project overview and context

Chemotherapy resistance remains a prominent issue in Acute Myeloid Leukaemia, particularly in patients over the age of 65. Our lab has previously identified the transcription factor NRF2 as being constitutively active in AML and this leads to resistance to frontline chemotherapy. miRNAs are 20-25 base pair RNA molecules that repress their complementary mRNA targets, and therefore play an important role in regulating gene expression. Given that NRF2 has previously been shown to regulate several miRNAs we wished to investigate whether this played a role in resistance in AML. Furthermore, we wished to explore the use of gene editing technology to further understand the role of NRF2 in AML.

1.1 Overview of Leukaemia

1.1.1 Haematopoiesis

Haematopoiesis refers to the formation of blood cells, in particular, the generation of mature myeloid, lymphoid and erythroid cells from primitive haematopoietic cells. The current accepted model suggests all haematopoietic cells are derived from Haematopoietic Stem Cells (HSC). HSCs are multipotent and have the ability to replicate themselves as well as produce any haematopoietic cells in the human body (Baum et al., 1992). One study showed HSC cells derived from murine bone marrow have the ability to differentiate into myeloid, B and T cells (Spangrude et al., 1988). As the HSCs divide they produce mature daughter cells with a narrower differentiation potential. The HSCs can form two lineages, myeloid and lymphoid and both are multipotent stem cells with a limited differentiation capacity. The myeloid progenitor cells have the ability to differentiate into immune cells such as megakaryocytes, erythrocytes, mast cells, basophils, neutrophils, eosinophils,

myeloid derived dendritic cells and macrophages. The lymphoid progenitors can differentiate into B and T lymphocytes, lymphoid-derived dendritic cells and natural killer cells. The myeloid system, derived from a common myeloid progenitor, plays a crucial role in the innate immune response. Dendritic cells present antigens to the lymphocytes and the macrophages/neutrophils play an important role in phagocytosis. Eosinophils and Mast cells protect cells from pathogens. The lymphatic system on the other hand plays a critical role in the adaptive immune response. B lymphocytes produce antibodies (through plasma cells) and the T lymphocytes can either activate the B lymphocytes/macrophages or directly induce cell death in virally infected cells (Kondo, 2010, Iwasaki and Akashi, 2007, Lai and Kondo, 2008).

The haemopoietic system is derived during embryogenesis, initially through specialisation of the mesoderm (one of the three germ layers). This process can be divided into primitive and definitive haematopoiesis. Primitive haematopoiesis occurs during the early stages of foetal development and results in the production of primitive haematopoietic cells including macrophages and nucleated erythrocytes (Baron, 2003). This provides oxygen during the early stages of embryogenesis (Orkin and Zon, 2008, Jagannathan-Bogdan and Zon, 2013). From the yolk sacs, the HSCs migrate towards the liver, before firmly establishing themselves in the bone marrow for definitive haematopoiesis. (Jagannathan-Bogdan and Zon, 2013). Definitive haematopoiesis produces all haematopoietic lineages in the human body. Like its primitive counterpart, definitive haematopoiesis initially begins in the yolk sac, before becoming widespread after

the formation of the circulatory system. In addition to generating all haematopoietic lineages required in the body, all “mature” cells are generated (such as anuclear erythrocytes) (Lux et al., 2008).

The origin of HSC cells is the subject of some debate with some evidence suggesting they may be derived from the yolk sac. One study isolated haemopoietic cells derived from the yolk sac and showed they can differentiate into different haematological types (Moore and Metcalf, 1970). However studies in avian models contradict these results suggesting the HSC originate from the extra-embryonic mesoderm (Tanaka et al., 2012).

There are several models that explore the ability of HSCs (or stem cells in general) to divide and populate the haematopoietic system. One such model is asymmetrical cell division. According to this model, every division of haematopoietic cells produces two daughter cells, one of which will have a more committed fate than the other which retains the parental cell’s stem cell characteristics. Asymmetrical division has the advantage of the haemopoietic cell population remaining at a constant level, keeping numbers of both the multipotent HSC population and the differentiated lineage specific cells constant. While this process will maintain cell numbers, there are times when the population needs to rapidly expand. Systemic division occurs when the HSC, or stem cell, divides with both daughter cells either becoming HSC, stem cells or differentiated cells (Måløy et al., 2017). This is particularly useful when it is necessary to replenish a certain cell type.

1.1.2 Subtypes of Leukaemia

Haematological malignancies refer to a diverse range of disorders primarily affecting the blood forming tissues. More specifically it refers to all leukaemias, lymphomas and myelomas. In leukaemias, the malignancy primarily occurs when myeloid or lymphocytic cells overcrowd the bone marrow preventing normal function. Lymphoma primarily affects the lymphocytic regions (notably the thymus, lymph nodes and spleen) and is commonly split into two subcategories Hodgkin and non-Hodgkin. Multiple myeloma occurs due to over-division of plasma cells in the bone marrow. Leukaemias can arise due to defects in the myeloid or lymphocytic progenitor cells and are commonly subdivided into four classes: Acute Myeloid Leukaemia (AML), Acute Lymphocytic Leukaemia (ALL), Chronic Myeloid Leukaemia (CML) and Chronic Lymphocytic Leukaemia (CLL).

Acute Myeloid leukaemia, (discussed in greater detail in the next section), refers to the excess proliferation of myeloid progenitor cells (Grove and Vassiliou, 2014). Compared to other haematological malignancies, AML is a heterogeneous disorder characterised by a plethora of molecular, genetic and chromosomal abnormalities resulting in abnormal myeloid cells (Kumar, 2011).

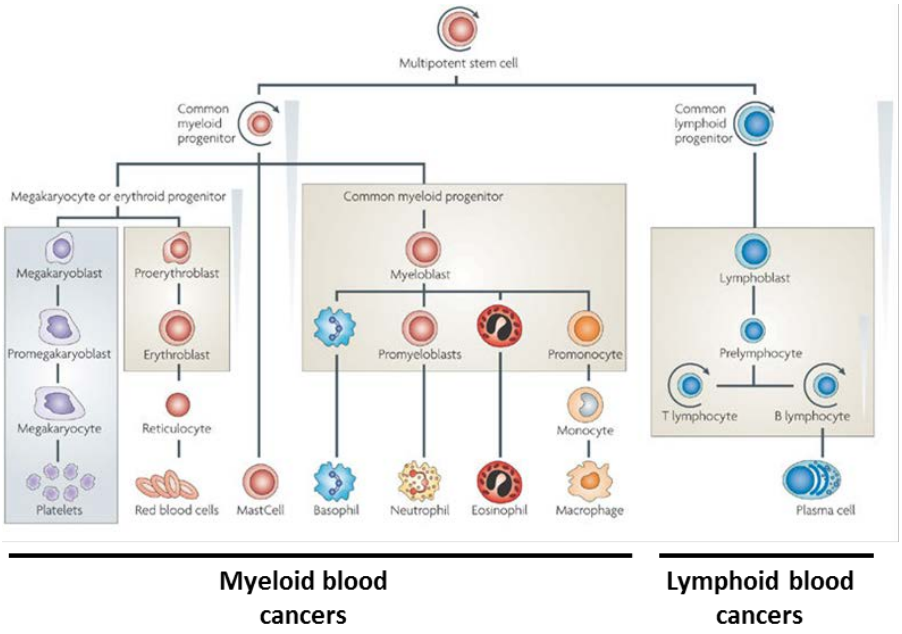

Figure 1.1: Schematic of the haematopoiesis process and the derivation of myeloid and lymphoid classes of blood cancers. The line thickness represents differentiation stage, from least to most differentiated. Adapted with permission from Springer Nature: Nature Reviews Cancer (Ramsay and Gonda, 2008)

Acute Lymphocytic Leukaemia (ALL) refers to the over-proliferation of B or T cells derived from a lymphoid progenitor. ALL predominately affects children and young adults. ALL is underlined by several genetic abnormalities and chromosomal translocations, including the BCR-ABL1 fusion or deletions in IKAROS (IKZF1) (Collins-Underwood and Mullighan, 2010). The repression or deletion of IKAROS is associated with poor prognosis and other chromosomal abnormalities including BCR-ABL1 (IKZA1 deletions are identified in approximately 80% of ALL cases with the translocation). Furthermore its deficiency in mice inhibits lymphocyte differentiation (Payne and Dovat, 2011).

Chronic Myeloid Leukaemia (CML) again refers to the over proliferation of myeloid progenitor cells, however unlike AML its cytogenetic profile is limited. Primarily CML is the result of the translocation of ABL (chromosome 9) and BCR (chromosome 11) which forms the Philadelphia chromosome, also known as the BCR-ABL fusion gene. This translocation is the primary abnormality in the disorder, and results in malignant cell transformation and increased cell proliferation (Haririan et al., 2012). CML progresses slower than AML, and can be segregated into three distinct phases: chronic, accelerated and blast (Calabretta and Perrotti, 2004). The initial chronic phase allows the slow proliferation and accumulation of myeloid progenitor cells in sites such as the bone marrow. The accelerated phase lasts up to six months and results in an increase of blast cells (Calabretta and Perrotti, 2004). The final blast crisis phase results in uncontrolled proliferation of the myeloid cells, not dissimilar from that in AML. Until recently, blast crisis was deemed fatal (Radich, 2007) but recent prognosis has drastically improved thanks to the introduction of tyrosine kinase inhibitors such as imatinib. Imatinib inhibits the activity of the BCR-ABL fusion protein and since its introduction CML survival rates have significantly increased, with the 8 year survival rates increasing from 6% in 1975 to 87% in 2001 (Kantarjian et al., 2012).

The most common leukemic subtype is Chronic Lymphocytic Leukaemia (CLL) and this again refers to the over proliferation of lymphocytic cells resulting in overcrowding in the lymph nodes and bone marrow. One of the most common defects in CLL is the dysregulation of the B cell signalling (BCR) transduction

pathway. The BCR pathway plays a crucial role in the growth and development of B cells (Shinners et al., 2007).

1.2 Acute Myeloid Leukaemia

1.2.1 Overview of Acute Myeloid Leukaemia

Acute Myeloid Leukaemia (AML) is responsible for 80% of acute leukaemias, affecting approximately 3-4 people per 100,000 (Almeida and Ramos, 2016). Whilst the five-year survival rate post diagnosis is 40% in young patients, it is less than 5% in patients aged over 65. Furthermore, 70% of patients over the age of 65 die within a year of being diagnosed (Meyers et al., 2013). This is of particular concern considering the average age of diagnosis of AML is 67. Despite this, the efficacy of AML treatment has improved in recent years, the historic 5-10 years survival rate of 10% has increased up to 40-50%. The majority of AML cases, approximately 97%, are as a result of mutation. One theory proposed to describe leukaemogenesis (as well as other cancers) is the “two-hit hypothesis” of Knudson’s (Conway O'Brien et al., 2014, Kelly and Gilliland, 2002). This states that leukaemia is caused by two main driving mutations which are required for oncogenesis. The first mutation (class one) allows cells to uncontrollably proliferate. The second mutation (class two) prevents the differentiation of the haematopoietic cells thereby allowing the leukaemia to develop (De Kouchkovsky and Abdul-Hay, 2016). Examples of a class one mutation include FLT3, c-Kit and TP53. Example of class two mutations include Core Binding Factor (CBF) and NPM1.

There has been criticism of this model, in particular due to a significant number of AML patients having epigenetic defects, i.e. in histone modification, DNA methylation and CpG hypermethylation (Shih et al., 2012). Some mutations, for example PML-RARα, occur at a certain point in myeloid cell development. For example, in the case of PML-RARα the translocation must occur at the pre myelocytic stage for it to have a prognostic effect (Reilly, 2005, Conway O'Brien et al., 2014). A third class of mutations has therefore been suggested which affect epigenetic-related genes, examples of these include IDH-1 and 2 (De Kouchkovsky and Abdul-Hay, 2016).

Acute Leukaemia is diagnosed by the presence of 20% (previously 30% before 2001) or more leukaemic blasts in the peripheral blood or bone marrow (Döhner et al., 2010). Myeloid leukaemia is defined by identifying the cell is of myeloid origin, through immunophenotyping. The primary symptoms of AML include bone marrow failure and leucocytosis. Other symptoms include fatigue, anorexia, anaemia and weight loss. Secondary death can occur due to bleeding or infection (De Kouchkovsky and Abdul-Hay, 2016).

1.2.2 Classification of AML

Classifying AML allows clinicians and scientists to group together different AML subtypes using either cytogenetics or through the prognostic outlook of patients. This allows us to better understand and diagnose similar AML subtypes, allowing better targeted treatments based on their characteristics. The French-American-British classification (FAB) was designed in 1976 and divides AML into eight

subtypes (M0-M7) based on immunological characteristics and morphology (Table 1.1). M0-M3 is primarily of a granulocytic lineage (with M0 being undifferentiated myeloblastic leukaemia, M1 refers to myeloblastic leukaemia without maturation, M2 refers to myeloblastic with maturation, and M3 refer to promyelocytic differentiation). M4 is primarily of both myleoblast and monocytic origin (here both the myleoblast and monocytic population are above 20% in the peripheral blood and bone marrow), a subtype M4eos is similar but also contains an increased eosinophils population. M5 refers to Acute Monocytic Leukaemia and defined by an excess monocytic population. M6 is erthyroid leukaemia and M7 refers to Acute megakaryoblastic leukaemia (referring to excess erythroid and megakaryoblastic cells respectively) (Bennett et al., 1976, Arber et al., 2003).

AML FAB designation	Name	Notes
M0	Undifferentiated myeloblastic leukaemia	Granulocytic lineage
M1	Myeloblastic leukaemia without maturation	Granulocytic lineage
M2	Myeloblastic leukaemia with maturation	Granulocytic lineage
M3	Acute promyelocytic leukaemia (APL)	Granulocytic lineage
M4	Myelomonocytic Leukaemia	Myleoblast and monocytic population above 20% in the peripheral blood and bone marrow
M4eo	Myelomonocytic Leukaemia with eosinophilia	Similar to M4 with increased eosinophils
M5	Acute Monocytic Leukaemia	
M6	Acute Erthyroid leukaemia	
M7	Acute Megakaryoblastic leukaemia	

Table 1.1: FAB classification of AML

This classification has been criticised for not giving enough weight to prognostic information. In 2001 the World Health Organisation (WHO) created a classification combining morphological, genetic, immunophenotyping and cytochemical information (Table 1.2). Since its creation in 2001, the classification has been

revised in both 2008 and 2016. This classification splits AML into several categories including “AML with recurrent genetic abnormalities”, “AML with myelodysplasia related changes”, “Therapy related myeloid neoplasms”, “Myeloid sarcoma” and “AML not categorised”.

AML with recurrent genetic abnormalities
t(8;21)(q22;q22)
t(15;17) (q24;q21)
t(16;16)
t(1;22)(p13;q13)
t(11;19)(q23;p13.1)
AML with myelodysplasia related changes
Therapy related myeloid neoplasms
Myeloid sarcoma
AML not categorised
AML (minimal differentiation)
AML (no maturation)
AML (maturation)
Myelomonocytic Leukaemia
Monocytic Leukaemia
Erythroid Leukaemia
Megakaryoblastic leukaemia
Basophilic Leukaemia
Acute Panmyelosis

Table 1.2: WHO classification of AML

1.2.3 AML Translocations and Cytogenetics

As previously mentioned, AML is a highly heterogeneous disorder exhibiting a range of mutations and chromosomal abnormalities. Understanding these genetic abnormalities is important as they have proven to relate to prognosis and response to chemotherapy (Tamamyan et al., 2017).

50-60% of AML patients suffer from chromosomal abnormalities, which result in the formation of fusion proteins, many of which cause aberrant transcriptional activity. Notable translocations include: t(16;16)(also known as inv (16)(p13q22)); as well as t(8;21)(q22;q22); t(1;22)(p13;q13); t(15;17)(q24;q21); 7q loss and t(11;19)(q23;p13.1) (Tamamyan et al., 2017, Mrózek et al., 2004). Due to the scope of this introduction only a few chromosomal translocations will be discussed in further detail.

t(16;16) results in the fusion of CBFB and MYH11 creating the fusion protein CBFB-MYH11. CBFB-MYH11 plays a critical role in AML, repressing differentiation through binding to CBFA2 (Delaunay et al., 2003, Kundu and Liu, 2001). Binding to CBFA2 allows it to recruit HDAC, which modifies acetyl groups post-translationally, thereby modulating gene expression (Delaunay et al., 2003). This alone is insufficient to act as a driving mutation (Kundu and Liu, 2001). t(16;16) patients are commonly classified with M4eo (high eosinophil count) (Le Beau et al., 1983). This translocation is associated with a favourable prognosis and a high proportion of patients reach complete remission. Despite this, older patients have a high risk of relapse and exhibit a poorer prognosis (Delaunay et al., 2003).

t(8;21)(q22;q22) involves a translocation between RUNX1 and RUNX1T1 (chromosomes 8 and 21 respectively), creating the fusion protein RUNX1-RUNX1T1 (also known as AML1-ETO). This translocation is responsible for 5-12% new AML cases and is predominately associated with FAB M2 (acute myeloblastic leukaemia with maturation), or in rare cases FAB M1 and M4 (Peterson and Zhang, 2004). RUNX1-RUNX1T1 blocks a myriad of cellular processes including myeloid differentiation and apoptosis, thereby allowing the cell to escape regulation (Peterson et al., 2007). Remission rates are high among patients who suffer from this translocation de novo, in particular in those treated with high levels of cytarabine (Bloomfield et al., 1998). However, the remission rates are lower in patients who gain this translocation as a response to their chemotherapy (known as therapy related AML or t-AML) (Gustafson et al., 2009).

Another translocation t(15;17) (q24;q21) causes a fusion between the Promyelocytic Leukaemia Protein (PML) and Retinoic Acid Receptor alpha (RARα) creating the PML-RARα fusion protein. This inhibits differentiation and increases proliferation (He et al., 1997). Meaning that the AML cells have had the "two hits" as discussed above (i.e. uncontrolled proliferation and arrest of differentiation) (Grimwade et al., 2000). This translocation is the most common molecular abnormality identified in patients suffering from Acute Promyelocytic Leukaemia (APL), classified in the French American British system as FAB M3. APL is responsible for 5% of all AML cases, and 15-18% of all acute non-lymphocytic leukaemia cases. Prior to 1985 patients were treated with daunorubicin

and cytarabine. While the complete remission rate were relatively high (up to 80%), remission on average only lasted up to 25 months (Wang and Chen, 2008). Patients suffered from bleeding diathesis (a defect in blood coagulation) which was responsible for a high proportion of deaths in APL patients (as opposed to resistance to the given chemotherapy agents), however these chemotherapy agents used did increase the severity of the condition (Wang and Chen, 2008, Coombs et al., 2015).

Retinoids have shown to be effective at causing granulocytic differentiation of APL cell lines and cultured patient samples, successfully differentiating the characteristic promyeloblasts to mature neutrophils (Breitman et al., 1981). This led to the development of the drug All-Trans Retinoic Acid (ATRA). ATRA induces differentiation by binding and conformationally changing PML-RARα, leading to the activation of various genes containing a retinoic response elements (RARE) motif in their promoter including C/EBP (critical in the differentiation process in neutrophils) (Raelson et al., 1996, Duprez et al., 2003). Furthermore it leads to the ubiquitination and degradation of PML-RARA (Zhu et al., 1999). ATRA was first used therapeutically in Shanghai, China and since then complete remission has increased up to 95%, and the 5 year disease free survival has increased to 74% (Huang et al., 1988, Wang and Chen, 2008). More recently arsenic has also been used in APL treatment, and has shown to be particularly effective when used either as a single agent, or in combination with ATRA (Chen et al., 1996, Tomita et al., 2013).

FMS like tyrosine kinase-3 (FLT-3), FLT-3 is a type III receptor tyrosine kinase initially identified on haematopoietic stem cells. It is located on chromosome 13 (13q2) and spans 100 kb with 24 exons. FLT3 is made up of five external immunoglobulin like domains, a transmembrane domain, and two kinase domains (Levis and Small, 2003). Upon binding FLT3 ligand (FLT3L) causes dimerization of the receptor creating a conformational change resulting in the auto-phosphorylation and a constitutively signalling receptor (Fathi and Chen, 2011).

FLT3 is predominately expressed in $CD34^+$ cells in the bone marrow and FLT3-deficient mice show a decrease in lymphoid population and a skew to the myeloid lineage (Mackarehtschian et al., 1995). FLT3 expression can be found in a high proportion of leukaemic cells, across all four subtypes, in the case of AML FLT3 expression is found in over 90% of AML cells (Carow et al., 1996). Ectopic expression of FLT3L causes leukaemia in mice (Hawley et al., 1998). In AML, a number of patients contain activating mutations in FLT3, these are mostly internal tandem duplications (ITD), which can be found in 23% of newly presented AML cases, and in a smaller subset of patients a point mutation occurs in the kinase domain resulting in its activation (Fathi and Chen, 2011). The ITD mutation is most commonly found in the vicinity of exon 14 (typically within the region coding for amino acids 590-600) but can occasionally span to exon 15. This primarily affects the juxtamembrane region (which regulates kinase activity) (Abu-Duhier et al., 2001). The ITD occurs in multiples of three (maintaining the reading frame) and can span from 3-400 bp (Schnittger et al., 2002). The duplication results in the constitutive activation of FLT3, which in turn activates downstream pathways

including STAT5, AKT and MAP kinase. The dysregulation of these signalling pathways in cancer cells can promote cell growth, whilst supressing apoptosis (Hayakawa et al., 2000). The most recent drug to be introduced for the treatment of AML is midostaurin, that is an inhibitor of FLT3 kinase activity (Stone et al., 2018).

Another crucial mutation is the phosphoprotein nucleophosphin 1 (NPM1), found in approximately 35% of AML cases (Falini et al., 2005). NPM1 is made up of 12 exons and contains nuclear export signals (NES) in its N-terminal, nuclear localisation signals (NLS) in the central region, the C-terminal also contains an NLS. The C-terminal region is also responsible for DNA binding (Heath et al., 2017). NPM1 is primarily located in the nucleolus, however due to the presence of NES and NLS domains, it translocates between the nucleus and cytoplasm (Federici and Falini, 2013). NPM1 has several roles including the regulation of genomic stability, promoting apoptosis, inhibiting proliferation, and the biogenesis of ribosomes (Heath et al., 2017). In AML, NPM1 can be mutated, predominately in exon 12, which creates a frameshift mutation towards the end of the exon (Falini et al., 2005). This causes the accumulation of NPM1 in the cytoplasm. These mutations are always heterozygous, with attempts to create murine models with homozygous mutated NPM1 being unviable, likely due to it being embryonic lethal (Grisendi et al., 2005). In AML, mutated NPM1 is therefore haploinsufficient (i.e. only partial production of the wild type protein). Murine models with mutated NPM1 showed excess proliferation of haematopoietic cells with a skew towards the myeloid lineage. The mutated NPM1 can repress apoptosis (through interfering with caspase 6/8 activity) and myeloid differentiation (Leong et al., 2010).

Furthermore it activates oncogenes such as Myc, due to the degradation of Fbw7y, a key factor in the ubiquitination and subsequent proteasomal degradation of c-Myc (Bonetti et al., 2008).

1.2.4 AML Treatment

AML is commonly treated using either induction or consolidation therapy. Initially newly diagnosed patients are treated with induction therapy. Induction therapy is underlined by the "7+3" regimen, which indicates seven days of cytosine arabinoside (cytarabine or Ara-C), alongside three days of anthracyclines (such as daunorubicin or doxycycline) (De Kouchkovsky and Abdul-Hay, 2016). This regimen is given to patients with a good or intermediate prognosis, in particular younger patients (Estey, 2014). The treatment gives complete remission in up to 80% of young patients, and 50% of patients above 65 (Seval and Ozcan, 2015, Menzin et al., 2002). Consolidation therapy is given to patients post induction therapy, with chemotherapy agents given to patients with low or intermediate prognosis. Older or less fit patients are considered not as healthy to receive combination therapy and are given cytarabine treatment alone. However, their resulting prognosis is poorer than patients deemed robust enough for combination therapy. Bone Marrow Stem Cell transplants (SCT) is given to those with severe prognosis or who relapse from their chemotherapy (Showel and Levis, 2014).

1.3 The redox-sensitive transcription factor - NRF2

1.3.1 Structure, activation and regulation by KEAP1

Reactive Oxygen Species (ROS) includes hydroxyl radicals, and superoxide anion, are produced from processes such as oxidative phosphorylation, NADPH oxidase and cytochrome P450 (Turrens, 2003). Hydroxyl radicals can be produced from H_2O_2through "Fenton-like" reactions catalysed by a transition metal (such as Fe(II))". ROS play an important role in cellular processes including signal transductions. Low levels of ROS can act as intracellular signalling intermediates, while high levels can act as anti-microbial protection (Finkel, 2011, Nathan, 2003). Altered ROS results in oxidative stress and its dysregulation is present in several diseases such as Huntington's, Atherosclerosis, Alzheimer's, Rheumatoid Arthritis and Parkinson's (Deshmukh et al., 2017). Oxidative stress can cause DNA damage directly through the formation of free radicals, but high levels also result in the repression of the DNA mismatch repair gene mutS as well as regulating DNA methyltransferases (Bridge et al., 2014, Wu and Ni, 2015). Collectively this can cause genomic instability or aberrant cellular proliferation leading to a number of malignancies (Visconti and Grieco, 2009).

Oxidative stress is regulated by antioxidants including the phase II cytoprotective enzyme Haem Oxygenase 1 (HO-1), NAD(P)H dehydrogenase [quinone] 1 (NQO1), glutathione-S-transferase (GST) and other redox proteins (Kim and Keum, 2016). The transcription factor Nuclear factor (erythroid-derived-2) like 2 (NFE2L2 or NRF2) is known as the master regulator of antioxidant genes. NRF2 is a member of the "Cap n Collar" (CNC) family and contains both a CNC and basic

leucine zipper domain (Moi et al., 1994). These domains allow NRF2 to regulate gene expression through binding to the "Antioxidant Response Element" (ARE) in the promoter region of its target genes. When NRF2 translocates to the nucleus it associates with small Maf proteins which aid its binding to AREs (Itoh et al., 1997).

NRF2 is made up of six NEH domains, NEH2 is located at the N-terminal, followed by NEH4, 5, 6, 1 and finally 3 (Figure 1.2). NEH 4 and 5 are activation domains and NEH 1 contains the CNC domain, as well as the basic leucine zipper region DNA binding domain. The NEH2 motif is important for regulation of NRF2 by binding to KEAP1 (Kelch-like ECH associated protein 1) (Taguchi et al., 2011). Under basal conditions NRF2 is kept in check by its inhibitor KEAP1.

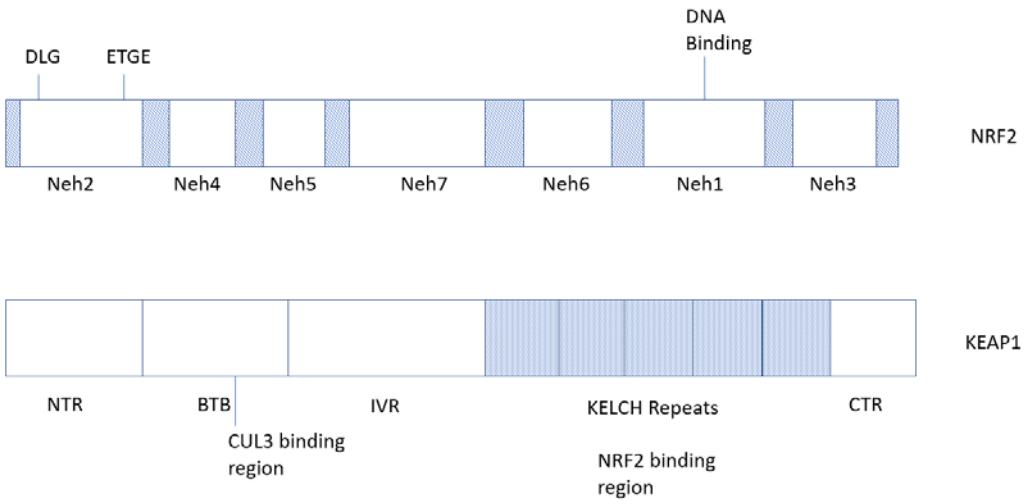

Figure 1.2: Domain structure of NRF2 and KEAP1

KEAP1 is made up of five domains (figure 1.2), the N terminal Region (NTR), Broad complex, tramtrack and "bric-a-brac" (BTB), intervening region (IVR), Kelch-like domain and C-terminal Region (CTR) (Itoh et al., 2004). KEAP1 binding to NRF2 is believed to occur as an "hinge and latch model", a Kelch domain

on KEAP1 binds strongly to the ETGE motif “Hinge” on NRF2, whereas a weaker interaction is seen between the binding of another Kelch domain to the DLG motif “Latch” on NRF2 (Tong et al., 2006). The DLG ensures NRF2s Neh2 domain is in the correct orientation to be ubiquitinated by Cul3. Ubiquitination of NRF2 causes proteasomal degradation ensuring it remains at low levels under basal conditions (Zhang and Hannink, 2003, Cullinan et al., 2004). In addition, NRF2 can be ubiquitinated and degraded in a KEAP1-independent manner. Neh6 contains two β-TrCP binding sites; DSGIS and DSAPGS, allowing SCF-mediated ubiquitination. The DSGIS motif can be phosphorylated by GSK-3 increasing its ability to bind to β-TrCP and therefore causing accumulation of NRF2. GSK-3 can be repressed by PI3K signalling, which is dysregulated in many malignancies (McMahon et al., 2004, Chowdhry et al., 2013).

The KEAP1/NRF2 complex is associated with the actin cytoskeleton through double glycine (Kelch) repeats on KEAP1, ensuring the complex remains in the cytoplasm until activated (Kang et al., 2004). In the presence of ROS, oxidation of Cys151 on KEAP1 prevents DLG-mediated binding NRF2 interfering with its ubiquitination. NRF2 subsequently becomes stabilised, *de-novo* synthesised NRF2 accumulates in the cytoplasm before translocating to the nucleus (Fig 1.3).(Stępkowski and Kruszewski, 2011).

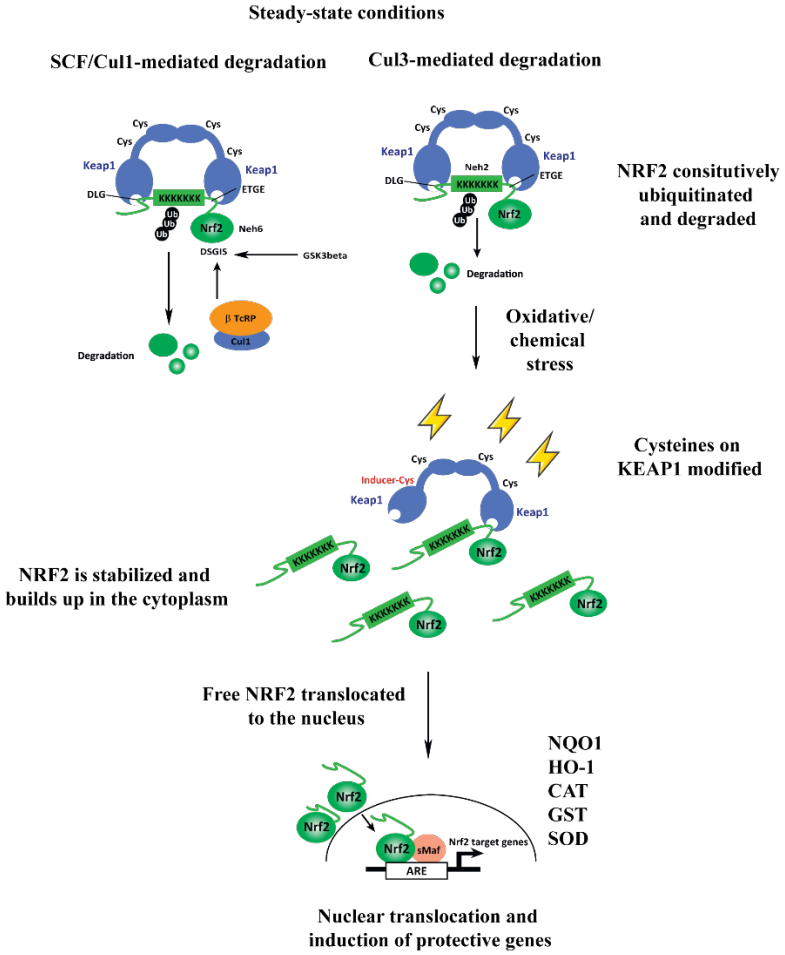

Figure 1.3: NRF2 activation in cells following oxidative/chemical stress. The figure legend was updated "Figure 1.3: NRF2 activation in cells following oxidative/chemical stress. Under basal conditions NRF2 is ubiquitinated by either by Cul3 in a KEAP1-dependent mechanism or by β-TcRP leading to its degradation. Following oxidative stress, KEAP1 is modified, and de-novo synthesised NRF2 accumulates in the cytoplasm before translocating to the nucleus, inducing its target genes. Adapted with permission from Elsevier: Trends in Pharmacological Sciences (Suzuki et al., 2013a)

1.3.2 Pathological roles of NRF2

The role of NRF2 expression has been indicated in several respiratory diseases. Patients with chronic obstructive pulmonary disease (COPD), show lower NRF2 and its downstream target, HO-1, levels in older patients who smoke than in age-matched controls. This is significant as low levels of NRF2 increases the risk of COPD (Suzuki et al., 2008). A polymorphism (617C/A) in the NRF2 promoter, which attenuates NRF2 expression, significantly increases the risk of lung injury post trauma (Marzec et al., 2007).

Chronic Kidney Disease (CKD) (caused mainly by chronic disorders such as hypertension and diabetes) is underlined by high levels of oxidative stress and inflammation. Murine models indicate NRF2 plays a protective role in CKD with NRF2-deficient female mice exhibiting glomerulonephritis and a lupus-like autoimmune nephritis (Yoh et al., 2001). ROS have previously been shown to aggravate immunological conditions and amplify tissue damage (Cooke et al., 1997).

In cancers, NRF2 has been dubbed as “Janus-faced” as it appears to play a dual role acting both as a tumour suppressor and an oncogene. Murine NRF2 knockout models appear to be protected against carcinogenesis. When exposed to benzo(a)pyrene, NRF2-deficient mice had an increased incidence in gastric neoplasia compared to their wild-type littermates. When treated with the chemoprotective agent Oltipraz a significant decrease in tumour burden was seen in the wild-type mice, with no reciprocal effect observed in NRF2-deficient mice.

This is likely due to Oltipraz inhibiting tumour growth through the induction of phase II enzymes (which are regulated by NRF2) (Ramos-Gomez et al., 2001).

Another study showed patients containing a SNP (rs6721961) which results in the repression of NRF2 expression, having an increased risk to lung cancers particularly in patients who smoke (Suzuki et al., 2013b). Furthermore, NRF2-deficient mice show increased metastasis in a Lewis Lung Carcinoma model with these cells exhibiting high levels of ROS. This effect was reversed in KEAP1-deficient mice (Satoh et al., 2010).

1.3.3 Oncogenic role of NRF2 in cancer

Upregulated or constitutive activation of NRF2 is found in a range of cancers including lung, ovarian, breast and head and neck (Jaramillo and Zhang, 2013). One study performing immunohistochemistry on 304 non-small cell lung cancer patients (NSCLC), detected high levels of NRF2, particularly in squamous cell carcinomas, while low levels of KEAP1 were detected, particularly in adenocarcinomas. High levels of NRF2 or low levels of KEAP1 both correlated with poor prognosis (Solis et al., 2010). In both of these studies high NRF2 levels were linked to resistance to frontline chemotherapy agents.

The role of NRF2 in resistance to chemotherapy has also been observed in primary gastric and pancreatic cancer samples and cell lines and this could be reversed by reducing NRF2 levels using siRNA (Hong et al., 2010, Hu et al., 2013). In the latter study NRF2 appeared to regulate the multidrug resistance genes ABCG2, GCLC,

MRP1,2,4 and 5 (Hong et al., 2010). This indicates NRF2's ability to protect against chemotherapy agents appears to go beyond its role in regulating oxidants and electrophiles.

Interestingly, several studies have identified many commonly used chemotherapy agents that activate or upregulate NRF2 signalling. The proteasome inhibitor Bortezomib, commonly used in MM, has been implicated in repressing Bach1, which allows NRF2 to bind to Maf unimpeded, thereby inducing expression of its downstream cytoprotective genes (Rushworth et al., 2011a). Histone deacetylase inhibitors (HDAC), work by causing histone acetylation, thereby altering gene expression which can result in increased differentiation or apoptosis (Wang et al., 2012, Bai et al., 2016).

In contrast, ATRA, which is commonly used in the AML subtype APL causes RARα and NRF2 to complex together, thereby preventing binding to its respective ARE sequences (Wang et al., 2007). Contrasting with its role in protecting against toxic compounds/insult, recent studies have suggested that NRF2 plays a larger role than simply protecting cells from chemotherapy agents and can also directly affect tumorigenesis in several cancer types. For example, in NSCLC high levels of NRF2 result in increased proliferation and cisplatin resistance, and this appeared to be linked indirectly to NRF2 by hyperphosphorylation of the Retinoblastoma (Rb) tumour suppressor gene and inhibition of p21CIP1/WAF1 (Homma et al., 2009). Moreover, in breast cancer there is a correlation between high levels of NRF2 and worse prognosis. This appeared to be linked to the effect of NRF2 on increased proliferation in these cells, partly due to stabilisation and elevated expression of

RhoA. When NRF2 levels are decreased a significant inhibition of proliferation and metastasis is seen (Zhang et al., 2016). The oncogenic function of NRF2 may also be due to its regulation of miRNA (discussed in more detail in the next section).

To further understand the role of NRF2 in cancer cell proliferation, one group used a range of lung cancer cell lines that were characterised with constitutive activation of NRF2 (Mitsuishi et al., 2012b). As expected NRF2 downregulation in these cells resulted in the attenuation of proliferation. The group next performed a microarray analysis using NRF2 siRNAs and identified a reduction in expression in several Pentose Phosphate Pathway (PPP)-related genes including G6PD, TALDO1, TKT, and PGD. Genes involved in NADPH production (such as IDH1 and ME1) were also reduced. The potential of NRF2 to bind to the promoters of these genes was confirmed by ChIP-Seq. This is significant because the PPP pathway is used to produce ribose 5-phosphate which is necessary for nucleotide synthesis, a process that requires NADPH. Additional experiments indicated that NRF2 was important in purine (but not pyrimidine) nucleotide synthesis. NRF2 was also shown to promote glutamine synthesis (through positive regulation of GCL) and involved in glutaminolysis (through ME1 regulation). In terms of NRF2's role in cellular proliferation, they showed this was predominately due to the upregulation of G6PD and TKT, which when attenuated, significantly reduced tumour growth in murine models. Furthermore, they identified PI3K/ATK dysregulation as being responsible for causing nuclear activation in several cancer types and thus altering the metabolic pathways of these cancers to increase proliferation (possibly thorough the regulation of the KEAP1 inhibitor GSK-3). However experiments carried out in

non-cancerous KEAP1 KD mice only showed alterations in the metabolic profiles cells located in certain regions (such as in the Forestomach Epithelium), suggesting that proliferative signalling in conjunction with constitutive activation of NRF2 is required to see the discussed metabolic reprogramming (Mitsuishi et al., 2012b).

Another group suggested that the PPP pathway is critical for NRF2s cytoprotective role (in particular NQO1 which uses NAPDH as a cofactor), and when the PPP pathway was inhibited (through altering glucose availability by serum starvation or by chemically disrupting G6PD) an inhibition in cytoprotective genes was seen (Heiss et al., 2013). This is at odds with the above Mitsuishi study which showed whilst serum starving KEAP1 KD MEFS reduced the expression of the cytoprotective gene NQO1, the cells still showed increased resistance to 1-chloro-2,4,dinitrobenzene (CDNB) in comparison to the wild type. This inconsistency could be down to both studies measuring different cytoprotective genes (one measuring HO-1 and glutathione reductase (GR) with the other using NQO1 as a cytoprotective marker). While both studies used serum starvation to attenuate PPP genes to basal conditions, the Heiss study additionally chemically disrupted G6PD. However, this study only measured cytoprotective gene expression, whilst the Mitsuishi additionally treated the serum starved cells with CDNB and looked at cell viability. This raises the possibility that NRF2 could still produce a cytoprotective response, despite low levels of PPP activity, however it may use cytoprotective genes that are independent of the PPP pathway (Heiss et al., 2013, Mitsuishi et al., 2012b).

As we have noted, NRF2 activity can be protective in some disorders and pathogenic in others, at times this "duality" can be seen in the same disorder. It has therefore been speculated that in a non-cancerous/early malignant cell, NRF2 predominately plays a protective role preventing further DNA damage through its anti-oxidative and anti-inflammatory mechanism thereby acting as a tumour suppressor. However as the cell becomes more malignant this mechanism is hijacked by the cancer cells to aid survival and growth, i.e. increase tumour proliferation (through mechanisms such as metabolomic reprogramming) and reduce sensitivity to chemotherapy agents (Sporn and Liby, 2012). This is supported by a study which investigated the role of NRF2 in inducing lung cancer. Lung cancer was induced in wild type or NRF2 KD mice using urethane (which also causes nuclear NRF2 accumulation). The NRF2-deficient mice developed more tumours in the early stages of urethane treatment in comparison to wild-type mice treated with urethane to induce NRF2. However, as treatment continued the urethane treated wild type mice grew larger tumours, which were generally more invasive and had a worse gene expression profile in comparison to the NRF2 KD mice. Of particular interest, the urethane induced wild-type mice were more likely to have constitutive activation of the oncogene KRAS (Satoh et al., 2013). Overall this study provides an interesting bridge between NRF2 role as a chemo-preventative and NRF2 as an oncogene.

1.3.4 Oncogenic activation of NRF2

As discussed previously, constitutive activation or overexpression of NRF2 can result in oncogenesis. There are three main mechanisms by which NRF2 can

become dysregulated in cancer, (i) mutations in either NRF2 or KEAP1, (ii) methylation of KEAP1, or (iii) activation of oncogenic signalling pathways (Taguchi and Yamamoto, 2017).

KEAP1 insertion, missense, or deletion mutations have been identified in lung carcinoma and these occurs throughout KEAP1 and not just within the NRF2 binding regions. In some circumstances this results in the loss of heterozygosity, causing impairment and/or loss of KEAP1 expression (Singh et al., 2006). This prevents KEAP1-NRF2 binding impeding NRF2 degradation (Taguchi and Yamamoto, 2017). These mutations have been found in several cancers including lung, breast, endometrial and hepatocellular carcinoma (Singh et al., 2006, Nioi and Nguyen, 2007, Wong et al., 2011, Schulze et al., 2015).

Mutations such as this are more common in KEAP1 than NRF2. NRF2 mutations are predominantly "gain-of-function" in nature and result in its constitutive activation. They often occur in the DLG and ETGE regions and therefore disrupting the binding between NRF2 and KEAP1. Mutations in the ETGE region prevent NRF2 ubiquitination (and therefore degradation) allowing it to accumulate in the cell. Similarly, mutations in DLG result in the stabilisation of NRF2 (Mitsuishi et al., 2012a). Again, these mutations have been identified in several cancers including head and neck, oesophageal and lung cancer (Shibata et al., 2008, Kim et al., 2010). Mutations have also been found in Cul3 in papillary renal cell carcinoma (Ooi et al., 2013).

Another way by which NRF2 may become constitutively expressed is through the methylation of CpG sites on the KEAP1 promoter, resulting in the repression of KEAP1 gene expression. This epigenetic regulatory mechanism is often seen in several cancer types including prostate and colorectal cancer (Jaramillo and Zhang, 2013, Zhang et al., 2010, Hanada et al., 2012).

Finally, NRF2 can be constitutively activated by oncogenic signalling. K-Ras, B-Raf and Myc oncogenes have all shown to increase transcriptional levels of NRF2 (DeNicola et al., 2011). Furthermore, as discussed in the next section, our lab have previously uncovered that the dysregulated NF-κB often found in cancer cells, results in constitutive activation of NRF2, a mechanism that was seen in AML cancer too (Rushworth et al., 2012).

1.4 NRF2 regulation by NF-κB in AML

In AML, the transcription factor nuclear factor-κB (NF-κB) was shown to be constitutively-activated by a number of signalling factors including the cytokine TNFα (Rushworth et al., 2010). The NF-κB family consists of p50 (NF-κB1), p52 (NF-κB2), p65 (RelA), RelB and c-Rel transcriptionally-active proteins. Their levels and functions are controlled by inhibitors such as IκBα, IκB, IκBε and BCL3 (Oeckinghaus and Ghosh, 2009). NF-κB can become activated through two pathways classical and non-canonical. In the classical (or canonical) pathway NF-κB is located in the cytoplasm. Here IκBα is phosphorylated at two sites- Ser32 and 36, resulting in its ubiquitination and proteasomal degradation. This results in the release of NF-κB subunits (such as a typical p50-p65 complex), allowing it to

undergo nuclear translocation before binding and regulating its target region in the DNA (Ghosh and Karin, 2002, Demchenko et al., 2010). NF-κB is constitutively activated in haematological malignancies (such as AML), resulting in an increase in proliferation and an reduction in responsiveness to apoptotic stimuli (Rushworth et al., 2010). Previous work in the MacEwan lab identified NF-κB repression did not result in TNFα-mediated apoptosis, this being due in part to the subsequent upregulation of HO-1, which plays a key protective role (Rushworth and MacEwan, 2008). HO-1 is regulated by NRF2, which was also found to be constitutively activated in AML, where it was identified that NF-κB positively regulated NRF2 through binding to two NF-κB sites on the NRF2 gene's promoter (Rushworth et al., 2012). The positive regulation between NF-κB and NRF2 may be cell type specific, as an inhibitory relationship is seen in other cell types (Wardyn et al., 2015). Furthermore, constitutive activation of NRF2 in AML was found to be the result of aberrant signalling, as opposed to any mutation in the NRF2/KEAP1 binding regions, that could account for dysregulation, as outlined above (Rushworth et al., 2012). This constitutive activation of NRF2 resulted in resistance to front-line chemotherapy agents in AML, most notably cytarabine and daunorubicin (Rushworth et al., 2011a, Rushworth et al., 2012).

1.5 micro RNAs (miRNAs)

1.5.1 miRNA biosynthesis and physiological role

miRNAs are small non-coding single-stranded RNA molecules that play a crucial role in epigenetic regulation by targeting and inactivating their corresponding mRNA sequences. The process of miRNA biogenesis begins with the transcription

of the primary miRNA transcript (pre-miRNA), this process occurs in the nucleus and is predominately carried out by RNA polymerase II but can also occur through RNA polymerase III (Lee et al., 2004, Borchert et al., 2006). The pre-miRNA generally contains the typical double stranded 33bp hairpin stem with a terminal loop, it is also flanked by a single stranded region both to the 5' and 3' of the stem (Winter et al., 2009). The pre-miRNA is cleaved by the Drosha/DGCR8 complex which leaves the precursor miRNA, this is a stem loop structure with a size of approximately 85 nucleotides (Han et al., 2006, Peng and Croce, 2016). Cytoplasmic translocation of the pre-miRNA is mediated by Ran/GTP and Exportin 5 (Yi et al., 2003) and once cytoplasmic the pre-miRNA are again processed by the RNAase III enzyme Dicer (in conjunction with the RNA binding protein TRBP) leaving 20-22 nucleotide mature miRNA and passenger strand in a duplex (Peng and Croce, 2016). After being unwound, the mature miRNA is loaded with Argonaute proteins and becomes incorporated into the RNA induced silencing complex (RISC). The RISC is guided to the complementary mRNA sequences (to that of the miRNA), where it binds and silences expression. The binding between the miRNA and mRNA is based on the 6-8 nucleotide "seed region" which binds to its complementary mRNA through Watson-Crick base pairing. This predominately results in a repression of protein translation and/or mRNA degradation (Peng and Croce, 2016, Winter et al., 2009).

miRNAs play a crucial role in modulating post-transcriptional expression from the earliest stages of development. Pluripotent embryonic stem (ES) cells have the ability to differentiate into any cells in the human body and are characterised by

high expression of transcription factors such as Nanog, Oct4, c-Myc and KLF4. Repression of these transcription factors results in differentiation of ES cells. ES cells have their own miRNA expression profiles and as these cells differentiate the mRNA profile changes (Houbaviy et al., 2003, Ivey et al., 2008). When Dicer (crucial for cleaving the pre-miRNA) was knocked-down in mice ES cells, they do not form teratomas with all three germ layers present (the "gold standard" requirement for determining pluripotency) and lacked several key differentiation markers (Kanellopoulou et al., 2005). Furthermore, the knockout was embryonically lethal (Bernstein et al., 2003).

1.5.2 miRNA in haematopoiesis

Dicer knockout in HSCs results in apoptotic cell death and this can be rescued by the ectopic overexpression of miR-125a (through targeting BAK), which returns the long term HSC population demonstrating its crucial role in haematopoiesis (Guo et al., 2010).

HSCs also have a unique miRNA profile, and several miRNA are upregulated in the long term HSC population (miR-125a, miR-125b, miR-129, miR-155, miR-130 and miR-181c). Ectopic overexpression of different miRNA skews differentiation towards certain haemopoietic lineages. miR-29a for example is upregulated in the long-term HSC population, and its expression decreases as the HSC cell becomes more committed (O'Connell et al., 2010). Ectopic expression results in a differentiation bias towards a myeloid lineage and miR-29a is upregulated in many patients with AML (Han et al., 2010). Similarly, when miR-125b is ectopically

expressed a myeloproliferative disorder is observed which can lead to AML (Bousquet et al., 2008a).

The miRNA expression profile differs between the myeloid and lymphoid progenitor stem cell. One study identified miR-130a, miR-31 and miR-203 as being upregulated in myeloid progenitors, while miR-126 and miR-23a are increased in the lymphoid progenitor (Petriv et al., 2010). Expression of miR-223 is low in HSCs but increases in expression during granulocytic differentiation and when its expression was repressed in murine models the granulocytes produced were defective (i.e. more sensitive to stimuli as well as terminal maturation) (Johnnidis et al., 2008).

In monocytes several miRNAs have been implicated in regulating differentiation into macrophages including miR-106a, miR-17 and miR-20a, which work through targeting M-CFR. These miRNAs also seem to be regulated by AML1 (which is upregulated during monocyte differentiation), as AML1 levels increase, these miRNAs decrease in expression (Fontana et al., 2007).

Once differentiated, macrophages can be classified into M1- or M2-type macrophages depending on several factors including their mechanism of activation, cytokine production and general function. miR-155 was shown to play a crucial role in regulating the two by targeting IL-13Rα1 (IL-13 being a key M2 cytokine) and inhibiting STAT6 phosphorylation (Martinez-Nunez et al., 2011). miR-155 is also important in dendritic cells as its deletion inhibits them from stimulating T-cells.

(Dunand-Sauthier et al., 2011). Dicer knockouts in B or T precursor cells results again in defects in cellular processes, leading to an inhibition in the precursor B cell differentiation and in T cells inhibits CD4 and CD8 T lymphocyte levels. In the case of $CD4^+$ cells this results in increased apoptosis (Koralov et al., 2008, Muljo et al., 2005). Overall miRNAs play a crucial role, transcriptionally regulating in both haematopoietic development and function. When dysregulated, these miRNAs can lead to a number of diseases and disorders including cancer.

1.5.3 miRNA dysregulation in cancer

miRNA expression profiling can be used to differentiate cancer types and can even be used to determine specific subtypes of cancers as well as their prognosis (Lu et al., 2005, Namkung et al., 2016). In pancreatic cancer, the expression of 19 miRNAs was sufficient to distinguish between high and mid/low risk prognosis (Namkung et al., 2016). In cancer, miRNAs can become dysregulated, acting either in an oncogenic manner (dubbed an OncomiR) or acting in a tumour-suppressor manner (dubbed a Tumour-Suppressor miR) (Fig 1.4).

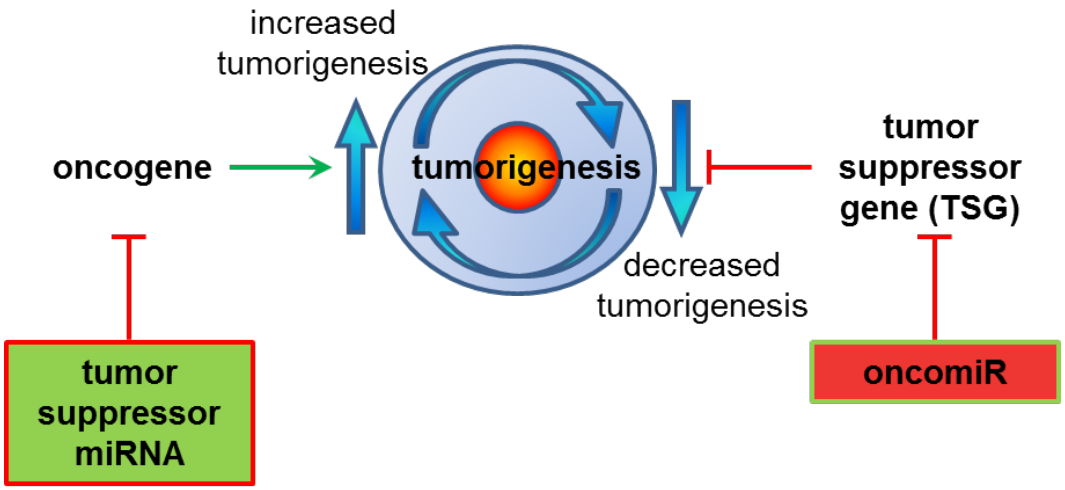

Figure 1.4: Dysregulation of cancer cells by miRNAs

miRNAs can act as tumour suppressors or an oncomiR. A tumour suppressor miRNA represses target oncogene expression decreasing tumorigenesis. An oncomiR represses target tumour suppressor genes, increasing tumorigenesis

miRNAs become dysregulated through three main mechanisms; amplification, deletion and through transcriptional regulation (Peng and Croce, 2016). The miR-143/145 cluster located on 5q33 can be deleted in lung cancer resulting in a decrease in miRNA expression (Peng and Croce, 2016). This miRNA cluster is also reduced in both breast and colon cancer (Calin and Croce, 2006). In CLL, the 13q deletion is responsible for approximately 55% of genomic aberrations and within this region lies the miR-15a/16-1miRNA cluster. The cluster acts as a tumour suppressor miR by targeting BCL2 and MCL1 (Döhner et al., 2000, Pekarsky and Croce, 2015).

miRNA expression can also be reduced through epigenetic modification. The tumour suppressor miR-127 is downregulated in breast cancer, primary prostate and bladder cancer and plays a key role by targeting BCL-6 (Chen et al., 2013, Saito et

al., 2006). miR-127 is located in the vicinity of several CpG islands and is epigenetically repressed in many cancer cells (Saito et al., 2006).

Amplification of miRNA can occur particularly through chromosomal translocations. 40% of Clear Cell Carcinoma (a subtype of Epithelial Ovarian Cancer) is characterised with an amplification of the 17q 23-25 region. miR-21 is located in an intron in the vicinity (17q23.2) and is upregulated in a range of cancers where it acts as an oncomiR by targeting PTEN expression. It is however unclear whether the amplification of the region is responsible for aberrant miR-21 expression as one study finding no correlation between the amplification and high miR-21 levels (Hirata et al., 2014).

miRNAs can also be regulated by transcription factors. For example, miR-34a is a tumour suppressor miR associated with apoptosis and directly regulated by p53 (which binds to the miR-34a promoter increasing its expression) (Raver-Shapira et al., 2007). miR-34a targets SIRT1 (which plays a key role in de-acetylating p53, thereby preventing p53 transcription), this results in an increase of acetylated p53 and thus an upregulation in the expression of p53 targets, including miR-34a creating a positive feedback loop (Luo et al., 2000, Yamakuchi and Lowenstein, 2009). Conversely, c-Myc represses the tumour suppressor miR-122 in hepatocellular carcinoma through binding to a non-canonical c-Myc site in the miR-122 promoter. miR-122 forms a negative feedback loop with c-Myc by targeting TFDP2 and E2F1 (E2F1 is a c-Myc activator with TFDP2 acting as a co-activator) (Wang et al., 2014a).

1.5.4 Oncogenic role of miRNA

When dysregulated in cancer miRNAs can affect a variety of processes including cell death, cell proliferation, angiogenesis, and metastasis (Peng and Croce, 2016). p53 is a key pro-apoptotic protein and, as previously discussed, can both regulate and be regulated by miR-34a (Yamakuchi and Lowenstein, 2009). p53 has also shown to positively regulate miR-192, miR-194 and miR-215 in multiple myeloma where they act as tumour suppressor miRs by negatively regulating Mdm2 expression (Pichiorri et al., 2010). Similarly, the tumour suppressor miR-122 represses expression of cyclin G1 (upregulated in hepatocellular carcinoma) which also plays a key role by repressing MDM2 resulting in increased sensitivity to doxorubicin (Fornari et al., 2009).

miR-221 and miR-222 have been characterised as both oncomiRs and tumour suppressors depending on the cancer type. In pancreatic cancer these miRNAs have been associated with an oncogenic role. Here one of their targets is the cyclin dependant kinase inhibitor (p27/Kip1), as well as capsase-10. Downregulation of p27/Kip1 is a known marker for an unfavourable prognosis. The upregulation of miR-221/222 was shown to increase proliferation in prostate cancer cells and repress sensitivity to TNFα (Galardi et al., 2007, Wang et al., 2015b). Conversely a study in lung cancer cells found another miRNA family (let-7) was downregulated compared to healthy patient samples. They also showed let-7 represses cell proliferation in both lung and liver cancer cell lines through the targeting of cell cycle targets including CDK6, cyclin D, Ras and CDC25a (thus inhibiting G1 to S-phase transition) (Johnson et al., 2007).

Another key characteristic of cancers is metastasis, this predominantly involves an epithelial-mesenchymal transition (EMT). miR-21 for example has shown to act as an oncomiR in several cancers including breast, colon and prostate cancer. In breast cancer high levels of miR-21 have been associated with poor prognosis and lymph node metastasis (Yan et al., 2008). Similarly it is associated with metastasis in colon cancer (Roldo et al., 2006). This may be because it targets tropomysin 1 (TPM1) and programmed cell death 4 (PDCD4) (Zhu et al., 2008). miR-155 has shown to act as an oncomiR in cancers such as hepatocellular carcinoma by promoting EMT. This is due to it targeting p85α (which represses the PI3K/AKT pathway)resulting in induction of SGK3 (Kong et al., 2016). SGK3 aids the phosphorylation of GSk3β, preventing it from degrading β-catenin. The stabilisation of β catenin is a key process in the Wnt pathway (whose activation is associated with EMT) (Kong et al., 2016).

Angiogenesis refers to the creation and development of new blood vessels from pre-existing vascular architecture, which supports the increasing growth of a tumour (Caporali and Emanueli, 2011). miRNAs can play a crucial role regulating this process, for example one study looked for miRNA that target VEGF. VEGF is a crucial factor in inducing both angiogenesis and vasculorigenesis. The study found several miRNA, including miR-16, miR-15b, miR-20a and b targeted and repressed VEGF levels (Hua et al., 2006). Furthermore these miRNA were repressed during hypoxic conditions (Hua et al., 2006). A subsequent study showed miR-20b also represses HIFα, thus creating a loop where miR-20b represses VEGFα and HIFα

expression, while HIFα represses miR-20b, this could possibly allow the tumours to adapt to different levels of oxygen (Lei et al., 2009). In breast cancer, miR-148a was shown to be downregulated, and when ectopically overexpressed can repress angiogenesis by targeting ERBB3 (a member of the EGFR family), VEGFα and HIF-1 (Yu et al., 2011, Mu et al., 2017).

1.5.5 NRF2 and miRNAs

Previous studies have shown NRF2 can be regulated and in turn regulate miRNA expression. For example, in Oestradiol induced breast cancer, miR-93 expression is increased and in turn targets NRF2. This results in a repression in apoptosis and an increase in oxidative stress mediated DNA damage (Singh et al., 2013b). In sickle cell anaemia, miR-144 was shown to target and reduce levels of NRF2, this results in a reduction of glutathione expression. The repression in glutathione levels can contribute to haemolysis (a crucial characteristic of sickle cell anaemia) (Sangokoya et al., 2010).

NRF2 can also regulate miRNAs, either through binding to the promoter of a miRNA or indirectly through the regulation of its target genes, this in part was shown by a ChIP-Seq experiment which identified NRF2 binding sites in the promoter of several miRNA in lymphoid cells (Chorley et al., 2012). A detailed review on these NRF2 regulated miRNA can be found here (Shah et al., 2013). NRF2 can indirectly regulate miR-1 and miR-206 through modulating HDAC4 (which translocates to the nucleus when reduced, this occurs with high levels of

NRF2 activation), resulting in increased expression of PPP genes (Singh et al., 2013a).

1.6 Gene Editing

1.6.1 Overview

Gene editing refers to the ability to make specific alterations of a targeted region of DNA. Prior to the era of targeted nucleases, several other methods were used for genetic manipulation. One such method is the Cre-Lox recombinase. The 38 kDa protein Causes (Cre) recombinase (derived from the P1 bacteriophage) plays a critical role in the recognition of LoxP sites, thereby mediating both inter/intra molecular recombination (Hamilton and Abremski, 1984). LoxP sites consist of two inverted 13 bp regions flanking an 8pb non-palandromic spacer region. Essentially, if both LoxP sites are orientated in the same direction, the flanked DNA will be excised. However, if the LoxP sites are in an opposing orientation (i.e. facing each other), the flanked DNA will be reversed (due to recombination). When the LoxP sites are on different chromosomes recombination is promoted between both sites (Medberry et al., 1995, Nagy, 2000).

Double-Strand Breaks can occur due to cellular processes (i.e. ROS as a by- product of metabolism) or through external sources (such as ionising radiation). During meiosis, double-strand breaks (DSB) occur to promote recombination by the enzyme Spo1 (Keeney et al., 1997). Two commonly used mechanisms to repair double-strand breaks are Non-Homologous End Joining (NHEJ) and Homologous Recombination (HR). During NHEJ, Ku70/80 responds to DSB by acting as a scaffold for other factors (Mari et al., 2006). This in turn activates DNA PKcs and Artemis, these two form a complex together. The PKcs/Artemis complex contains endonuclease activity allowing the removal of DNA overhangs (Lieber, 2010).

DNA polymerase μ and λ are recruited to fill in the overhang using dNTPs and rNTPs to polymerise the template (Davis and Chen, 2013, Nick McElhinny et al., 2005). λ has the ability to remove damaged DNA bases (Ramadan et al., 2004). The DNA ends are ligated together using DNA ligase IV (Davis and Chen, 2013). This process is error-prone and can lead to insertion or deletion mutations (INDELs) (Rodgers and McVey, 2016).

Homologous recombination is an accurate repair process as it uses the sister chromatid as a repair template (Rodgers and McVey, 2016). After a double strand break occurs, it is recognised by the MRN complex (Mre11 RAD50, and Nbs1) which contains exonuclease activity, thereby allowing the 5' end to be "nibbled"-back (leaving 3' overhangs). The exposed 3' strand then invades the complementary sister chromatid (which is used as a repair template), this process is mediated by RAD51, thereby creating a region of heteroduplex DNA (DNA containing both invading strand and the sister chromatid). The displaced and invading strand forms a displacement loop (D Loop). The invading strand is extended and can be resolved by two mechanisms, double strand break repair (DSBR), which can result in a crossover, or synthesis dependent strand annealing (SDSA). In gene-editing the process of homologous recombination can use a donor DNA template, (with homology to target sequence) to create a custom modification in the genome (Ran et al., 2013b).

1.6.2 Zinc Finger Nucleases

One of the first targeted nucleases were Zinc Finger-fused nucleases. Zinc Finger proteins (Cys2His2) are based on the IIIA transcription factor found in *Xenopus*. Zinc fingers are between 28-30 amino acids in a Beta-Beta-Sheet-Alpha Helix (BBA) configuration.

The alpha helix contains amino acids in contact with base pairs (typically three) in the major grooves of the DNA (Gaj et al., 2013). This ability allows Zinc Fingers to bind to most triplet bases in the genome. Zinc Finger proteins are fused with the FOK1 nuclease, thereby combining the DNA binding ability of the Zinc Finger with the nuclease activity of FOK1. Each Zinc Finger module will bind to a triplet code of DNA. Two Zinc Finger proteins (made up of approximately 3-6 modules) are designed to target opposite strands of DNA region of interest, binding in a "tail to tail" orientation with a 5-7 bp spacer region, which is used by FOK1 to dimerise (hence why the binding of both zinc finger proteins is necessary) and cleave, thereby creating a double strand break (Gaj et al., 2013).

1.6.3 TALENs

Transcription activator-like effector nuclease (TALENS) are an alternative nuclease used in gene editing. Derived from the proteobacteria *Xanthomonas* TALEs (transcription activator-like effectors). Similar to Zinc Fingers, TALEs are fused to FOK1. The TALEs are comprised of repeat arrays of 33-35 amino acids allowing specific base targeting. Binding is determined by the hypervariable region (amino acids 12 and 13) known as the repeat variable di residue (RVD). Amino acid 13 is crucial in recognising the base to bind to, while 12 is important in stabilising

the interaction (Deng et al., 2012). There are four commonly found hypervariable regions NN (guanine), NI (adenine), HD (cytosine), and NG (thymine) (Joung and Sander, 2013, Miller et al., 2011). Similar to the Zinc- Finger nucleases, TALEN arrays bind to opposing DNA strands (separated by a short spacer region generally between 12-21 bp). With the spacer region binding to adjacent DNA strands, FOK1 dimerises causing a DS break.

While both ZFN and TALENS are challenging to design and construct, TALEN synthesis is streamlined using "Golden Gate Cloning". This uses Type-IIS restriction enzymes, and plasmids that are configured to have non-compatible initial overhangs, but allow the next complementary construct to ligate . Each RVD is modularised allowing the TALEN constructs to be custom designed for the area of choice (Cermak et al., 2011).

The effectiveness of TALENs is also dependent on the location of the targeted genomic location. A major setback to TALEN use is their inability to bind to methylated genomic regions (in particular 5'methylated cytosine). One study using TALE to target Oct-4 showed a significant decrease in transcription activation post-methylation. Treatment with a DNA methyltransferase can successfully reverse this inactivation suggesting chemical treatment may be a viable solution (Bultmann et al., 2012). However treatment with methyltransferases can cause a myriad of secondary effects such as genomic instability and cytotoxicity (Palii et al., 2008), Valton et al instead show using the RVD N*, instead of the HD hypervariable region (the * referring to a missing residue at that location.) (Valton et al., 2012)

Due to the missing glycine, the TALE is able to bind to the methyl group in the 5mC, and therefore editing can reliably occur in cytosine methylated regions (Valton et al., 2012).

1.6.4 CRISPR-Cas9

Clustered Regulatory Interspaced Short Palindromic Repeats or CRISPR-Cas9 system has recently been identified as an alternative to ZFN or TALENS.

The CRISPR locus was originally identified in E.coli, where they play a crucial role as a reprogrammable adaptive immune response to protect these bacteria cells from viruses (Rath et al., 2015). Viral DNA is exposed to the Cas complex, where it is cleaved by Cas proteins and incorporated into as a sequence in a CRISPR array. These are transcribed and the pre-cRNA is processed into shorter, separate crRNA, complementary sequences on the invading viruses are recognised and targeted by Cas proteins (Rath et al., 2015, Koonin and Wolf, 2015).

There are two main classes of CRISPR-associated (Cas) proteins, Class 1 (which encompasses approximately 90% of Cas loci) and Class 2 (Makarova et al., 2015). Class 1 (encompassing type I, III and IV) Cas systems requires several Cas proteins to form an effector complex that can target either DNA or RNA (Makarova et al., 2015). In contrast Class 2 (encompassing type II, V and VI) only requires one Cas protein, thereby making them useful for gene editing. The most commonly used example of a Type-2 CRISPR system is Cas9, specifically that found in Streptococcus pyogenes (spCas9). Unlike the Class 1 systems, Cas9 alone can

process and cleave the DNA causing a double strand-break. Here the CRISPR-RNA (crRNA) hybridises with the trans-activating cDNA (which binds to the palindromic repeat on the crRNA), this in turn is processed by RNase III, allowing it to bind to Cas9. The Cas9-tracRNA (trans-activating crRNAs) complex will be directed to the region of DNA complementary to the corresponding crRNA sequence. Cas9 requires a consensus Protospacer Adjacent Motif (PAM) site 3' downstream of the crRNA sequence (in the case of spCas9 5'-NGG-3') in order to dock and bind that region of DNA. Assuming the crRNA sequence is complementary to the DNA sequence preceding the PAM site, Cas9 will cleave the DNA resulting in a double-strand break, which will be repaired by either NHEJ or HDR (Tsai and Joung, 2016). The recognition of the gRNA with its complementary DNA counterpart, along with the presence of a PAM motif, results in the unwinding of DNA strands, and forms an R-loop, thereby allowing the DNA strands to be exposed to cleavage by Cas9 (Jiang et al., 2016). The ability for Cas9 to cleave double-stranded DNA is due to the HNH (complementary) and RuvC (non-complimentary) nuclease domains. Cas9 undergoes a conformational change upon binding of the guide RNA to genomic DNA, resulting in both the HNH and RuvC domains cutting their respective DNA strand (Sternberg et al., 2015).

The realisation that the tracr- and CRISPR-RNA can be fused to create a single guide RNA (sgRNA) has meant that CRISPR-Cas9 has become the preferred tool for genome editing as it its easily "re-taskable". The sgRNA is the synthetic fusion of the tracrRNA and crRNA and acts to target Cas9 to precise genomic locations (as discussed below).

The sgRNA retains the ability to bind to Cas9 and cause a conformational change, as well as direct it to regions of DNA complementary to that of the gRNA (Cong et al., 2013, Jinek et al., 2012). A schematic of Cas9 binding to double stranded DNA, in the presence of an sgRNA guide and PAM site can be seen in Fig 1.5A, Interestingly, in mammalian cells RNAse III (required for the processing of the tracrRNA and maturation of the crRNA in the prokaryotic systems) is not required for successful editing. This suggests the RNAse/s present in mammalian cells are sufficient for processing and successful CRISPR editing (Cong et al., 2013). As discussed above a double strand break will be repaired by either NHEJ or HDR (Fig 1.5B). NHEJ generally results in an INDEL mutation in the vicinity of the double strand-break, and is a useful mechanism for creating "knock -out" cells. Unlike NHEJ, HDR (in conjunction with a DNA repair template) can be used to accurately edit the targeted locus allowing for specific targeted changes to be made to the genome (Ran et al., 2013b).

spCas9 is the most commonly used Cas9, with its NGG PAM site occurring approximately once every 8 bp (Graham and Root, 2015). While this is sufficient for experimental CRISPR knockout/knock-ins, it does pose a problem for those wishing to generate cells with a specific targeted mutation. The size of the Cas9 protein also makes it difficult to introduce into cells or incorporate into viral vectors, which is required for editing in hard to transfect cells (such as most AML cell lines). Recently there has been a push to identify additional Cas9 variants or orthologues. One example of this is SaCas9 (derived from *Staphylococcus aureus*) which is a

smaller variant the regular Cas9 being 3.2 kb in size and recognises a PAM site consisting of NGRRT or NGRRN. An initial *in vivo* study packaged SaCas9 into an AAV vector with guides targeting PCSK9, they showed 35-45% INDEL, and no detectable off-target effects. They also found SaCas9 requires a slightly larger guide sequence (20-23 bp) in comparison to that of SpCas9 (17-20bp) (Ran et al., 2015).

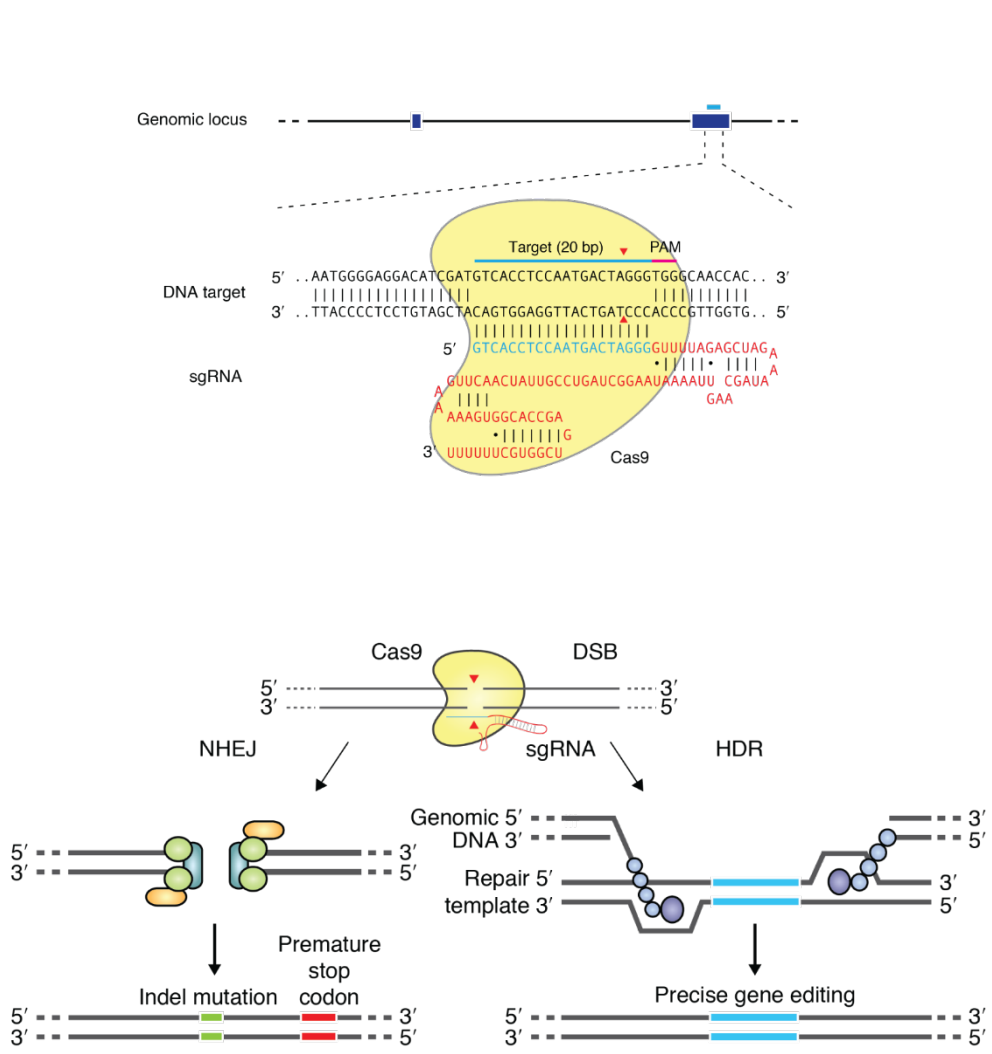

Figure 1.5: Overview of Gene editing with CRISPR-Cas9 A) Cas9 binds to DNA complementary of the sgRNA (in blue), upstream of the NGG PAM site. Triangles indicate location of double strand break. B) The double strand break can be resolved

by either NHEJ or HDR. NHEJ results in insertion or deletion mutations. HDR requires the presence of a repair template and results in precise editing based on the template sequence. Adapted with permission from Springer Nature: Nature Protocols (Ran et al., 2013b).

1.6.5 Other nucleases (i.e. CPF1) C2C2 FnCas9 Cas13 (RNA)

The class II type V Cas9 variant, Cpf1, was first derived from *Francisela novicida*, and is made up of nine spacer regions, separated by 36 nucleotide repeats (Schunder et al., 2013). Subsequently several additional CPF1 orthologs have been identified including AsCpf1 (from *Acidaminococcus* sp. BV3L6) and LbCpf1 (from *Lachnospiraceae* bacterium). Similar to Cas9, Cpf1 contains a RuvC nuclease domain, however it lacks the HnH domain. Instead RuvC is sufficient to cleave both DNA strands, as shown in mutations to the RuvC domain in fnCPF1, which ablate DNA cleavage. Contrasting mutations in Cas9 turn it into a "nickase", which is only able to cleave one strand of DNA. (Zetsche et al., 2015a). Cpf1 has shown to have similar editing efficiency to Cas9, and has a TTTN PAM site (Zetsche et al., 2015a). This T-rich PAM site allows the targeting of AT rich regions, which may lack the Cas9 NGG PAM site.

There are several advantages to CPF1 over Cas9, for example CPF1 does not require a tracerRNA sequence to aid crRNA processing, thereby reducing the size of the guide RNAs (to approximately 42 nucleotides) which provides an advantage when using viral vectors. CPF1 also cuts 18-23 nucleotides downstream of the PAM site, and leaves a staggered overhang (Zetsche et al., 2015a). This provides two

advantages, first since Cas9 cuts approximately 3 nucleotides 5' to the PAM site, NHEJ often results in the destruction of the PAM site, preventing further editing at this locus. This problem is not seen with Cpf1 due to it cutting away from the PAM site, meaning further editing could occur, this may be particularly useful when generating "knock-in" mutations. Secondly, the staggered ends themselves are thought to improve editing in quiescent cells (Zetsche et al., 2015a). The Cpf1 guides can also be multiplexed and expressed from a single CRISPR array. While multiple Cas9 guides can be expressed, additional regulatory sequences are required (for example separate promoters per guide), thus increasing the size of the construct. Cpf1 on the other hand, can express multiple guides from a single U6 Polymerase III promoter (Zetsche et al., 2017).

Cas13a (formally named C2C2), was initially identified as a Class 2-type VI Cas variant which targets single-stranded RNA (ssRNA). Cas13a contains a double Higher Eukaryotes and Prokaryotes Nucleotide binding (HEPN) site, which allows it to act as a ribonuclease (i.e. binds and cleaves RNA molecules) (Abudayyeh et al., 2016). Despite studies in bacteria, which show off-target cleavage by Cas13a due to its remaining activity post binding, studies in mammalian cells have shown no evidence for off target cleavage of RNA (Abudayyeh et al., 2017). Cas13a has shown to have similar targeting efficiency with significantly lower off-target effects in comparison to shRNA (Abudayyeh et al., 2017). Furthermore, similar to Cpf1, Cas13a orthologs (such as LwaCas13a) have also been shown to be able to be easily multiplexed (Abudayyeh et al., 2017).

1.6.6 Research and Therapeutic Potentials

Gene editing is revolutionising research and shows promise therapeutically. Mutations in CCR5, a crucial receptor for HIV entry, have shown to increase viability of CD4 T cells, and thus resistance to HIV. One study designed two Zinc finger arms to target CCR5 in CD4 T cells *in vitro*. The cells were expanded and a sample of patients suffering from HIV infections were treated with the modified $CD4^+$ T cells. The treatment succeeded in increasing resistance to the HIV virus (Tebas et al., 2014). Another study used Zinc finger proteins to accurately correct a mutation on IL2RG in HSCs. This mutation is responsible for X-linked severe combined immunodeficiency (SCID-XI), and the HSCs were derived from a patient suffering from the disease. The corrected HSCs were expanded allowing the potential for them to be re-transplanted into a patient (Genovese et al., 2014).

Mutations in cystic fibrosis transmembrane regulator (CTFR) inhibits the function of chloride transporters, thereby causing cystic fibrosis. One study wished to use CRISPR to target and repair the ΔF508 mutation. Skin cells were derived from a patient carrying this mutation and iPSC cells were derived. The ΔF508 mutation was targeted by CRISPR in iPSC cells using a donor vector containing a GFP-Puro-TK cassette flanked by piggyBac (a transposon) sites and the corrected CTFR sequence. The cassette was integrated into the iPSC cells, and positive clones were selected for by puromycin selection. The cassette was then excised using the piggyBac transposase, leaving behind the corrected ΔF508 mutations without any residual DNA. Cells without the donor cassette removed are selected against through ganciclovir treatment (which targets TK). The corrected iPSCs were then

differentiated into lung epithelial cells and normal function was shown. This study provides a viable methodology to treat patients suffering from cystic fibrosis by genetically editing the ΔF508 from their derived cells (Firth et al., 2015).

Despite the relative ease of designing and using CRISPR constructs, there still remains several issues which prevent it from being used in the clinic. Off- target effects remain the primary issue and this is less of a concern with TALENS and ZFN due to them acting as monomers (i.e. both arms are required for successful editing) (Nemudryi et al., 2014). Hence despite being less versatile, TALEN and Zinc Fingers are still predominately used in a therapeutic setting.

Improvements have been made to the CRISPR Cas9 system to address this problem including the use of a Cas9 nickase (nCas9). These Cas9 variants are designed with a mutation at either D10A in RuvC domain or H840A in HnH domain, thereby only having one active nuclease domain (Cong et al., 2013). The Cas9n are used in conjunction with sgRNA. Nickases like TALENS and Zinc-finger nucleases act as monomers and both must be introduced to get a DSB. On their own an individual nickases will cause a single-strand break, which is repaired by using base excision repair. The use of nCas9 results in a 50-1000 fold reduction in off-target effects (Ran et al., 2013a). Other methods include shortening the region of the sgRNA complementary to the target, the synthesis of catalytically inactive Cas9 (dCas9) (these can be fused to Fok1 to improve specificity) and the generation of high fidelity variants of Cas9 (Fu et al., 2014, Guilinger et al., 2014, Kleinstiver et al., 2016).

Recent work in ALL has shown the potential for TALEN gene-editing to be used to modify the patient's own cells. Such an approach has been seen to be effective in the treatment of chemotherapy-resistant B-ALL children, in at least two cases (11 and 18 month old children) where CAR-T cells with TALEN-modified target TCRαβ, were used as this novel treatment option (Qasim et al., 2017).

The success of the TALEN-based editing 'living drug' breakthrough has led those research teams to look towards CRISPR- or other targeted nuclease-based technologies to improve genetic modification of donor cells for common use in cancer patients worldwide.

dCas9 has no endonuclease activity, preventing editing from occurring, however it still retains its ability to bind to DNA which means it can be used to target specific DNA sequences. Studies have combined the dCas9 or Cas9 nickases with a cytidine deaminase resulting in "base-editors" which allow the conversion of cytosine to thymine without the need for a DSB (Komor et al., 2016). The first generation of base editing used the cytosine deaminase rAPOBEC1 and this was sufficient to convert C-T within 5 nucleotides of the targeted sequence (Komor et al., 2016). The third generation (BE3) used the "nickase" ability of Cas9 to create a single strand break on the non- targeted strand, the rationale being the previously edited strand will act as a template, therefore copying the mutation on the targeted strand (i.e. C-G will become T-A). While this increased efficiency, it also increased the number of off-target effects (Komor et al., 2016). Since then improvements have been made to increase both efficiency and specificity of the base editing enzymes. These improvements include the use of other deaminases (such as AID), allowing for a higher level of customisation (Nishida et al., 2016). One study mutated the cytidine

deaminase allowing for C-T targeting within 2bp (Kim et al., 2017). Recently, studies have created a DNA adenosine deaminase through directed evolution from a transfer RNA adenosine deaminase (as none existing naturally). Four adenine base editors (ABEs) were developed, allowing an A to G alteration to occur with the targeting to be between 4-9 nucleotides (Gaudelli et al., 2017). Both the Cas9-fused cytidine and adenosine deaminase provide a potential mechanism to correct specific targeted mutations in the genome with little off target effects.

In addition to its potential therapeutic use, CRISPR has tremendous potential in research and diagnostics. For example, the CRISPR system can be used to identify the role of genes or signalling pathways in a disease of interest. Combining large CRISPR libraries with Lentiviral delivery has revolutionised forward genetic screening.

One study used a CRISPR library with an enriched pool of 73,151 sgRNA (targeting 7114 genes) and a lentiviral vector for delivery. Cells were transduced with the library, before being treated with the selection control drug 6-thioguianine (6-TG). The treated cells were compared to those not exposed to 6-TG by high throughput sequencing. Here the sgRNA act as a barcode allowing identification (Wang et al., 2014b). This is an example of a negative screen. Alternatively, post treatment, the surviving cells can be analysed by sequencing, with those that have survived contain mutations that provide a survival advantage. This is known as a positive screen method. Overall these CRISPR libraries provide an invaluable tool

to better understand the role of different genes in diseases and thus find novel prognostic targets.

1.7 Aims

Our lab has previously shown the presence of constitutively-activated NRF2 in AML, with its activation being linked to chemotherapy-resistance. In this study we wished to fully elucidate the effect of NRF2 signalling in Acute Myeloid Leukaemia. Despite a fair understanding of its role in chemo-resistance, its impact in promoting oncogenesis is still to be determined. Recently, miRNAs have been shown to play a key role in regulating a myriad of cellular mechanisms, and of particular relevance in cancer. They can function in both an oncogenic and tumour suppressor capacity.

In this study, we will investigate:

a) The capacity of the transcription factor NRF2 to regulate miRNAs in AML,

b) Characterise the NRF2-regulated miRNAs and explain their function in AML.

c) The potential for gene-editing technology to further understand NRF2 signalling networks in AML.

Chapter 2

Materials and Methods

2.1 Materials

All reagents and consumables were purchased from either the Sigma Aldrich Chemical Company (Poole, Dorset) or as otherwise stated. Biological samples and cells are described below, where appropriate.

2.2 Cell Biology Protocols

2.2.1 Cell Culture

All cell lines were obtained from either ATCC (Virginia, USA), ECACC (Salisbury, UK) or DSMZ (Braunschweig, Germany). AML cell lines (THP-1, HL-60, U937, OCI-AML3 and MV4-11) and the CML cell line K652s were cultured in Roswell Park Memorial Institute (RPMI) 1640 containing 1% GlutaMax, 10% heat-inactivated Foetal Bovine Serum (FBS) and 10 U/ml Penicillin and Streptomycin. HEK-293 and HCT-116 were cultured in Dulbecco's Modified Eagle Medium (DMEM) containing high glucose (5000 mg/ml), L-glutamine, and HEPES. As before the media is supplemented with 10% FBS and 10 U/ml Penicillin and Streptomycin. Cell were grown at 37°C in a humidified atmosphere containing 5% CO_2 and were maintained by routine passage every 2-3 days.

2.2.2 Freezing cells

Cells were grown to confluency, before being centrifuged at 500 x g for 5 minutes. Cell pellets were resuspended in freezing media (FBS containing 10% DMSO) at a concentration of around 5 x 10^6 cells/ml. Cells were then frozen in 1.8 ml CryoTubes (Nunc) and placed into a 'Mr Frosty' Freezing Container (ThermoFisher Scientific, Loughborough UK) containing isopropanol. Storage of

this container at -80°C allows samples to freeze slowly (at 1°C per minute). Following overnight storage cells were transferred to liquid nitrogen for long-term storage. To resurrect cells, Cryotubes were placed in a 37°C water bath, once defrosted the cells were washed in medium (to remove residual DMSO), centrifuged then resuspended in either fresh RPMI or DMEM media before being placed into a T25 flask (Nunc, ThermoFisher Scientific).

2.2.3 Assessment of cell viability using Cell Titer Glo™

The Cell-Titer Glo Luminescent Cell Viability Assay (Promega) determines cell viability through determination of cellular ATP content. The assay was carried out according to the Manufacturer's instruction. Briefly, cells were transferred to an opaque 96 well plate and the Cell-Titer-Glo reagent added to 5 x 10^5 cells at a 1:1 ratio. Cells were incubated for 5 minutes on an orbital shaker after-which the plate was read on a plate reader with luminescence detection capabilities, FLUOstar Omega Microplate Reader (BMG Labtech, Germany). Luminometric results were normalised and expressed as a percentage compared to the control samples.

2.2.4 Annexin-V and Propidium Iodide staining

Apoptosis was assessed using Annexin-V/Propidium Iodide (AV/PI) staining. 1 x 10^6 cells were pelleted, washed in PBS and resuspended in Annexin buffer (10 mM HEPES, pH 7.5, 137 mM NaCl and 2.5 mM $CaCl_2$). Cells were then stained with an Annexin-V-FITC conjugate for 10 minutes in the dark. Propidium Iodide (0.1 mg/ml in PBS) was then added and cells stained for a further 5 minutes on ice before analysis by flow cytometry BD Acuri C6, or the Attune Acoustic Focusing

Cytometer (Applied Biosystems). Annexin-V detects apoptotic cells by binding to phosphatidylserine on the outer leaflet of the plasma membrane. PI detects late apoptosis with staining indicating both the plasma and nuclear membranes have both ruptured.

2.3 Primary cell culture

2.3.1 AML patient samples

Primary AML patient samples were collected from the Norfolk and Norwich University Hospital (NNUH) under ethical approval (LRECref07/HO310/146). Peripheral blood was carefully layered on Histopaque™ (Sigma) before spinning at 400 x g for 20 minutes (with both accelerator and break turned off). The "buffy-coast" layer containing AML blasts were extracted and washed in Hank's Balanced Salt Solution, before being frozen down or cultured in RPMI 1460 (with GlutaMax, supplemented with 10% FBS). Before use, the AML blast percentage was calculated using a flow cytometer measuring CD34+ cell surface marker. If the population contained less than 80% AML blasts, the sample was further purified with using the Miltenyi MACs system and CD34 Microbead selection kit (Miltenyi Biotec, Surrey UK).

2.4 Biochemical Techniques

2.4.1 Preparation of lysates for SDS-PAGE

Cell lysates were prepared either in SDS sample buffer (50 mM Tris/HCl pH 7.5, 4% SDS containing 0.01% Bromophenol Blue) or Triton lysis buffer (50 mM Tris/HCl pH 7.5, 150 mM NaCl, 10% Glycerol, 1% Triton X-100 (v/v)

supplemented with protease inhibitors aprotinin, pepstatin A, E64 and leupeptin (all at 1 µg/ml)). When using the SDS sample buffer, the cell pellet was mixed with the buffer prior to sonication (to aid cell lysis). When using the Triton lysis buffer cells were lysed on ice for 30 minutes following which lysates were cleared by centrifugation at 12,000 RPM for 20 minutes. Supernatant was collected and protein concentration was determined using the DC Protein Assay (BioRad).

2.4.2 SDS-PAGE

Protein lysates were reduced using β-mercaptoethanol, boiled (>95ºC), before being separated on a Tris-Glycine PAGE gel. The percentage of acrylamide in the gel used is based on the molecular weight of the protein being examined. The gel was electrophoresed at 100 V until the samples had passed the stacking gel following which the voltage was increased to 135 V.

	7%	**10%**	**15%**	**stacking**
ddH_2O	12.5 ml	10.1 ml	6 ml	12 ml
Acrylamide (30%)	6 ml	8.4 ml	12.5 ml	3 ml
5 x gel buffer	6.5 ml	6.5 ml	6.5 ml	5 ml
10% APS	150 µl	150 µl	150 µl	150 µl
TEMED	30 µl	30 µl	30 µl	30 µl

Table 2.1: SDS-PAGE gel recipes: Ammonium Persulphate (APS) and Tetramethylethylenediamine (TEMED) were added last to facilitate polymerisation. Resolving Gel Buffer: 1.5 M Tris/HCl (pH 8.8) containing 0.4% SDS. Stacking Buffer: 0.5M Tris/HCl (pH 6.8) containing 0.4% SDS.

2.4.3 Western Blotting

Following electrophoresis, proteins were transferred to Nitrocellulose at 100V for 60 minutes. Membranes were then washed in TBST (Tris-buffered Saline containing 0.1% Tween-20) and blocked with TBSMT (TBST containing 5% (w/v) Marvel^{TM}) for 30 minutes. After a brief wash with TBST membranes were incubated in primary antibody overnight at 4ºC (Table 4.2). The next day membranes were washed twice for 10 minutes then incubated with the appropriate HRP-conjugated secondary antibody (NEB, Nottingham UK for 1 h. The membrane was again washed twice in TBSMT followed by two further washes in TBST before being developed with enhanced chemiluminescence (ECL). Membranes were visualised either by X-ray film or by using the ChemiDoc Imaging System (BioRad).

Antibody	Source	Species	Dilution
NRF2 (c-20)	Santa Cruz	Rabbit	1:200
NRF2 (16396-1-AP)	Proteintech	Rabbit	1:1,000
NRF2 (ab62352)	Abcam	Rabbit (mAb)	1:2,000
NRF2 (D1Z9C)	CST	Rabbit (mAb)	1:100 (ChIP)
KEAP1 (10503-2 AP)	Proteintech	Rabbit	1:1,000
HO-1 (ab13248)	Abcam	Mouse (mAb)	1:1,000
NQO1 (ab80588)	Abcam	Rabbit	1:10,000
Cas9	CST	Mouse (mAb)	1:5,000
B-actin (A53-16)	Sigma	Mouse (mAb)	1:5,000
Anti-mouse HRP	CST	Horse	1:2,000
Anti-rabbit HRP	CST	Goat	1:2,000
Anti-goat HRP conjugate	Santa Cruz	Donkey	1:2,000

Table 2.2: Antibody sources and dilutions used for Western blotting or CHiP

CST- Cell Signaling Technology

2.4.4 Chromatin immunoprecipitation assay (CHiP)

CHiP was performed using the Simple CHiP Enzymatic Chromatin Immunoprecipitation (IP) kit according to the manufacturer's protocol (Cell Signaling Technology (CST)). Briefly, 4 x 10^6 cells were plated in 15 cm dishes and grown till ~90% confluent. Following treatments, cells were first fixed with Formaldehyde and then lysed using micrococcal nuclease. Chromatin was then sheered by probe sonication and the cross-linked DNA immunoprecipitated with an NRF2 antibody (CST). Positive (Histone H3) and negative (control IgG) were included as control IPs. IPs were performed overnight at 4°C using magnetic Protein-G Sepharose beads (CST). The next day following a washing step, the cross-linking was reversed and bound DNA purified. qPCR was then carried out to quantify the "input DNA" and results were presented relative to the control. The primers used for qPCR are shown in the table below (Table 2.3).

	5'-3' oligos for ChIP analysis	
miRNA	**Forward Primer**	**Reverse Primer**
miR-125B1 **ARE1**	ATGTTTCCAAACCAGGCTGA	CTAACACTGCAGGCTCACCA
miR-125B1 **ARE2**	CAGAGCCAGCTGTCAATGAA	CCAGAATGGGAGAAATGGAG
miR-125B1 **ARE3**	GTTGAGGCCTCTCCAGTGTC	GCCACCAAAAATGAAAGGAA
miR-29B1 **ARE4**	TCAAGGTGCAGGATCTTTCC	GTCTACCTTGGATGGCCTCA
miR-29B1 **ARE5**	CACATCTGGGCAACATCATC	CTCCAAGGGGGTGTCCTTAT

Table 2.3: qPCR primers used for ChIP analysis on the ARE sites

2.4.5 Luciferase Reporter Assay

A 2.6 kb fragment of the miR-125B1 promoter (which included the ARE3 site) was cloned into the pGL4.11 promoter/reporter plasmid. Briefly, we designed primers (Forward: 5′ AGAAAGGCCACCAAGATTCAC 3′ and Reverse: 5′ TGAGAGGAGCGCAACAATG 3′) and cloned a 2.6 kb fragment to create ppGL4.11 p125b. Both pGL4.11 (Empty vector) and the p125b were transfected into THP-1 cells using Diethylaminoethyl (DEAE) dextran. Cells were incubated for 48 hours then washed in PBS and lysed with passive lysis buffer (Promega). Lysates were treated with LARII and "Stop and Glo" reagent, before luminescence measurements for FireFly and Renilla were taken using the plate reader, FLUOstar Omega Microplate Reader (BMG Labtech, Germany).

2.4.6 Site Directed Mutagenesis

The ARE site in the miR-125b1 promoter was mutated using the QuikChangeXL kit (Agilent) according to the manufacturer's instructions. Briefly, a primer containing the required point mutations was designed, 5′-GCTGTGGCTGtTTTGTtATTCTCTTTGACTAG-3′, and used to mutate the wild-type pGL4.11 125b plasmid. The non-mutated plasmid was digested with Dpn1 before the mutated nicked plasmid was transformed into *E.coli* XL10 Gold cells and plated onto agar plates containing ampicillin (100 µg/ml). The following day colonies were picked and DNA was extracted using the miniprep protocol (see Section 2.5.5). The mutated plasmid was sequenced prior to transfection into THP-1 cells.

2.5 Molecular Biology Techniques

2.5.1 Plasmids

All plasmids were from AddGene (Boston, USA) or constructed and a kind gift from Dr Nicholas Harper (University of Liverpool, UK), unless otherwise indicated.

2.5.2 Bacterial strains and Culture conditions

NEB "Stable" *E.coli* (New England Biolabs) were used for all manipulation as its $RecA^-$ phenotype making it particularly suitable for cloning repeated sequences (such as the 3' and 5' Lentiviral repeats).

2.5.3 Preparation of Competent Cells

Competent cells were generated using the Mix and go *E.coli* transformation kit (Zymo Research, Cambridge Bioscience). A 5 ml culture of SOB medium (10% Tryptone, 5% Yeast Extract, 1 mM $MgCl_2$, 1 mM $MgSO_4$ and 0.5 mM KCl) was inoculated and grown overnight without antibiotics. The following day 500 µl of this culture was used to inoculate a 50 ml culture of SOB in a 500 ml Erlenmeyer Flask. Bacteria were grown at 26°C with shaking until the Optical Density (OD) 600 nm was between 0.4 and 0.6. The cells were rapidly chilled on ice and processed according to the Manufacturer's instructions. Competent *E.coli* were aliquoted and stored at-80°C until required.

2.5.4 Transformation of *E.coli*

Plasmid DNA was added to an aliquot of competent *E.coli* and incubated on ice for 20 minutes. Bacteria were then subjected to heat-shock (42°C, 1 minute) and allowed to recover on ice for 5 minutes. 350 µl of SOC medium (SOB including 1% glucose) was then added and the cells grown at 37°C with shaking for 1 hour. The transformation was then plated onto a Luria Broth (LB)-Agar plate containing the required antibiotic for colony selection. Plates were then incubated overnight at 37°C.

2.5.5 Isolation of Plasmid DNA

DNA Mini-prep was carried out using the Qia-Quick Mini-Prep kit (Qiagen) according to the manufacturer's instructions. Briefly, 4 ml of an overnight bacterial culture was pelleted and re-suspended in Buffer P1. Cells were then lysed in Buffer P2, and proteins and genomic DNA precipitated with Buffer N3. Precipitated was removed by centrifugation and the supernatants added to the provided spin columns. Columns were washed sequentially with Buffers PB and PE and finally plasmid DNA eluted with DNase/RNase-free water.

MAXI-Preps were performed using the PureLink HiPure Plasmid Filter Maxiprep Kit (Invitrogen, ThermoFisher Scientific) were used when larger amounts of plasmids were required. 1 ml of bacteria from a 5 ml starter culture was used to inoculate a 200 ml LB culture (containing the relevant antibiotic) and shaken overnight at 37°C. The culture was pelleted then resuspended in Buffer R3 (containing RNaseA), lysed with L7, and protein/genomic DNA precipitated with

Buffer N3. The precipitate was removed by filtration and supernatant applied to the provided maxiprep columns (which has been pre-equilibrated). The columns were washed in buffer W8, before DNA eluted using Buffer E4. DNA was precipitated using Isopropanol and at this stage was stored at -20ºC overnight (to aid precipitation). DNA was pelleted by centrifuging out the isopropanol solvent at 1,400 x g for one hour, then washed in 70% ethanol before being resuspended in DNA/RNase-free water.

2.5.6 DNA Electrophoresis - Agarose and PAGE

Agarose (Invitrogen, ThermoFisher Scientific) powder was weighed out and mixed with 1 x TAE buffer (40 mM TRIS, 20 mM acetic acid and 1 mM EDTA), the exact percentage of agarose used is dependent on the PCR product size tested. Ethidium bromide (EtBr) was added to the molten gel before pouring into the gel tank, EtBr is a DNA intercalator which fluoresces when exposed to UV light. The DNA was run at 135 V until sufficient separation of was seen. Separation was initially judged by the running of the loading dye, then visualised through exposure to UV light.

Polyacrylamide gel electrophoresis (PAGE) was carried out to determine the size of an DNA product with higher resolution than agarose gels. The PAGE gels were set up (10 ml 30% acrylamide, 12.5 ml 2 x TAE, 2.5 ml H_20, 150 µl APS, and 30 µl TEMED) and 1.5 mm 10-well combs were used. DNA samples were separated on the gel for 90 minutes at 135 V. After running, the gels were post-stained with EtBr and visualised through exposure to UV light.

2.5.7 Cloning of DNA

The DNA sequence for the region of interest was identified from the NCBI database (https://www.ncbi.nlm.nih.gov/nucleotide/) and flanking primers designed (Integrated DNA Technologies, Leuven Belgium). Primers were made up to the working concentration of 10 µM. The region of DNA was amplified by polymerase chain reaction technique.

2.5.8 Polymerase chain reaction (PCR)

PCR conditions varied depending on the experiment, with conditions such as annealing temperature changing based on predicted product size and/or the G:C ratio of the fragment being cloned. The two polymerases most commonly used in this thesis are OneTaq and Phusion High Fidelity Polymerase (NEB). Below (Table 2.4) is a typical PCR reaction with OneTaq and Phusion.

Polymerase	One Taq	Phusion
Buffer	5 µl (2x)	10 µl (5x)
H_2O	2 µl	31 µl
dNTPs (10 µM)	N/A	1 µl
Forward and Reverse primer mix (10 µM)	0.5 µl	5 µl
DNA (250 ng)	2 µl	2 µl
Polymerase	n/a	1 µl

Table 2.4: Example of typical PCR reaction with One Taq or Phusion

2.5.9 Restriction Digestion of Plasmid DNA

Restriction enzymes were used to digest either the Plasmid DNA or the amplified DNA fragment (dubbed the “insert”). Plasmid maps were used to determine restriction enzyme sites. 5 µg of plasmid was digested with the appropriate enzyme.

See Table 2.5 below for a typical digest. Control samples were also made up omitting the restriction enzyme (thus no DNA cleavage). Samples were incubated for four hours at 37°C, before being either gel extracted or PCR purified using the Wizard SV Gel and PCR Clean-up system (Promega).

Component	
Plasmid	5 µg
CutSmart (10 x)	8 µl
Restriction Enzyme	2 µl (per enzyme)
H_2O	up to 80 µl

Table 2.5: Example of a typical Restriction Digest

2.5.10 Ligation of digested DNA fragments

Ligation reactions were set up as detailed in the table below in 0.5ml microcentrifuge tubes as (Table 2.6). Reactions were incubated at 4°C overnight, before being used for transformation (see Section 2.5.4)

Component	Vector + Ligase	V:I (1:2)	V:I (1:4)
Vector	25 ng	25 ng	25 ng
Insert	n/a	100 ng	200 ng
T4 DNA ligase	0.5 µl	0.5 µl	0.5 µl
10x ligase buffer	1 µl	1 µl	1 µl
H_2O	to 10µl	to 10 µl	to 10 µl

Table 2.6: Example of a typical ligation reaction

Vector and Insert was incubated at a ratio of 1:2 and 1:4

2.5.11 Colony PCR

Colony PCR was used to check correct insertion of ligated DNA fragments. Bacterial colonies were picked and a PCR screen was carried out (following the OneTaq polymerase protocol and using a vector and insert-specific primer pair). Positive clones were marked and used to inoculate overnight cultures.

2.5.12 Transfection of DNA into Mammalian Cells

With adherent cells, DNA was transfected into cells using JetPei (Polyplus Transfection). Essentially 3.5×10^5 HEK-293 or 5×10^5 HCT-116 cells were seeded into a six-well plate. The following day following the manufacturer protocol, 100 µl of 150 mM NaCl was mixed with 4 µl of JetPei. Separately 100 µl of NaCl was mixed with between 1-2 µg of plasmid DNA. The NaCl/JetPei mix was then added to the NaCl/DNA, vortexed and incubated at room temperature for 20 minutes. DNA/JetPEI complexes were then added to the cells dropwise and cells incubated at 37°C for 72 hours. An eGFP control plasmid was included to ensure the transfection has been performed correctly.

2.5.13 Transfection of siRNA

Suspension cells were centrifuged, washed in serum-free RPMI media and resuspended at a density of 1×10^6 cells/ml. 100 µl of cells were then aliquoted into 1.5 ml microcentrifuge cells and siRNA was added (the concentration of siRNA was varied depending on the experiment). The cell/siRNA mix was transferred to an electroporation cuvette (Lonza) and electroporated (Program T-001) in an Amaxa Nucleofector II (Lonza, Cambridge U.K). Following electroporation, the

cells were mixed with complete RPMI media, seeded into a six-well plate and incubated for 72 hours before analysis.

2.5.14 Isolation of Genomic DNA

Cells were either scraped (adherent) or thoroughly mixed (suspension) and transferred to a 1.5 ml microcentrifuge tube. Cells were then pelleted and washed in PBS. Cells were then resuspended in 300 µl of "tail" lysis buffer (50 mM Tris/HCL (pH 7.5), 150 mM NaCl, 1 mM EDTA and 0.2% SDS) containing 20 mg/ml proteinase-K and 50 mg/ml RNaseA.

Cells were then left to digest overnight at 55°C. The following day the proteinase-K was inactivated at 95°C for 10 minutes then left on ice to cool for 5 minutes. DNA was precipitated by the addition of 400 µl of isopropanol and glycogen (1 µl of a 100 mg/ml stock). Tubes were incubated on ice for up to 30 minutes before the DNA pelleted by centrifugation at 20,000 x g for 1 h. The pellet was then washed in 70% ethanol before being resuspended in DNase/RNase-free water. Samples were then incubated at 55°C to allow for resuspension of DNA and quantified by nanodrop.

2.6 Real-time PCR

2.6.1 RNA extraction

RNA extraction was carried out using the RNeasy Mini Kit (Qiagen). We followed the manufacturer protocol but essentially cells were pelleted in 1.5 ml microcentrifuge tubes and washed in PBS. Cells were lysed in RLT buffer using the included QiaShredder columns. 70% ethanol was added to the lysate which was

then applied to an RNeasy Spin Column. The column was washed with the buffers RW1 and RPE. After which the empty spin column was centrifuged to remove any traces of ethanol before being eluted using 50 µl DNase/RNase-free water. The concentration of the extracted RNA was determined by nanodrop.

2.6.2 Reverse Transcription

RNA was converted to cDNA using the iSCRIPT Select cDNA Synthesis Kit (BioRad). The amount of RNA used in the reverse transcription (RT) was dependent on the individual experiment, but generally 100-200ng of DNA was added to each RT reaction. A typical RT reaction can be seen below (Table 2.7).

Component	
RNA (100-200 ng)	(100-200 ng)
5 x iScript select reaction mix	4 µl
Oligo dT	1 µl
Random Hexamers	1 µl
iSCRIPT Reverse Transcriptase	1 µl
DNase/RNase-free water	to 20 µl

Table 2.7: Example of a typical Reverse Transcription reaction using iSCRIPT

Once the above reaction was set up, the samples were incubated for 5 minutes at 25°C (required for Random Hexamer cDNA synthesis), 90 minutes at 42°C (required for Oligo-dT cDNA synthesis), and finally 5 minutes at 85°C (to inactivate the reverse transcriptase).

2.6.3 Quantitative real time-PCR (qPCR)

qPCR was used to quantify gene expression in cells. cDNA was diluted 1:10 to make up the working solution for qPCR. A typical qPCR reaction is shown below (Table 2.8).

Component	Amount
2 x SYBR Green Mix (Roche)	10 µl
Forward and Reverse primers (10 µM)	1 µl
DNase/RNase-free water	to 20 µl
cDNA	5 µl

Table 2.8: Example of a typical 20µl qPCR reaction using SYBR Green

Short Spanning Forward and Reverse primers were designed to flank the genomic regions of interest (see table 2.8). Reactions were set up as in the table above and plated into white-walled 96-well plates (Roche). Plates were then sealed with PCR sealing foil (Roche) and briefly spun. qPCR was performed using the LightCycler 480 (Roche) and used the SYBR Green qPCR protocol. SYBR Green binds to double stranded DNA and emits fluorescence at 520 nm. Therefore, as PCR cycles increase so does the fluorescence (known as acquisition).

The qPCR protocol was carried out as follows, initial denaturation (95°C, 2 minutes), then followed 45 amplification cycles of 95°C (denaturing), 60°C (annealing) and 72°C (extension) for 10 seconds each stage. Acquisition was taken at each cycle end. Once the PCR was complete, the samples were heated to 97°C, with the acquisition every 0.5°C, the aim here was to observe the temperature that the PCR products denature (known as the melt curve analysis). The presence of a single peak on the melt curve indicates a single PCR product has been amplified.

GAPDH was used as an internal control/housekeeping gene for mRNA and SnU6B as an internal control for miRNA. To generate the threshold cycle (CT) value, a threshold is set at the point where the PCR products have reached amplification. The cycle number where the individual PCR products have reached this threshold is noted as the CT value. The qPCR results are analysed using the change in CT (ΔCT) method. Essentially the CT values of the samples were subtracted from the CT values of GAPDH (ΔCT). ΔCT values were then subtracted from the experimental control and the fold change was calculated.

2.7 Lentivirus

2.7.1 Lentiviral vectors

A 3rd generation lentivirus system was used composing of pCMV-VSVG, pMDLG and pRSV-Rev as packaging plasmids. Gene of interest (GOI) plasmids included a modified LentiCRISPR plasmid containing an SFFV promoter, pLJM1 and pLeGO. All plasmids were obtained from AddGene, Boston USA.

2.7.2 Production of lentivirus

4 x 10^7 HEK-293T cells were plated into 10 cm^3 dishes and allowed to adhere overnight. Lentiviral plasmids were then transfected into the cells using JetPei. Essentially 200 µl of 50 mM NaCl and 20 µl of JetPei (1 mg/ml) were mixed. Separately 2 µg of each packaging vector (pRev, pMDLG, and pVSVG) and 4 µg of a GOI plasmid was diluted in another 200 µl of NaCl. The NaCl/JetPei mix was added to the NaCl/DNA followed by vigorous vortex mixing. Following incubation for 20 minutes at room temperature the DNA/PEI complex was added to the cells.

24 hours after transfection, the media was changed and 72 hours post-transfection, the media (containing the viral particles) was removed, cleared using a 0.45 µm filter and concentrated in an SW40Ti rotor at 110,000 x g for 2 hours. The supernatant was then removed and the pellet air dried then resuspended in 200 µl OptiMEM (ThermoFisher Scientific)

2.7.3 Transduction with Lentivirus

Six-well plates were set up with either adherent or suspension cells. Polybrene (4 µg/ml) and 20 µl of concentrated virus was added to each well and the cells were spinoculated for one hour at 400 x g, then incubated. 24 h after the transduction, medium was replaced and cells incubated for a further 48 h after which they were either genotyped or passaged on for selection.

2.8 miRNA techniques

2.8.1 miRNA extraction

miRNAs were extracted and purified using the miRvana miRNA isolation kit (miRvana, ThermoFisher Scientific). The kit uses a mixture of both solid phase and organic extraction. Briefly, the cells are lysed and RNA is purified using an acidic phenol/chloroform solution. Total RNA is precipitated using ethanol (1.25 × volumes) and purified on the supplied spin-columns. To extract enriched small RNA (siRNA or miRNA) ethanol was added (1/3rd volume) and spun through a second column. After-which the column is washed again with ethanol (2/3^{rds} volume), and washed several times using a wash buffer. Finally, small RNA are

eluted. Quantification of both total and small RNA was carried out using the nanodrop.

2.8.2 miRNA Reverse Transcription and real time PCR (miRNA)

Reverse transcription was carried out using the miScript kit (Qiagen). The proprietary 5× HighFlex buffer was used along with the extracted RNA and a reverse transcriptase. miRNA were first polyadenylated (using polyA polymerase) before being converted to cDNA using an oligo dT primer. RNA was incubated for 60 minutes at 37°C, before being heated up to 90°C for 5 minutes (to inactivate the reverse transcriptase). The RNA was diluted for use in qPCR.

2.8.3 miR-mimics and antagomir

miRNA levels were manipulated using miRNA mimics and antagomirs. In haematopoetic cells (such as THP-1s), the same protocol was followed as siRNA transfection as described in Section 2.5.13. The miRNA mimic/antagomir was transfected using the Amaxa nucleofector and cells incubated for 48-72 h before harvesting.

2.8.4 Designing miRNA primers

Real-time PCR primers for mature miRNA were designed using the mature sequence of miRNA with a universal reverse primer. The immature miRNA primers were designed using the DNA sequence for the miRNA being tested and sequences flanking the miRNA, these primer sequences were subjected to BLAST (NCBI) analysis (https://blast.ncbi.nlm.nih.gov/Blast.cgi) to ensure specificity.

2.9 qPCR primers

Gene	Forward Primer	Reverse Primer
GAPDH	GAPDH was purchased from Qiagen	
NRF2	TGATTCTGACTCCGGCATTT	GCCAAGTAGTGTGTCTCCATAG
HO-1	TCTTGGCTGGCTTCCTTAC	CATAGGCTCCTTCCTCCTTTC
NQO1	GGGATGAGACACCACTGTATTT	TCTCCTCATCCTGTACCTCTTT
KEAP1	TGTCCTCAATCGTCTCCTTTATG	CTCGTTCCTCTCTGGGTAGTA
MYBL2	CACACTGCCCAAGTCTCTATC	GAGCAAGCTGTTGTCTTCTTTG
AKT2	AGTGGCTCATGCCTGTAATC	GATGAAGGTCTCCCTATGATGC
CXXC6	CCAGAGATTCCTGGTGCTATTC	GGACAACACTCCCACTCATAC
Dnmt1	CGGCCTCATCGAGAAGAATATC	TGCCATTAACACCACCTTCA
TGFβ	CCTGCCTGTCTGCACTATTC	TGCCCAAGGTGCTCAATAAA
PIK3R1	GCTTTGCCGAGCCCTATAA	ACATTGAGGGAGTCGTTGTG
CDK4	ATGTGGAGTGTTGGCTGTATC	CAGCCCAATCAGGTCAAAGA
SP1	GATGTGTGGGCTTCTGAGTTTA	ACTGGCTGATGCTCCTTATTG
CBFB	CACAGGAACCAATCTGTCTCTC	CCTTGCCTGCTTCTCTTTCT
KLF13	GTCTGGGAGAGAGAGTGGAATA	TTTGGAACTGGGCATGAAGA
ABTB1	ACAGTGACGTGGTCTTTGTAG	ACACTCTTGCCCTTCCATTT
MAPK14	GGCCAAGGTGTTTCCATTTC	CCTTCCTTCTTGCTCCAGTT
STAT3	GAGAAGGACATCAGCGGTAAG	CAGTGGAGACACCAGGATATTG
CDK6	CTAGCAACCATCCCTCCATTAC	CTCAGAGCATTCTGAAGACAGTA
BCL2	GGCCAGGGTCAGAGTTAAATAG	GGAGGTTCTCAGATGTTCTTCTC
MCL1	GTGAAGATGGTAGGGTGGAAAG	TCGGCGGGTAATCAATTCTATG
BAK1	AGGGCTTAGGACTTGGTTTG	GGGATTCCTAGTGGTGTTGATAG

Table 2.9 Primer sequences used for qPCR. All primers (except GAPDH) were designed and purchased from Integrated DNA Technologies (www.idtdna.com).

2.9 Statistical analysis

Statistical analysis was carried out using Microsoft Excel or GraphPad Prism 6. Densitometry was performed using Image J. Further details on the precise statistical tests used can be found in the results section for the individual experiments

Chapter 3

Regulation of miRNAs by NRF2

3. 1 Introduction

Acute Myeloid Leukaemia (AML) is underpinned by a myriad of genetic abnormalities found predominantly in myeloid progenitor cells. Despite the heterogeneous nature of this disorder, the existence of shared signalling abnormalities between subtypes is highly likely (Kvinlaug et al., 2011).

Our lab has previously worked on the transcription factor NRF2, the master regulator of the antioxidant response mechanism which protects cells from reactive oxygen species through the regulation of cytoprotective genes such as HO-1, NQO1 and GCLM (Alam et al., 1999, Venugopal and Jaiswal, 1996, Zipper and Mulcahy, 2000). This mechanism can be hijacked in a range of malignancies (for example breast, lung and liver cancer), resulting in resistance to chemotherapy. (Solis et al., 2010, Yoo et al., 2012, Nioi and Nguyen, 2007). Furthermore, recent studies have demonstrated that aberrant NRF2 signalling often results in malignant cells becoming more tumorigenic, displaying increased proliferation and resistance to apoptosis (Zhang et al., 2010). This dysregulation in signalling predominately occurs due to somatic mutations in either NRF2 or its inhibitor KEAP1. These mutations usually prevent NRF2-KEAP1 binding allowing NRF2 to freely enter the nucleus and leads to cells having higher basal NRF2 activity (Sporn and Liby, 2012, Shah et al., 2013).

We have previously shown the presence of elevated levels of NRF2 in AML, and this results in resistance to commonly used chemotherapy agents in both AML cell lines and primary patient samples (Rushworth et al., 2011b). Interestingly in AML,

unlike solid tumours, we identified aberrant NRF2 signalling was not due to a mutations in NRF2 or KEAP1 but instead as a result of upstream signalling pathways, in particular NF-κB (Rushworth et al., 2012).

miRNAs are short non- coding RNA molecules (approximately 20-30 bp) that bind and repress their target mRNA. Under normal conditions they play a crucial role in regulating various cellular processes, under pathological conditions, however, tumour cells can hijack their normal physiological roles leading to the terms OncomiR and Tumour Suppressor miR (Hwang and Mendell, 2006). OncomiRs are miRNAs traditionally elevated in cancer cells that target and repress tumour suppressor genes. Tumour suppressor miRs target oncogenes and are traditionally downregulated in cancer cells (Svoronos et al., 2016). Studies looking at global miRNA expression have not only shown changes between different cancers, but significant variation can be detected within subsets of the same malignancy (Lu et al., 2005, Marcucci et al., 2009). Theoretically these miRNAs can regulate a plethora of mRNA targets, however the exact mRNA target being regulated, and the cellular effect of miRNA expression, often varies between different tissues.

3.1.1 Aims/Rational

Our previous work has indicated that NRF2 potentially plays a greater role in AML than just the regulation of antioxidant genes. We therefore wished to investigate the ability of NRF2 to regulate miRNA and further explore the significance of these NRF2 regulated miRNA in primary AML samples.

3.2 Results

3.2.1 miRNA array methodology

To establish whether NRF2 plays a role in modulating miRNA in AML we used miRNA expression profiling. A real-time PCR-based miRNA array consisting of primers to detect 93 miRNAs commonly dysregulated in cancer was designed (Fig 3.1A). miRNA profiling was then performed by qPCR on RNA extracted from THP-1 and HL60 AML cell lines following treatment with the NRF2 activator sulforaphane.

A

	1	2	3	4	5	6	7	8	9	10	11	12
A	let-7-family	miR-7	miR-92a	miR-93	miR-9	miR-101	miR-103	miR-106a	miR-106b	miR-107	miR-10b	miR-122
B	miR-125a-5p	miR-125b	miR-126	miR-128	miR-132	miR-133a	miR-134	miR-140	miR-141	miR-142-3p	miR-143	miR-145
C	miR-146a	miR-149	miR-150	miR-151	miR-154	miR-155	miR-15a	miR-15b	miR-16	miR-17*	miR-17	miR-181a
D	miR-181b	miR-181c	miR-181d	miR-183	miR-185	miR-186	miR-188-5p	miR-18a	miR-191	miR-192	miR-194	miR-195
E	miR-196a	miR-197	miR-30b	miR-19a+b	miR-95	miR-20a	miR-200a	miR-200b	miR-200c	miR-202	miR-205	miR-21
F	miR-210	miR-214	miR-372	miR-373	miR-219	miR-22	miR-221	miR-222	miR-223	miR-23a	miR-24	miR-25
G	miR-26a	miR-26b	miR-27a+b	miR-30c	miR-30a	miR-296	miR-34a	miR-34b	miR-144	mir-144*	miR-377	miR-217
H	miR-28	mir-301	miR-193b	miR-29a	miR-29b	miR-203	miR-1224	Sn25	U6 snRNA			

B

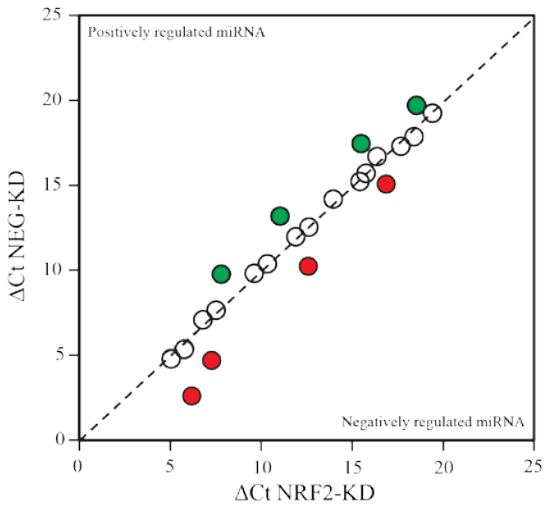

Figure 3.1: miRNA Screening Array Schematic A) Schematic of a miRNA array based on commercially available SA Bioscience array consisting of probes to detect 93 miRNA commonly dysregulated in cancers. B) Criteria for determining miRNA

regulation by NRF2. Change in CT values following NRF2 knockdown plotted against control cells miRNA showing either a 1.5-fold increase or 0.2-fold decrease were chosen

The CT values were plotted, and a standard curve was generated, this was used as a threshold determining which miRNA are positively or negatively regulated by NRF2 is shown in Fig 3.1B. The ΔCT values were plotted onto a scatter graph (after being subtracted from the internal control RNU6B). A trendline was plotted and any miRNA above the line was determined to have increased expression in response to elevated NRF2, miRNA below the line represent decreased expression. We were interested in any miRNAs which showed either a 1.5-fold increase or 0.2-fold decrease in CT values in response to both sulforaphane and the NRF2 lentiviral KD. Whilst these were arbitrary cut-off values, steps were taken to reduce false positives and negatives. Sulforaphane treatment was repeated in two AML cell lines, and these results were combined with that of the NRF2 KD. Only miRNAs which were consistently altered in all three conditions would be taken forward. Potential targets will be further confirmed by additional qPCR experiments

3.2.2 Effect of NRF2 activation on miRNA expression array

The effect of sulforaphane (5 μM) on the 93 cancer-related miRNAs in the array are shown in Fig 3.2. miRNAs were standardised against the control RNU6B (U6) with Sn25 also present as an additional control. For the purposes of this study we were interested in both miRNA that were positively and negatively regulated by increased levels of NRF2 in two AML cell lines, THP-1 and HL-60. In THP-1 cells

sulforaphane-induced miRNA included the let-7 family, miR-7, miR-92a, miR-103, miR-107, miR-125a/b, miR-15a, miR-21, miR-25, miR-132, miR-181d, miR-185, miR-191, miR-192, miR-196a, miR-197 and miR-200a. Those with decreasing expression included miR-29b, miR-140, miR-193b and miR-200c (Fig 3.2A). To demonstrate activation of NRF2 by sulforaphane in these cells we analysed the expression of two NRF2 targets, HO-1 and NQO1. As expected we saw over a 12-fold increase in HO-1 and over a 3-fold increase in NQO1 expression by sulforaphane indicating activation of NRF2 targeted gene products (Fig 3.2C). The increased expression of HO-1, compared to NQO1 in response to sulforaphane is in line with previous studies in our lab (Rushworth et al., 2008).

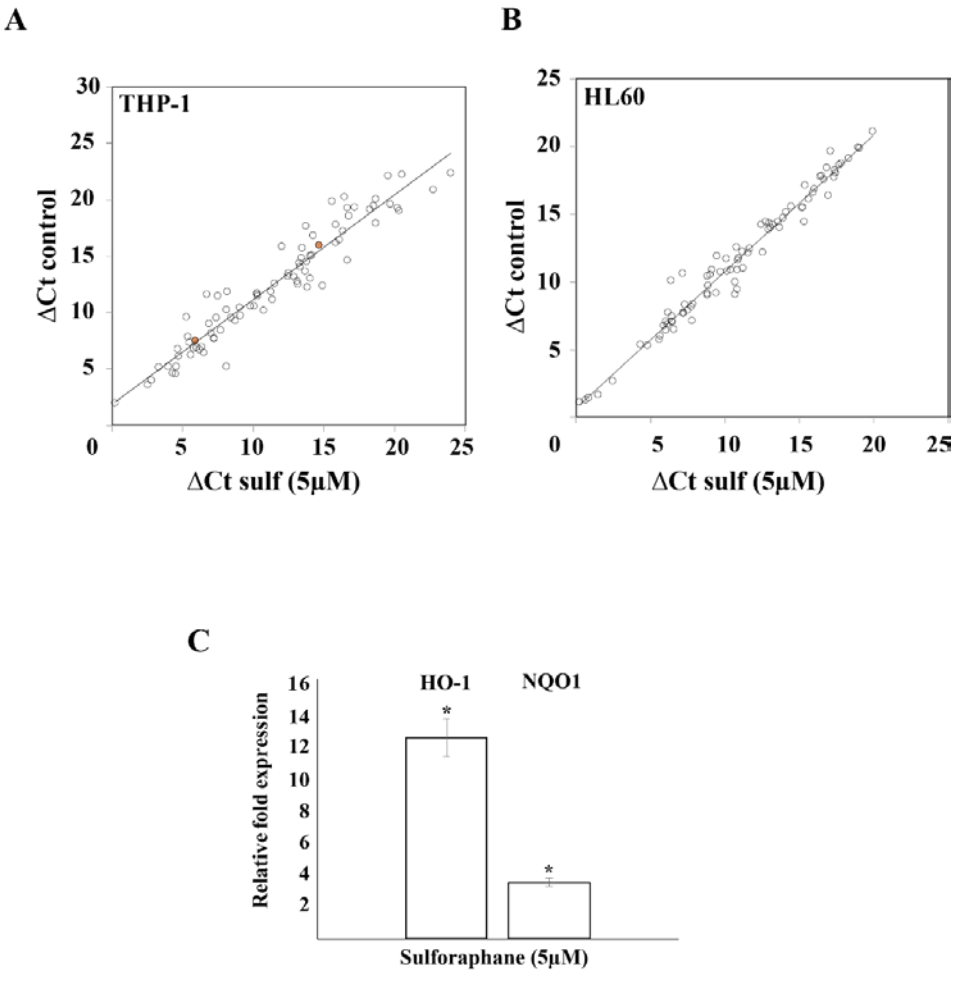

Figure 3.2: Effect of Sulforaphane on miRNA expression in AML cells Nrf2 was induced using 5uM Sulforaphane in THP-1 and HL-60 cells and miRNA signature was detected using qPCR. Delta CT values were calculated by subtracting the CT values for RNU6B from the CT values post Sulforaphane treatment, these are shown in the graphs. A) qPCR array in THP-1 cells. B) qPCR array in HL-60 cells. C) THP-1 cells treated with 5μM of Sulforaphane and mRNA levels of Nrf2 targets HO-1 and NQO1 were measured by qPCR. GAPDH was used as an internal control. Statistical significance was determined by a student's t-test (p=0.05).

In HL-60s there were increases in the let-7 family, miR-103, miR-125a, miR-125b, miR-15a, miR-17, miR-17*, miR-191, miR-195, miR-196a, miR-197, miR-95, miR-200b, miR-210, miR-222, miR-223, miR-23a, miR-24, miR-28, and miR-301. We saw a decrease in miR-21, miR-26b, miR-26b, miR-377, and miR-29b (Fig 3.2B).

Taken together this data shows that the NRF2 activator sulforaphane can induce or decrease several miRNA and NRF2 target genes in AML cell lines.

3.2.3 miRNA profile following NRF2 knockdown

While sulforaphane is known as a potent activator of NRF2, it also activates ERK, AKT and other pathways that interact with the NRF2 signalling pathway, such as NFκB (Negi et al., 2011). To demonstrate the miRNA changes observed were a direct result of its effects on NRF2 and not on any of these other pathways, we used a lentiviral NRF2 miRNA knockdown construct to reduce NRF2 levels. To

specifically increase NRF2 levels we used a viral construct that would knockdown the NRF2 inhibitor KEAP1. THP1 cells were transduced at 5 x 10^4 cells for 72 hours after which knockdown was confirmed by Western blot (Fig 3.3A). Basal levels of NRF2 were low in these cells however we saw a decrease in protein levels following NRF2 miRNA Lentiviral transduction. We saw an increase in NRF2 levels post transduction with an KEAP1 miRNA Lentivirus. As shown in Fig 3.3B, in response to the NRF2 KD, we identified 29 miRNA that showed greater than 0.2-fold decrease in expression, including miR-125b, miR-200b, miR-221, mR-15b, miR-30a, miR-200c, miR-18a, miR-27a/b, miR-195, miR-196, miR-141 and miR-34a. We also identified several miRNAs which increased in expression (by at least 1.5-fold) as a result of the NRF2 KD, these included miR-29a/b, miR-93, miR-132, miR-146a, miR-154, miR-181b, miR-200a, miR-202, and miR-372.

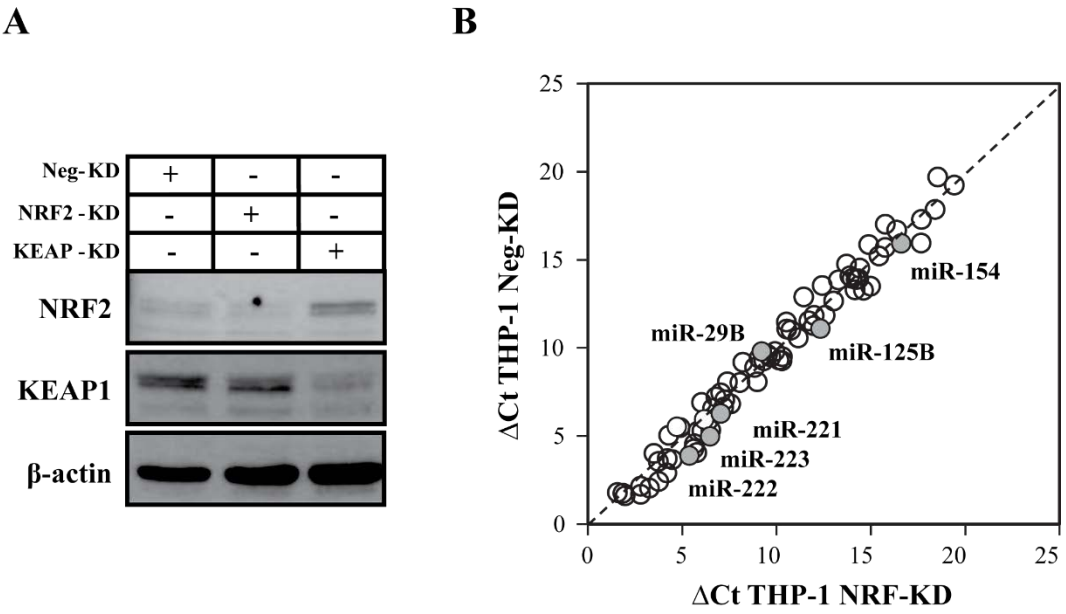

Figure 3.3: miRNA expression changes following NRF2 knockdown THP-1 cells were transduced with a lentivirus to knockdown NRF2. and miRNA signature detected using qPCR. A) NRF2, KEAP1 and β-actin protein levels were detected by Western Blot post NRF2 or KEAP1 lentiviral knockdown. B) qPCR miRNA

array carried out in THP-1 cells post NRF2 lentiviral knockdown. ΔCT values were plotted on a scatter graph and calculated by subtracting the control miRNA RNU6B from the CT value.

Overall, this data provides a more specific assessment of the miRNAs modulated by NRF2 in the AML cell line THP-1. Taken together with the sulforaphane data, there does seem to be a change in the expression of a subset of miRNA in response to NRF2 modulation.

3.2.4 Analysis of miRNA array data: identification of NRF2-regulated miRNAs

To identify just the NRF2-regulated miRNAs, we combined the results of miRNA profiling obtained following sulforaphane treatment and NRF2 KD (Fig 3.3). We were particularly interested in miRNA which showed a 0.2-fold decrease or a 1.5-fold increase in NRF2 expression. We also ensured the miRNAs chosen were responding to NRF2 modulation, ie higher expression with increased NRF2 and lower expression with the NRF2 KD or vice versa. We also took into consideration the individual CT values and melt curves from the qPCR. SYBR Green can only bind to double stranded DNA, thus its fluorescence increases through successive PCR cycles. As the amplicon is heated to 95°C, the DNA denatures (the exact temperature depending on the constituent nucleotides) creating a decrease in fluorescence. Generally, if a single PCR amplicon is present, then a single denaturing peak will be observed. We identified several miRNAs that met our criteria including miR-125a, miR-125b, miR-221, miR-222, miR-223, miR-29b,

miR-154, miR-15a, miR-17, miR-191, miR-195, miR-196, miR-197, miR-200b, miR-210, let-7-a1, and miR-103.

3.2.5 Identification of NRF2-regulated miRNA promoters using bioinformatics

Having identified a correlation between NRF2 and specific miRNAs, we now wished to investigate whether NRF2 was directly regulating these miRNA through ARE elements within the miRNA promoter regions. We used public databases such as NCBI to identify nucleotide sequences 5000 bp upstream and downstream from the miRNA start sequence. While we were primarily interested in putative binding sites in the 5' promoter regions near the miRNA start sequence, we were also aware that in certain circumstances transcription factors are known to regulate mRNA/miRNA at a large distance from the consensual promoter site (known as distal regulatory regulation) (Maston et al., 2006). A transcription factor binding programme-P-match (http://gene-regulation.com/cgi-bin/pub/programs/pmatch/bin/p-match.cgi), was used to identify consensual ARE motifs. P-match uses the Transfec database (in particular its weight matrix) as well as pattern recognition (Chekmenev et al., 2005).

Consensus ARE sites were identified with a 95% match. These sites were also compared against the ENCODE database (https://genome.ucsc.edu/encode/) in particular, transcription factor binding "hotspots" were focused on, as well as typical Pol2 sites within the vicinity of these miRNAs. We were also interested in

areas with high methylation. A schematic of the putative ARE binding sites is shown in Fig 3.4.

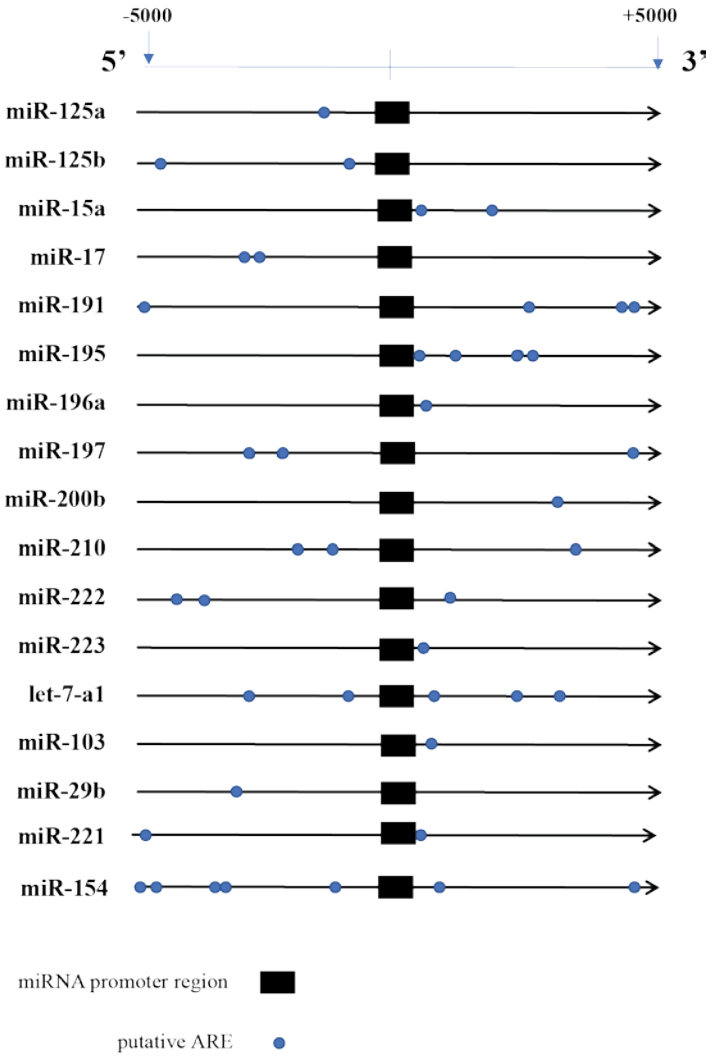

Figure 3.4: Schematic of miRNA promoter regions with putative NRF2 ARE binding sites. Putative ARE sites were identified using the transcription factor binding program p-match. Binding sites identified 5000bp 5' and 3' to the miRNA start sites are indicated.

3.2.6 Validation of putative NRF2-regulated miRNA

We next wished to further validate several of the miRNAs identified using the array. As discussed above sulforaphane is not a specific NRF2 activator, therefore, in order to specifically implicate NRF2 in the regulation of these miRNAs we also created a lentiviral-mediated KD construct for the NRF2 inhibitor KEAP1. Reduction of KEAP-1 leads to the direct upregulation of NRF2 in cells (Zhang and Hannink, 2003).

THP-1 cells transduced with the KEAP-1 KD showed significant increases in miR-125b, miR-221, miR-222 and miR-223 levels and this was accompanied by a decrease in miR-29b expression. As before, reduction in NRF2 resulted in a significant decrease in miR-125b and an increase in miR-29b expression (Fig 3.5). Although there was a slight decrease in expression of other miRNAs, such as in miR-221 and miR-222, but this was not found to be statistically significant.

mRNA expression for KEAP1, NRF2 and its target gene HO-1 were used as a negative and positive control respectively. As expected NRF2 KD in THP-1 cells resulted in a significant decrease in NRF2 and HO-1 expression but no change in KEAP-1 mRNA. Whereas the KEAP-1 KD resulted in a significant increase in HO-1 expression (around 3-fold) and as expected a decrease in KEAP-1 expression.

The KEAP1 KD showed a decrease in KEAP1 protein levels, and a slight increase (0.6 fold) of NRF2 levels. This indicated that while a KEAP1 KD does not increase NRF2 on a mRNA level, it does seem to increase the amount of NRF2 protein possibly by preventing its Cul3 mediated ubiquitination and degradation and

increasing the ability for NRF2 to translocate to the nucleus and regulate its target genes, as demonstrated by the strong increase in HO-1 at both the mRNA and protein levels.

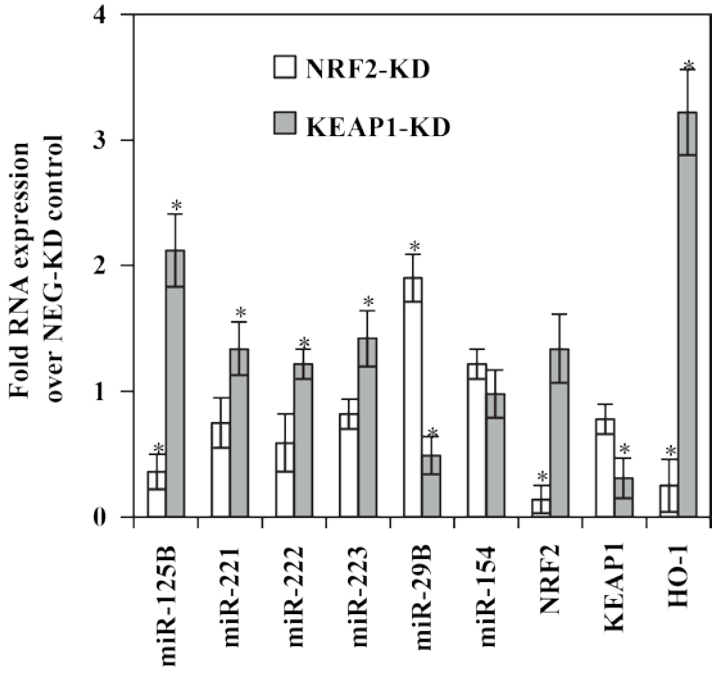

Figure 3.5: Confirmation of NRF2 dependent miRNA regulation miRNAs were measured by qPCR (miR-125b, miR-221, miR-222, miR-223, miR-29b, miR-154) along with HO-1, NRF2 and KEAP1. Student's t-test carried out to determine statistical significance, * indicates $P < 0.05$ (n=3).

3.2.7 Correlation between NRF2 and expression levels of miRs-125b and -29b in AML patient samples

The qPCR data identified a correlation between NRF2 expression and levels of miR-125b and miR-29b (Fig 3.5). So far, all experiments were carried out in AML cell lines, while these provide a useful model to characterise the disease they have inherent limitations. For one, the cell lines are only representative of the specific AML subsets they represent. THP-1s for example are acute monocytic leukaemia

(FAB M5), while HL-60 are acute promyelocytic leukaemia (FAB M2/3). AML is a heterogeneous disorder made up of a range of various cytogenetic abnormalities, each with different prognostic outlook and variable sensitivity to chemotherapy agents.

We therefore wished to look at the regulation of these miRNAs in primary AML blasts extracted from the peripheral blood of AML patients. AML patient samples were characterised, by World Health Organisation (WHO) classification and cytogenetics (Table 3.1). The percentage of AML blasts present in each sample was also calculated. Samples used were from patients with a spectrum of cytogenetic and genetic disorders. CD34+ cells (n=8) were isolated from normal healthy volunteers to act as controls.

Number	Age	Gender	WHO diagnosis	Cytogenetics	% Blasts	Fold NRF2 mRNA over CD34+	Fold RNA over CD34+	
							miR-125B1	miR-29B1
AML#1	49	M	AML with maturation	Normal	80	3.35	6.57	0.04
AML#2	39	M	AML with maturation	Normal	65*	6.89	12.33	0.11
AML#3	64	M	AML with RUNX1-RUNX1T1	t(8;21)	85	1.26	1.09	1.01
AML#4	92	F	AML with myelodysplasia related changes	Not available	70*	1.23	1.70	0.20
AML#5	82	F	AML with MDSrelated changes	Deletion 13	85	3.39	3.20	0.07
AML#6	46	F	AML with maturation	+4,+8, t(9;22)	70*	4.99	12.51	0.10
AML#7	66	F	AML with maturation	t(2;12)	65*	1.23	5.22	0.27
AML#8	78	M	AML with MDS related changes	Not available	85	4.19	9.85	0.01
AML#9	57	M	AML without maturation	Not available	95	4.35	4.59	0.09
AML#10	27	M	AML with RUNX1-RUNX1T1	t(8;21)	60*	4.99	10.93	0.08
AML#11	25	M	AML with maturation	Normal	50*	4.81	6.63	0.37
AML#12	61	M	Relapsed AML without maturation	Not available	95	1.96	1.07	0.71
AML#13	28	F	Acute Monoblastic and Monocytic Leukaemia	Normal	90	4.68	6.52	0.33
AML#14	31	F	AML without maturation	Trisomy 8	75*	2.73	6.37	0.03
AML#15	84	M	Acute meyloid leukaemia, NOS	Not available	70*	3.99	2.43	0.24
AML#16	53	M	AML with t(6;9)(p23;q34);*DEK-NUP214*	t(6;9)	65*	3.25	9.13	0.24
AML#17	51	F	AML with maturation	Normal	40*	4.54	3.45	0.02
AML#18	47	M	Acute myeloid leukaemia without maturation	Not available	90	4.20	2.07	1.33
AML#19	77	F	AML with maturation	Normal	70*	2.78	7.70	0.21
AML#20	62	M	AML with maturation	Complex	55*	2.96	2.67	0.59
AML#21	70	M	AML with minimal differentiation	Normal	95	2.01	1.98	0.64
AML#22	65	F	AML with maturation	Normal	40*	1.44	2.75	0.24
AML#23	77	M	Therapy related AML	Complex	70*	3.24	3.10	0.24
AML#24	40	F	AML with minimal differentiation	Normal	90	1.77	3.23	1.09
AML#25	70	M	AML without maturation	Complex	95	3.18	6.54	0.42
AML#26	91	F	AML NOS	Not available	75*	1.08	1.63	0.97
AML#27	59	F	AML with t(8;21)(q22;q22); RUNX1-RUNX1T1	t(8;21)	85	1.17	1.44	0.53

Table 3.1: Characterisation of the 27 primary AML samples used in this study

WHO and cytogenetics have been characterised, percentage of AML BLASTS were determined through Flow Cytometry. NRF2, miR-125b1 and miR-29b1 expression was determined by qPCR (relative to that in CD34+ cells).

We first aimed to identify basal NRF2, miR-125b and miR-29b expression in AML blasts compared to the normal CD34+ cells. As previously shown in the AML cell lines, there is a significant increase in NRF2 mRNA and miR-125b expression, and a significant decrease in miR-29b in the AML blasts (Fig 3.6). We then compared the expression of total miR-125b or miR-29b levels with that of miR-125b1 or miR-29b1 in primary AML Blasts. We found a similar expression in these miRNA paralogs in comparison to the total levels, perhaps indicating they are the subset partly responsible for the aberrant expression of these miRNA in AML (Fig 3.6).

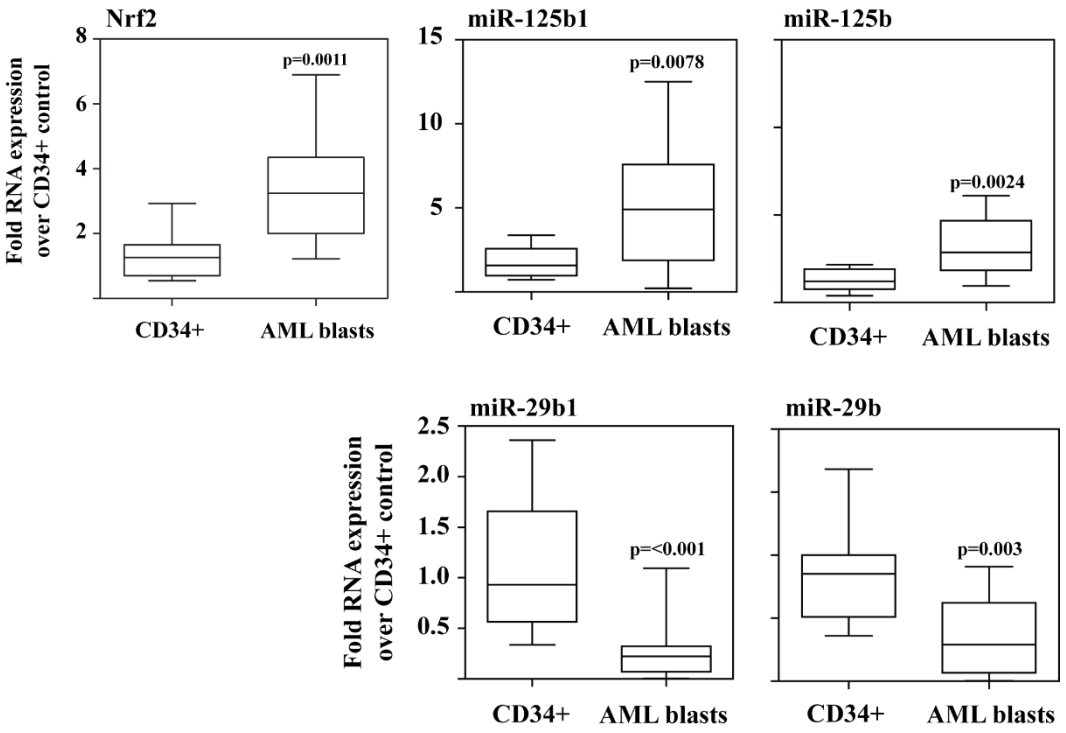

Figure 3.6: Expression of miRNA in AML blasts compared to normal CD34+ cells RNA was extracted from AML patient blasts and CD34+ cells. Using qPCR NRF2 and total miR-125b/miR-125b1 and miR-29b/miR-29b1 levels were measured.

Using Pearson correlation analysis, a significant positive correlation was seen between NRF2 mRNA and miR-125b expression and a negative correlation between NRF2 mRNA and mir-29b in the AML blasts (Fig 3.7A). Taken together these results confirm the results seen in the AML cell lines, suggesting that NRF2 regulates miR-125b and miR-29b, possibly through binding to an ARE site in their respective promoter regions.

To modulate NRF2 levels in the patient samples we transfected both a scrambled, and NRF2 targeting siRNA (Fig 3.7B). We found in general AML samples with a higher transfection efficiency (i.e. lower levels of NRF2), for example AML #25, also had lower levels of miR-125b1 and higher levels of miR-29b1. Likewise, AML samples with a lower transfection efficiency, such as AML #4 showed no change in miR-125b or 29b levels compared to cells treated with the control scrambled siRNA.

A

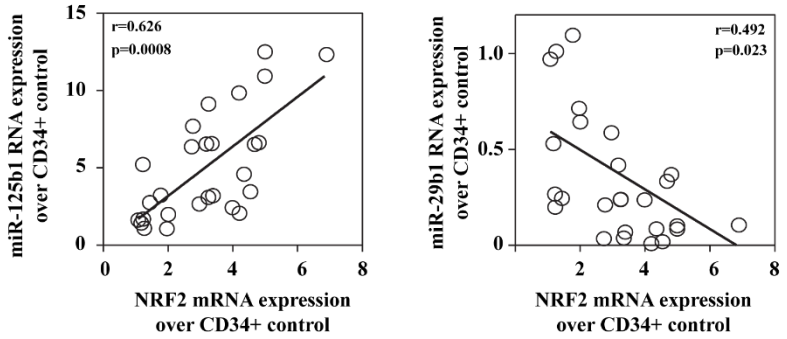

B

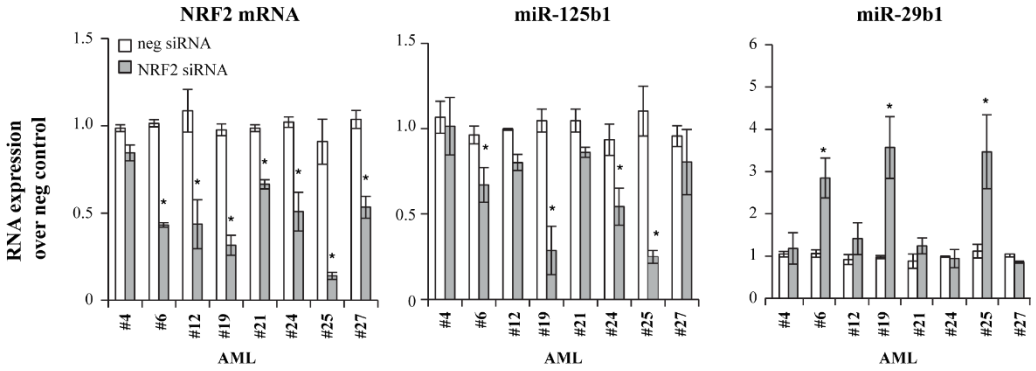

Figure 3.7: miR-125b and miR-29b in primary AML NRF2 levels were measured by qPCR in primary AML blasts (n=18) and CD34+ cells (n=8) from healthy donors. A) Pearson's correlation between NRF2 and miR-29b1/miR-125b1 B) qPCR on mRNA extracted from primary AML blasts transfected with NRF2 siRNA.

3.3 Conclusions and Discussion

In this chapter, we aimed to show whether NRF2 could modulate miRNA expression in AML. We analysed 93 miRNA that had previously been associated with malignancies in AML cell lines and modulated NRF2 expression using the NRF2 activator sulforaphane or an NRF2 miRNA lentiviral knockdown in THP-1 and HL60s. We identified several miRNAs (miR-125b, miR-29b, miR-221, miR-222, miR-223 and miR-154) from the array that showed either a positive or negative correlation with NRF2 levels. Further, both lentiviral KEAP1 and NRF2 KD identified miR-125b and miR-29b as being positively and negatively regulated by NRF2.

In primary AML cells, higher levels of NRF2 was identified in the AML blasts compared to the CD34+ cells. We also found a positive correlation between NRF2 and miR-125b, and a negative correlation between NRF2 and miR-29b. To show NRF2 affects miR-29b and miR-125b levels, we modulated NRF2 levels in the AML blasts using either a control or NRF2 siRNA. Here we saw a trend between AML samples successfully transfected with NRF2 siRNA, and levels of miR-125b or miR-29b. Finally, we found the miRNA paralogs (miRNA sequence with the same core "seed" region but resides on another chromosome) miR-125b1 and miR-29b1 showed similar expression to that of miR-125b or miR-29b suggesting they may be the subset dysregulated in AML.

This study demonstrated that both AML cell lines and patient samples have high levels of NRF2 and miR-125b and low levels of miR-29b. With regards to the high

mRNA levels of NRF2 in the primary AML blasts (compared to the CD34+ cells), it must be remembered the patients these samples are derived from are likely undergoing chemotherapy treatment, which may explain the high NRF2 levels. However our lab has previously shown that NRF2 is constitutively active in a high proportion of AML samples than control CD34+ cells (Rushworth et al., 2012).

Both miR-125b and miR-29b have been implicated in a range of cancers including AML. miR-125b is a known oncogene in glioblastoma, colorectal cancers, and non-small cell lung cancer (Wu et al., 2013, Nishida et al., 2011, Yuxia et al., 2012). In haematological malignancies, it is particular associated with the t(2;11)(p21;q23) translocation which can lead to between a 6–90 fold upregulation found in a subset of patients with MDS or AML (Bousquet et al., 2008b). miR-125b is also important in the AML subtype acute promyelocytic leukaemia (FAB M3) where its upregulation blocks differentiation and reduces its sensitivity to apoptotic signalling (Bousquet et al., 2012).

The negatively regulated miR-29b is a known tumour suppressor in several cancers, including leukaemias. It was previously shown to be downregulated in several AML cell lines and patient samples and when expression was increased, the cells became more sensitive to apoptosis and AML mouse xenografts showed a reduction in their tumours (Garzon et al., 2009a). miR-29b can also regulate promoter methylation through the regulation of DNMTs. In AML for example miR-29b can regulate and repress DNMT1, DNMT3A and DNMT3B, resulting in the expression of several tumour suppressor genes (Garzon et al., 2009b).

The role between NRF2 and miR-125b/ miR-29b in AML cells requires further investigation. So far, we have shown a correlation between NRF2 and both miRNA, however we have not demonstrated whether NRF2 directly regulated these miRNA by binding to an ARE site in their promoters, or if its indirect through NRF2 target genes. To do this we need to further characterise the ARE binding sites in the vicinity of both miRNA, and test the ability of NRF2 to bind to these sites using a chromatin immunoprecipitation assay (ChIP), DNA-binding assays or a promoter-reporter assays.

miRNA can exist as paralogs, i.e. multiple copies of the same miRNA in the genome. These paralogs contain the same functional seed region but exist in different genomic locations indicating that these paralogs can be individually regulated. Initial work in this study (Fig 3.7) has demonstrated total levels of miR-125b and miR-29b is similar to that of the paralogs miR-125b1 and 29b1. Further studies need to be undertaken to understand whether NRF2 can modulate the expression of the paralogs miR-125b1 / miR-29b1, or if another paralog is responsible (i.e. miR-125b2 or miR-29b2). We also need to elucidate the function of miR-125b and miR-29b in AML and their downstream targets.

As mentioned above miR-125b and miR-29b has previously been characterised as a oncomiR/ tumour suppressor miR respectively. We would therefore like to characterise the miRNA targets genes important in AML and elucidate if NRF2 can indirectly regulate these targets.

Chapter 4

Regulation of miR-125b and miR-29b by NRF2

4.1 Introduction

miR-125b is a member of the miR-125 miRNA family and has been associated with a wide range of pathologies (Sun et al., 2013). As with other miRNAs, when dysregulated miR-125b can act as an oncomiR or tumour suppressor miR by repressing the expression of tumour suppressor or oncogene mRNA targets respectively. For example, in hepatocellular carcinoma miR-125b is downregulated and when overexpressed decreases cell proliferation (Jia et al., 2012). Furthermore, miR-125b reduces metastasis in hepatocellular carcinoma through repression of LIN28B (Liang et al., 2010). miR-125b is also downregulated in breast cancer, ectopic upregulation of the miRNA inhibits proliferation and migration through the targeting of ERBB2, ERBB3, EST1, and MUC1 (Scott et al., 2007, Zhang et al., 2011b, Rajabi et al., 2010).

miR-125b plays a key role in regulating haematopoiesis, It is one of the most upregulated miRNA in long-term cultured haematopoietic stem cells (HSC) and its expression decreases as the HSC cells differentiate into a more mature lineage (O'Connell et al., 2010). Overexpression results in an increased myeloid and lymphoid population along with a marked decrement in differentiation (Bousquet et al., 2008b). One study using bone marrow-derived murine 32D cells identified miR-125b as being regulated by G-CSF and ectopic expression resulted in the arrest of granulocytic differentiation (Surdziel et al., 2011). miR-125b has also shown to play a role in inflammation through targeting the TNF pathway through stabilisation of the NF-κB inhibitor NKIRAS2 (Murphy et al., 2010). There is

evidence that NF-κB can both increase and repress miR-125b expression, thereby creating a feedback loop (Tili et al., 2007).

miR-125b has also been shown to play a key role in leukaemias. In AML (and MDS), miR-125b is upregulated in patients exhibiting the translocation t(2;11)(p21;q23) (Bousquet et al., 2008b). Its upregulation in AML leads to the arrest of differentiation and the promotion of proliferation. Ectopic overexpression of miR-125b in mouse bone marrow models results in leukaemia, with the exact subtype being dependent on the level of expression of miR-125b (Bousquet et al., 2010). As shown in other cancers, increased miR-125b levels also inhibits differentiation and decreases its responsiveness to apoptotic signalling. According to one study miR-125b blocks apoptosis through the targeting of several proteins in the p53 pathway (such as BAK1) and differentiation through targeting CBFB, a key transcription factor involved in myeloid differentiation (Bousquet et al., 2012, Vargas Romero et al., 2015).

Similar to miR-125b, miR-29b can act both as an oncomiR or tumour suppressor miR but in the case of AML, it has previously been characterised as a tumour suppressor miR. miR-29b is downregulated in AML Blasts, and when ectopically overexpressed in murine models results in increased apoptosis and a decrease in tumour size (Garzon et al., 2009a, Yan et al., 2015). The increase in apoptosis is partly down to the regulation of the anti-apoptotic genes MCL-1 and BCL-2 (Garzon et al., 2009a, Xu et al., 2014). miR-29b also controls the expression of tumour suppressor genes through the targeting of DNA methylation. miR-29b was

shown to directly bind and target DNMT3A and DNMT3B and indirectly regulate DNMT1 through modulation of SP1 (resulting in demethylation of tumour suppressor genes such as ESR1 and CDKN2B (Garzon et al., 2009b). The AML subtype AML-ETO (characterised by chromosomal rearrangement affecting the transcription factor RUNX1) shows downregulation of miR-29b (due to direct repression of AML1-ETO). miR-29b, on the other hand, can also target and therefore repress AML1-ETO, thereby creating a feedback loop. One result of dysregulated AML1-ETO is an arrest in myeloid differentiation, which is partially prevented if miR-29b levels are ectopically over-expressed (Zaidi et al., 2017).

4.1.1 Aims and Rationale

In the previous chapter we identified two miRNAs, miR-125b and miR-29b, regulated by the transcription factor NRF2. We next wished to understand the regulatory relationship between NRF2 and both miR-125b and miR-29b, in particular, the capability of NRF2 to directly regulate both miRNAs.

Both miRNA have previously been shown to play a significant role in various malignancies and we wished to characterise the role of both miRNA in AML cell lines and AML Blasts to elucidate the functional relationship between NRF2 and both miRNA expression in AML.

Finally, if successful we aim to characterise the mRNA targets which these miRNAs bind to and repress with a particular emphasis on those important in AML.

4.2 Results

4.2.1 Genomic location of miRs-125b and miR-29b paralogs

In the previous chapter we identified a correlation between NRF2 and levels of the miRNAs, miR-125b and miR-29b. As this regulation is most likely by NRF2 binding to the promoter region of these miRNA, we looked at the genomic regions in the vicinity of these miRNA. miR-125 and miR-29 both exist in miRNA families which consist of several miRNA homologs; miR-125a, and miR-125b; miR-29a, miR-29b and miR-29c. These homologs share the same seed region, the region where miRNAs bind to repress their target mRNA, but differ in their end mature sequences.

miRNAs also exist as paralogs, miR125b for example exists as two paralogs, miR-125b1 and miR-125b2, both with the same core seed region, but residing in different genomic locations (miR-125b1 is located on chromosome 11, while miR-125b2 is located on chromosome 21). Similarly, miR-29b exists as two paralogs, miR-29b1 (chromosome 7) and miR-29b2 (chromosome 1). A schematic of these miRNA is shown in Fig 4.1. The differing locations of these paralogs suggest they are likely to be independently regulated.

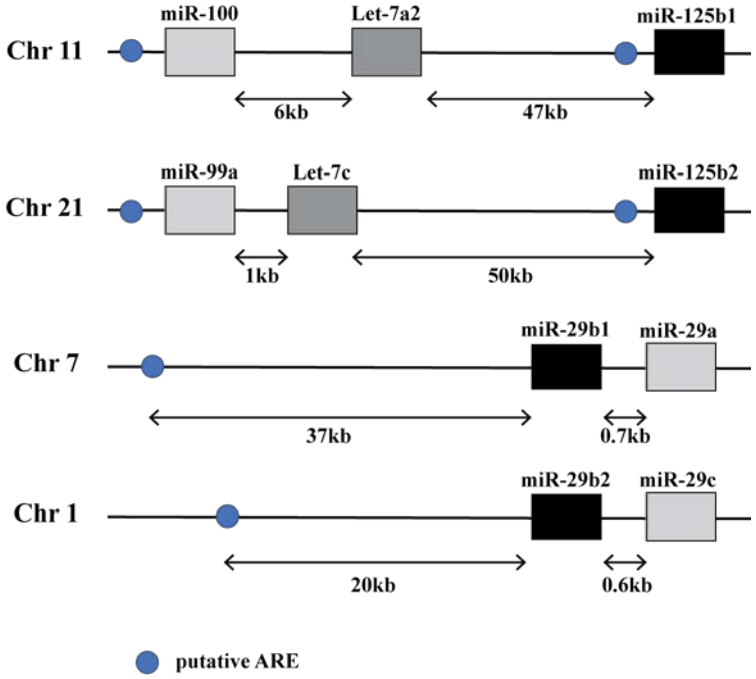

Figure 4.1: Schematic of genomic location of miR-125b and miR-29b and paralogs. miRNA in the vicinity of miR-125b1, miR-125b2, miR-29b1 and miR-29b2 can be seen in boxes. Putative NRF2 "ARE" binding sites are indicated in circles.

4.2.2 NRF2 regulation of miRs-125b and miR-29b homologs and paralogs

We next wished to identify which miR-125 and miR-29 family members were being regulated by NRF2. Since these miRNAs have the same seed region and similar mature sequences it is likely that they have similar functions and may tend to synergise with each other. As before we used specific primers to the miRNA-specific mature sequences following NRF2 knockdown.

We found significant modulation (Fig 4.2) in expression in miR-125b (downregulation), miR-29a and miR-29b (upregulation). miR-125b1 showed a 40% downregulation in expression, while miR-29b expression increased by two-fold.

miR-29a increased to a lesser extent by 1.8-fold., while no significant changes were seen in miR-29c levels.

We next wished to identify which miRNA paralogs are (i.e. miR125b1/2 and miR-29b1/2) regulated by NRF2. As these miRNA paralogs have the same seed region and mature sequence (despite residing in separate genomic location) they both, should in theory, have the same function. However, due to differences in their genomic location, they may be independently regulated differently (i.e. by different transcription factors), thereby changing their exact physiological role despite coding for the same mature sequence/targeting the same mRNAs. To identify which paralog NRF2 was regulating, qPCR was once again used to following NRF2 lentiviral knockdown. In the previous miRNA qPCR amplification, we used the mature sequence as the forward primer and a universal primer as the reverse. This was not possible when measuring miRNA paralogs as they contain the same mature sequence. We therefore designed primers for the flanking regions (i.e. the immature miRNA sequences) around the different paralogs (which would differ to one another due to locational differences). Several primers were designed and tested on an agarose gel post-PCR endpoint (data not shown), the best primers were utilized in qPCR (using the normal mRNA PCR method).

Knock-down of NRF2 resulted in a significant decrease in miR-125b1 expression (approximately 40%) and upregulation of miR-29b1 (around 2-fold). No significant change was seen in miR-125b2 and miR-29b2 expression (Fig 4.2). This indicates

while NRF2 regulates miR-125b1 and miR-29b1, it likely does not regulate miR-125b2/29b2 expression.

Of interest, the total levels of miR-125b and miR-29b, following NRF2 knockdown, (Fig 3.5) are comparable with levels of miR-125b1 and miR-29b1 under the same conditions. This further suggests the dysregulation of miR-125b/29b by NRF2 is down to 125b1/29b1 rather than its paralogs.

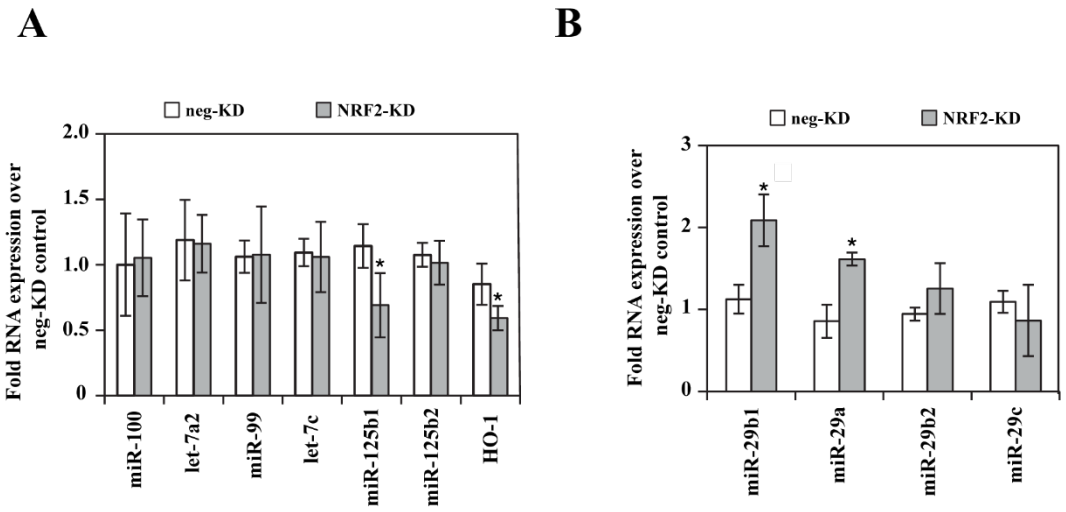

Figure 4.2 Real time PCR detection of miRNA cluster members in THP-1 cells following NRF2 lentiviral knockdown A) miR-125b1 (miR-125b1, miR-100, and let-7-a2) miR-125b2 (miR-125b2, miR-99a and let-7c) and HO-1 B) miR-29b1 (miR-29b1 and miR-29ba) and miR-29b2 (miR-29b2 and miR-29 c) Student's t-test carried out to determine statistical significance, * indicates $P< 0.05$.

4.2.3 NRF2 regulates miRs-125b and -29b through their individual promoters

We next wished to understand the mechanism by which NRF2 regulates miR-125b and miR-29b. miRNAs can be regulated through their own individual promoter or co-regulated alongside other miRNAs in "miRNA clusters". miR-125b1 lies

downstream (approx. 47 kb) from miR-100 and let-7-a2. miR-125b2 similarly lies downstream (50 kb) of miR-99a and let 7-c. The miR-29b paralogs lie closer to their respective clusters with miR-29b1 located approximately 700 bp away from miR-29a, while miR-29b2 is approximately 600 bp from miR-29c (Fig 4.3). Admittedly 50 kb is a large distance for miRNA co-regulation however reports have suggested these miRNA do associate with one another to create a physiological effect (Wang et al., 2011). These miRNA cluster regions also exhibit a high genomic conservation suggesting they can be of regulatory importance.

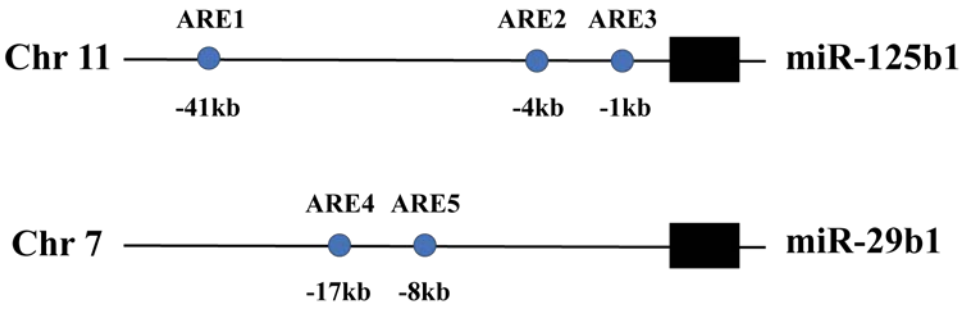

Figure 4.3: Schematic of the miR-125b-1 and miR-29b-1 promoter regions

Putative "ARE" binding sites in the vicinity of the miRNA paralogs miR-125b1 and miR-29b1.

The first question we wished to answer was whether miR-125b or miR-29b were being regulated through their own independent promoters, or alongside other miRNA clusters. Again, we used qPCR (on THP-1 cells treated with the lentiviral NRF2 KD) to amplify the mature miRNA in the cluster (i.e. miR-100, let 7-a2, miR-99, let7c, miR-29a, miR-29c) and the immature miRNA sequences for those with the same seed region (i.e. miR-125b1, miR-125b2, miR29b1 and miR-29b2). mRNA for the NRF2 HO-1 was used as a positive control. As shown in Fig 4.2

there was no change in miR-100, let-7-a2, miR-99, let7. As discussed above only a slight increase in miR-29a expression was observed following NRF2 knockdown.

As no significant change in expression was seen in the miR-125b1 or miR-125b2 cluster this suggested that NRF2 may regulate miR-125b1 and miR-29b1 independently of the other miRNA in its cluster. This also suggests that the ARE binding site responsible for miR-125b1/29b1 is likely to be in the vicinity of these miRNA (as opposed to around the other miRNA cluster members).

4.2.4 Identification of potential ARE sites in the miRs-125b and -29b promoters

We have identified miR-125b1 and miR-29b1 as the miRNAs targeted by NRF2. As described previously, we used the transcription factor binding program, Pmatch, to identify novel NRF2 (ARE) binding sites close to miR-125b1 and miR-29b1 start sites. We identified three putative ARE sites in the vicinity of miR-125b1, one located at -41 kb, another at -4.3 kb and the third one at 900 bp from the miRNA start site. We also identified two sites near miR-29b1 located approximately 17 kb and 8 kb from the miRNA start site. While these putative AREs are located a fair distance away from miR-29b1 start site there are reports indicating SMAD3 binding sites exist 22 kb away from the miR-29b paralog miR-29b2. This suggests it is possible for a transcription factor to bind and regulate miR-29b1 from such a distance (Kriegel et al., 2012). Another study used RACE to amplify the genomic 5' ends of miR-29b1 and identified a primary miRNA start site and promoter region approximately 36 kb upstream of the mature miRNA start site (Eyholzer et al.,

2010, Chang et al., 2008), again indicating the possibility of NRF2 regulating miR-29b1 from quite a distance away from its mature sequence. A diagram of the miR-125b1 and 29b1 schematic can be seen in Fig 4.3 along with a visual schematic detailing the ARE sites 1-5. The exact genomic locations seen in Table 4.1.

miRNA	Sites	position	ARE sequence
miR-125B1	ARE1	40923-40933	ATGACTCAGTG
miR-125B1	ARE2	4537-4548	TGATCTCAGCA
miR-125B1	ARE3	1357-1368	GCTTTGTCATT
miR-29B1	ARE4	16788-16799	AGCTGAGTCAC
miR-29B1	ARE5	7647-7658	TGCTGAGTCAT

Table 4.1: Location and sequences of putative ARE sites in the miR-125b1 or miR-29b1 promoters

4.2.5 Identification of ARE binding sites using CHiP

As discussed above three ARE sites were identified on miR-125b1 and two on miR29b1. To determine which, if any, of these sites NRF2 binds to, we used a Chromatin Immunoprecipitation Assay (CHiP).

CHiP was performed on THP-1 cells using an antibody to immunoprecipitate NRF2 and any bound DNA, following cross-linking with formaldehyde. Specific PCR primers were designed to flank the regions of each putative ARE site for qPCR analysis (Fig 4.4). From the five ARE sites identified we saw the biggest enrichment

in NRF2 at ARE3 (-1 kb from miR-125b1) and ARE5 (-8 kb from miR-29b1). The enrichment on ARE5 seems to be larger than that of the other ARE sites tested. To further confirm site activity in vivo, we upregulated NRF2 expression by targeting KEAP1 suppression with siRNA. In agreement with our previous results we saw a significant enrichment in AREs 3 and 5 in comparison to cells treated with a scrambled siRNA control suggesting increased NRF2 is binding to these areas of DNA upon up-regulation. We did see small, but not statistically significant, enrichment in ARE2 and ARE4 when compared with the control IgG immunoprecipitation. When KEAP1 was downregulated, no significant change was seen in ARE2, but a small enrichment was seen at ARE4, raising the possibility this site may not be completely transcriptionally inactive, however for the purposes of our study only AREs 3 and 5 were used.

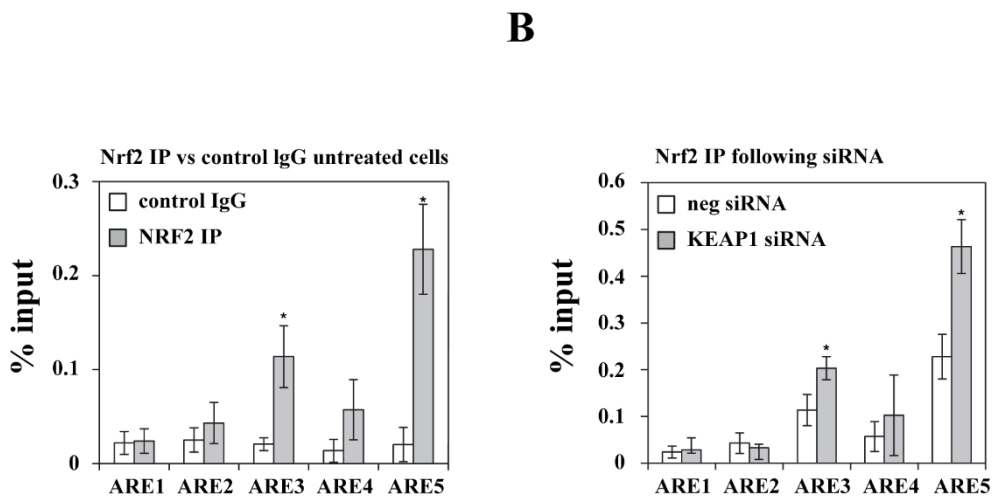

Figure 4.4: Chromatin Immunoprecipitation assay (ChIP) was used to determine Transcription factor (TF) binding NRF2 antibody was used with rabbit IgG as the control. A) qPCR was carried out on both immunoprecipitated and input DNA. B) qPCR was carried out on both immunoprecipitated NRF2 DNA from THP-1 cells post negative or KEAP1 siRNA transfections for 24 hours. A

two-way Anova was carried out prior to the post-hoc Bonferroni correction, and used to determine statistical significance within each ARE site, * indicates $P< 0.05$

Overall, the CHiP assay indicates that NRF2 can bind *in vivo* to ARE3 on miR-125b1 and ARE5 on miR-29b1. Furthermore, when NRF2 levels are raised, increased NRF2 recruitment is seen at these sites, thereby attesting to NRF2's ability to bind to both ARE sites.

4.2.6 Development of Luciferase p125b and p125bAREmut constructs

The previous data has demonstrated that NRF2 can bind to ARE3 (on miR-125b1) and ARE5 (on miR-29b1) in AML cells (Fig 4.3 and 4.4). To test whether these sites were transcriptionally active, we used a luciferase-based promoter/reporter assay. We cloned each of the ARE sites into the pGL4.11 luciferase vector (Fig 4.5A) upstream of the FireFly luciferase reporter. To clone the promoter for miR-125b1 we designed primers- Forward 5′-AGAAAGGCCACCAAGATTCAC-3′ and Reverse 5′-TGAGAGGAGCGCAACAATG-3′) to clone the 2.6 kb fragment (which included the ARE3 site). Site-directed mutagenesis was carried out on the p125b sequence using the primer 5′-GCTGTGGCTGtTTTGTtATTCTCTTTGACTAG-3′ to introduce a single point mutation to generate the p125b NRF2 MUT. A schematic of the site directed mutagenesis can be seen in Fig 4.5B. The pGL4 (empty vector) p125b and p125b NRF2 MUT were all transfected into THP-1 cells using the transfection reagent diethylaminoethyl (DEAE) dextran for 48 hours, after which, a luciferase assay was conducted.

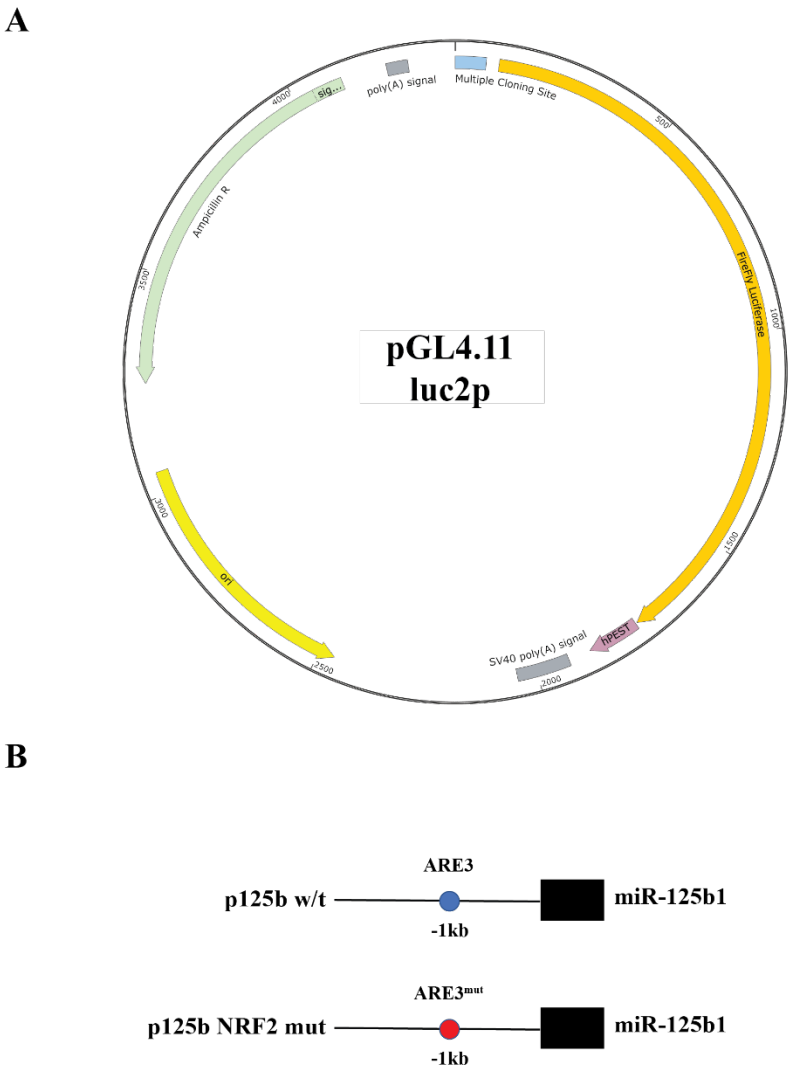

Figure 4.5: miRNA promoter/reporter assay A) Map of pGL4.11 Luciferase reporter construct B) A cartoon of w/t and mut ARE 3 (miR-125b1) promoter/reporter inserts

4.2.7 Validation of the miR-125b ARE site

As discussed above, we designed the dual luciferase pGL4 miR-125b constructs to test the transcriptional activity of ARE3. ARE5 is ~8 kb away from the miR-29b1 start site and we were unable to clone a fragment of that size into the pGL4.11

plasmid. We first transfected both the pGL4 and p125b (0.5 μg) into THP-1 cells without a NRF2 modulator, as previous work in our lab had demonstrated AML cells are characterised with high basal expression levels of NRF2. As shown in Fig 4.6A, when the p125b plasmid was transfected alone into THP-1 cells, we found an eight-fold upregulation in reporter activity in comparison to the empty vector pGL4 control. When we treated THP-1 cells with pGL4/ p125b alongside siRNA to KEAP1, the p125b reporter showed significant increased reporter activity, no such change was seen in the pGL4 control vector.

We performed site directed mutagenesis on site ARE3 (as discussed in the previous section): the construct was designated p125b NRF2 MUT. Admittedly, when transfected into THP-1 cells, we saw a four-fold increase in reporter activity (compared to the vector control), however this is still significantly lower (four-fold) then the results seen with the p125b plasmid. Furthermore, in cells treated with KEAP1 siRNA, we found no change in reporter activity with p125b NRF2 MUT, but significant increase activity in p125b. When treated with NRF2 siRNA no change in reporter activity was seen in either p125b or p125b NRF2 MUT. The results (shown in Fig 4.6B) seen were in line with what was expected, increasing levels of NRF2 correlated with increased levels of p125b activity, plus decreased NRF2 levels resulted in p125b activity to decrease to that of p125b NRF2 MUT. This shows that NRF2 can transcriptionally control the ARE3 site on miR-125b1.

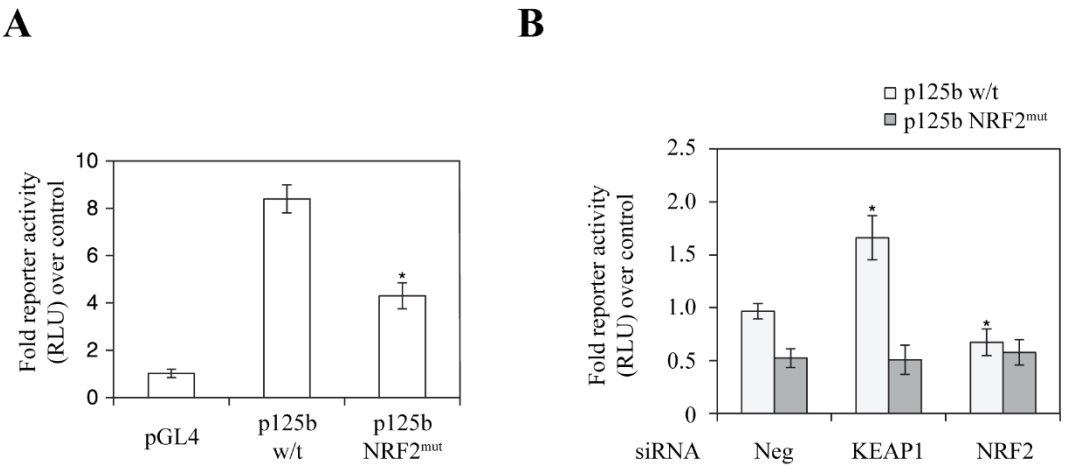

Figure 4.6 Transcriptional activity of the putative NRF2 binding sites on the miR-125b1 promoter. A) Luciferase reporter expression in THP-1 cells transfected with p125b NRF2 w/t and mut. B) Reporter expression of p125b wt/ p125b NRF2 mut in THP-1 cells following NRF2 or KEAP1 knockdown. Student's t-test carried out to determine statistical significance, * indicates $P< 0.05$.

4.2.8 Manipulation of miR-125b and miR-29b using antagomiRs and miR mimics

We have shown NRF2 can transcriptionally regulate miR-125b1 (through ARE3) and can bind to the miR-29b1 promoter (through ARE5). We next wished to identify the functional role of both miR-125b1 and miR-29b1 towards NRF2 signalling. To do this we manipulated expression of these miRNAs using an miRNA mimic (miR-29b) or an antagomiRs (miR-125b). Mimics are small molecules made to mimic the function of a particular miRNA i.e. bind and repress their target mRNA. AntagomiRs are complementary to the miRNA of interest and therefore duplex to and block the miRNA function.

We first had to validate that the mimic and the antagomir blocked their respective miRNA function and so both were transfected into THP-1 cells and levels of each miRNA analysed using qPCR. When transfected the miR-29b mimic resulted in a 3.5-fold increase in total miR-29b expression and conversely, the miR-125b antagomiR resulted in a significant decrease in total miR-125b levels (Fig 4.7). No changes were observed with the scrambled miRNA control. As an additional control, we measured miRNA levels following NRF2 or KEAP1 knockdown. In the NRF2 knockdown cells, we found decreased levels of miR-125b to the same level as the cells treated with the miR-125b antagomiR. The miR-29b levels increased (by just under two-fold), however, not to the same extent as when cells were treated with the miR-29b mimic, although this was to be expected as the mimic artificially increases specific miRNA expression. Furthermore, in the KEAP1 knockdown cells we saw increased levels of miR-125b, and lower levels of miR-29b. This data shows that both the mimic and antagomir are capable of modulating expression of their respective miRNAs in the THP-1 cells.

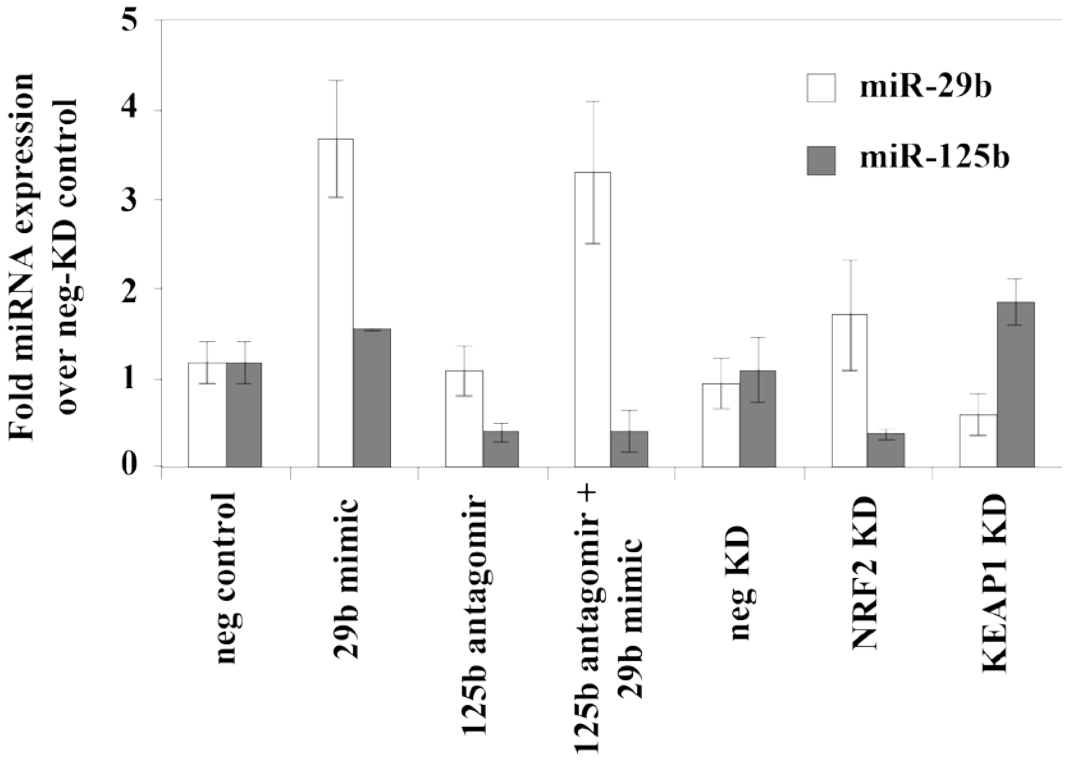

Figure 4.7: Effect of a miR125b anatagomiR and a 29b mimic on miR125b and 29b expression in THP-1 cells A miR-125b antagomir and a mIR-29b mimic were transfected into THP-1 cells for 48h following which miR-125b and miR-29b levels were detected by qPCR. NRF2 and KEAP1 Lentiviral knockdown were used as positive/negative controls respectively.

4.2.9 Modulation of miR-125b and miR-29b using antagomiRs and miRNA mimics induces apoptosis in AML cell lines

Previous studies have shown both miR-125b and miR-29b play a role in regulating apoptosis. miR-125b is a well-known oncogenic miRNA in haematological malignancies, and miR-29b is a known tumour suppressor miR (Bousquet et al., 2012, Garzon et al., 2009a).

In order to assess their role in apoptosis in AML, THP-1 cells were transfected with an miR-125b antagomiR or an miR-29b mimic for 48 hours, after which apoptosis was measured using Annexin V and Propidium Iodide (PI) staining. As shown in Fig 4.8A we saw a minor increase in cell death when miR-125b levels were decreased (approximately 8%) or miR-29b levels were increased (approximately 10%). We did not see any significant change in Annexin V/ PI levels when miR-125b levels were increased or miR-29b was decreased, this could possibly be due to their aberrant expression in AML (data not shown). As discussed previously miR-125b levels are increased in AML blasts compared to CD34+ cells and miR-29b shows the opposite trend. We speculated as levels of miR-125b are already raised in AML, its target mRNAs are already being repressed and therefore artificially increasing levels of miR-125b have no apparent functional effect. We further speculate miR-29b shows the opposite trend. While both the mimic and antagomir had only minor effects on cell death when transfected individually, more surprisingly, when the two miR regulators were co-transfected there was a singularly more impressive 43% increase in the amount of cell death observed.

Similar to the AV/PI results, Fig 4.8B shows a decrease in miR-125b (or increase in miR-29b) resulting in a minor decrease in cell viability (around 12–15%), however when cells were transfected with both the miR-125b antagomir / miR-29b mimic, the cell viability fell by 63%. To show this synergistic effect was not specific to THP-1, the Cell-Titer Glo was repeated in Kasumi-1 cells (an AML cell line characterised by the translocation t(8;21)). The same trend was seen, however the Kasumi-1 cells seemed less sensitive to alteration by individual miR-125b

antagomiR (3% reduction in cell viability) or miR-29b mimic (8% reduction in cell viability). Synergistic expression of both the miR-125b antagomiR and miR-29b mimic resulted in a 43% reduction in cell viability.

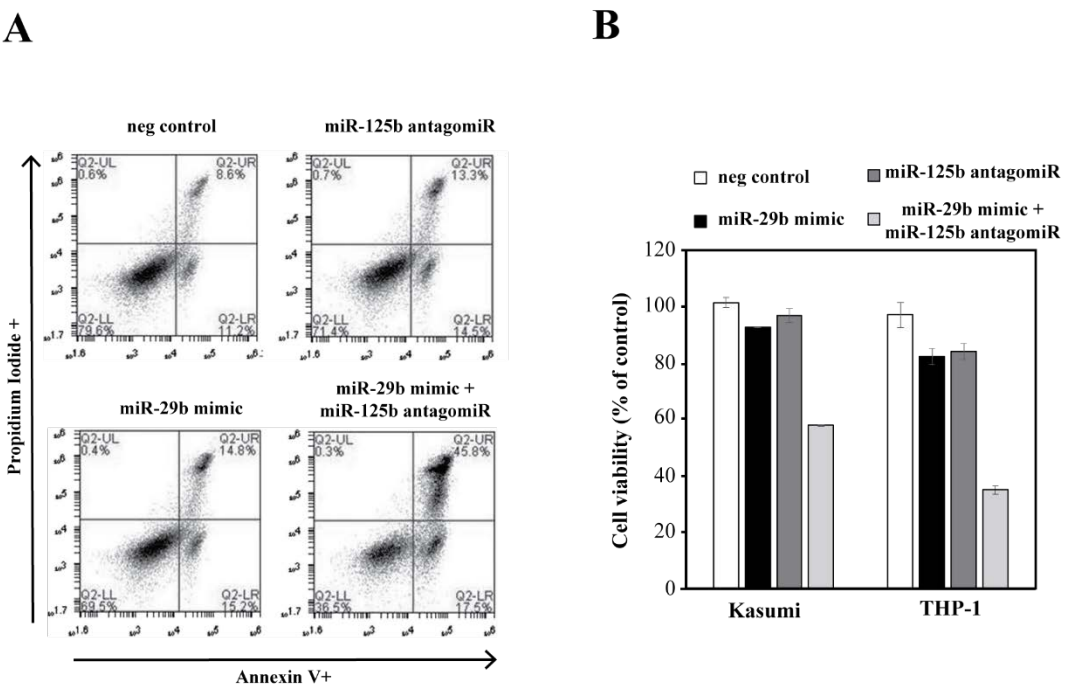

Figure 4.8: Modulation of miR-125b/29b induces cell death in AML A) Annexin V/PI staining on THP-1 cells post modulation of miR-125b and/or miR-29b. B) Cell viability assays on THP-1 and Kasumi cells post modulation of miR-125b and/or miR-29b.

We have shown NRF2 can increase levels of miR-125b1 and repress miR-29b1 through binding to an ARE sites on their promoter. Whist only a modest response was seen when miR-125b levels were decreased or miR-29b levels were increase, we were surprised to see a large increase in apoptosis when the miR-125b antagomiR and the miR-29b mimic were co-transfected together. Overall this suggests NRF2 can synergistically regulate miR-125b1 and miR-29b1. Levels in AML cells

4.2.10 Cell death induction by antagomiRs and miRNA seen in primary AML blasts

We have successfully shown manipulating levels of both miR125b and miR-29b in AML cell lines can modulate cell death. As previously discussed, AML is a heterogeneous disorder made up of a vast number of cytogenic and genetic abnormalities. While AML cell lines provide useful models they represent a limited repertoire of the complexities clinically seen in primary AML. We therefore wished to look at the effect of the miRNA mimics and antagomiRs in primary AML blasts derived from patients. AML blasts were extracted from the peripheral blood of AML patients samples and $CD34^+$ cells from the peripheral blood of healthy volunteers. Both $CD34^+$ cells and AML blasts were transfected with mimic and antagomiR for 24 hours after which cell death was measured using an ATP-utilisation assay (Cell-Titer Glo) (Fig 4.9A and B).

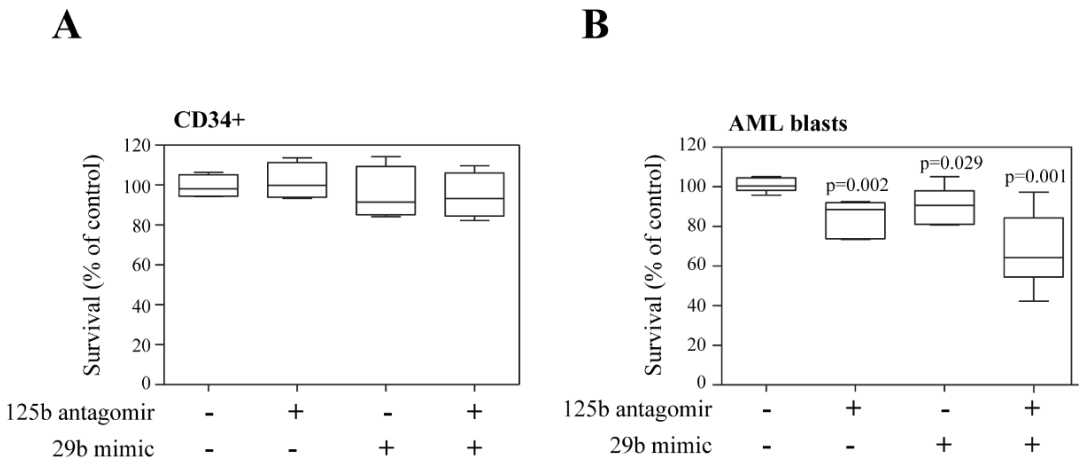

Figure 4.9 miR-125b/29b modulation induces cell death in primary AML cells

Cell viability assay was carried out on A) CD34+ and B) AML blasts following transfection with miRNA mimics and/or antagomIRs. Student's t-test carried out to determine statistical significance.

A decrease in viability was seen when AML blasts were treated with a miR-125b antagomiR, while a lesser decrease was seen in blasts treated with the miR-29b mimic. As previously shown in the AML cell lines, when the AML blasts were transfected with both the miR-125b antagomiR and the miR-29b mimic, a significant decrease (around 40%) in cell viability was seen. The $CD34^+$ cells showed no difference in cell viability post transfection with the miR-125b antagomiR. Meanwhile a slight (but not significant) decrease was seen upon transfection with the miR-29b mimic alone or when co-transfected with both the miR-125b antagomiR and miR-29b mimic.

In agreement with the AML cell lines, the primary AML blasts showed significant (but limited response) to single mimic or antagomiR, but a much larger decrease in cell viability when both the miR-125b antagomiR and miR-29b mimic were combined. The large sensitivity towards the miR-125b antagomiR / miR-29b mimic in primary samples is further evidence that NRF2 synergistically regulates both miR-125b1 and miR-29b1 to increase cell survival and proliferation. Some variation was seen within the AML blasts (and the $CD34^+$ cells), particularly when co-transfected with the miRNA mimic and antagomiR, which is to be expected due to the rather heterogeneous nature of these samples.

4.2.11 AntagomiRs and miRNA mimics sensitise AML cells to chemotherapeutic agents

Chemotherapy-resistance is a major problem in AML. While remission rates are approximately 75-85%, the five-year survival rate is only around 30–40%. Survival

rates are particularly low in patients over the age of 65 and this can be further complicated by resistance occurring to currently available chemotherapy (De Kouchkovsky and Abdul-Hay, 2016, Almeida and Ramos, 2016). Previous work in our lab has identified NRF2 as a key regulator of chemotherapy-resistance in AML. We therefore wished to investigate whether the dysregulation of miRNA by NRF2 plays a role in this resistance.

THP-1 and Kasumi-1 cells were transfected with miRNA mimic and antagomiR, 24 hours later increasing concentrations of daunorubicin were added. Viability was measured and IC_{50} measurements were carried out (Table 4.2),

As expected, we found a slight increase in daunorubicin sensitivity following transfection with the miR-125b antagomiR or the miR-29b mimic. The highest levels of sensitivity were seen when cells were co-transfected with both the miR-125b antagomir and the miR-29b mimic. THP-1 cells seemed to show a greater response to miRNA manipulation then Kasumi-1s, with a 20% decrease in IC_{50} post miR-125b downregulation, a 45% decrease post miR-29b mimic, and a 65% decrease consequently when transfected with both miRNA simultaneously. The Kasumi-1 cells showed a 17% decrease post transfection with a miR-125b antagomiR, an 8% decrease post miR-29b mimic and a 30% decrease when presented with both miRNAs.

	IC_{50} daunorubicin [μM]	
	THP-1	Kasumi1
negative control	0.276	0.092
α125B	0.221	0.077
29B mimic	0.153	0.085
α125B + 29B mimic	0.123	0.066

Table 4.2: Modulation of miR125b and miR-29b increases daunorubicin sensitivity in AML cell lines Cell viability was calculated on THP-1 IC50 was measured on THP-1 and Kasumi cells treated with increasing concentrations of daunorubicin for 48 hours post miRNA mimic or antagomir transfection

4.2.12 Increased sensitivity to chemotherapeutic agents in primary AML samples following treatment with antagomiRs and miRNA mimics

We next wished to confirm drug-sensitivity in primary AML blasts. In the previous section we confirmed the trend that AML blasts were susceptible to manipulation of miR-125b and miR-29b levels. Next, we compared a $CD34^+$ cell alongside primary AML BLAST with both high (sample AML#25) and normal levels of NRF2 (sample AML#27). As shown in both Table 4.3 and Fig 4.10A, AML#27 from the outset were more sensitive to daunorubicin treatment than AML #25. Primary samples were transfected with either the miRNA mimic or antagomiR before treatment with daunorubicin. AML # 25 when transfected with the miR-125b

antagomiR showed a decrease in IC_{50} by 26%, while the miR-29b mimic had a 49% decrease in its IC_{50}. When co-transfected with both the miR-125b antagomiR and miR-29b mimic, there was a 64% decrease in the IC_{50}. AML#27 showed no sensitivity towards either the miRNA mimic or antagomiR individually or in conjunction with one another following daunorubicin treatment. Likewise, normal CD34+ cells, which contain lower levels of NRF2 than that of most AML cases, showed limited sensitivity towards daunorubicin.

We decided to closely compare the two AML samples, AML #25 and #27 which are characterised by different underlying disorders, AML#25 has the WHO classification of "AML without maturation" with complex cytogenetics (Table 3.1). In the previous chapter qPCR was carried out comparing levels of NRF2, miR-125b1 and miR-29b1 in all primary AML blasts used, relative to that of the $CD34^+$ cells (Table 3.1). In AML #25, we identified a 3.2-fold upregulation in NRF2 mRNA, 6.5-fold upregulation in miR-125b1 and a 0.4-fold downregulation in miR-29b1 levels.

	IC_{50} daunorubicin [μM]		
	CD34+	AML#25	AML#27
negative control	0.207	0.293	0.037
α125B	0.186	0.219	0.036
29B mimic	0.187	0.152	0.034
α125B + 29B mimic	0.157	0.106	0.033

Table 4.3: Daunorubicin sensitivity of AML blasts following miRNA manipulation Daunorubicin sensitivity was measured in AML BLASTS characterised with high (AML-25)/normal (AML-27) NRF2 levels and normal CD34+ cells.

AML #27 is characterised as a core binding factor (CBF) AML which contains a t(8;21) (q22;q22) translocation between the RUNX1 and RUNX1T1. In table 3.1, we saw a 1.2-fold increase in NRF2 mRNA, a 1.4-fold increase in miR-125b1 and a 0.5-fold decrease in miR-29b1 levels. As expected AML #27 showed NRF2 levels closely resembling that of $CD34^+$ cells (and therefore only a minor increase in miR-125b1 levels). Despite the normal basal levels of NRF2, we did see a significant decrease seen in miR-29b1 levels, however this may be more attributable to the underlying cytogenetics of this sample. The t(8;21) translocation is strongly associated with a gain of KIT function. KIT has been reported to indirectly represses miR-29b through aberrant Myc signalling. Myc alongside SP1 (also an miR-29b target) represses levels of miR-29b (Liu et al., 2010a).

NRF2 levels were next increased in AML #27 by transduction with an KEAP1 KD (Fig 4.10B), these cells were then treated with daunorubicin. The KEAP1 KD AML #27 showed a higher resistance to daunorubicin then those with the control treatment, further illustrating the importance of NRF2 levels in mediating drug-resistance in AML (Fig 4.10C). KEAP1 KD AML #27 was transfected with the miR-125b antagomiR and a miR-29b mimic, after which cells were treated with daunorubicin (Fig 4.10D). We saw little change in daunorubicin-resistance post-

treatment with the antagomiR and mimic, however when both the miR-125b antagomiR and miR-29b mimic was co-transfected together, we did observe a significant decrease in daunorubicin-resistance, which once again suggests aberrant NRF2 activity is partially responsible for the oncogenic role of miR-125b and miR-29b in AML.

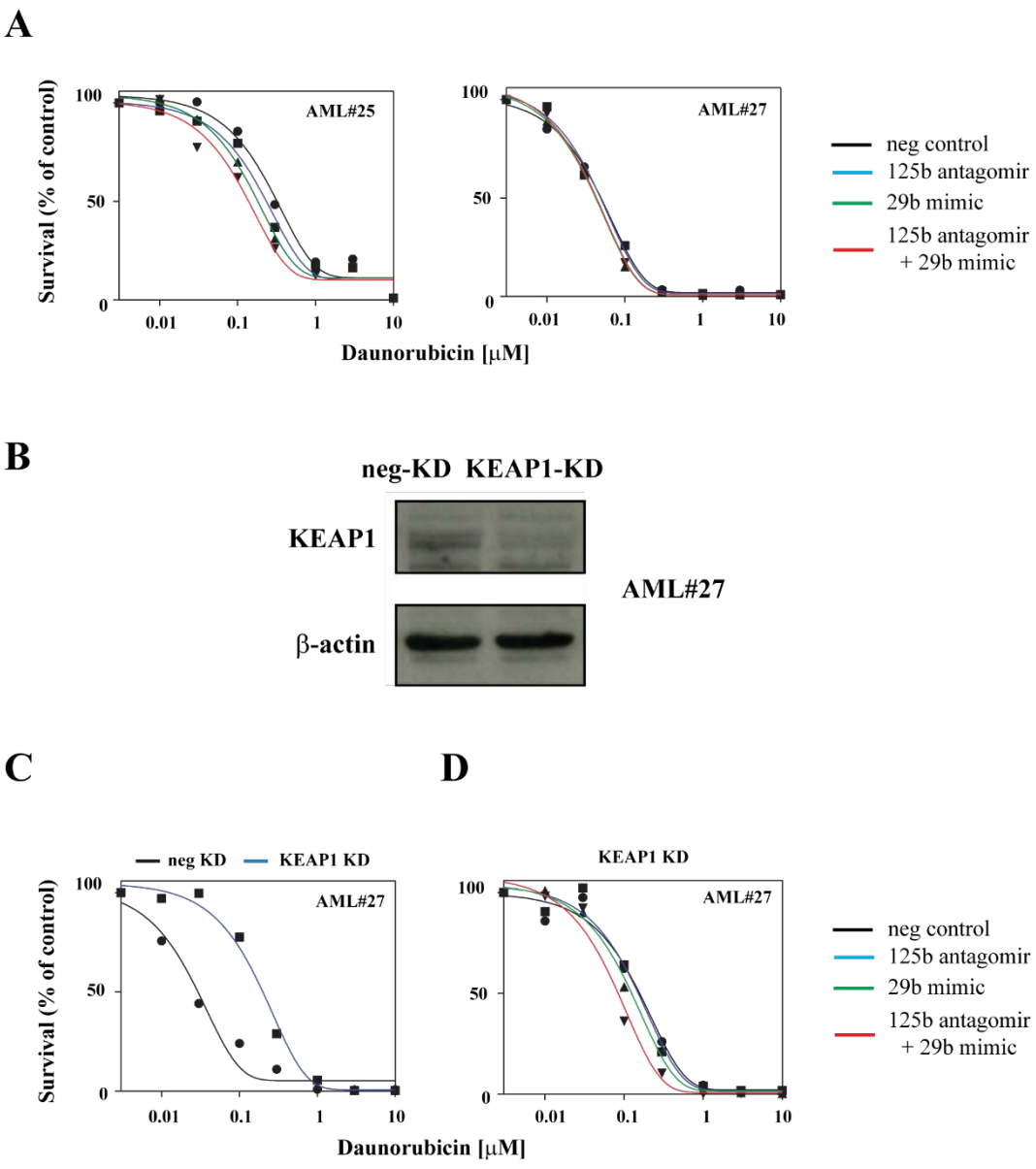

Figure 4.10 Modulation of miR-125b and miR-29b increases daunorubicin sensitivity in AML blasts A) AML BLASTs #25 and #27 were transfected with miRNA control, miR-125b antagomir, 29b mimic and combined miR-125b

antagomir and miR-29b mimic for 24 hours. After which cells are treated with increasing doses of daunorubicin for 48 hours. Cell viability is calculated by Cell-Titer Glo.

B) AML BLAST #27 was transduced with a KEAP1 KD lentivirus, after-which treated with increasing doses of daunorubicin and KEAP1 protein was detected by Western Blot. C) Cell viability was detected in AML BLAST #27 after transduction with an KEAP1 KD lentivirus. Cells were then treated with increasing doses of daunorubicin for 48 hours, after which a Cell-Titer Glo assay was performed. D) The transduced AML #27 was transfected with miRNA mimics and antagomir. Cells were then treated with increasing doses of daunorubicin for 48 hours, after which a Cell-Titer Glo assay was performed.

4.2.13 Identification of miRNA targets through manipulation of miR-125b / miR-29b

We have identified NRF2 can synergistically regulate miR-125b and miR-29b, and NRF2 dependent dysregulation of these miRNA lead to a decrease in apoptosis and a resistance to frontline chemotherapy agents such as daunorubicin. miRNAs can traditionally target a range of mRNAs, many of which are disease-dependent. We therefore wished to elucidate which mRNAs (and resulting proteins) were being affected by both miRNAs (miR-125b1 / miR-29b1) in AML. Using both a literature search and public miRNA target databases (such as miRdb) we identified seventeen experimentally validated targets for either miR-125b and miR-29b, the majority of

which had previously been validated as targets in haematological malignancies (see Table 4.4).

Gene name	Function/disease	Reference
miR-29B targets		
MYBL2	AML	(Garzon et al., 2009a)
AKT2	EOC	(Teng et al., 2015)
Cxxc6	AML	(Garzon et al., 2009a)
DNMT1	AML	(Garzon et al., 2009b)
TGFB1	Trabecular meshwork	(Chou et al., 2013)
PIK3R1	Liver	(Wang et al., 2015a)
CDK4	Osteosarcoma	(Zhu et al., 2016)
SP1	AML	(Liu et al., 2010b)
miR-125B targets		
CBFβ	AML subtype-APL	(Bousquet et al., 2012)
KLF13	Haematopoietic stem cells	(Ooi et al., 2010)
ABTB1	AML subtype-APL	(Bousquet et al., 2012)
MAPK14	Head and neck squamous cell carcinoma	(Zhang et al., 2014)
STAT3	Myelopoiesis	(Surdziel et al., 2011)
miR-125B/mIR-29B targets		
CDK6	Mantle cell lymphoma	(Iqbal et al., 2012)
BCL2	Hepatocellular carcinoma	(Zhao et al., 2012)
MCL1	Hepatocellular carcinoma	(Jia et al., 2012)
BAK1	AML/Breast Cancer	(Zhou et al., 2010)

Table 4.4: List of putative miR-125b and miR-29b mRNA targets and their associated disorders.

THP-1 cells were transfected with miR mimic and antagomiR both singularly and in combination with one another. mRNA of miR-125b and miR-29b targets were measured by qPCR (Fig 4.11A). Treatment with the miR-125b antagomiR resulted in a significant increase in the miR-125b targets MAPK14, STAT3, and BAK1. We also saw no change in CBFB. Treatment with the miR-29b mimic resulted in a significant decrease in the miR-29b targets MYBL2, AKT2, CDK4, SP1 and BCL2. When both the miR-125b antagomiR and miR-29b mimic were co-transfected together, we saw a significant decrease in CDK4, and AKT2. A significant up-regulation of MAPK14 and BAK1 was also identified. We next measured the whole-cell protein expression of three of the miRNA targets: AKT2, STAT3, and BAK1 (Fig 4.11B). After transfection with the miR-125b antagomiR, we saw no increase in AKT2 protein levels, but an increase in STAT2 and BAK1.

A

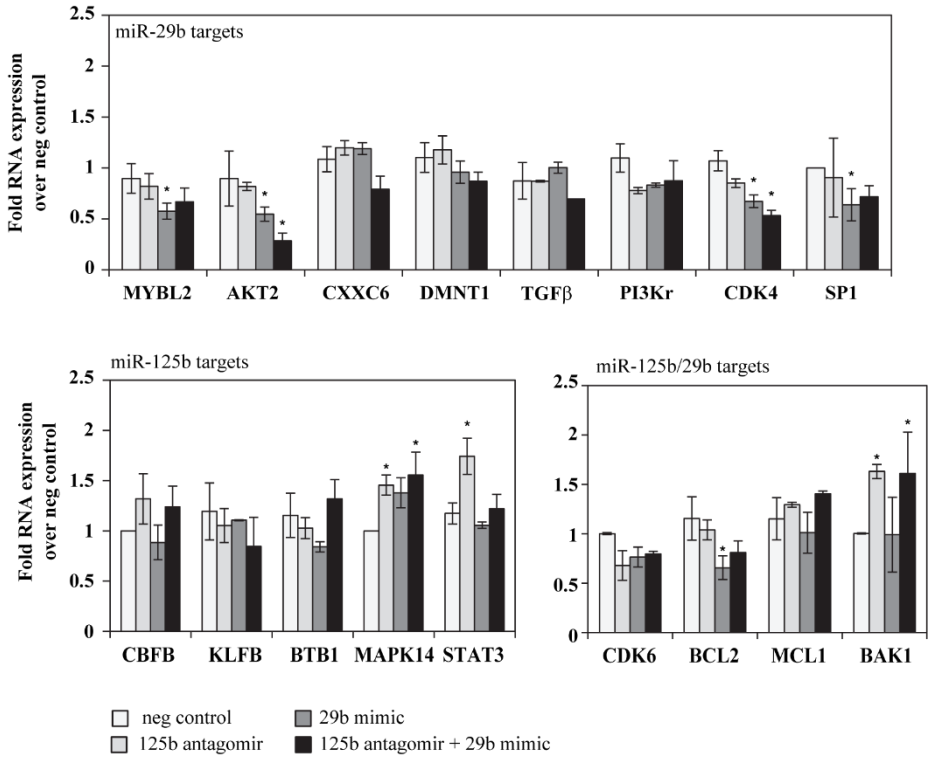

B

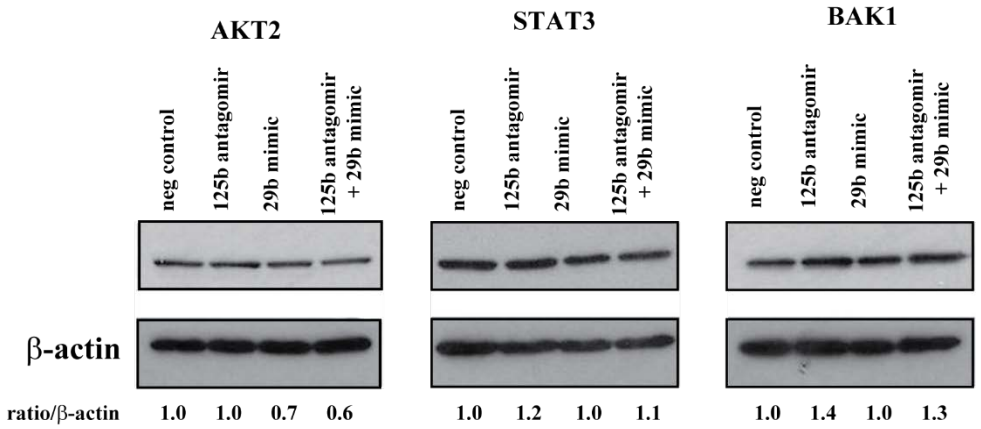

Figure 4.11: Detection of miR-125b and miR-29b targets THP-1 cells were transfected with miR-125b antagomir and miR-29b mimic A) mRNA levels of miRNA targets were detected by qPCR. Student's t-test was carried out to determine statistical significance, * indicates $p < 0.05$. B) Western blot was used to measure protein levels of AKT2, STAT3, and BAK1. Levels of AKT2, STAT3 and BAK1 were normalised against β-actin by densitometry.

4.2.14 Confirmation of targets miRNA targets through NRF2 inhibition and KEAP1 knockdown

We have identified potential targets for miR-125b and miR-29b in AML. We next wished to test the regulation of these mRNA targets by NRF2 and KEAP1. Fig 4.12A indicates that when NRF2 was knocked down in AML, we saw a significant decrease in mRNA levels of AKT2, while a significant increase was seen in STAT3 and BAK1. When cells were transfected with a KEAP1 KD, we saw an increase in AKT2 levels, but no significant change in STAT3 or BAK1. No change was seen either in MCL1 levels post NRF2 or KEAP1 KD. When protein expression was measured (Fig 4.12B), we saw a slight decrease in AKT2, an increase in BAK1,

and no change in STAT3 (post NRF2 KD). Post KEAP1 KD, we saw a slightly larger increase in AKT2 (0.7-fold) and a slight decrease in STAT3 and BAK1 protein levels. It should be noted that while the change in protein levels is not large, it is in line with the subtle changes that we have observed and typically expect of miRNA regulation.

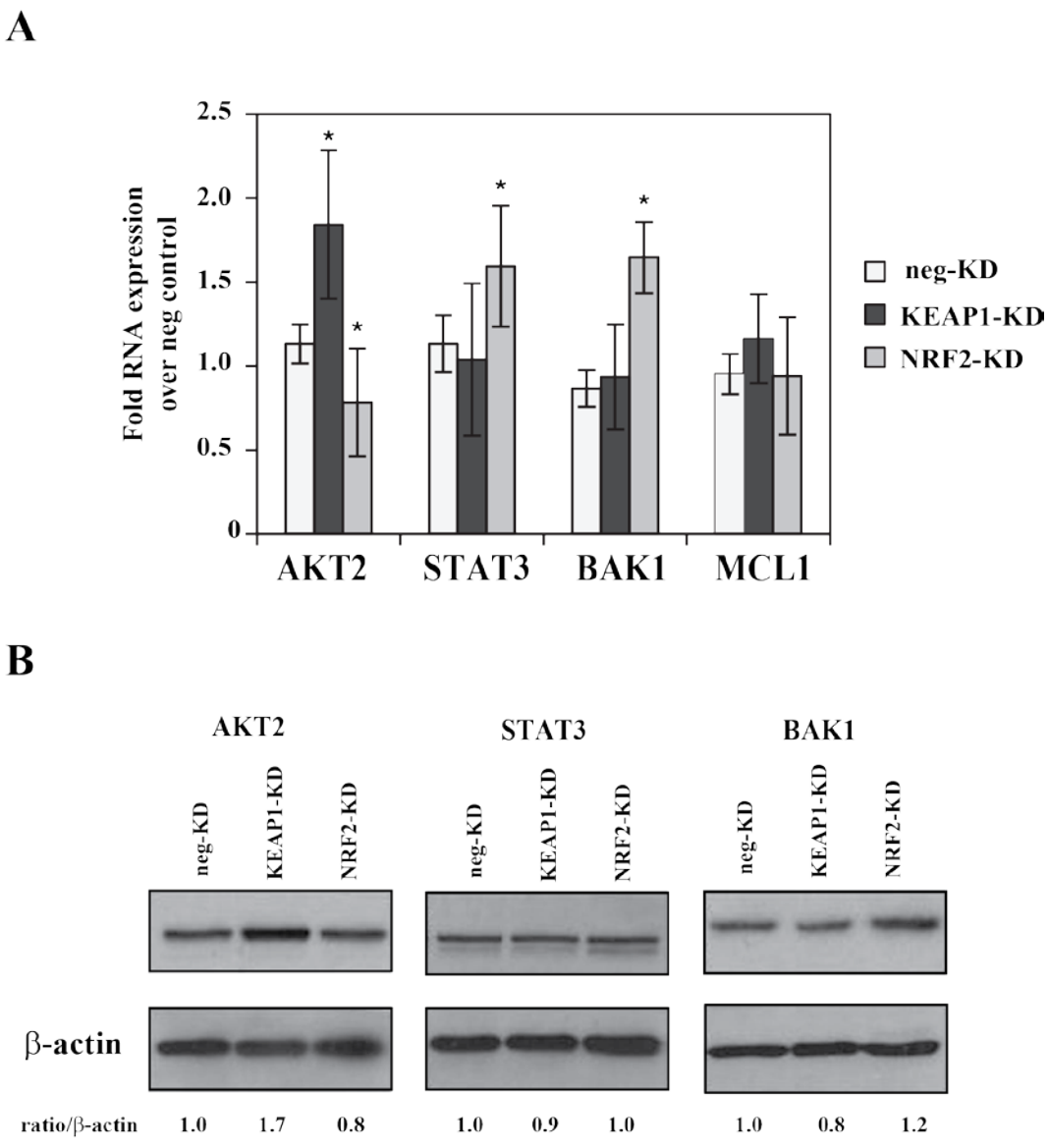

Figure 4.12: miRNA targets confirmed through NRF2 modulation THP-1 cells were transduced with an NRF2 or KEAP KD lentivirus. a) qPCR was used to

measure AKT2, STAT3, BAK1, and MCL1 mRNA levels in transduced cells. Student's t-test carried out to determine statistical significance, * indicates $p< 0.05$. b) AKT2, BAK1 and STAT3 protein levels were measured by Western blot.

4.3 Conclusions and Discussion

We have identified NRF2 can manipulate miRNA expression, including positively regulating miR-125b1 and negatively regulating miR-29b1 through binding to their promoter regions at -1 kb (miR-125b1) and -8 kb (miR-29b1). A CHiP assay was used to show the potential of NRF2 to binds to the ARE site on the miR-125b1 and miR-29b1 promoter. The functional regulation of the miR-125b1 ARE site by NRF2 was shown by a luciferase assay. We next showed we could successfully manipulate NRF2, miR-125b and miR-29b in our AML cell lines and AML blasts. Manipulating the dysregulated miRNA levels indicated they play a crucial role in protecting the AML cells from apoptosis. Furthermore, dysregulation of both miRNA are in part responsible for resistance to front line chemotherapy agents in AML. We took an AML blast sample (AML#27) which was underlined by low levels of NRF2 and found to be more sensitive to daunorubicin treatment than other AML Blasts characterised by high NRF2 levels. When NRF2 was ectopically overexpressed in AML#27 using a lentiviral mediated KEAP1 KD, we found a significant increase in resistance to daunorubicin. The KEAP1 KD AML#27 was then transfected with both an miR-125b antagomir and a miR-29b mimic. The synergistic reduction in miR-125b and increase in miR-29b attenuated its resistance to daunorubicin. We finally looked at the mRNA levels of several miR-125b and

miR-29b targets, identifying STAT3, AKT2, and BAK1. Of these targets we confirmed at a protein level STAT3 and BAK1 are indirectly regulated by NRF2.

The oncogenic role of NRF2 has been alluded to in other studies, from chemo-resistance to metabolic reprogramming (Rushworth et al., 2012, Mitsuishi et al., 2012b). This study demonstrates an interesting mechanism by which NRF2 can post-transcriptionally regulate a range of anti-apoptotic and pro-proliferative targets through the regulation of miR-125b1 and miR-29b1. Due to the scope of this study we only analysed a limited number of well characterised miR-125b and/or miR-29b target genes. While this did provide a useful insight into the role of these miRNAs in AML, a more thorough global profiling of the target mRNAs, would be required to fully establish their role in AML and in particular the effect of NRF2 on miR-125b1 and miR-29b1. Of interest are the DNA methylation genes DMNT1, 3A and B. DNA hypermethylation remains an issue in AML, in particular with those suffering from myelodysplastic syndrome or relapsed patients (Ley et al., 2010, Kroeger et al., 2008). Whilst we did not see any changes in the indirect miR-29b target DMNT1, DNMT3A or B were not analysed in this study. It would therefore be of great interest to see if NRF2 regulation of miR125b/29b results in the methylation of tumour suppressor genes. It should also be noted this study only used one AML cell line THP-1 (FAB M5) to determine miR-125b/29b target genes. While we did see an increase in cell death in a range of AML Blasts upon treatment with an miR-125b antagomiR and miR-29b mimic, indicating a shared or similar mechanism of action, a further study needs to be done to establish if the same or

different mRNA targets are responsible for the miRNA effects in different AML subtypes.

Both miR-125b and miR-29b have both been previously characterised as key oncomiR and tumour suppressor miR respectively in AML (Bousquet et al., 2010, Garzon et al., 2009a). It would be interesting to determine whether the cumulative effect of NRF2 on miR-125b1/ miR-29b1 expression is significant in other malignancies.

In this study we provide a rationale behind the plausibility of targeting either NRF2 or miR-125b1/29b1 as a future therapeutic target in AML, both to increase apoptosis among the leukaemic blasts and to improve sensitivity towards chemotherapy agents used in the clinic.

Chapter 5

Modulating the NRF2 Pathway Through Gene Editing

5.1 Introduction

NRF2 plays a dual role in a myriad of oncogenic malignancies, in that it protects healthy cells from DNA damage caused by ROS, however it can also protect malignant cells from chemotherapy-induced damage.

Recent evidence suggests high NRF2 levels (for example in lung, and breast cancers) can aid various oncogenic processes such as cell proliferation, metabolomic and oncogenic reprogramming (Jaramillo and Zhang, 2013). Despite this, more needs to be done to elucidate the mechanisms by which NRF2 acts, in particularly in haematological malignancies, where this pathway is not well characterised.

Manipulation of genes in haematological cells is particularly challenging. Previous attempts to manipulate NRF2 (i.e. through siRNA and Lentiviral mediated miRNA knock-down) while effective were transient and relatively inefficient.

Lately there has been increasing interest in gene-editing technologies such as TALENS and CRISPR-Cas9. Gene editing allows alterations to be made to a specific area of DNA, in recent times using targeted nucleases guided by user-defined sequences to bind and cleave DNA. This results in a double-strand break which can be repaired by the cell using one of two mechanisms; Non-Homologous End Joining (NHEJ) or Homologous Recombination (Zaboikin et al., 2017).

NHEJ is an “error-prone” mechanism which results in an insertion or deletion (INDEL) mutation leading to the disruption of a gene (Rodgers and McVey, 2016). Homologous Recombination is a more specific process, which can accurately repair DNA when presented with a DNA template homologous to the “break”, this is

generally the opposing DNA strand (Rodgers and McVey, 2016). If, an additional "repair" template is available (i.e. through co-transfection with the nuclease) this process can be leveraged to introduce custom modifications into the genome. These two mechanisms make site-directed nucleases invaluable tools in genomic research.

The Type 2 CRISPR system nuclease, Cas9, was initially identified as a member of the bacterial adaptive immune response (Rath et al., 2015). Cas9 derived from Streptococcus pyogenes (spCas9) is the most common type used in gene editing (Gasiunas et al., 2012). The CRISPR-Cas9 system is made up of the nuclease Cas9 (containing both HNH and RuvC nuclease domains) and a crRNA fused to a tracer RNA known as the single-guide RNA (sgRNA) (Cong et al., 2013, Jinek et al., 2012).

The sgRNA is responsible for directing Cas9 to the region of DNA complementary of itself. In the presence of an Protospacer Adjacent Motif (PAM), NGG in the case of spCas9, Cas9 will bind DNA and create a double strand break 3-5bp upstream (5') to the PAM site (Tsai and Joung, 2016). This process can be used to create an INDEL (through NHEJ) or, in the presence of a repair template, insert a custom DNA sequence (through HDR). Despite suffering from increased off-target effects compared with previous iterations of targeted nucleases (such as TALENs), CRISPR has become the preferred method of gene editing. This is in part due to its ease of use, requiring the design of a sgRNA guide to target a specified region of DNA (Cong et al., 2013).

To date, there are several issues with SpCas9, including limited targeting to sequences near an NGG PAM site, off-target cleavage, and targeting efficiency (a problem in "hard to transfect" cells). To account for these limitations, several

modifications have been made to the CRISPR system including the modification of sgRNA (increasing targeting efficiency), discovery of other Cas9 variants (containing different PAM sequences) and other class II CRISPR variants (Ding et al., 2016).

Aims and rationale

To date we have used a miRNA-based system to manipulate levels of NRF2 and KEAP-1. While this system significantly reduces the mRNA levels, the knockdown is not complete and residual mRNA levels are still present. The knockdown is transient, and over a period of time the cells regain levels of NRF2.

We would like to explore the use of a number of gene-editing techniques to see whether we can effectively and efficiently use a site directed nuclease to create cells with disrupted NRF2.

5.2 Results

5.2.1 Cloning guides into LentiCRISPR

LentiCRISPR-V2 was a gift from Feng Zhang (as described in (Sanjana et al., 2014)). The plasmid contains an ampicillin resistance and puromycin selection markers and the original EFS-NS promoter was replaced with an SFFV promoter as this has previously been shown to work well in haematopoietic cells lines (Baum et al., 1997).

To determine the guide RNA (gRNA) sequences we obtained the DNA sequence of NRF2 using the NCBI database (https://www.ncbi.nlm.nih.gov/). To design the guide sequences, we used the CRISPR design tool at the Broad Institute https://portals.broadinstitute.org/gpp/public/analysis-tools/sgrna-design). As with all PCR primers, the gRNA sequence was synthesised and ordered from IDT. The oligos were phosphorylated with T4 Polynucleotide Kinase and annealed. Before the guides were ligated into the plasmid, the plasmid was digested with BsmB1 to remove the stuffer leaving 3' and 5' overhangs. Guide oligos were also designed with overhangs already available when annealed.

Following transformation and plasmid extraction (as described in Materials and Methods) the plasmids were sequenced to ensure correct guide incorporation. The plasmid map and cloning strategy for LentiCRISPR is shown in Fig 5.1.

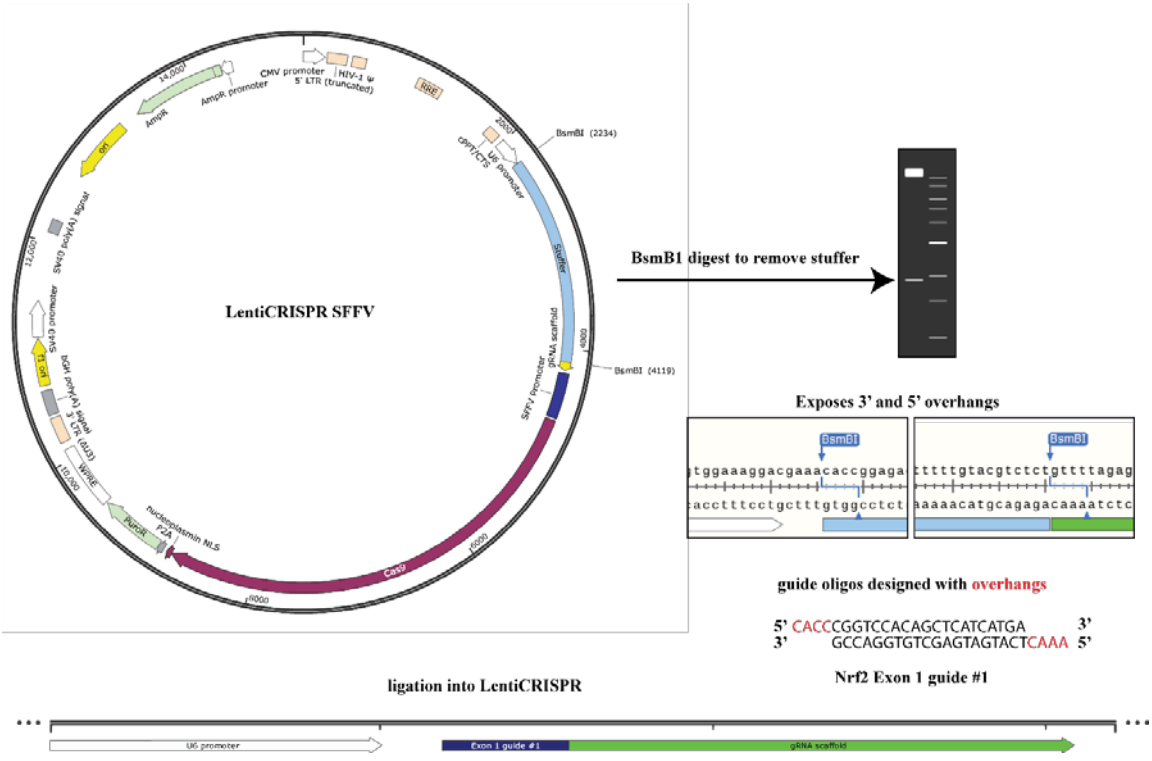

Figure 5.1: **Overview of CRISPR guide cloning** LentiCRISPR-SFFV plasmid is digested with BsmB1 to remove the stuffer region. This generates overhangs for insertion of a guide oligo with compatible sequences (in red). Annealed oligos are ligated into digested plasmid.

5.2.2 Genotyping Primers

Before testing the guide plasmids, we designed and optimised primers to detect the genomic regions being targeting (Exons 1, 2 and 4 in NRF2 and Exon 1 in KEAP1). Primer design spanned each Exon ensuring the guide sequences and PAM sites were within the amplified region. A schematic of the primers and their location with-respect-to the guide sequences is shown for NRF2 Exon 1 (Fig 5.2A) NRF2 Exon 2 (Fig 5.3A) and NRF2 Exon 4 (Fig 5.4A). All primers sets were checked

using the NCBI BLAST algorithm (https://blast.ncbi.nlm.nih.gov/Blast.cgi) to ensure specificity.

Multiple primer sets were tested on genomic DNA extracted from HEK-293 cells.

Exon 1: multiple PCR products were detected in the genotyping PCR for NRF2 Exon 1, and some primer sets (such as NRF2 Exon1 1F/2R) resulted in products that differed from the predicted sizes (Fig 5.2B and C). These regions appeared GC rich and we therefore repeated the Exon 1 genotyping PCR using a "Hot-Start" polymerase (NEB) (data not shown).

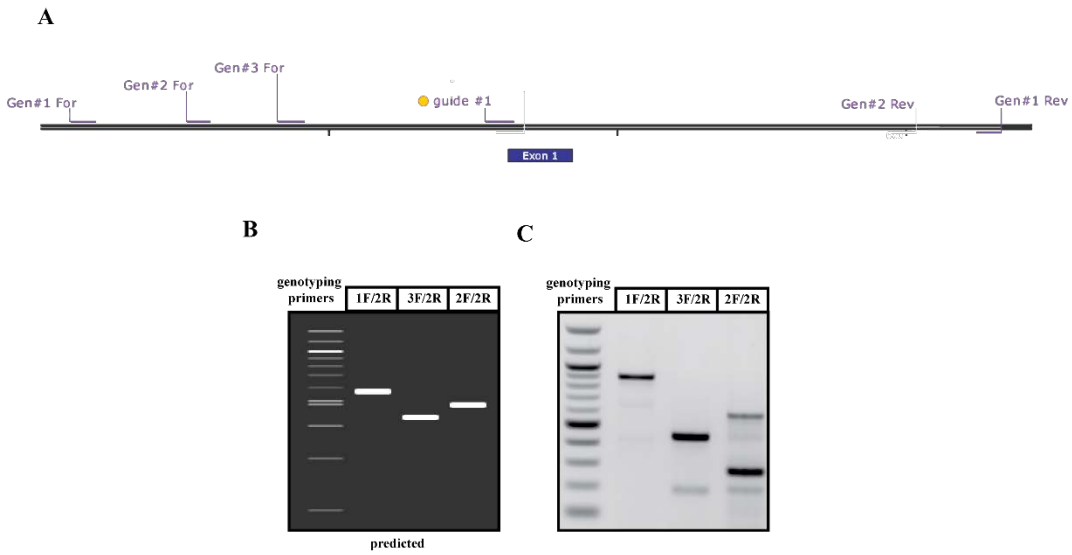

Figure 5.2: **NRF2 Exon 1** A) Exon 1 location of genomic primers and guide sequences B) simulated agarose gel showing predicted product size using Exon 1 genotyping primers. C) agarose gel showing actual product size using Exon 1 genotyping primers.

Exon 2: a genotyping PCR was carried out for NRF2 Exon 2 using a combination of two forward and two reverse primers. No difference was observed between the predicted product size and that found when carrying out the PCR, indicating all tested primers work successfully (Figs 5.3B and C).

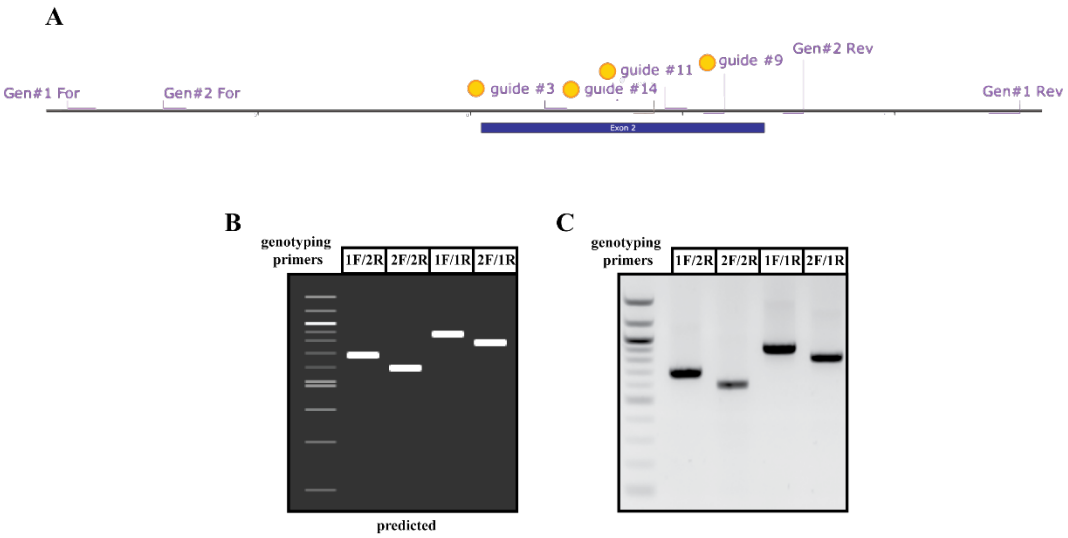

Figure 5.3: NRF2 Exon 2 A) Exon 2 location of genomic primers and guide sequences. B) simulated agarose gel showing predicted product size using Exon 2 genotyping primers. C) agarose gel showing product size of PCR using Exon 2 genotyping primers.

Exon 4: two forward and reverse primer combinations were tested for NRF2 Exon 4, and all primer pairs amplified products matching the predicted size (Figs 5.4 B and C) again indicating all pairs work successfully.

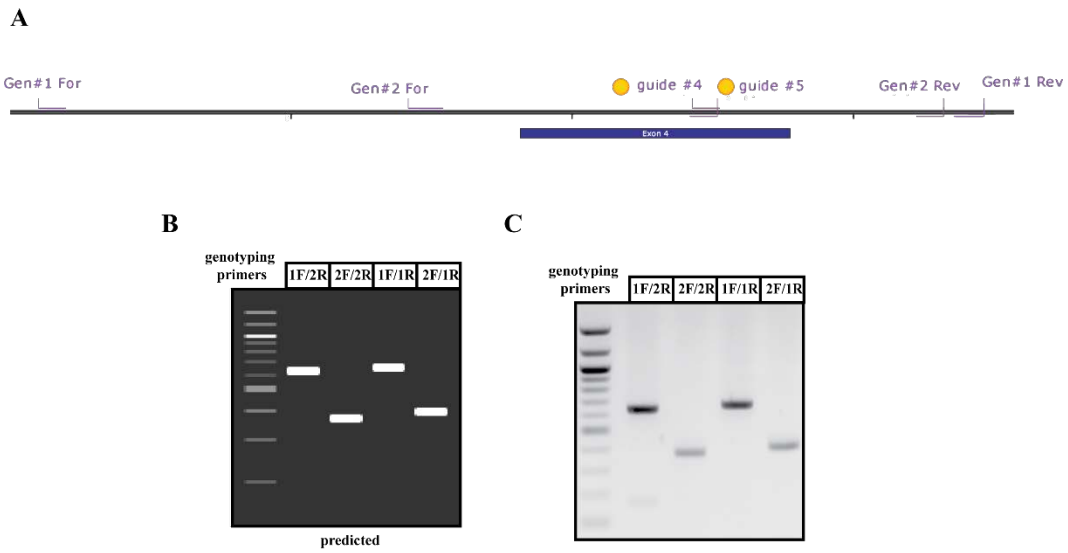

Figure 5.4: **NRF2 Exon 4** A) Exon 4 location of genomic primers and guide sequences. B) Simulated agarose gel showing predicted product size using Exon 4 genotyping primers. C) agarose gel showing product size of PCR using Exon 4 genotyping primers.

5.2.3 Determining CRISPR editing by T7 endonuclease assay

CRISPR-Cas9 disrupts gene function by creating a double-stranded break at a specific locus which, due to the inefficiency of the NHEJ pathway, results in small indels being introduced into the genomic DNA. These indels are too small to resolve from a non-modified genomic locus and therefore we use a DNA-mismatch assay to assess editing efficiency (Fig 5.5).

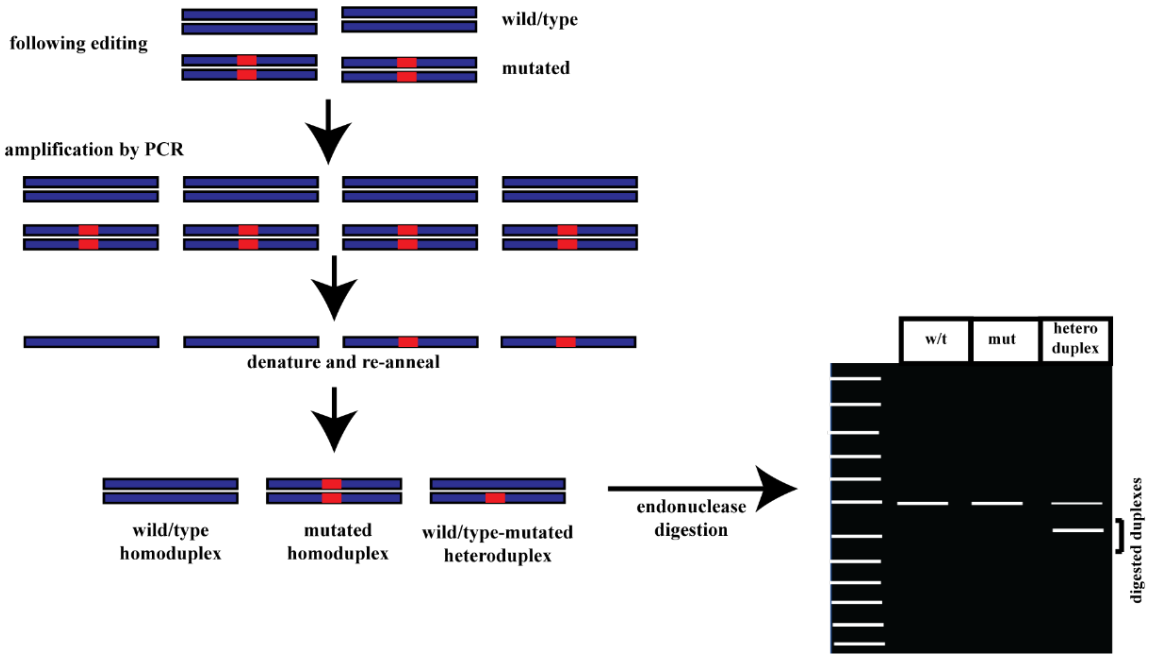

Figure 5.5: DNA mismatch assay using a T7 Endonuclease genotyping on edited cells will result in homoduplexes of both w/t and mutated products. Denaturing and Re-annealing will result in the formation of some heteroduplex DNA (w/t bound to mutated). These mis-matched duplexes can be cleaved by a T7 Endonuclease and the resulting cleaved products are detected using DNA-PAGE.

This assay relies on the fact that a DNA endonuclease can digest mismatched or cruciform DNA structures. Following genotyping at a given modified locus, the PCR products will consist of homoduplexes of wild-type and modified sequences. By denaturing and re-annealing the PCR products heteroduplexes of wild-type and modified DNA will then be present (as well as the wild-type and modified homoduplexes). The endonuclease is then able to cleave the mismatched heteroduplexes fragments which are then resolved using DNA-PAGE (see **Materials and Methods**).

5.2.4 Guide efficiency in HEKs

A schematic of the guide sequences and adjacent PAM sites can be seen for NRF2 Exon 1 (Fig 5.6A), Exon 2 (Fig 5.7A) and Exon 4 (Fig 5.8A). All Exons apart from Exon 1 (due to its size) were targeted with at least 2 guide sequences. LentiCRISPR plasmids containing the various guide sequences were then transfected into HEK293T cells for 72 h before genomic DNA was extracted and analysed. HEK293T cells were used for guide validation as they are easy to transfect with high efficiency. Genotyping PCRs were performed for all targeted Exons and a small amount of the PCR reaction was separated on a 1.5% agarose gel to check for amplification.

The remainder of the PCR reaction was denatured and slowly re-annealed to allow formation of heteroduplex DNA. The re-annealed product was either left untreated (uncut) or digested with a T7 Endonuclease (cut) prior to separation on a DNA PAGE gel.

Exon 1: The PCR product for NRF2 Exon 1 showed successful amplification showing a product running at the same size as the untransfected, control genomic DNA (Fig 5.6B). Unexpectedly, when the PCR products were denatured and annealed two additional bands were seen in the control genomic DNA sample and these were processed with the T7 endonuclease. It is unclear what these bands represent but as they were not apparent on the Agarose gel and are not smears they likely represent specific mutations introduced by the Taq polymerase. When genomic DNA was analysed from 2 repeats of a guide#1 transfection these bands were absent and only 2 cleavage products were observed with a combined size of the intact PCR product (Fig 5.6C). These fragments are thus a consequence of guide#1 cleaving the genomic DNA and suggests INDEL mutations have occurred.

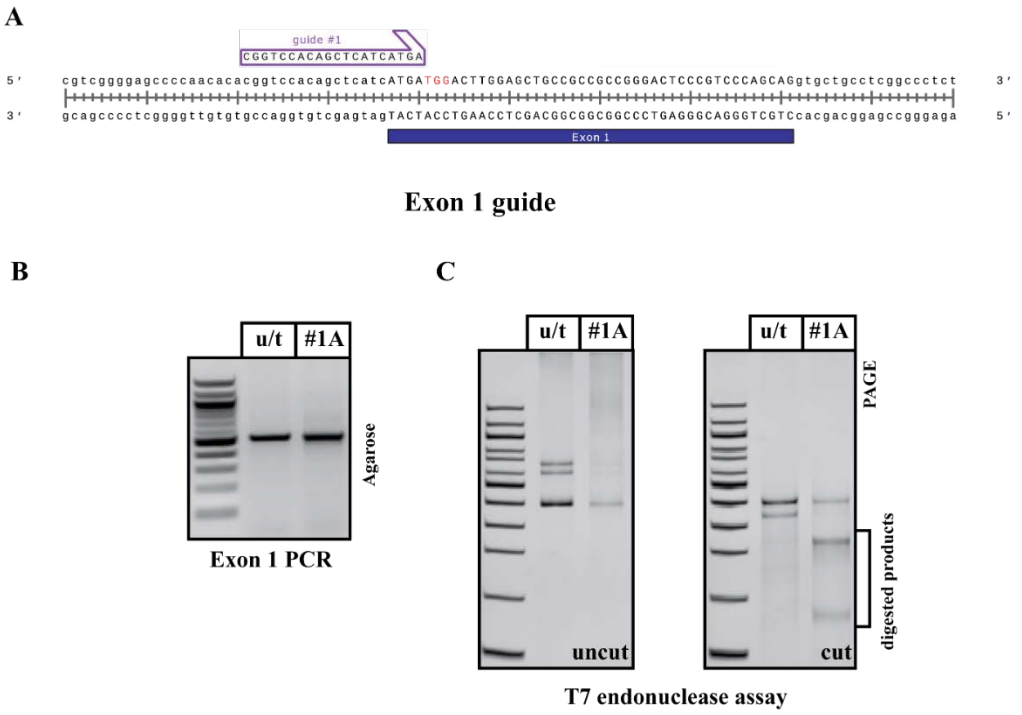

Figure 5.6: T7 endonuclease assay on Exon 1 guides A) Sequence of guide and corresponding PAM site (red). B) Amplified Exon 1 DNA run on an agarose gel. DNA was extracted from control (u/t) or HEK-293 cells transfected with guide #1. Transfection was repeated twice (#1A and #1B). C) Amplified DNA was denatured and re-annealed. Re-annealed DNA was separated on a DNA PAGE gel without (uncut) or following incubation with the T7 Endonuclease (cut).

Exon 2: Four guides were tested targeting Exon 2 (#3, #9, #11, and #14). Successful amplification from transfected cells was seen on an agarose gel (Fig 5.7B). No cleavage fragments were on the uncut gel however smearing was apparent above guides #9, #11 and #14. Mobility of heteroduplex DNA on DNA PAGE gels is retarded compared to homoduplexes and the smearing is a good early indicator that editing has occurred. Following incubation with the endonuclease a number of cleavage products were observed with guides #9, #11 and #14 (Fig 5.7C). The

"smearing" in these lanes was also reduced. This indicates these guides were cutting efficiently. No cleavage fragments or smearing was observed with guide #3, indicating no editing has occurred.

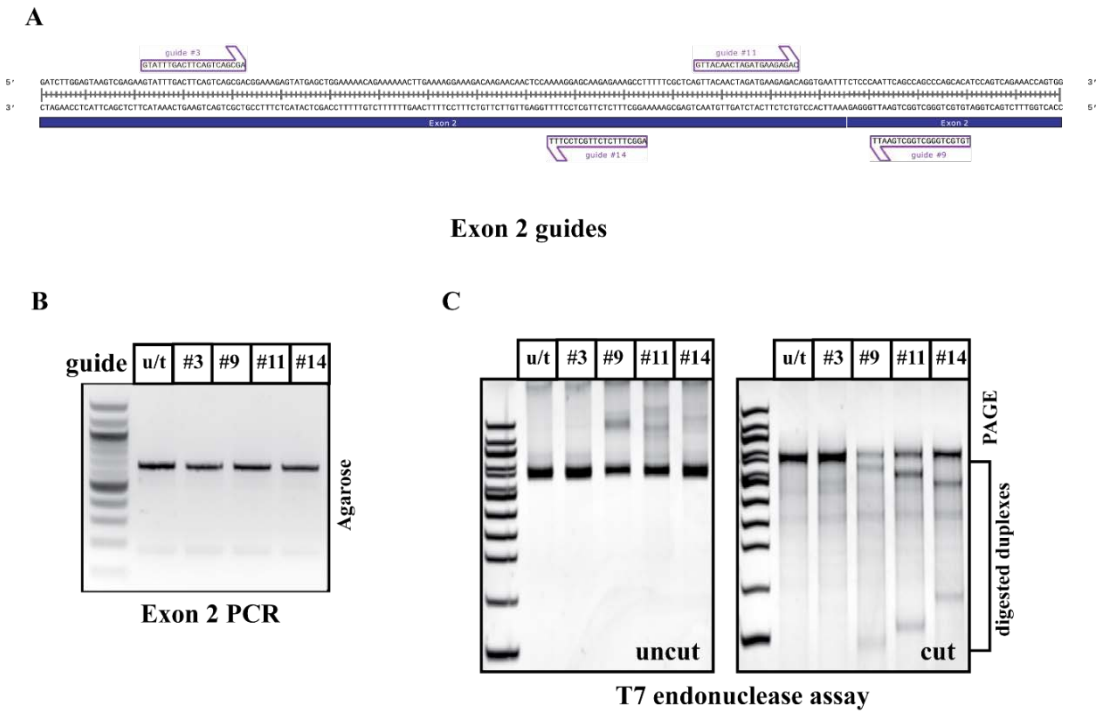

Figure 5.7: T7 endonuclease assay on Exon 2 guides A) Sequence of guide #3, 9, 11 and 14 and corresponding PAM site (in red). B) Amplified Exon 2 DNA separated on an agarose gel. DNA was extracted from control (u/t) or HEK-293 cells transfected with guide #3, 9, 11 or 14. C) Amplified DNA was denatured and re-annealed. Re-annealed DNA was separated on a DNA PAGE gel without (uncut) or following incubation with the T7 Endonuclease (cut).

Exon 4: Two guides (#4 and #5) were tested targeting NRF2 exon 4. Both guides were transfected individually or co-transfected (4+5). Exon 4 was PCR amplified and subjected to a T7 assay. No band-shift was seen in the uncut gel, however post

incubation with T7-endonuclease, a successful band-shift is seen in #4, #5 and #4+5 (Fig 5.8C). This again confirms the ability of the CRISPR/guide construct to target exon 4 of NRF2.

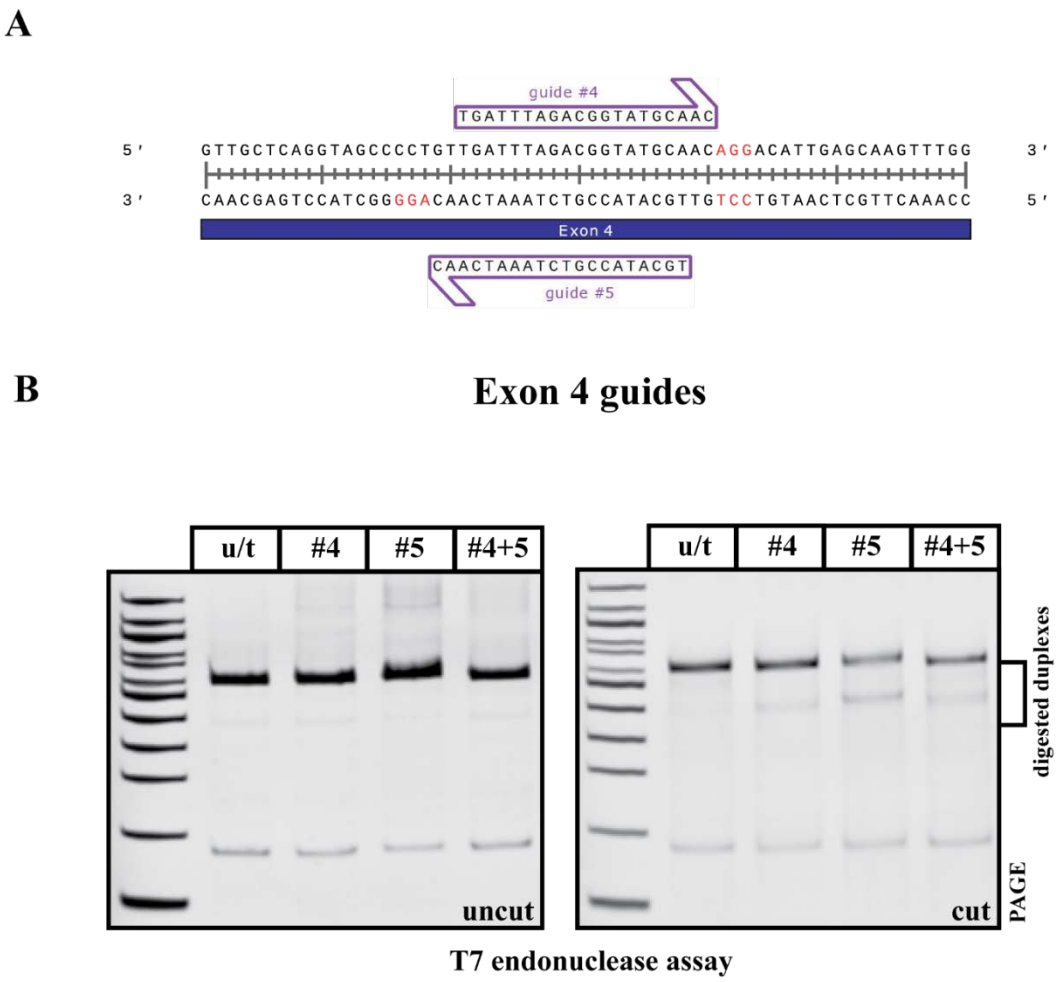

Figure 5.8: T7 endonuclease assay on Exon 4 guides A) Sequence of guide #4 and 5, along with the corresponding PAM site (in red). B) Amplified Exon 4 PCR was denatured and re-annealed. Re-annealed DNA was separated on a DNA PAGE gel without (uncut) or following incubation with the T7 Endonuclease (cut).

5.2.5 Editing NRF2 Exon 4 with TALENs

One alternative to using CRISPR is Transcription Activator-Like Effector Nucleases or TALENS. Unlike CRISPR-Cas9 or CRISPR-Cpf1 which both use an RNA component to target DNA with TALENS the DNA recognition domain is a protein component fused to the Fok1 nuclease.

CRISPR is popular as it is easily "re-taskable", and multiple guide constructs can be made and validated within a short time period. TALEN construction is somewhat challenging, and the entire array must be re-made to "re-task". TALENS are also much more sensitive to base changes (such as SNPs) or DNA methylation (Valton et al., 2012). However, because of this and the bipartite structure of the Fok1 nuclease their "off-target" effects are considerably lower than with CRISPR. The only reported gene-editing on primary cells that have been "returned" to patients has been using TALENs (Qasim et al., 2017).

We designed a TALEN pair targeting Exon 4 of NRF2 using ChopChop (http://chopchop.cbu.uib.no/) (Montague et al., 2014). Each TALEN targets opposing strands of DNA and when both bind within ~20bp of each other, then the Fok1 nuclease is able to dimerise and create a double-strand DNA break. The sequence of the chosen TALEN pair is shown in Fig 5.9A.

The TALE modules are identical apart from two central amino acid residues the RVDs which confer the DNA binding ability of the TALEN. NN binds Guanine, NI -Adenine; HD – Cytosine and NG – Thymidine. When arrayed within each plasmid and fused to the Fok1 nuclease they collectively make up the DNA binding domain. The two TALENs containing the arrayed repeats are shown in Fig 5.9B.

TALENs are constructed using “golden-gate” cloning. This relies on Type II restriction enzymes (e.g. Bsa1, Bbs1 or BsmB1) which unlike other restriction enzymes cleave adjacent to their binding site. The orientation of the binding site determines whether the cleavage is 5’ or 3’ to binding, importantly this also means that the exposed DNA ends can be incompatible.

The set of plasmids used here were from the Voytas lab (Cermak et al., 2011). Each RVD module is contained within one plasmid flanked by Bbs1 restriction sites. Each RVD is contained within 1 of 10 plasmids and each plasmid must be used sequentially. For example, if HD NI NG is required plasmids pHD1, pNI2 and pNG3 are used for assembly. The plasmids are arranged within one digestion/ligation reaction and cycled (37°C and 16°C) for digestion and ligation.

The arrays are made in 2 parts. Part 1 assembles the first 8 RVDs, part 2 RVDs 9-18 with the final RVD added when the two parts are assembled. Construction of the Left-Hand TALEN is shown in Fig 5.10. DNA from clones were mini-prepped and PCR screened. The repetitive nature of the TALEN repeats means that positive clones do not give a single band (corresponding to however many TALE repeats are in the assembly) but instead show a smearing or ladder-like effect due to polymerase slippage (Hommelsheim et al., 2014). We obtained several clones (marked in green) which exhibited this smearing, and these were used for the final assembly. The finished TALEN constructs were sequenced before use and a linear schematic of both is shown in Fig 5.11A.

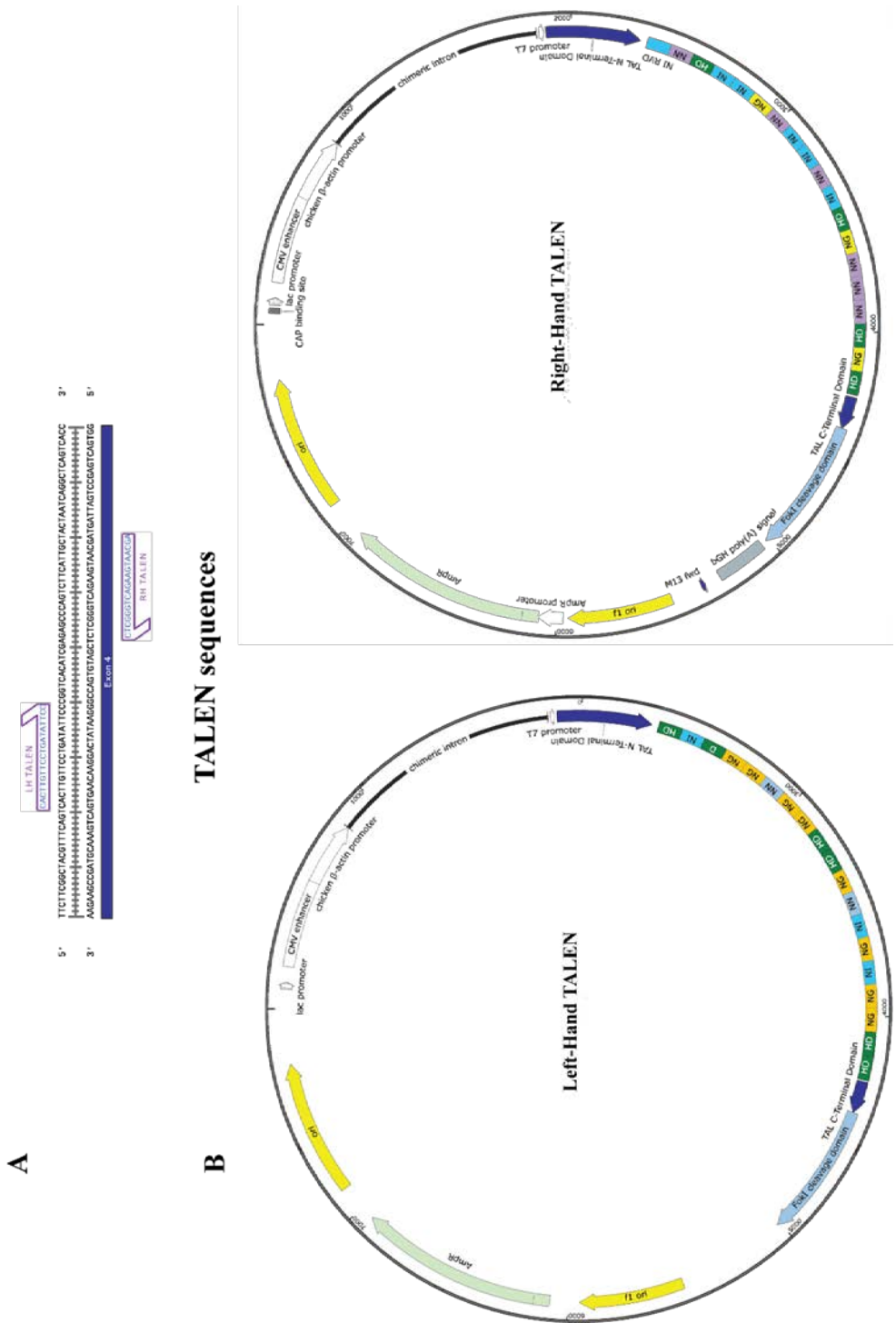

Figure 5.9: Construction of TALEN pair targeting NRF2 Exon 4 A) map of Nrf2 Exon 4 with Left- and Right-Hand TALEN target sites on opposing DNA

strands B) maps of Left- and Right-Hand TALEN pair, the RVD repeats on both pairs are shown

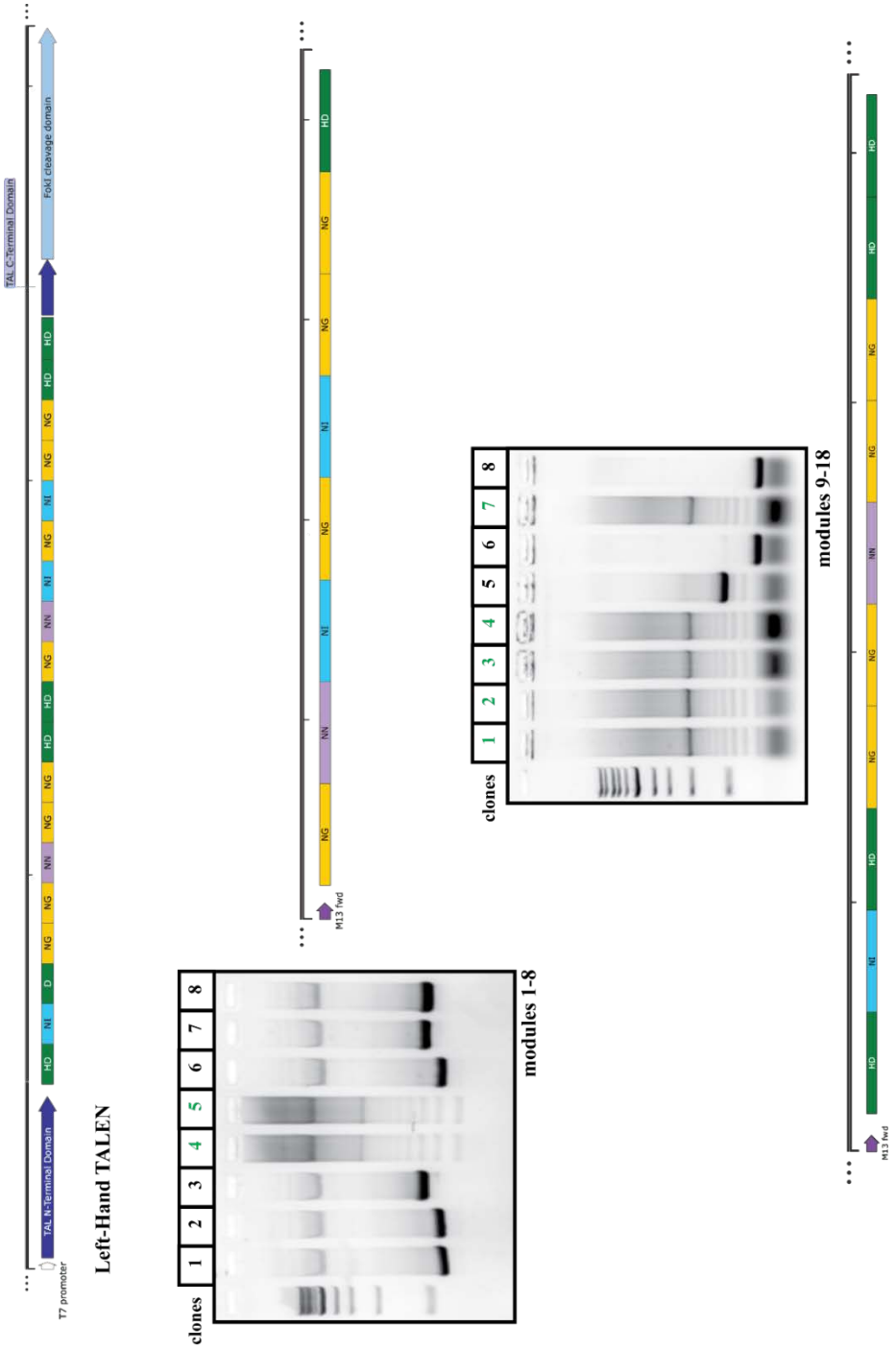

Figure 5.10: Construction of Left-Hand TALEN construct linear map of Left-Hand TALEN. Map and PCR screen of part#1 (modules #1-8) and part#2 (modules

#9-18). Due to nature of the repeated sequences smears and laddered bands indicate successful assembly - positive lanes marked in green

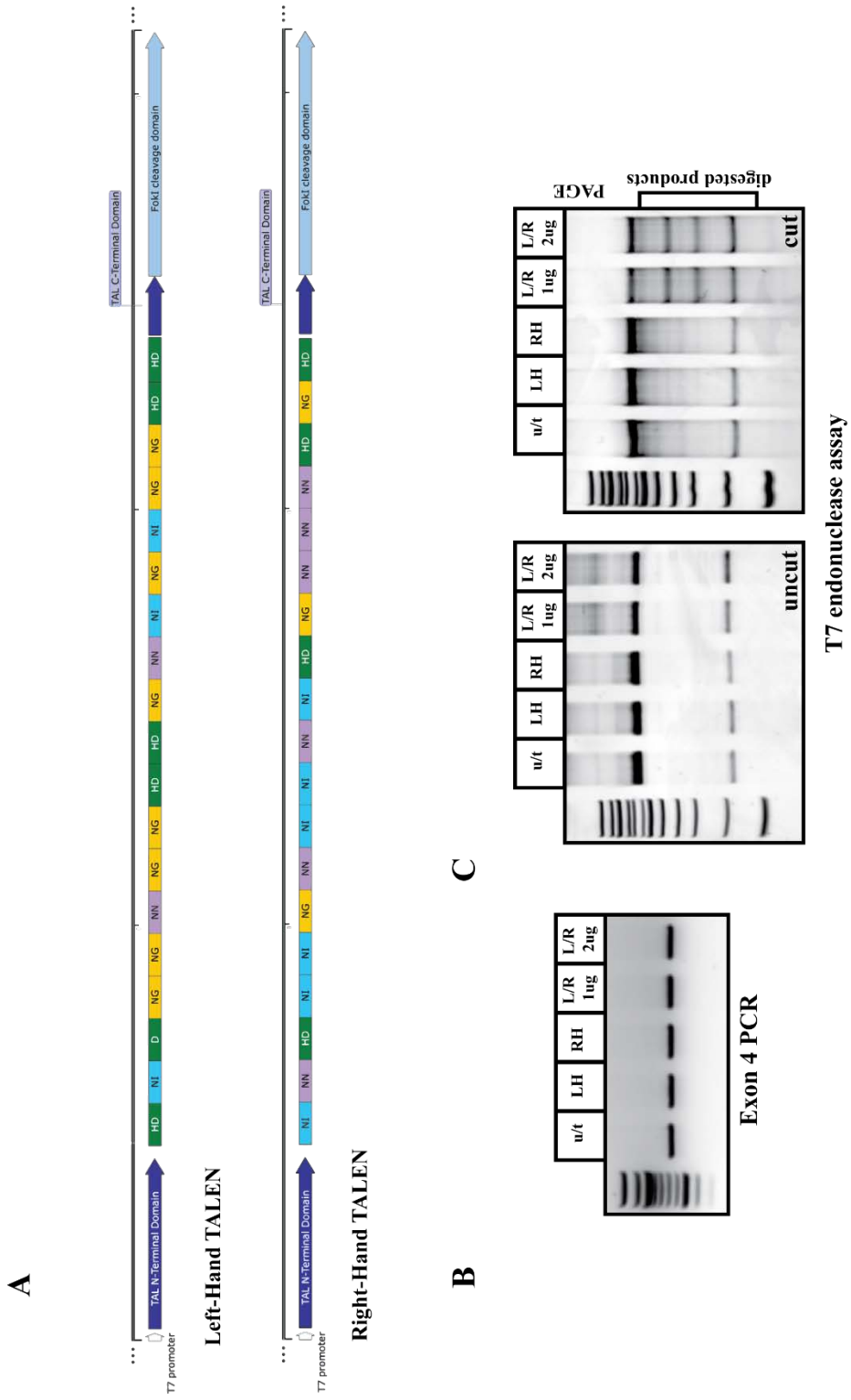

Figure 5.11: Validation of TALEN pairs on NRF2 Exon 4 A) linear map of final Left and Right Hand TALENs B) Exon 4 PCR following transfection of HEKs with single and TALEN pairs. C) Amplified DNA (from TALEN - transfected HEKs) was denatured and re-annealed. Re-annealed DNA was separated on a DNA PAGE gel without (uncut) or following incubation with the T7 Endonuclease (cut).

The TALENS were validated in HEK293T cells and transfected both as single plasmids and as pairs. As with CRISPR the cells were left for 72h before cells were harvested for genotyping and T7 assay. A single band was seen on an Agarose gel following genotyping of this region (Fig 5.11B) although TALENs act in pairs they create only one double-strand break unlike when using CRISPR pairs. When a T7 Endonuclease assay was performed no cleavage was observed in untransfected, or when the TALENs were transfected alone Fig 5.11C. However, when they were transfected as a pair extensive heteroduplex formation was seen on the uncut PAGE gel and these products were heavily processed following incubation with the Endonuclease.

This data shows that the constructed TALEN pair is capable of efficiently editing Exon 4 in NRF2.

5.2.6 Cpf1 guides targeting NRF2 Exon 4

Cpf1 is a Class II Type-V variant of Cas9 which contains the RuvC but not the HnH domain with the RuvC being able to cleave both DNA strands. There are several advantages of using Cpf1 compared with Cas9 these include; shorter guide sequences, a different PAM site and a cleavage site distal to the PAM leaving a staggered end. Perhaps most importantly, unlike Cas9, Cpf1 guides can be easily

multiplexed without the need for additional/individual promoters or splicing elements (Zetsche et al., 2015a).

To assess whether Cpf1 would be able to edit NRF2 we designed guides to Exon 4 using the design tool at Benchling (https://benchling.com/). Cpf1 has an unusual requirement as its tracer RNA is located 5' to the guide sequence (unlike that with Cas9) and it favours a 5' XTTT 3' PAM site. Guides were cloned into pY108, a lentiviral plasmid which expresses AsCpf1 and the tracer RNA under the control of a U6 RNA promoter (Fig 5.12A).

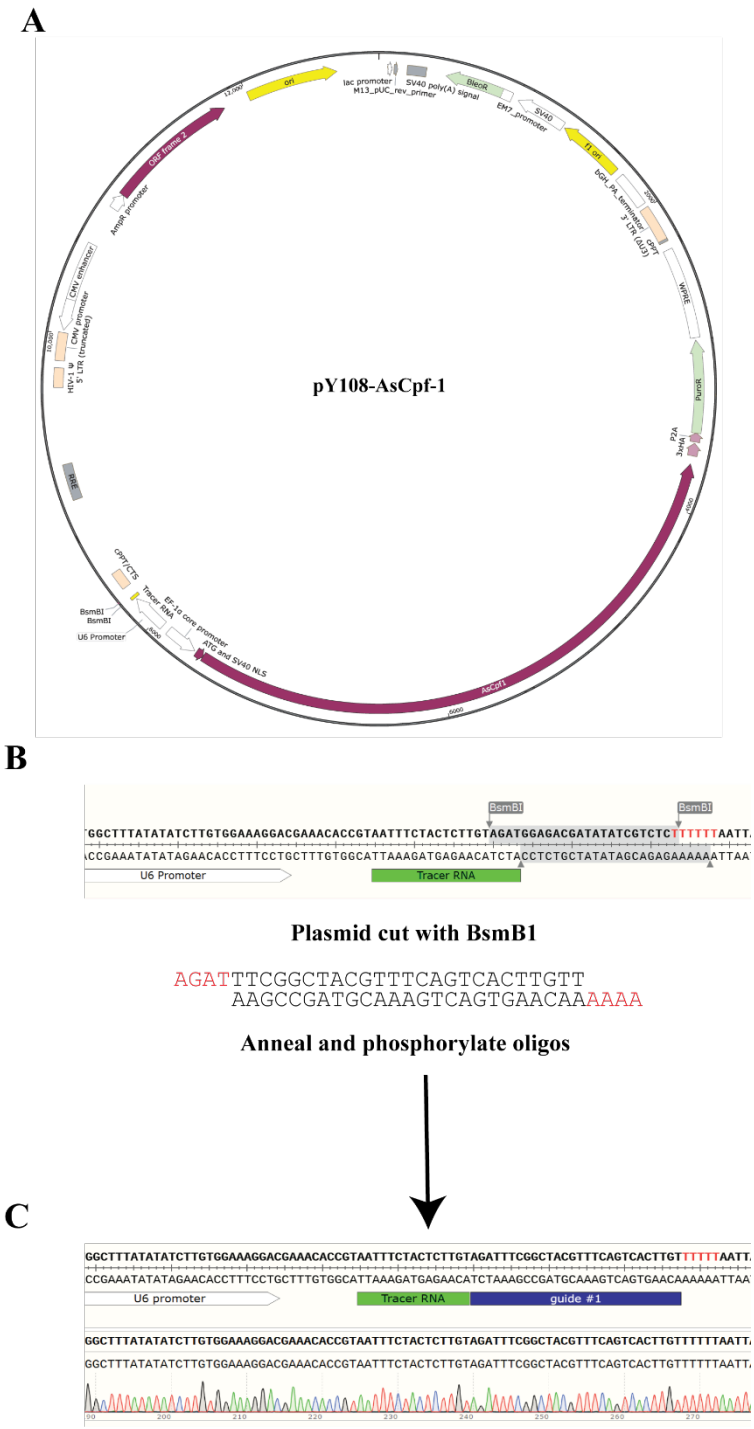

Figure 5.12: Cloning Cpf-1 guides A) map of pY108 plasmid, expressing both the Cpf1 nuclease and tracer RNA B) overhangs following BsmB1 digestion with an

example annealed guide oligonucleotides C) guide ligation into the pY108 plasmid under a U6 promoter.

As before, the plasmid was cut with BsmB1, and the stuffer excised. Five guides were designed, targeting Exon 4 of NRF2. Oligos were annealed and phosphorylated, before being ligated into BsmB1-digested pY108 and sequenced (5.12B and C). A linear map of NRF2 Exon 4 detailing the Cpf1 guide sequences is shown in Fig 5.13A.

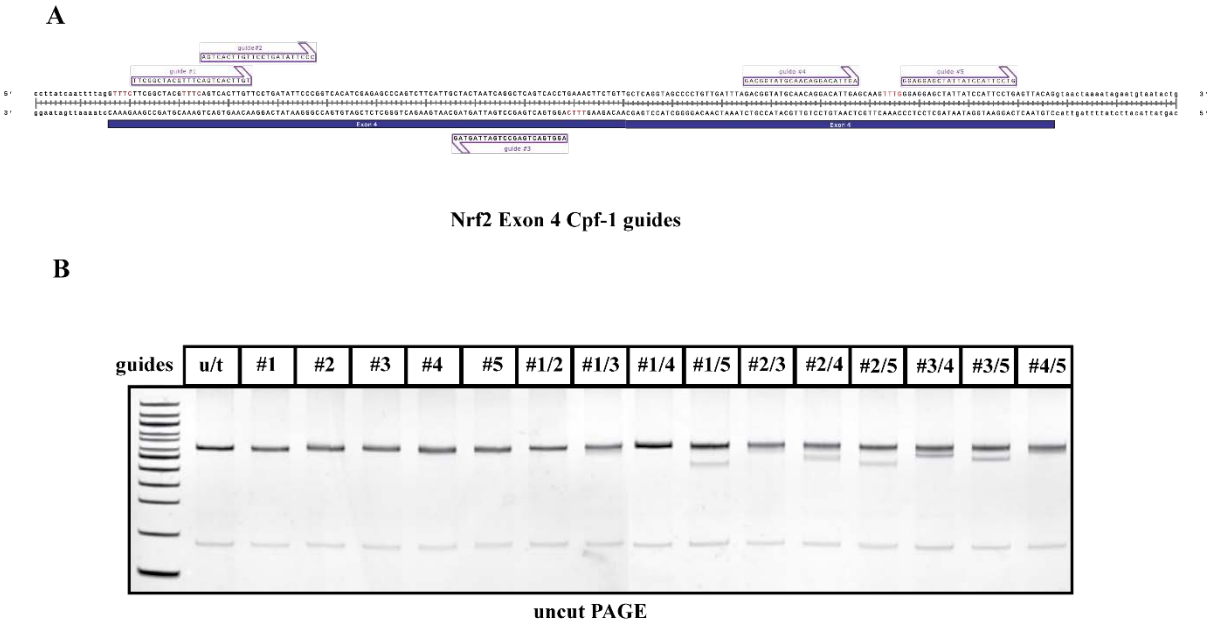

Figure 5.13: Validation of Cpf1 guides on NRF2 Exon 4 A) The location and sequences of Cpf1 guides and the corresponding XTTT PAM sites (in red) B) Cpf1 guides were transfected into HEK-293 cells as single or paired plasmids for 72h. Genotyping of Exon 4 following guide transfection paired guides will remove a region of genomic DNA resulting in a smaller PCR product.

Plasmids were transfected into the HEK-293 cells individually or as pairs. As with the Cas9 constructs, cells were incubated for 72 hours then genomic DNA was extracted and Exon 4 amplified. A single product was seen in all single guide samples and no other bands were present (Fig 5.13B). However, when transfected as pairs an additional band was seen below the band seen in the untransfected cells. Guide pairs #1/5, #2/4, #2/5, #3/4 and #3/5 all produced a double band indicating these guide combinations are successfully excising part of Exon 4.

This data shows that Cpf1 guides are able to edit NRF2 Exon 4 especially when paired with other guides. The guides pairs were transfected as separate plasmids but the fact that Cpf1 guides can easily be multiplexed under the same U6 promoter within the same plasmid means several of those identified here could be assembled without significantly affecting plasmid size.

Some of the single guides are likely to successfully edit cells, a T7 endonuclease assay is required to confirm this. Clearly though the use of multiple guides facilitates genotyping of edited cells as it negates the requirement for the Endonuclease assay.

5.2.7 Cloning KEAP1 guides and editing KEAP1 in HEK-293 cells

Similar to NRF2, guides were designed to target Exon 1 of KEAP1 using the online tool at the Broad website. Unlike NRF2, the guides were spaced apart from each other the rationale being if successful cleavage occurs by two guides simultaneously excision of a fragment from Exon 1 would occur. This could potentially allow us to genotype cells without the use of a T7 endonuclease assay. Genotyping primers were also designed to flank the guide sequences Fig 5.14A. The sequence of the

two CRISPR guides targeting KEAP1 (#1 and #3) can be seen in Fig 5.14B along with the PAM sites (in red).

Guides were cloned into the LentiCRISPR-SFFV gRNA vector using the same method as previously described for NRF2. Guides were sequenced and before transfection into HEK-293T cells. Cells were incubated for 72 hours before DNA was extracted, and KEAP1 Exon 1 was amplified. The amplified DNA was denatured and slowly reannealed before being separated by DNA-PAGE.

The uncut gel showed a single band in the u/t, guide #1 and guide#2. Multiple products were seen when both guide #1 and 2 were transfected together (Fig 5.14C). There appeared to be very little of the intact Exon 1 PCR product remaining suggesting a fragment of Exon 1 has been excised. When these products were digested with the T7 endonuclease cleavage products were observed with the two single guides, but the digestion was even more extensive when both guides were used together. This again indicates successful genome editing has occurred.

The use of the two guides together appears to have two consequences a) it makes genotyping easier as only an agarose gel is required to see whether both guides have cut and b) the efficiency of the guides together appeared to be much greater than when used individually.

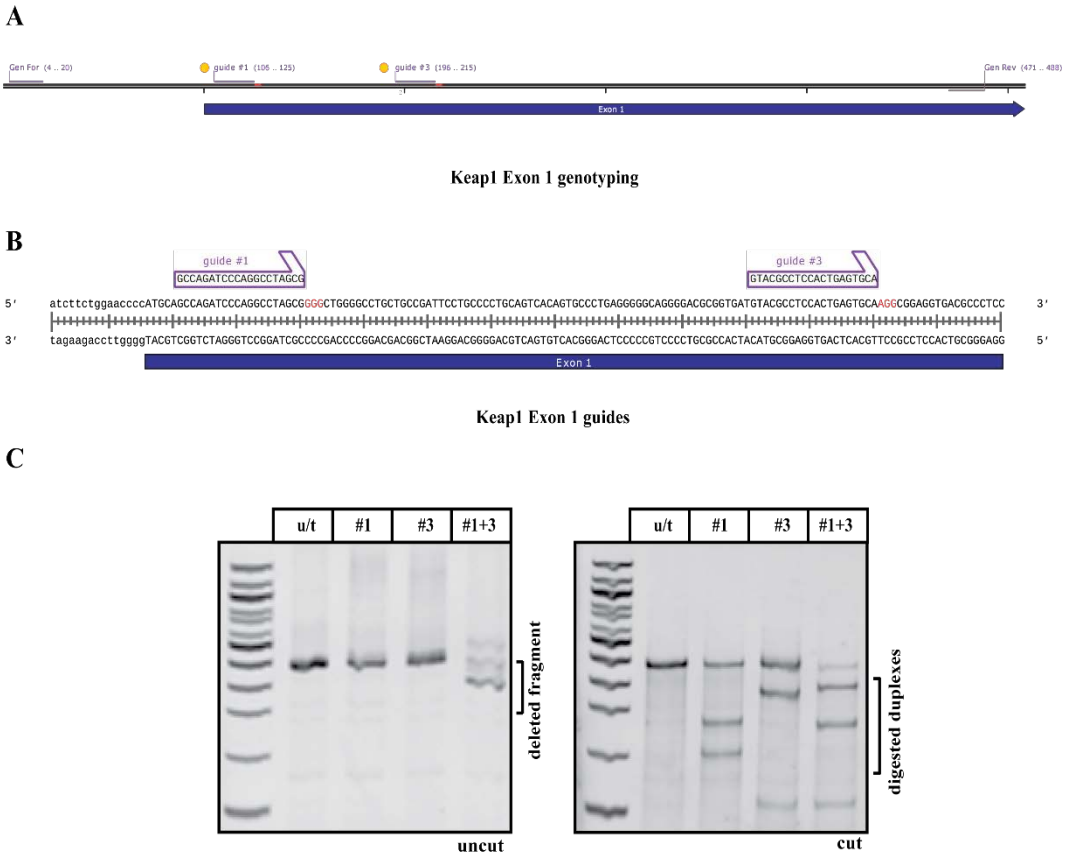

Figure 5.14: Keap1 guides A) Keap-1 Exon 1 schematic showing position of genotyping primers and guides B) sequence of two Exon 1 guides (#1 and #3) C) DNA was extracted and amplified post transfection with Keap1 Exon 1 guides. Amplified DNA was denatured and re-annealed. Re-annealed DNA was separated on a DNA PAGE gel without (uncut) or following incubation with the T7 Endonuclease (cut).

5.2.8 Generation of NRF2 and KEAP1 deficient HCT-116

Now we have shown the LentiCRISPR constructs can successfully show genome editing, we wished to create an NRF2 edited cell line. Whilst we still aim to make NRF2 deficient leukaemia cells, AML cells are torturously difficult to transfect and a viral vector will likely be necessary. We picked an easier to transfect cell line and thus decided to modify both NRF2 and KEAP1 in the colorectal cancer cell line HCT-116. $4x10^5$ cells HCT-116 cells were transfected with LentiCRISPRv2 targeting exon 4 of NRF2 (using the guides NRF2 #4, #5 and #4+#5). Exon 1 of KEAP1 was also targeted (KEAP1 #1, #2 and #1+#2). Genomic DNA was extracted after 72 hours, however limited evidence of editing was seen (data not shown).

The LentiCRISPRv2 plasmid contains a puromycin selection marker, thus allowing us to positively select those successfully transfected with the plasmid. Two concentrations of puromycin was used (2.5 and 5 µg/ml), and the cells were incubated for 72 hours. after-which genomic DNA was extracted from these cells. NRF2 exon 4 and KEAP1 exon 1 was amplified. The DNA was denatured and re-annealed before being run on a PAGE gel with/ without T7 endonuclease incubation.

The NRF2 Exon 4 (Fig 5.15A) uncut gel showed a single PCR product in all samples. Smears were seen above all NRF2 samples transfected with a guide and with both concentrations of puromycin, suggesting the presence of heteroduplex DNA. This was confirmed by the cut gel, showing a band shift in all transfected samples compared to the u/t. The lack of the upper band in samples treated with

5ug/ml puromycin suggests a high proportion of the selected population has undergone editing.

Similarly KEAP1 exon 1 (Fig 5.15B) uncut gel showed a single PCR product for the individual guides (#1 and #2) in both concentrations of puromycin. The double guide (#1+#2) showed multiple bands in both puromycin concentrations, indicating successful editing has occurred. The cut gel confirmed these results, with a band shift detected in all transfected sample.

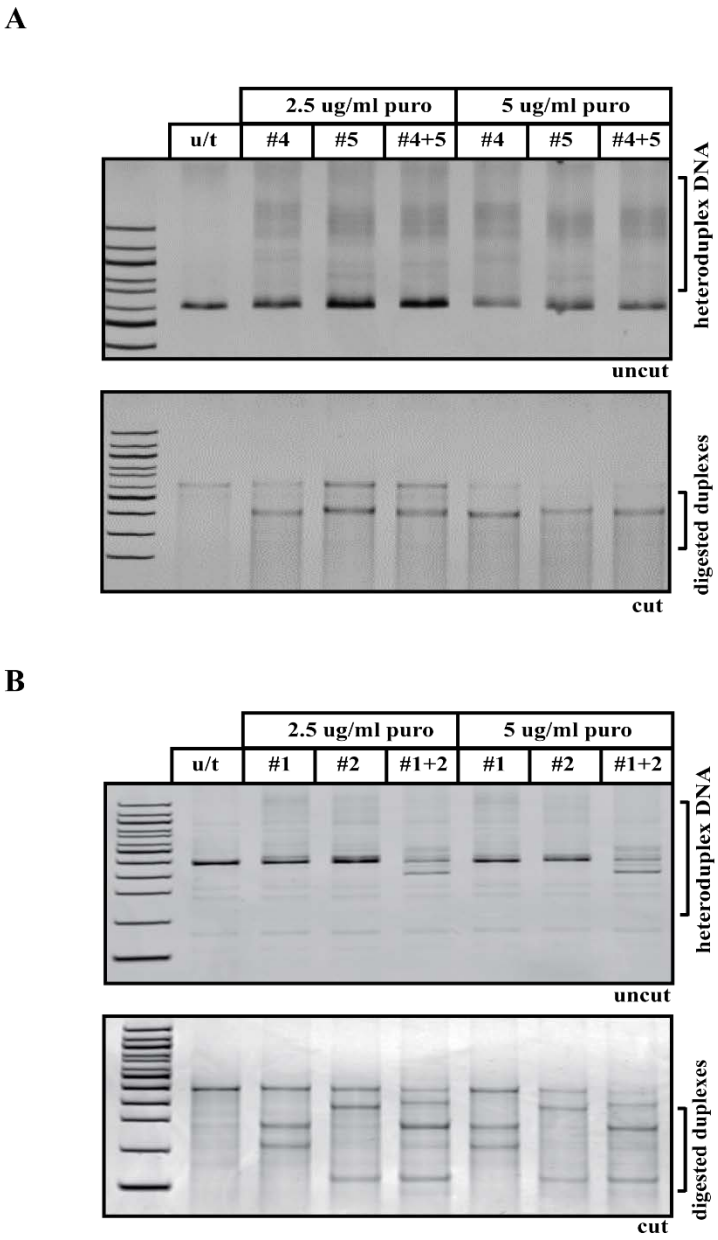

Figure 5.15: Generation of NRF2- and KEAP1-deficient HCT116 cells A) NRF2 Exon 4 guides #4, #5 and #4+5. b) KEAP1 guides #1. #2 and #1+2. Cells were transfected with NRF2 and KEAP1 guides for 72 hours before the addition of puromycin (2.5 or 5µg/ml). DNA was amplified and denatured/ re-annealed. T7 endonuclease assay was performed on un-transfected and puromycin-selected cells as indicated

The CRISPR-Cas9 system does not create a defined mutation instead most commonly creates an INDEL 3-5bp upstream of the PAM. The puromycin-selected cells will therefore contain a population with varied mutations both heterozygous and homozygous.

In order to create populations of HCT-116 cells deficient in NRF2 we would need to clonally isolate the cells. To achieve this, we performed serial dilutions of the selected cells and plated them at approximately 0.5 cells/well into 96-well plates.

We identified individual clones visually using standard light microscopy. Wells with colonies originating from a single source were identified as single clones. Those with cells growing from multiple sources (or containing no clones) were also marked. Once the clones had reached confluency, they were split into 2x further 96-well plates.

At this stage we needed to identify which clones were expressing NRF2 and so one the "daughter" plates was treated with the proteasome inhibitor MG-132 (to stabilise NRF2) for 2h. Protein was extracted (using SDS sample buffer), and lysates Western blotted for NRF2 or β-actin. 48 clones were tested per guide (144 in total). The lack of an NRF2 band in a lane with a β-actin band would correspond to a deficient clone.

As shown in Fig 5.16, NRF2 expression was detected in a number of clones (i.e. Guide #4 clone 3+4), however we were unable to detect NRF2 in several clones (for example Guide #4 clone 2 and 5). In addition, we also detected clones expression NRF2 but running at a lower molecular weight than expected (for example Guide #2 clone 43). This could indicate a truncation has occurred. We

picked 34 clones that were negative for NRF2 and expanded them for further analysis

Once confluent, we tested three clones per guide to confirm the absence of NRF2. Clones were again treated with MG-132 but as there were more cells available lysates were prepared and protein assays performed to normalise protein loading. Lysates were then Western blotted for NRF2 and β-actin with untransfected HCT-116 cells used as a positive control.

MG-132 was able to induce NRF2 expression in the wild-type HCT-116 cells, but not in any of the nine clones chosen. The β-actin band present in all the clonal samples re-confirms these clones were deficient in NRF2 (Fig 5.17).

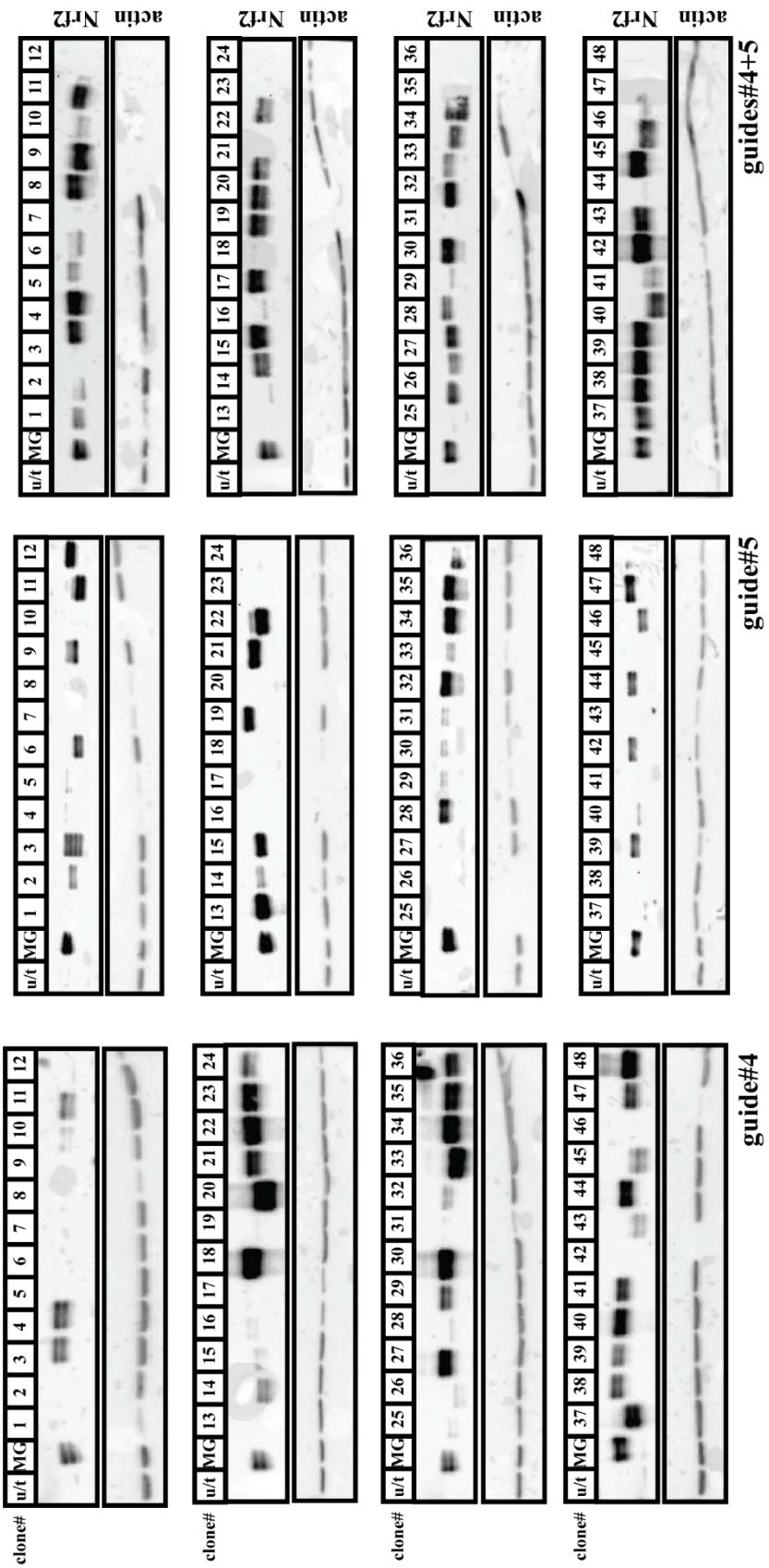

Figure 5.16: Deriving NRF2-edited clones from puromycin selected HCT-116 cells A polyclonal pool of puromycin-selected HCT116 cells single cell cloned by limiting dilution in 96-well plates. 48 clones from each guide (#4, #5 and #4+#5) were isolated and treated with 10μM MG-132 for two hours to stabilise NRF2. Protein expression was detected by Western blot using NRF2 and β-actin antibodies

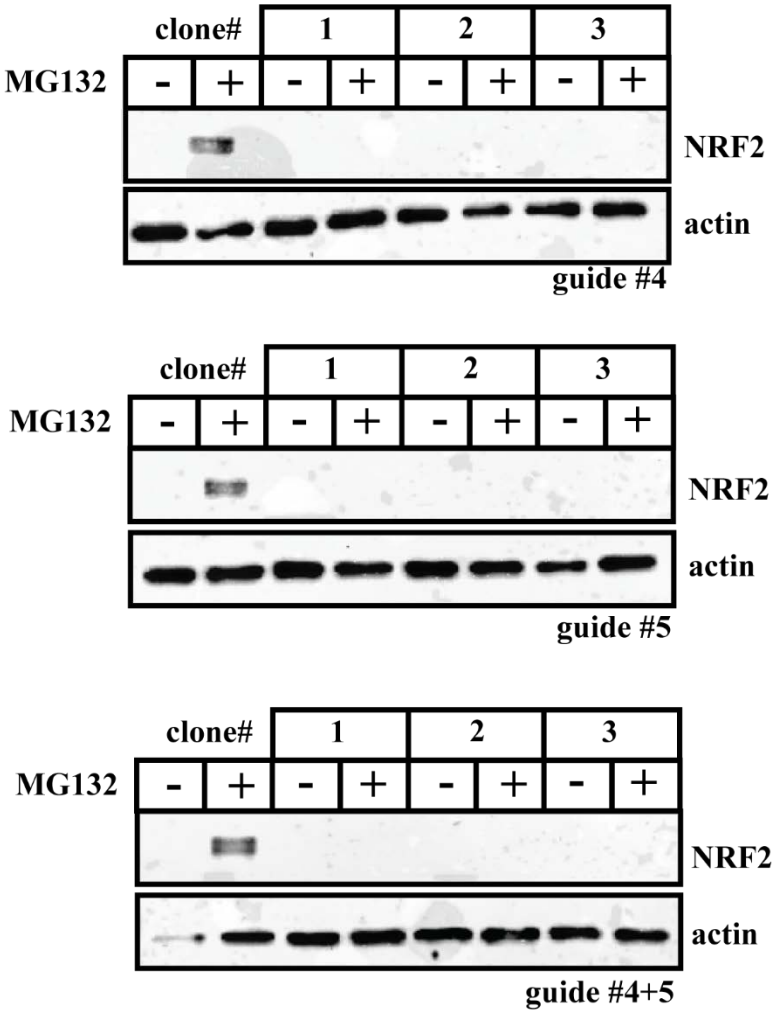

Figure 5.17: Confirmation of NRF2-deficient HCT-116 clones 3 clones per guide were treated without/ with 10μM MG-132 for two hours to stabilise NRF2. Protein expression was detected by Western blot using NRF2 and β-actin antibodies.

5.2.9 Generation of NRF2-deficient K562 cells

We next wished to see whether we could use some of the NRF2 targeting plasmids we have characterised earlier to knock-out NRF2 in haematopoietic cells lines. These lines are notoriously hard to transfect, compared to HEK293T or HCT-116

cells, and therefore we used the Exon 4 LentiCRISPR plasmids to make Lentivirus to transduce the cells. We initially started out in the Chronic Myeloid Leukaemia cell line, K562 as they have been shown to be more transducible with Lentivirus than AML lines (such as THP-1s). To create viral particles HEK-293T were transfected with the viral packaging vectors pRSV-REV, pMDLG-RRE and pCMV-VSVG and either LentiCRISPR containing NRF2 guide #4 or #5. The lentiviral particles were harvested in the supernatant and concentrated by ultracentrifugation before use. To test the editing ability of the viral particles, we first transduced HEK-293T cells. DNA was extracted from the virally transduced cells, after 72 h and Exon 4 amplified and a T7 endonuclease assay was carried out. A cleavage fragment was observed with guide #5 but not #4 (data not shown).

K562 cells were then transduced with two concentrations of concentrated guide #5-expressing virus for 72 hours before the transduced cells were selected with puromycin for 7 days. Genomic DNA was extracted from cells both before and after puromycin selection. Again, NRF2 Exon 4 was amplified before being incubated with T7 endonuclease.

As shown in Fig 5.18, the uncut gel showed a single specific PCR product in all samples. A smear is seen above post puromycin selection indicating the presence of heteroduplex DNA. These results are confirmed upon incubation with T7 endonuclease where a cleavage fragment is present in these samples, but not in the wild type or non-puromycin selected samples.

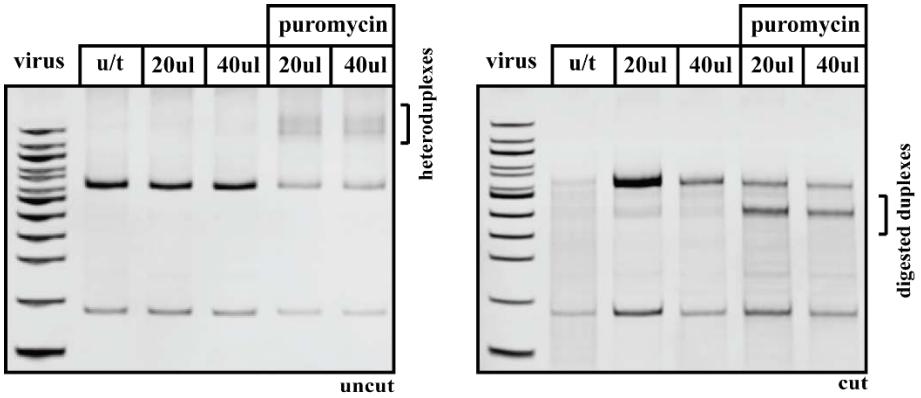

Figure 5.18: Generation of NRF2-deficient K562 cells K562 cells were transduced with two concentrations Lentiviral particles expressing NRF2 guide #5 for 72 hours. Cells were selected with 6µg/ml puromycin as indicated. A T7 assay was performed on selected cells to assess editing efficiency.

The puromycin selection creates a heterogeneous population of cells. Some will have mutations in both Exon 4 alleles some in just one, while others may not be modified at all. As with the HCT-116 cells we needed to obtain clonal lines from this population. Since K562 is a suspension cell line, we could not use limiting-dilution as we have previously been unable to generate clonal haematopoietic cell lines using this method.

To this end we used a “semi-solid” media based on resuspending the cells in 2.5% Methycellulose dissolved in RPMI. 700 cells/ml were mixed with the Methylcellulose/RPMI solution using a syringe with a blunt ended needle before being plated 1ml/well into 12 well plates. The plates were incubated without disturbance for 7-10 days when discreet clumps of cells became apparent.

Colonies were picked into 96-well plates using a light microscope which had been placed in a hood, an inbuilt screen allowed for accurate colony identification and picking. Clones were then grown to confluency and expanded.

As with the HCT-116 cells, the 96-well plate was split and one "daughter" plate treated with MG-132 for two hours. Cells were lysed, and lysates analysed for NRF2 by Western blot. By this large-scale screening we identified several clones deficient in NRF2 expression and several clones were chosen and expanded further (data not shown). To confirm the results from the 96 well plate, 12x clones were grown to confluency before being treated with MG-132 (10µM) for two hours. Protein lysates were subsequently extracted and NRF2 detected by Western blot.

MG-132 increased NRF2 expression in un-transfected K562 cells. Of the 12x clones picked 9 failed to show NRF2 induction following MG132 treatment suggesting the editing had been successful in these lines (Fig 5.19). NRF2 induction was seen in clones #2, 7 and 11 indicating the CRISPR editing was not successful or complete, or the population was mixed. A slight induction is also seen in clone 5. Clones #4, #5, and #6 were passaged onwards.

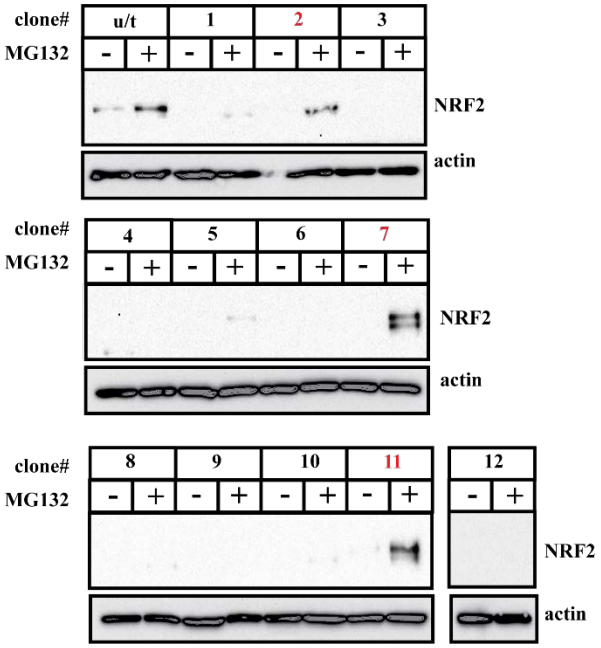

Figure 5.19: Deriving NRF2-edited clones from puromycin-selected K562 cells

Puromycin-selected K562 cells were single-cell cloned by culturing in semi-solid medium before expansion. Isolated clones were treated with MG-132 (10 μM) for two hours to stabilise NRF2. Protein expression was detected by Western Blot using NRF2 and β-actin antibodies

MG-132 is a proteasome inhibitor and therefore acts by preventing NRF2 degradation allowing the protein to stabilise, however it remains unclear if it is able to transcriptionally activate NRF2 expression. Thus, to confirm these clones were indeed NRF2 deficient, we treated them with the NRF2 inducers CDDO and Sulforaphane. Protein was extracted, normalised through protein determination assays and western blots were performed (Fig 5.20).

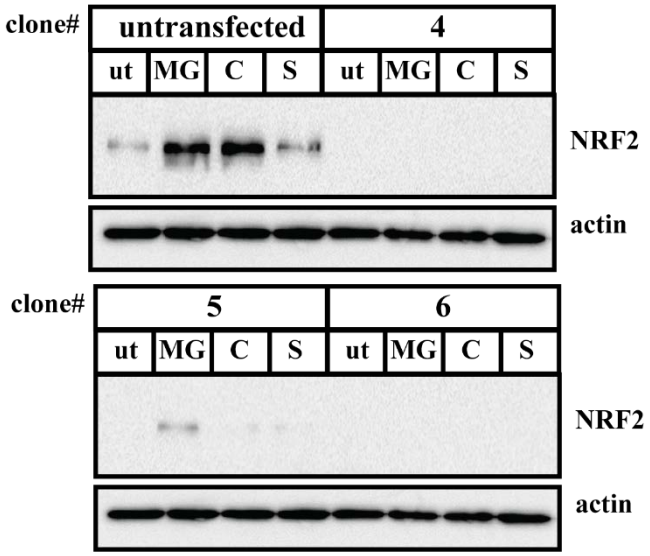

Figure 5.20: NRF2 inducers CDDO and Sulforaphane in NRF2-deficient K562 cells K562 clones (#4, #5 and #6) were treated with 10uM MG-132 (MG) or the NRF2-inducers (100mM) CDDO-Me (C) and (5 µM) Sulforaphane (S). Protein expression was detected by Western Blot using NRF2 and β-actin antibodies.

As expected we saw positive NRF2 induction with MG132 and both CDDO and Sulforaphane in the wild-type K562 cells, and clone#5, but no induction in was seen in clone #4 and #6. The fact that neither a proteasome inhibitor can stabilise NRF2 or that NRF2 can be induced by known activators indicate these cells were deficient in NRF2.

Genomic DNA was extracted from these clones, Exon 4 amplified and the resulting PCR product purified and sequenced (Fig 5.21). We included an additional clone #8 as clone #5 appeared to still express NRF2. All clones were disrupted at or very near to the site at which the guide RNA is predicted to cleave the Exon 4 (3 bp downstream (3' to) the PAM site). Clone #4 had insertion of a C. Clones #6 and #8 had extensive deletion of Exon 4 starting near this site. The lack of uniformity in

the mutations in the clones reflects the fact that only a single guide was used for deletion.

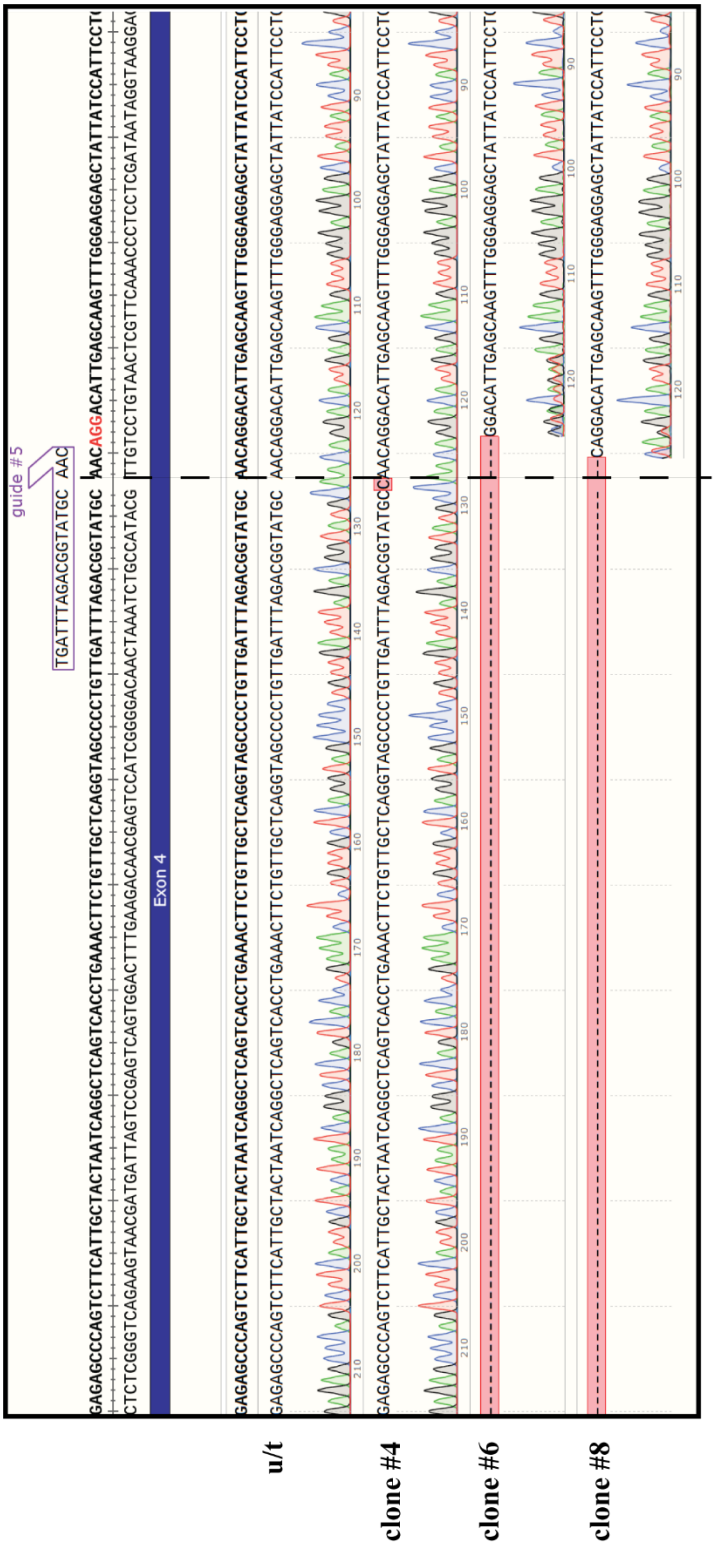

Figure 5.21: Sanger sequencing of NRF2-edited K562 clones
Exon 4 of NRF2 was amplified from several K562 clones, purified by gel extraction and sequenced. Chromatograms were aligned using Snapgene.

5.2.10 Generation of NRF2 deficient THP-1 cells

We next wished to see whether we could edit NRF2 in an AML cell line. The Lentiviral particles containing NRF2 guide #5 were used as for the K562 cells (see above). THP1 cells were transduced with two concentrations of LentiCRISPR NRF2 guide #5 for 72 hours, before being selected for with puromycin. DNA was extracted from these cells, NRF2 exon 4 was amplified before being denatured/ reannealed and a T7 endonuclease assay was carried out. The uncut gel showed a single PCR product in the correct size. Upon incubation with T7 endonuclease, a cleavage fragment was seen in both puromycin selected cells indicating cleavage has occurred (Fig 5.22). No band shift was seen in the untreated or non-selected cells.

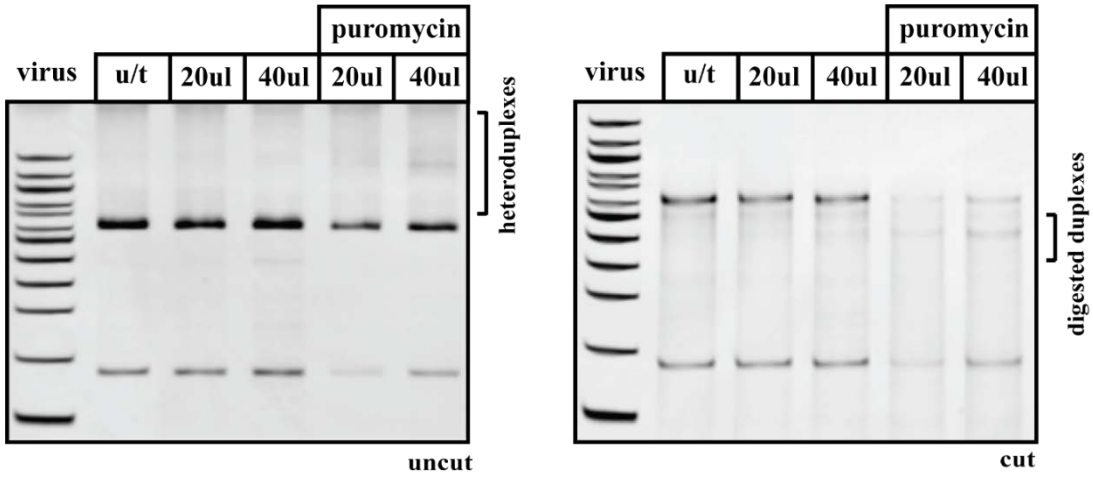

Figure 5.22 Generation of NRF2-deficient THP1s cells THP-1 cells were transduced with two concentrations Lentiviral particles expressing NRF2 guide #5 for 72 hours. Cells were selected with 6µg/ml puromycin as indicated. DNA was amplified and denatured/ re-annealed. T7 endonuclease assay was performed on un-transfected and puromycin-selected cells as indicated

Like the K562 cells, single-clones of selected THP-1s were obtained by cloning the cells in Methylcellulose then transferring colonies to 96-well plates. Protein lysates were extracted and NRF2 detected by Western blot. We identified several clones (data not shown) that did not show any NRF2 expression, and 19 clones were passaged onwards. To confirm the results from the 96 well plate, the clones were once again treated with MG-132 and screened for NRF2/β actin expression by Western blot (Fig 5.23).

NRF2 antibodies are notoriously poor and this was especially true for the THP-1 cells. A band is present in untreated cells around the molecular weight we would expect to see NRF2 but following MG132 treatment upper bands are clearly visible which are not in the untreated sample. It appears that the lower band is non-specific.

Whilst we identified several false negatives from the 96 well plate, we identified several clones with no detectable NRF2 expression including #1, #2, #10 and #16-19. These clones were expanded for further investigation.

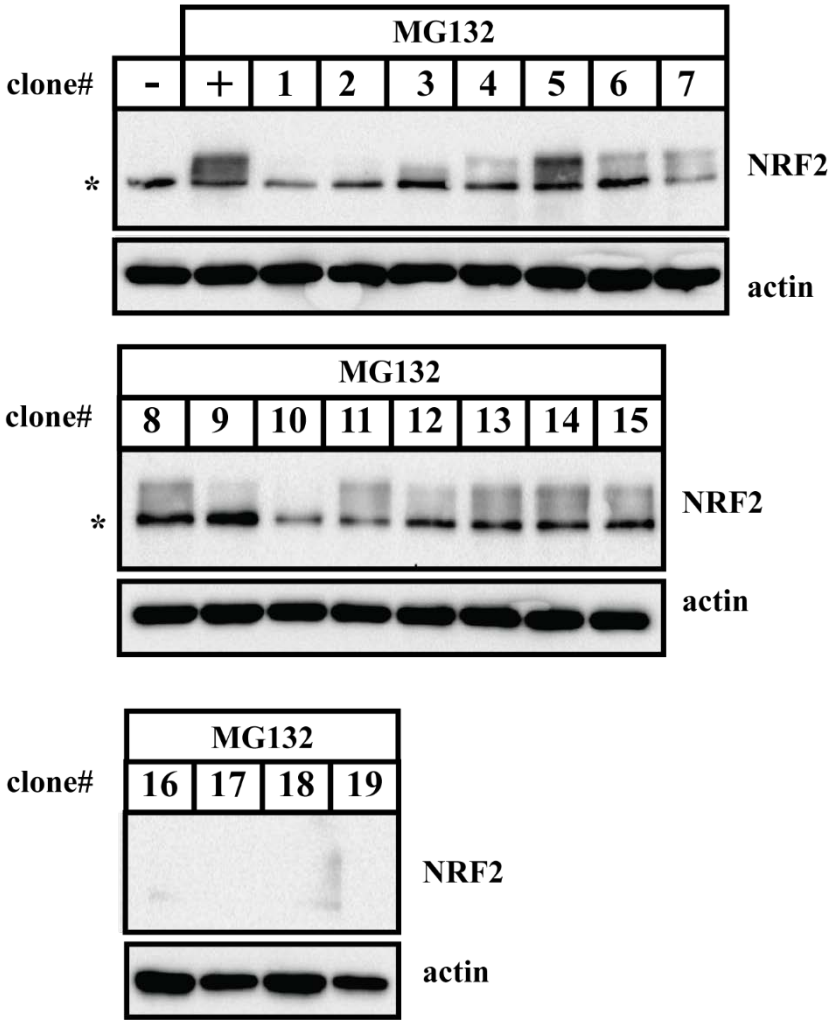

Figure 5.23: Deriving an NRF2 edited clones from puromycin-selected THP-1 cells Puromycin-selected THP-1 clones were single-cell cloned using semi-solid medium before expansion. Isolated clones were treated with MG-132 (10μM) for two hours to stabilise NRF2. Protein expression was detected by Western Blot using NRF2 or β-actin antibodies. * indicates a non-specific band

Four of these clones (#1, #2, #10, and #19) were treated with MG-132 and the NRF2 inducers CDDO-Me, and sulforaphane. Protein was extracted from these cells and

normalised and Western Blots were used to determine protein expression for NRF2 and β-actin (Fig 5.24).

As expected MG-132, CDDO-me and sulforaphane were able to induce NRF2 in the wild-type THP-1 cells, with CDDO-Me being the most potent. No NRF2 expression was detected in any of the clones with any of the treatments indicating its expression is disrupted in the clones.

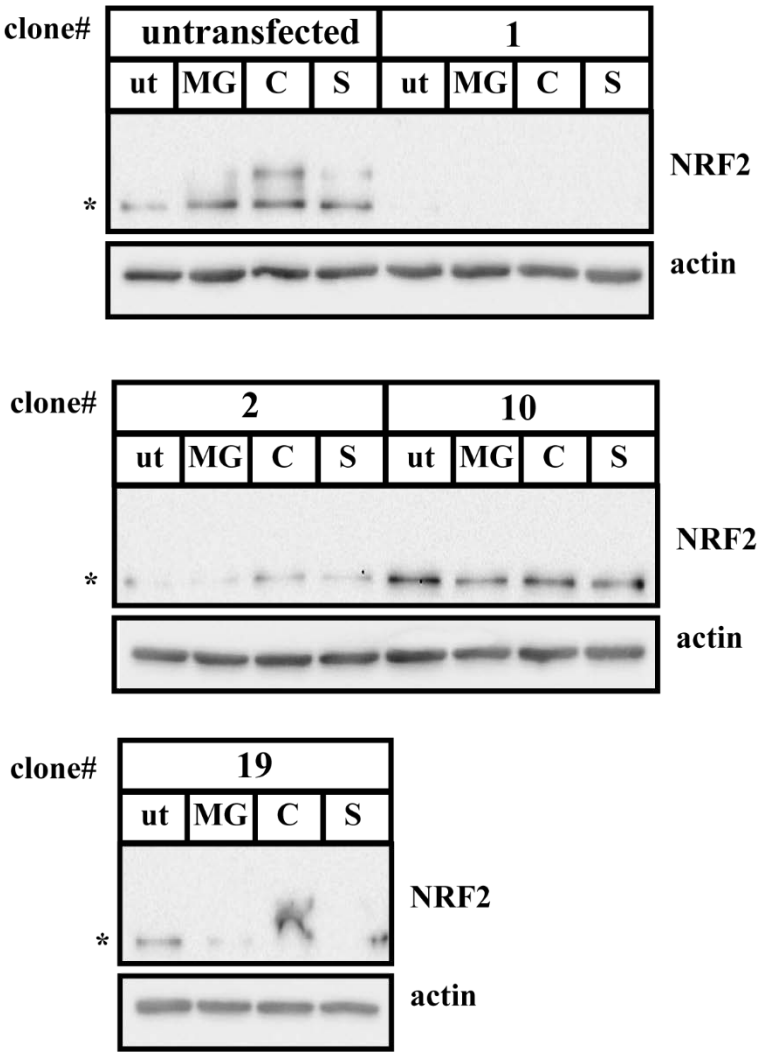

Figure 5.24: NRF2 inducers CDDO and Sulforaphane in NRF2-deficient THP-1 cells. THP-1 clones (#1, #2, #10 and #19) were treated with MG-132 (10 μM) or the NRF2 inducers CDDO-Me (100 nM) and Sulforaphane (5 μM). Protein expression was detected by Western Blot using NRF2 and β-actin antibodies. * indicates non-specific band

DNA was extracted from two of these clones and as with the K562 cells Exon 4 was sequenced (Fig 5.25). Clone #1 showed a large deletion starting just 4bp 3' to the expected cleavage site. Clone #19 showed a small deletion starting 3bp 3' to the expected cleavage site. As with the K562 cells, the modifications in the clones varies when a single guide is used for editing.

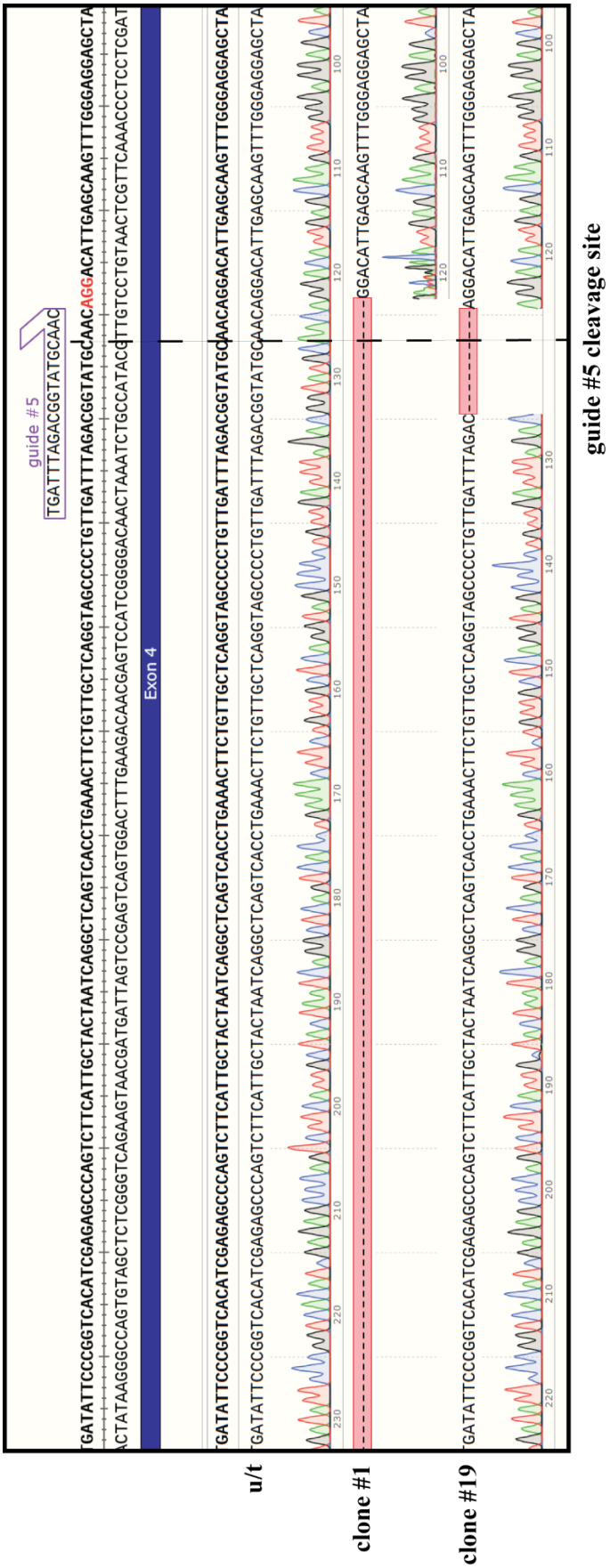

Figure 5.25: Confirmation of NRF2 edited THP-1 cells by Sanger sequencing
Exon 4 of NRF2 was amplified from several THP-1 clones, purified by gel extraction and sequenced. Chromatograms were aligned using Snapgene.

5.3 Conclusions and Discussion

In this Chapter we designed constructs with the aim of targeting and disrupting NRF2 and KEAP1 gene expression in AML cells. Whilst we predominately focussed on CRISPR-Cas9 (due to its simplicity) we also explored some additional gene-editing methods. All have their strengths and weaknesses.

Guides targeting different exons in NRF2 and KEAP1 were designed and subsequently cloned into a LentiCRISPR plasmid that had an AML "friendly" SFFV promoter. HEK293T cells were used to validate all the initial experiments as they are highly transfectable.

The editing ability of these guides were tested in HEK-293T cells and five successful guides were identified in NRF2, and two in KEAP1 (Figs 5.6, 5.7, 5.8 and 5.14). In addition to transfecting these guides individually, we identified that CRISPR guides targeting the same exon can be used in tandem successfully with a high targeting efficiency. If the guides are spaced sufficiently far apart, a high proportion of cleavage shows the excision of bases between the two guide sites (as shown when KEAP1 guides #3 and 7 are co-transfected) (Fig 5.14).

We initially tested our constructs in HEK-293 cells. NRF2 guides targeting exon 4 were transfected and positively selected for with puromycin. While this created a highly selected population of edited HEK-293 cells, the exact mutation in exon 4 can vary. For us to perform comparative studies, we required a homogeneous population of cells with the exact mutation being fully characterised. It was therefore necessary to derive an isogenic population from a single CRISPR clone.

We derived several HEK-293 clones containing disruptions to exon 4 of NRF2. Disrupted NRF2 clones of HCT-116 cells were made in a similar manner. To create NRF2 knockout leukaemia cell lines (K562 and THP-1), we transduced cells with an NRF2 guide #5 lentivirus. Similar to the HEK-293 cells, clonal populations were created from transduced K562 and THP1. The clonal mutations were confirmed through Sanger sequencing.

CRISPR guides targeting KEAP1 was cloned into the Lentiviral SFFV plasmid and used to make clonal HEK-293 knockouts. We attempted to make KEAP1 edited HCT-116 cells, while we were able to develop a selected population of KEAP1 edited HCT cells, we were unable to develop a clonal population of these cells.
As well as Cas9 we also explored the use of alternate nucleases/editing methodologies TALENs and another CRISPR nuclease, Cpf-1.

The only published studies on primary cells being manipulated and "returned" to patients is using TALENs. Both the Left- and Right-Hand TALEN is attached to one part of the bipartite Fok1 nuclease. This in part explains the reduction of off-target effects compared to CRISPR as both 20 bp TALEN targeting sequences must occur within 20-30 bp of each other in order for Fok1 to dimerise and cause a double-strand break (Christian et al., 2010). Further specificity can be achieved using a heterodimerizing Fok1 (Miller et al., 2007), so in the unlikely event two Left- or Right-hand TALENs bind no cutting will occur (Cade et al., 2012). This specificity is their key advantage in a clinical setting.

The TALENs we designed efficiently edited exon 4 in NRF2 (Fig 5.11). The design and construction however, is much more complicated than with CRISPR-Cas9 or -Cpf-1. While "Golden-Gate" cloning using the Type II restriction enzymes makes

this much easier it still requires a few weeks to synthesise the final TALENs and they require at least an intermediate knowledge of molecular biology. The main issue lies with delivery. *In vivo* delivery generally requires the use of viruses. Introducing plasmids/proteins into certain cell types (such as AML and B-cell lines) also requires the use of viruses. Due to the nature of their structure (each RVD is contained within the Helix-Loop-Helix motif) TALENS (and Zinc Fingers contain many repeated sequences) this effectively rules out the use of viral methods of delivery.

There have been attempts to reduce the off-target effect when using CRISPR and the initial studies mimicked the TALEN pairs and resulted in the use of a Cas9 "nickase". This enzyme has one of the active sites, either D10 in the HNH domain or H588 in the RuvC domain mutated to alanine. This renders Cas9 unable to create double- but only single-strand breaks (Cong et al., 2013). Cutting one strand of DNA results in the cell repairing the "nick" through the Base-Excision Repair pathway which is highly accurate, so no mutations will occur. If, however two "nicks" occur within 40-50bps a double-stand break will occur (Ran et al., 2013a). Later studies following the publication of structural information on Cas9 binding and mechanism have led to so called "enhanced" Cas9 nucleases with purported lower "off-target" such as eSpCas9 and SpCas9-HF1 (Kleinstiver et al., 2016, Slaymaker et al., 2016).

The other current drawback for using CRISPR-Cas9 therapeutically is its size. At ~4.2 kb (~150 kD) Cas9 is a large protein which makes it difficult to introduce efficiently into cells. While studies have tried to address this for example by using "split" Cas9 these proteins still have their issues (Zetsche et al., 2015b). The CRISPR system is very diverse and bacteria contain many CRISPR nucleases.

There is a tremendous push to find other Cas9-related nucleases that are smaller than SpCas9 or have differing specificities. One such from Staphylococcus aureus (SaCas9) is 300bp small than SpCas9 (115 kD) and has a longer PAM sequence NNGRRT which occurs less in genome, reducing the "off-target" effects. However, this also limits its list of targetable sites making it more of a complimentary tool (Ran et al., 2015).

Cpf-1 is another such variant which, while only being slightly smaller than SpCas9, has some features that make it useful. Its PAM TTTN is T-rich meaning it can be used to target AT-rich genomic locations. The Tracer RNA is only 24 bp (compared to over 100 bp for Cas9 proteins) and perhaps more importantly its sgRNAs can be easily multiplexed without resorting to extra promoter or RNA splicing elements (Zetsche et al., 2017). We found that Cpf-1 could efficiently edit exon 4 in NRF2 and when used as pairs was able to excise a piece of DNA from the exon (Fig 5.13). We were unable to try multiplexing these guides within one plasmid. But it would be envisaged that 3-4 of these guides including the TRACER RNA could be packaged into the same Lentiviral plasmid and only be around 300bp in total.

The NGG PAM is fairly abundant in the genome but its efficiency is known to vary depending on the genomic location (for example in AT -rich regions). Its position may not always be optimal to edit a target gene while producing a guide sequence with low "off-target" effects. By engineering SpCas9 non-canonical PAM sequences (e.g. NAG and NGA) PAM specificity has been expanded to include NAG and NGA (Kleinstiver et al., 2015).

In this study we attempted to overcome the problem of using a mixed CRISPR population by creating a clonal population of cells containing a single CRISPR

mutation. One problem we anticipate if undertaking comparison studies with these clones, is the lack of parental population for the individual clones. The clonal populations would therefore be compared against the wild-type cell line (which while similar, will inevitably contain a slightly different genetic makeup). If repeated we would aim to create and characterise the clonal populations first before editing them with CRISPR, thereby creating a more reliable method to determine the function of the mutated gene.

Due to time constraints we have been unable to fully characterise NRF2 signalling in the edited leukaemic cells. We have shown no NRF2 protein was induced in these cells when stimulated with NRF2 activating compounds sulforaphane and CDDO (Fig 5.20 and 5.24). In the future we would like to characterise the expression of NRF2 target genes, in particular HO-1, NQO1 and GCLM. Whilst we expect no mRNA or protein change among the NRF2 targets, some minor modulation is to be expected due to the compounds being “dirty” and regulating other pathways in addition to NRF2.

We would also like to do a more thorough investigation of downstream targets of NRF2 in particular to characterise the proteins binding to the promoters of certain NRF2-regulated genes. To do this we could like to perform an engineered DNA binding molecule mediated chromatin immunoprecipitation (enChiP). EnChip is a methodology that uses the binding ability of dCas9 to bind to a region of DNA, thereby creating an RNA/DNA complex. The dCas9 is tagged, which can be used to enrich the region of interest through chromatin immunoprecipitation. This can then be used for RNA, DNA or protein analysis. One study used enCHIP on a region of IRF-1 and mass spectrometry to identify all proteins that interacting with this locus (Fujita and Fujii, 2013).

Chapter 6

General Discussion

6.1 Final Discussion

6.1.1 NRF2 regulation of miR-125b and miR-29b

The dysregulation of NRF2 results in chemotherapy-resistance and oncogenesis in several malignancies including AML. This work follows on from earlier observations in the laboratory which demonstrated AML cells exhibit constitutive NRF2 activation (Rushworth et al., 2012). In this study we aimed to investigate the function of NRF2 in AML, in particular, its ability to regulate miRNAs.

We performed a miRNA array following treatment with an NRF2 activator or genetic perturbation of NRF2. The array identified several miRNAs that exhibited modulated expression in response to changes in NRF2. miRNAs were further validated through knockdown of NRF2 or KEAP-1 and a correlation was observed between NRF2 and miR-125b and miR-29b. NRF2 positively regulates miR-125b1 and negatively regulates miR-29b1 in both AML cell lines and primary patient samples. A reporter assay demonstrated that this occurs through NRF2 binding to ARE sites in the promoter sequences of both miRNA.

To understand the function these dysregulated miRNAs play in AML we directly modulated their levels using miRNA “mimics” and antagomiRs. Increasing or decreasing levels of miR-125b and miR-29b, resulted in only a slight increase in apoptosis respectively. However, simultaneously modulating levels of both miR-125b and miR-29b resulted in a significant increase in apoptosis and increased sensitivity to front-line chemotherapy drugs such as Daunorubicin. This suggests NRF2 synergistically regulates both miRNAs to increase resistance to

chemotherapy and decrease sensitivity to apoptotic signalling. This is in part due to the repression of pro-apoptotic BAK and STAT3, while anti-apoptotic proteins such as AKT2 were induced.

Of the 93 miRNAs tested we were only able to fully characterised miRs-125b and -29b. In the future it would be interesting to investigate the role the other NRF2 regulated miRNA play in AML. For example miR-221 and -222 have been known to act as both oncomiRs and tumour suppressor miRs, with their exact role dependent on the malignancy involved (Garofalo et al., 2012). In breast and prostate cancer they act as oncomiRs by regulating ERα and the pro-apoptotic protein Bim (Di Leva et al., 2010, Tanaka et al., 2015). This results in increased proliferation and a reduction in apoptosis. In erythroleukaemia they repress c-Kit expression, thereby reducing cell growth (Felli et al., 2005).

It would be interesting to characterise the expression of NRF2-regulated miRNAs in different AML subtypes to identify any prognostic link. For example, dysregulated miR-125b expression is more highly associated with APL compared to other AML subtypes (Zhang et al., 2011a). The miRNAs we identified in AML would be compared to their expression in other malignancies to examine whether dysregulation is tissue specific or has global consequences to the disease progression as a whole.

Despite significant research, chemotherapy agents such as daunorubicin and cytarabine still remain the predominant treatments used for AML (De Kouchkovsky

and Abdul-Hay, 2016). Kinase and Bcl-2 inhibitors are revolutionising the treatment of CML and CLL however these breakthroughs are not being transferred to AML (Kantarjian et al., 2012, Roberts et al., 2016). Haematopoietic stem cell transplantation (allogenic bone marrow transplant) remains the treatment option for many and the end of the line for clinical options if it fails.

We have a good understanding of the underlying cytogenetics characterising AML, and the idea of targeted therapy, is becoming increasingly popular. The FLT3 inhibitor Midostaurin is the only example of a new drug that has been approved for AML treatment in the last half century, but is suitable for only a subset of AML patients (Levis, 2017). The hope is that more novel drugs will be developed and made currently available to treat all classes of AML.

miRNAs predominately play a role in the "fine tuning" of gene expression, correcting their expression when dysregulated could provide a viable therapeutic option. Examples of miRNA-regulating agents (miR-mimics or antagomiRs) have shown promise, the most notable being an antisense oligonucleotide-based drug to treat Huntington's disease (Zaghloul et al., 2017). A Phase 1/2a trial demonstrated that mutant Huntingtin protein levels could be reduced. Our data suggests this could be an avenue of interest in AML.

6.1.2 Gene Editing NRF2

Gene editing using site-directed nucleases (such as TALENS or CRISPR-Cas9) can be used to target specific regions of DNA leading to gene disruption. Due to their

"programmable" nature theoretically any area of the genome is targetable, and we wished to see whether we could use these targeted nucleases to disrupt NRF2 and KEAP1 in AML cells.

We successfully validated a number of gene-editing methods targeting NRF2 in HEK-293T cells. Of these the CRISPR-Cas9 or CRISPR-Cpf1 were the easiest constructs to generate and multiple guides could easily be cloned and tested at one time. The TALEN pair did seem to be highly efficient in the HEK293Ts but was time-consuming to generate, however, this is currently the only gene-editing technology to date to be used therapeutically (Qasim et al., 2017). As our aim was to modify AML cell lines we would ultimately have to resort to using lentivirus to introduce the guides and Cas9 into the cells. TALENs cannot be packaged by lentiviruses due to the presence of many repeated sequences.

We cloned CRISPR guides targeting Exons 1, 2 and 4 of NRF2 and observed editing in all these exons. However, guides targeting Exon 4 were used throughout this study as the genotyping primers were more robust.

To test the methodology Exon 4 of NRF2 was targeted in HCT-116 colon cancer cells and in order to obtain "knock-out" cells, clonal populations were made from puromycin-selected cells. A total of 96 clones were screened per CRISPR guide, using Western Blot following treatment with MG-132. The clones which showed no NRF2 expression were further passaged and re-tested for NRF2 expression. Screening many clones by Western blot was time-consuming but the only other

method of verification would require genomic DNA extraction followed by the T7 assay which could be prohibitively expensive.

When validating guides targeting Exon 1 of Keap-1 and, also when using the Cpf-1 plasmids as pairs we noticed the removal of the sequence in between the two guides. This was an interesting observation and suggests in future we could use guides as pairs and simply screen clones using agarose gels following a genotyping PCR. For this to work with Lentiviral plasmids the two guides would have to be clones within the same backbone.

We were unable to directly transfect the plasmids into THP-1 cells. Although we have previously, successfully used nucleofection for AML lines we needed as high transfection efficiency as possible as the editing efficiency will always be low. We had to therefore package the Cas9 and guides into a lentivirus.

Both the CML cell line K562 and the AML cells line THP-1 cells were transduced with lentiviral particles containing CRISPR targeting Exon 4 of NRF2.

Positively-edited clones were selected by puromycin and clonal expansion of positive populations were obtained by plating cells in a Methylcellulose-based semi-solid medium. We tried cloning the cells by limiting dilution into 96-well plates but failed to obtain any clones growing out.

The “micro-environment” surrounding cells trapped in the semi-solid medium must allow them to divide and form colonies, which were identified by transmission light microscopy and could be picked using a pipette tip into 96 well plates. While this approach could at times be somewhat tedious it was the only reproducible way we could get clonal AML lines. Expanded clones were treated with MG132 and NRF2 was detected by Western blot post treatment with MG-132. As with the HCT116 cells this was incredibly time-consuming and would benefit from a simplified genotyping approach to identify null cells.

Several colonies negative for NRF2 expression were further expanded. They were subsequently treated with the NRF2 activating drugs CDDO and sulforaphane to assess any responsiveness and to confirm no NRF2 activity was present. We were successful in identifying positive NRF2 KD colonies which were absent in NRF2 expression.

6.1.3 Future work

We successfully used CRISPR-Cas9 to generate NRF2-deficient AML and CML cell lines. Importantly, we were able to obtain single cell clones of these cells. This means we are now in a position to utilise our experience with both CRISPR and Lentiviral delivery in haematopoietic cell lines to further study NRF2 and other pathways in AML.

Using NRF2-deficient AML cells to further explore the role NRF2 plays in miRNA regulation

Given time constraints we were only able to briefly characterise these cells. We would first analyse the expression of miR-125b1 and miR-29b1 in these cells to see if any mis-regulation supports our experimental hypotheses from Chapters 3 and 4. We would also like to analyse the expression of the miR-125b1/29b1 target genes and proteins, confirming the ones identified are indeed causing the anti-apoptotic/pro-proliferative effects seen in the AML cell lines and patient samples.

We are also able to "re-introduce" NRF2 into the deficient cells under the control of a Tet-On promoter which enables us to use Doxycycline to directly activate NRF2 in these cells. Although this is a non-physiological stimulus it is a "cleaner" method of activating NRF2 than drugs such as Sulforaphane and CDDO.

Targeting miRNA "seed" regions

We identified a number of ARE sites that NRF2 may use to regulate miR-125b1, and successfully modulated expression of miR-125b and miR-29b using miRNA mimics and antagomiRs. Clearly, we could use CRISPR to more precisely investigate the regulation of these miRNAs. Targeting a miRNA seed region with a guide RNA would effectively delete the miR from the cells. A more targeted promoter approach would be used to target individual ARE sites within the miRNA promoters in order to specifically identify those responsible for NRF2 regulation. Finally, by combining pairs of guides theoretically it would be possible to delete

specific seed regions from a given genomic location. All these approaches would give us a better insight into the role of both miRNAs in AML cells.

Analysis of NRF2 target genes in AML

NRF2 activation in AML is linked to resistance to commonly used chemotherapy drugs. It would be interesting to further characterise the NRF2-deficient versus parental cells to ascertain if any of the changes in gene expression can account for this. Although the cells we produced are clonal, they are not isogenic (as they were not derived from a single clone). So, it would be of use to generate clonal lines from untransfected AML cell lines prior to modifying them. The rationale behind performing editing in this way, would be to ensure an identical genetic background between the parental and "edited" clones.

The clones could then be characterised before further comparative studies are carried out such as ChIP Seq or RNA Seq which can be used to characterise all binding sites and mRNA influenced by "knocking-out" NRF2. Other members of the laboratory have successfully used CRISPR to endogenously tag NRF2 and it would be interesting to use these plasmids in some of the AML cell lines as it would greatly simplify any ChIP-Seq methodologies. This would allow us to identify novel NRF2-targets and categorise the genes that are affected by NRF2 and responsible for chemoresistance.

We have also noticed the NRF2-deficient THP-1 clones tend to grow at a slower rate than the wild-type cells (data not shown), this may be due to clonal variation

or due to NRF2-dependent changes in their metabolomic profiles. As previously discussed, NRF2 has been shown to regulate various cancer metabolism genes (in particular the phosphate pentose pathway (PPP) and NADPH synthesis) (Mitsuishi et al., 2012b). We would like to investigate NRF2's role in regulating metabolism genes in AML, while we would focus on the PPP pathway we would also like to see if any additional metabolomic pathways are under the influence of NRF2 regulation.

Crosstalk of NRF2 and other transcription factors

As previously discussed, despite AML cells being characterised by constitutive activation of NRF2, there is no mutation disrupting the NRF2/KEAP1 binding sites. Instead NRF2 is dysregulated due to additional upstream signalling pathways such as NF-κB (Rushworth et al., 2012). However, it is likely that NRF2 is regulated by additional upstream signalling.

In order to identify upstream signalling factors we intend to use the technique enChIP (Fujita and Fujii, 2013). enChIP uses a catalytically inactive Cas9 (dCas9) which retains the binding ability of Cas9 to DNA but prevents DNA cleavage. We have previously made dCas9n which targets Exon 4 of NRF2, however we intend to redesign the dCas9 to target Exon1, the construct would also contain a tag. The dCas9 would bind to the targeted region of NRF2 and this region of DNA is purified and immunoprecipitated through antibodies against the tag. This can then be combined using techniques such as mass spectrometry or RNA seq to identify

proteins or RNA sequences which associate with the region. This will give us a greater understanding of the upstream regulators of NRF2 transcription factor.

Genome screening to identify NRF2 target genes

To further study other associated downstream targets of NRF2, we could carry out a CRISPR screening library. This would allow us to screen a high number of functional processes through the designing panels of multiple sgRNA per gene of interest. These are transduced using a lentiviral vector and a selection drug would be used (for example daunorubicin or cytarabine). DNA would be extracted from the surviving cells, and using the sgRNA barcode for identification, next generation sequencing could be performed. The surviving cells would assumedly contain a mutation in a gene that provides a survival advantage to them. We would perform the screen on both parental THP-1 clones and those with edited NRF2, looking in particular at guides which aid cell survival in one drug-resistant situation, but not the other.

Overall this study gives us a greater insight into the role of NRF2 in AML, and, in particular, its contribution to oncogenesis through the regulation of miRNAs. Furthermore, the tools developed in this study have the potential to greatly expand our understanding of NRF2 signalling.

References

ABU-DUHIER, F. M., GOODEVE, A. C., WILSON, G. A., CARE, R. S., PEAKE, I. R. & REILLY, J. T. 2001. Genomic structure of human FLT3: implications for mutational analysis. *Br J Haematol,* 113**,** 1076-7.

ABUDAYYEH, O. O., GOOTENBERG, J. S., ESSLETZBICHLER, P., HAN, S., JOUNG, J., BELANTO, J. J., VERDINE, V., COX, D. B. T., KELLNER, M. J., REGEV, A., LANDER, E. S., VOYTAS, D. F., TING, A. Y. & ZHANG, F. 2017. RNA targeting with CRISPR-Cas13. *Nature,* 550**,** 280-284.

ABUDAYYEH, O. O., GOOTENBERG, J. S., KONERMANN, S., JOUNG, J., SLAYMAKER, I. M., COX, D. B., SHMAKOV, S., MAKAROVA, K. S., SEMENOVA, E., MINAKHIN, L., SEVERINOV, K., REGEV, A., LANDER, E. S., KOONIN, E. V. & ZHANG, F. 2016. C2c2 is a single-component programmable RNA-guided RNA-targeting CRISPR effector. *Science,* 353**,** aaf5573.

ALAM, J., STEWART, D., TOUCHARD, C., BOINAPALLY, S., CHOI, A. M. & COOK, J. L. 1999. Nrf2, a Cap'n'Collar transcription factor, regulates induction of the heme oxygenase-1 gene. *J Biol Chem,* 274**,** 26071-8.

ALMEIDA, A. M. & RAMOS, F. 2016. Acute myeloid leukemia in the older adults. *Leuk Res Rep,* 6**,** 1-7.

ARBER, D. A., STEIN, A. S., CARTER, N. H., IKLE, D., FORMAN, S. J. & SLOVAK, M. L. 2003. Prognostic impact of acute myeloid leukemia classification. Importance of detection of recurring cytogenetic abnormalities and multilineage dysplasia on survival. *Am J Clin Pathol,* 119**,** 672-80.

BAI, X., CHEN, Y., HOU, X., HUANG, M. & JIN, J. 2016. Emerging role of NRF2 in chemoresistance by regulating drug-metabolizing enzymes and efflux transporters. *Drug Metab Rev,* 48**,** 541-567.

BARON, M. H. 2003. Embryonic origins of mammalian hematopoiesis. *Exp Hematol,* 31**,** 1160-9.

BAUM, C., ITOH, K., MEYER, J., LAKER, C., ITO, Y. & OSTERTAG, W. 1997. The potent enhancer activity of the polycythemic strain of spleen focus-forming virus in hematopoietic cells is governed by a binding site for Sp1 in the upstream control region and by a unique enhancer core motif, creating an exclusive target for PEBP/CBF. *J Virol,* 71**,** 6323-31.

BAUM, C. M., WEISSMAN, I. L., TSUKAMOTO, A. S., BUCKLE, A. M. & PEAULT, B. 1992. Isolation of a candidate human hematopoietic stem-cell population. *Proc Natl Acad Sci U S A,* 89**,** 2804-8.

BENNETT, J. M., CATOVSKY, D., DANIEL, M. T., FLANDRIN, G., GALTON, D. A., GRALNICK, H. R. & SULTAN, C. 1976. Proposals for the classification of the acute leukaemias. French-American-British (FAB) co-operative group. *Br J Haematol,* 33**,** 451-8.

BERNSTEIN, E., KIM, S. Y., CARMELL, M. A., MURCHISON, E. P., ALCORN, H., LI, M. Z., MILLS, A. A., ELLEDGE, S. J., ANDERSON, K. V. & HANNON, G. J. 2003. Dicer is essential for mouse development. *Nat Genet,* 35**,** 215-7.

BLOOMFIELD, C. D., LAWRENCE, D., BYRD, J. C., CARROLL, A., PETTENATI, M. J., TANTRAVAHI, R., PATIL, S. R., DAVEY, F. R., BERG, D. T., SCHIFFER, C. A., ARTHUR, D. C. & MAYER, R. J. 1998.

Frequency of prolonged remission duration after high-dose cytarabine intensification in acute myeloid leukemia varies by cytogenetic subtype. *Cancer Res,* 58**,** 4173-9.

BONETTI, P., DAVOLI, T., SIRONI, C., AMATI, B., PELICCI, P. G. & COLOMBO, E. 2008. Nucleophosmin and its AML-associated mutant regulate c-Myc turnover through Fbw7 gamma. *J Cell Biol,* 182**,** 19-26.

BORCHERT, G. M., LANIER, W. & DAVIDSON, B. L. 2006. RNA polymerase III transcribes human microRNAs. *Nat Struct Mol Biol,* 13**,** 1097-101.

BOUSQUET, M., HARRIS, M. H., ZHOU, B. & LODISH, H. F. 2010. MicroRNA miR-125b causes leukemia. *Proceedings of the National Academy of Sciences of the United States of America,* 107**,** 21558-21563.

BOUSQUET, M., NGUYEN, D., CHEN, C., SHIELDS, L. & LODISH, H. F. 2012. MicroRNA-125b transforms myeloid cell lines by repressing multiple mRNA. *Haematologica,* 97**,** 1713-21.

BOUSQUET, M., QUELEN, C., ROSATI, R., MANSAT-DE MAS, V., LA STARZA, R., BASTARD, C., LIPPERT, E., TALMANT, P., LAFAGE-POCHITALOFF, M., LEROUX, D., GERVAIS, C., VIGUIE, F., LAI, J. L., TERRE, C., BEVERLO, B., SAMBANI, C., HAGEMEIJER, A., MARYNEN, P., DELSOL, G., DASTUGUE, N., MECUCCI, C. & BROUSSET, P. 2008a. Myeloid cell differentiation arrest by miR-125b-1 in myelodysplastic syndrome and acute myeloid leukemia with the t(2;11)(p21;q23) translocation. *J Exp Med,* 205**,** 2499-506.

BOUSQUET, M., QUELEN, C., ROSATI, R., MANSAT-DE MAS, V., LA STARZA, R., BASTARD, C., LIPPERT, E., TALMANT, P., LAFAGE-POCHITALOFF, M., LEROUX, D., GERVAIS, C., VIGUIÉ, F., LAI, J. L., TERRE, C., BEVERLO, B., SAMBANI, C., HAGEMEIJER, A., MARYNEN, P., DELSOL, G., DASTUGUE, N., MECUCCI, C. & BROUSSET, P. 2008b. Myeloid cell differentiation arrest by miR-125b-1 in myelodysplastic syndrome and acute myeloid leukemia with the t(2;11)(p21;q23) translocation. *J Exp Med,* 205**,** 2499-506.

BREITMAN, T. R., COLLINS, S. J. & KEENE, B. R. 1981. Terminal differentiation of human promyelocytic leukemic cells in primary culture in response to retinoic acid. *Blood,* 57**,** 1000-4.

BRIDGE, G., RASHID, S. & MARTIN, S. A. 2014. DNA mismatch repair and oxidative DNA damage: implications for cancer biology and treatment. *Cancers (Basel),* 6**,** 1597-614.

BULTMANN, S., MORBITZER, R., SCHMIDT, C. S., THANISCH, K., SPADA, F., ELSAESSER, J., LAHAYE, T. & LEONHARDT, H. 2012. Targeted transcriptional activation of silent oct4 pluripotency gene by combining designer TALEs and inhibition of epigenetic modifiers. *Nucleic Acids Res,* 40**,** 5368-77.

CADE, L., REYON, D., HWANG, W. Y., TSAI, S. Q., PATEL, S., KHAYTER, C., JOUNG, J. K., SANDER, J. D., PETERSON, R. T. & YEH, J. R. 2012. Highly efficient generation of heritable zebrafish gene mutations using homo- and heterodimeric TALENs. *Nucleic Acids Res,* 40**,** 8001-10.

CALABRETTA, B. & PERROTTI, D. 2004. The biology of CML blast crisis. *Blood,* 103**,** 4010-22.

CALIN, G. A. & CROCE, C. M. 2006. MicroRNAs and chromosomal abnormalities in cancer cells. *Oncogene,* 25**,** 6202-10.

CAPORALI, A. & EMANUELI, C. 2011. MicroRNA regulation in angiogenesis. *Vascul Pharmacol,* 55**,** 79-86.

CAROW, C. E., LEVENSTEIN, M., KAUFMANN, S. H., CHEN, J., AMIN, S., ROCKWELL, P., WITTE, L., BOROWITZ, M. J., CIVIN, C. I. & SMALL, D. 1996. Expression of the hematopoietic growth factor receptor FLT3 (STK-1/Flk2) in human leukemias. *Blood,* 87**,** 1089-96.

CERMAK, T., DOYLE, E. L., CHRISTIAN, M., WANG, L., ZHANG, Y., SCHMIDT, C., BALLER, J. A., SOMIA, N. V., BOGDANOVE, A. J. & VOYTAS, D. F. 2011. Efficient design and assembly of custom TALEN and other TAL effector-based constructs for DNA targeting. *Nucleic Acids Res,* 39**,** e82.

CHANG, T. C., YU, D., LEE, Y. S., WENTZEL, E. A., ARKING, D. E., WEST, K. M., DANG, C. V., THOMAS-TIKHONENKO, A. & MENDELL, J. T. 2008. Widespread microRNA repression by Myc contributes to tumorigenesis. *Nat Genet,* 40**,** 43-50.

CHEKMENEV, D. S., HAID, C. & KEL, A. E. 2005. P-Match: transcription factor binding site search by combining patterns and weight matrices. *Nucleic Acids Res,* 33**,** W432-7.

CHEN, G. Q., ZHU, J., SHI, X. G., NI, J. H., ZHONG, H. J., SI, G. Y., JIN, X. L., TANG, W., LI, X. S., XONG, S. M., SHEN, Z. X., SUN, G. L., MA, J., ZHANG, P., ZHANG, T. D., GAZIN, C., NAOE, T., CHEN, S. J., WANG, Z. Y. & CHEN, Z. 1996. In vitro studies on cellular and molecular mechanisms of arsenic trioxide (As2O3) in the treatment of acute promyelocytic leukemia: As2O3 induces NB4 cell apoptosis with downregulation of Bcl-2 expression and modulation of PML-RAR alpha/PML proteins. *Blood,* 88**,** 1052-61.

CHEN, J., WANG, M., GUO, M., XIE, Y. & CONG, Y. S. 2013. miR-127 regulates cell proliferation and senescence by targeting BCL6. *PLoS One,* 8**,** e80266.

CHORLEY, B. N., CAMPBELL, M. R., WANG, X., KARACA, M., SAMBANDAN, D., BANGURA, F., XUE, P., PI, J., KLEEBERGER, S. R. & BELL, D. A. 2012. Identification of novel NRF2-regulated genes by ChIP-Seq: influence on retinoid X receptor alpha. *Nucleic Acids Res,* 40**,** 7416-29.

CHOU, J., LIN, J. H., BRENOT, A., KIM, J. W., PROVOT, S. & WERB, Z. 2013. GATA3 suppresses metastasis and modulates the tumour microenvironment by regulating microRNA-29b expression. *Nat Cell Biol,* 15**,** 201-13.

CHOWDHRY, S., ZHANG, Y., MCMAHON, M., SUTHERLAND, C., CUADRADO, A. & HAYES, J. D. 2013. Nrf2 is controlled by two distinct β-TrCP recognition motifs in its Neh6 domain, one of which can be modulated by GSK-3 activity. *Oncogene,* 32**,** 3765-81.

CHRISTIAN, M., CERMAK, T., DOYLE, E. L., SCHMIDT, C., ZHANG, F., HUMMEL, A., BOGDANOVE, A. J. & VOYTAS, D. F. 2010. Targeting DNA double-strand breaks with TAL effector nucleases. *Genetics,* 186**,** 757-61.

COLLINS-UNDERWOOD, J. R. & MULLIGHAN, C. G. 2010. Genomic profiling of high-risk acute lymphoblastic leukemia. *Leukemia,* 24**,** 1676-85.

CONG, L., RAN, F. A., COX, D., LIN, S., BARRETTO, R., HABIB, N., HSU, P. D., WU, X., JIANG, W., MARRAFFINI, L. A. & ZHANG, F. 2013. Multiplex genome engineering using CRISPR/Cas systems. *Science,* 339**,** 819-23.

CONWAY O'BRIEN, E., PRIDEAUX, S. & CHEVASSUT, T. 2014. The epigenetic landscape of acute myeloid leukemia. *Adv Hematol,* 2014**,** 103175.

COOKE, M. S., MISTRY, N., WOOD, C., HERBERT, K. E. & LUNEC, J. 1997. Immunogenicity of DNA damaged by reactive oxygen species--implications for anti-DNA antibodies in lupus. *Free Radic Biol Med,* 22**,** 151-9.

COOMBS, C. C., TAVAKKOLI, M. & TALLMAN, M. S. 2015. Acute promyelocytic leukemia: where did we start, where are we now, and the future. *Blood Cancer J,* 5**,** e304.

CULLINAN, S. B., GORDAN, J. D., JIN, J., HARPER, J. W. & DIEHL, J. A. 2004. The Keap1-BTB protein is an adaptor that bridges Nrf2 to a Cul3-based E3 ligase: oxidative stress sensing by a Cul3-Keap1 ligase. *Mol Cell Biol,* 24**,** 8477-86.

DAVIS, A. J. & CHEN, D. J. 2013. DNA double strand break repair via non-homologous end-joining. *Transl Cancer Res,* 2**,** 130-143.

DE KOUCHKOVSKY, I. & ABDUL-HAY, M. 2016. 'Acute myeloid leukemia: a comprehensive review and 2016 update'. *Blood Cancer J,* 6**,** e441.

DELAUNAY, J., VEY, N., LEBLANC, T., FENAUX, P., RIGAL-HUGUET, F., WITZ, F., LAMY, T., AUVRIGNON, A., BLAISE, D., PIGNEUX, A., MUGNERET, F., BASTARD, C., DASTUGUE, N., VAN DEN AKKER, J., FIÈRE, D., REIFFERS, J., CASTAIGNE, S., LEVERGER, G., HAROUSSEAU, J. L., DOMBRET, H., INTERGROUP, F. A. M. L., MYÉOBLASTIQUES, G. O.-E. D. L. A., L'ENFANT, L. A. M. D., ASSOCIATION, A. L. F. & GROUPS, B.-G.-M.-T. C. 2003. Prognosis of inv(16)/t(16;16) acute myeloid leukemia (AML): a survey of 110 cases from the French AML Intergroup. *Blood,* 102**,** 462-9.

DEMCHENKO, Y. N., GLEBOV, O. K., ZINGONE, A., KEATS, J. J., BERGSAGEL, P. L. & KUEHL, W. M. 2010. Classical and/or alternative NF-kappaB pathway activation in multiple myeloma. *Blood,* 115**,** 3541-52.

DENG, D., YAN, C., PAN, X., MAHFOUZ, M., WANG, J., ZHU, J. K., SHI, Y. & YAN, N. 2012. Structural basis for sequence-specific recognition of DNA by TAL effectors. *Science,* 335**,** 720-3.

DENICOLA, G. M., KARRETH, F. A., HUMPTON, T. J., GOPINATHAN, A., WEI, C., FRESE, K., MANGAL, D., YU, K. H., YEO, C. J., CALHOUN, E. S., SCRIMIERI, F., WINTER, J. M., HRUBAN, R. H., IACOBUZIO-DONAHUE, C., KERN, S. E., BLAIR, I. A. & TUVESON, D. A. 2011. Oncogene-induced Nrf2 transcription promotes ROS detoxification and tumorigenesis. *Nature,* 475**,** 106-9.

DESHMUKH, P., UNNI, S., KRISHNAPPA, G. & PADMANABHAN, B. 2017. The Keap1-Nrf2 pathway: promising therapeutic target to counteract ROS-

mediated damage in cancers and neurodegenerative diseases. *Biophys Rev,* 9**,** 41-56.

DI LEVA, G., GASPARINI, P., PIOVAN, C., NGANKEU, A., GAROFALO, M., TACCIOLI, C., IORIO, M. V., LI, M., VOLINIA, S., ALDER, H., NAKAMURA, T., NUOVO, G., LIU, Y., NEPHEW, K. P. & CROCE, C. M. 2010. MicroRNA cluster 221-222 and estrogen receptor alpha interactions in breast cancer. *J Natl Cancer Inst,* 102**,** 706-21.

DING, Y., LI, H., CHEN, L. L. & XIE, K. 2016. Recent Advances in Genome Editing Using CRISPR/Cas9. *Front Plant Sci,* 7**,** 703.

DUNAND-SAUTHIER, I., SANTIAGO-RABER, M. L., CAPPONI, L., VEJNAR, C. E., SCHAAD, O., IRLA, M., SEGUÍN-ESTÉVEZ, Q., DESCOMBES, P., ZDOBNOV, E. M., ACHA-ORBEA, H. & REITH, W. 2011. Silencing of c-Fos expression by microRNA-155 is critical for dendritic cell maturation and function. *Blood,* 117**,** 4490-500.

DUPREZ, E., WAGNER, K., KOCH, H. & TENEN, D. G. 2003. C/EBPbeta: a major PML-RARA-responsive gene in retinoic acid-induced differentiation of APL cells. *EMBO J,* 22**,** 5806-16.

DÖHNER, H., ESTEY, E. H., AMADORI, S., APPELBAUM, F. R., BÜCHNER, T., BURNETT, A. K., DOMBRET, H., FENAUX, P., GRIMWADE, D., LARSON, R. A., LO-COCO, F., NAOE, T., NIEDERWIESER, D., OSSENKOPPELE, G. J., SANZ, M. A., SIERRA, J., TALLMAN, M. S., LÖWENBERG, B., BLOOMFIELD, C. D. & LEUKEMIANET, E. 2010. Diagnosis and management of acute myeloid leukemia in adults: recommendations from an international expert panel, on behalf of the European LeukemiaNet. *Blood,* 115**,** 453-74.

DÖHNER, H., STILGENBAUER, S., BENNER, A., LEUPOLT, E., KRÖBER, A., BULLINGER, L., DÖHNER, K., BENTZ, M. & LICHTER, P. 2000. Genomic aberrations and survival in chronic lymphocytic leukemia. *N Engl J Med,* 343**,** 1910-6.

ESTEY, E. H. 2014. Acute myeloid leukemia: 2014 update on risk-stratification and management. *Am J Hematol,* 89**,** 1063-81.

EYHOLZER, M., SCHMID, S., WILKENS, L., MUELLER, B. U. & PABST, T. 2010. The tumour-suppressive miR-29a/b1 cluster is regulated by CEBPA and blocked in human AML. *Br J Cancer,* 103**,** 275-84.

FALINI, B., MECUCCI, C., TIACCI, E., ALCALAY, M., ROSATI, R., PASQUALUCCI, L., LA STARZA, R., DIVERIO, D., COLOMBO, E., SANTUCCI, A., BIGERNA, B., PACINI, R., PUCCIARINI, A., LISO, A., VIGNETTI, M., FAZI, P., MEANI, N., PETTIROSSI, V., SAGLIO, G., MANDELLI, F., LO-COCO, F., PELICCI, P. G., MARTELLI, M. F. & PARTY, G. A. L. W. 2005. Cytoplasmic nucleophosmin in acute myelogenous leukemia with a normal karyotype. *N Engl J Med,* 352**,** 254-66.

FATHI, A. T. & CHEN, Y. B. 2011. Treatment of FLT3-ITD acute myeloid leukemia. *Am J Blood Res,* 1**,** 175-89.

FEDERICI, L. & FALINI, B. 2013. Nucleophosmin mutations in acute myeloid leukemia: a tale of protein unfolding and mislocalization. *Protein Sci,* 22**,** 545-56.

FELLI, N., FONTANA, L., PELOSI, E., BOTTA, R., BONCI, D., FACCHIANO, F., LIUZZI, F., LULLI, V., MORSILLI, O., SANTORO, S., VALTIERI, M., CALIN, G. A., LIU, C. G., SORRENTINO, A., CROCE, C. M. & PESCHLE, C. 2005. MicroRNAs 221 and 222 inhibit normal erythropoiesis and erythroleukemic cell growth via kit receptor down-modulation. *Proc Natl Acad Sci U S A,* 102**,** 18081-6.

FINKEL, T. 2011. Signal transduction by reactive oxygen species. *J Cell Biol,* 194**,** 7-15.

FIRTH, A. L., MENON, T., PARKER, G. S., QUALLS, S. J., LEWIS, B. M., KE, E., DARGITZ, C. T., WRIGHT, R., KHANNA, A., GAGE, F. H. & VERMA, I. M. 2015. Functional Gene Correction for Cystic Fibrosis in Lung Epithelial Cells Generated from Patient iPSCs. *Cell Rep,* 12**,** 1385-90.

FONTANA, L., PELOSI, E., GRECO, P., RACANICCHI, S., TESTA, U., LIUZZI, F., CROCE, C. M., BRUNETTI, E., GRIGNANI, F. & PESCHLE, C. 2007. MicroRNAs 17-5p-20a-106a control monocytopoiesis through AML1 targeting and M-CSF receptor upregulation. *Nat Cell Biol,* 9**,** 775-87.

FORNARI, F., GRAMANTIERI, L., GIOVANNINI, C., VERONESE, A., FERRACIN, M., SABBIONI, S., CALIN, G. A., GRAZI, G. L., CROCE, C. M., TAVOLARI, S., CHIECO, P., NEGRINI, M. & BOLONDI, L. 2009. MiR-122/cyclin G1 interaction modulates p53 activity and affects doxorubicin sensitivity of human hepatocarcinoma cells. *Cancer Res,* 69**,** 5761-7.

FU, Y., SANDER, J. D., REYON, D., CASCIO, V. M. & JOUNG, J. K. 2014. Improving CRISPR-Cas nuclease specificity using truncated guide RNAs. *Nat Biotechnol,* 32**,** 279-284.

FUJITA, T. & FUJII, H. 2013. Efficient isolation of specific genomic regions and identification of associated proteins by engineered DNA-binding molecule-mediated chromatin immunoprecipitation (enChIP) using CRISPR. *Biochem Biophys Res Commun,* 439**,** 132-6.

GAJ, T., GERSBACH, C. A. & BARBAS, C. F. 2013. ZFN, TALEN, and CRISPR/Cas-based methods for genome engineering. *Trends Biotechnol,* 31**,** 397-405.

GALARDI, S., MERCATELLI, N., GIORDA, E., MASSALINI, S., FRAJESE, G. V., CIAFRÈ, S. A. & FARACE, M. G. 2007. miR-221 and miR-222 expression affects the proliferation potential of human prostate carcinoma cell lines by targeting p27Kip1. *J Biol Chem,* 282**,** 23716-24.

GAROFALO, M., QUINTAVALLE, C., ROMANO, G., CROCE, C. M. & CONDORELLI, G. 2012. miR221/222 in cancer: their role in tumor progression and response to therapy. *Curr Mol Med,* 12**,** 27-33.

GARZON, R., HEAPHY, C. E., HAVELANGE, V., FABBRI, M., VOLINIA, S., TSAO, T., ZANESI, N., KORNBLAU, S. M., MARCUCCI, G., CALIN, G. A., ANDREEFF, M. & CROCE, C. M. 2009a. MicroRNA 29b functions in acute myeloid leukemia. *Blood,* 114**,** 5331-41.

GARZON, R., LIU, S., FABBRI, M., LIU, Z., HEAPHY, C. E., CALLEGARI, E., SCHWIND, S., PANG, J., YU, J., MUTHUSAMY, N., HAVELANGE, V., VOLINIA, S., BLUM, W., RUSH, L. J., PERROTTI,

D., ANDREEFF, M., BLOOMFIELD, C. D., BYRD, J. C., CHAN, K., WU, L. C., CROCE, C. M. & MARCUCCI, G. 2009b. MicroRNA-29b induces global DNA hypomethylation and tumor suppressor gene reexpression in acute myeloid leukemia by targeting directly DNMT3A and 3B and indirectly DNMT1. *Blood,* 113**,** 6411-8.

GASIUNAS, G., BARRANGOU, R., HORVATH, P. & SIKSNYS, V. 2012. Cas9-crRNA ribonucleoprotein complex mediates specific DNA cleavage for adaptive immunity in bacteria. *Proc Natl Acad Sci U S A,* 109**,** E2579-86.

GAUDELLI, N. M., KOMOR, A. C., REES, H. A., PACKER, M. S., BADRAN, A. H., BRYSON, D. I. & LIU, D. R. 2017. Programmable base editing of A•T to G•C in genomic DNA without DNA cleavage. *Nature,* 551**,** 464-471.

GENOVESE, P., SCHIROLI, G., ESCOBAR, G., TOMASO, T. D., FIRRITO, C., CALABRIA, A., MOI, D., MAZZIERI, R., BONINI, C., HOLMES, M. C., GREGORY, P. D., VAN DER BURG, M., GENTNER, B., MONTINI, E., LOMBARDO, A. & NALDINI, L. 2014. Targeted genome editing in human repopulating haematopoietic stem cells. *Nature,* 510**,** 235-240.

GHOSH, S. & KARIN, M. 2002. Missing pieces in the NF-kappaB puzzle. *Cell,* 109 Suppl**,** S81-96.

GRAHAM, D. B. & ROOT, D. E. 2015. Resources for the design of CRISPR gene editing experiments. *Genome Biol,* 16**,** 260.

GRIMWADE, D., BIONDI, A., MOZZICONACCI, M. J., HAGEMEIJER, A., BERGER, R., NEAT, M., HOWE, K., DASTUGUE, N., JANSEN, J., RADFORD-WEISS, I., LO COCO, F., LESSARD, M., HERNANDEZ, J. M., DELABESSE, E., HEAD, D., LISO, V., SAINTY, D., FLANDRIN, G., SOLOMON, E., BIRG, F. & LAFAGE-POCHITALOFF, M. 2000. Characterization of acute promyelocytic leukemia cases lacking the classic t(15;17): results of the European Working Party. Groupe Français de Cytogénétique Hématologique, Groupe de Français d'Hematologie Cellulaire, UK Cancer Cytogenetics Group and BIOMED 1 European Community-Concerted Action "Molecular Cytogenetic Diagnosis in Haematological Malignancies". *Blood,* 96**,** 1297-308.

GRISENDI, S., BERNARDI, R., ROSSI, M., CHENG, K., KHANDKER, L., MANOVA, K. & PANDOLFI, P. P. 2005. Role of nucleophosmin in embryonic development and tumorigenesis. *Nature,* 437**,** 147-53.

GROVE, C. S. & VASSILIOU, G. S. 2014. Acute myeloid leukaemia: a paradigm for the clonal evolution of cancer? *Dis Model Mech,* 7**,** 941-51.

GUILINGER, J. P., THOMPSON, D. B. & LIU, D. R. 2014. Fusion of catalytically inactive Cas9 to FokI nuclease improves the specificity of genome modification. *Nat Biotechnol,* 32**,** 577-582.

GUO, S., LU, J., SCHLANGER, R., ZHANG, H., WANG, J. Y., FOX, M. C., PURTON, L. E., FLEMING, H. H., COBB, B., MERKENSCHLAGER, M., GOLUB, T. R. & SCADDEN, D. T. 2010. MicroRNA miR-125a controls hematopoietic stem cell number. *Proc Natl Acad Sci U S A,* 107**,** 14229-34.

GUSTAFSON, S. A., LIN, P., CHEN, S. S., CHEN, L., ABRUZZO, L. V., LUTHRA, R., MEDEIROS, L. J. & WANG, S. A. 2009. Therapy-related acute myeloid leukemia with t(8;21) (q22;q22) shares many features with de novo acute myeloid leukemia with t(8;21)(q22;q22) but does not have a favorable outcome. *Am J Clin Pathol,* 131**,** 647-55.

HAMILTON, D. L. & ABREMSKI, K. 1984. Site-specific recombination by the bacteriophage P1 lox-Cre system. Cre-mediated synapsis of two lox sites. *J Mol Biol,* 178**,** 481-6.

HAN, J., LEE, Y., YEOM, K. H., NAM, J. W., HEO, I., RHEE, J. K., SOHN, S. Y., CHO, Y., ZHANG, B. T. & KIM, V. N. 2006. Molecular basis for the recognition of primary microRNAs by the Drosha-DGCR8 complex. *Cell,* 125**,** 887-901.

HAN, Y. C., PARK, C. Y., BHAGAT, G., ZHANG, J., WANG, Y., FAN, J. B., LIU, M., ZOU, Y., WEISSMAN, I. L. & GU, H. 2010. microRNA-29a induces aberrant self-renewal capacity in hematopoietic progenitors, biased myeloid development, and acute myeloid leukemia. *J Exp Med,* 207**,** 475-89.

HANADA, N., TAKAHATA, T., ZHOU, Q., YE, X., SUN, R., ITOH, J., ISHIGURO, A., KIJIMA, H., MIMURA, J., ITOH, K., FUKUDA, S. & SAIJO, Y. 2012. Methylation of the KEAP1 gene promoter region in human colorectal cancer. *BMC Cancer,* 12**,** 66.

HARIRIAN, M., KAVIANI, S., SOLEIMANI, M., GHAEMI, S. R., DELALAT, B. & ATASHI, A. 2012. Morpholino Oligo Antisense efficiently suppresses BCR/ABL and cell proliferation in CML: specific inhibition of BCR-ABL gene expression by Morpholino Oligo Antisense in BCR-ABL(+) cells. *Hematology,* 17**,** 28-34.

HAWLEY, T. S., FONG, A. Z., GRIESSER, H., LYMAN, S. D. & HAWLEY, R. G. 1998. Leukemic predisposition of mice transplanted with gene-modified hematopoietic precursors expressing flt3 ligand. *Blood,* 92**,** 2003-11.

HAYAKAWA, F., TOWATARI, M., KIYOI, H., TANIMOTO, M., KITAMURA, T., SAITO, H. & NAOE, T. 2000. Tandem-duplicated Flt3 constitutively activates STAT5 and MAP kinase and introduces autonomous cell growth in IL-3-dependent cell lines. *Oncogene,* 19**,** 624-31.

HE, L. Z., TRIBIOLI, C., RIVI, R., PERUZZI, D., PELICCI, P. G., SOARES, V., CATTORETTI, G. & PANDOLFI, P. P. 1997. Acute leukemia with promyelocytic features in PML/RARalpha transgenic mice. *Proc Natl Acad Sci U S A,* 94**,** 5302-7.

HEATH, E. M., CHAN, S. M., MINDEN, M. D., MURPHY, T., SHLUSH, L. I. & SCHIMMER, A. D. 2017. Biological and clinical consequences of NPM1 mutations in AML. *Leukemia,* 31**,** 798-807.

HEISS, E. H., SCHACHNER, D., ZIMMERMANN, K. & DIRSCH, V. M. 2013. Glucose availability is a decisive factor for Nrf2-mediated gene expression. *Redox Biol,* 1**,** 359-65.

HIRATA, Y., MURAI, N., YANAIHARA, N., SAITO, M., URASHIMA, M., MURAKAMI, Y., MATSUFUJI, S. & OKAMOTO, A. 2014. MicroRNA-

21 is a candidate driver gene for 17q23-25 amplification in ovarian clear cell carcinoma. *BMC Cancer,* 14**,** 799.

HOMMA, S., ISHII, Y., MORISHIMA, Y., YAMADORI, T., MATSUNO, Y., HARAGUCHI, N., KIKUCHI, N., SATOH, H., SAKAMOTO, T., HIZAWA, N., ITOH, K. & YAMAMOTO, M. 2009. Nrf2 enhances cell proliferation and resistance to anticancer drugs in human lung cancer. *Clin Cancer Res,* 15**,** 3423-32.

HOMMELSHEIM, C. M., FRANTZESKAKIS, L., HUANG, M. & ÜLKER, B. 2014. PCR amplification of repetitive DNA: a limitation to genome editing technologies and many other applications. *Sci Rep,* 4**,** 5052.

HONG, Y. B., KANG, H. J., KWON, S. Y., KIM, H. J., KWON, K. Y., CHO, C. H., LEE, J. M., KALLAKURY, B. V. & BAE, I. 2010. Nuclear factor (erythroid-derived 2)-like 2 regulates drug resistance in pancreatic cancer cells. *Pancreas,* 39**,** 463-72.

HOUBAVIY, H. B., MURRAY, M. F. & SHARP, P. A. 2003. Embryonic stem cell-specific MicroRNAs. *Dev Cell,* 5**,** 351-8.

HU, X. F., YAO, J., GAO, S. G., WANG, X. S., PENG, X. Q., YANG, Y. T. & FENG, X. S. 2013. Nrf2 overexpression predicts prognosis and 5-FU resistance in gastric cancer. *Asian Pac J Cancer Prev,* 14**,** 5231-5.

HUA, Z., LV, Q., YE, W., WONG, C. K., CAI, G., GU, D., JI, Y., ZHAO, C., WANG, J., YANG, B. B. & ZHANG, Y. 2006. MiRNA-directed regulation of VEGF and other angiogenic factors under hypoxia. *PLoS One,* 1**,** e116.

HUANG, M. E., YE, Y. C., CHEN, S. R., CHAI, J. R., LU, J. X., ZHOA, L., GU, L. J. & WANG, Z. Y. 1988. Use of all-trans retinoic acid in the treatment of acute promyelocytic leukemia. *Blood,* 72**,** 567-72.

HWANG, H. W. & MENDELL, J. T. 2006. MicroRNAs in cell proliferation, cell death, and tumorigenesis. *Br J Cancer,* 94**,** 776-80.

IQBAL, J., SHEN, Y., LIU, Y., FU, K., JAFFE, E. S., LIU, C., LIU, Z., LACHEL, C. M., DEFFENBACHER, K., GREINER, T. C., VOSE, J. M., BHAGAVATHI, S., STAUDT, L. M., RIMSZA, L., ROSENWALD, A., OTT, G., DELABIE, J., CAMPO, E., BRAZIEL, R. M., COOK, J. R., TUBBS, R. R., GASCOYNE, R. D., ARMITAGE, J. O., WEISENBURGER, D. D., MCKEITHAN, T. W. & CHAN, W. C. 2012. Genome-wide miRNA profiling of mantle cell lymphoma reveals a distinct subgroup with poor prognosis. *Blood,* 119**,** 4939-48.

ITOH, K., CHIBA, T., TAKAHASHI, S., ISHII, T., IGARASHI, K., KATOH, Y., OYAKE, T., HAYASHI, N., SATOH, K., HATAYAMA, I., YAMAMOTO, M. & NABESHIMA, Y. 1997. An Nrf2/small Maf heterodimer mediates the induction of phase II detoxifying enzyme genes through antioxidant response elements. *Biochem Biophys Res Commun,* 236**,** 313-22.

ITOH, K., TONG, K. I. & YAMAMOTO, M. 2004. Molecular mechanism activating Nrf2-Keap1 pathway in regulation of adaptive response to electrophiles. *Free Radic Biol Med,* 36**,** 1208-13.

IVEY, K. N., MUTH, A., ARNOLD, J., KING, F. W., YEH, R. F., FISH, J. E., HSIAO, E. C., SCHWARTZ, R. J., CONKLIN, B. R., BERNSTEIN, H. S.

& SRIVASTAVA, D. 2008. MicroRNA regulation of cell lineages in mouse and human embryonic stem cells. *Cell Stem Cell,* 2**,** 219-29.
IWASAKI, H. & AKASHI, K. 2007. Myeloid lineage commitment from the hematopoietic stem cell. *Immunity,* 26**,** 726-40.
JAGANNATHAN-BOGDAN, M. & ZON, L. I. 2013. Hematopoiesis. *Development,* 140**,** 2463-7.
JARAMILLO, M. C. & ZHANG, D. D. 2013. The emerging role of the Nrf2-Keap1 signaling pathway in cancer. *Genes Dev,* 27**,** 2179-91.
JIA, H. Y., WANG, Y. X., YAN, W. T., LI, H. Y., TIAN, Y. Z., WANG, S. M. & ZHAO, H. L. 2012. MicroRNA-125b functions as a tumor suppressor in hepatocellular carcinoma cells. *Int J Mol Sci,* 13**,** 8762-74.
JIANG, F., TAYLOR, D. W., CHEN, J. S., KORNFELD, J. E., ZHOU, K., THOMPSON, A. J., NOGALES, E. & DOUDNA, J. A. 2016. Structures of a CRISPR-Cas9 R-loop complex primed for DNA cleavage. *Science,* 351**,** 867-71.
JINEK, M., CHYLINSKI, K., FONFARA, I., HAUER, M., DOUDNA, J. A. & CHARPENTIER, E. 2012. A programmable dual-RNA-guided DNA endonuclease in adaptive bacterial immunity. *Science,* 337**,** 816-21.
JOHNNIDIS, J. B., HARRIS, M. H., WHEELER, R. T., STEHLING-SUN, S., LAM, M. H., KIRAK, O., BRUMMELKAMP, T. R., FLEMING, M. D. & CAMARGO, F. D. 2008. Regulation of progenitor cell proliferation and granulocyte function by microRNA-223. *Nature,* 451**,** 1125-9.
JOHNSON, C. D., ESQUELA-KERSCHER, A., STEFANI, G., BYROM, M., KELNAR, K., OVCHARENKO, D., WILSON, M., WANG, X., SHELTON, J., SHINGARA, J., CHIN, L., BROWN, D. & SLACK, F. J. 2007. The let-7 microRNA represses cell proliferation pathways in human cells. *Cancer Res,* 67**,** 7713-22.
JOUNG, J. K. & SANDER, J. D. 2013. TALENs: a widely applicable technology for targeted genome editing. *Nat Rev Mol Cell Biol,* 14**,** 49-55.
KANELLOPOULOU, C., MULJO, S. A., KUNG, A. L., GANESAN, S., DRAPKIN, R., JENUWEIN, T., LIVINGSTON, D. M. & RAJEWSKY, K. 2005. Dicer-deficient mouse embryonic stem cells are defective in differentiation and centromeric silencing. *Genes Dev,* 19**,** 489-501.
KANG, M. I., KOBAYASHI, A., WAKABAYASHI, N., KIM, S. G. & YAMAMOTO, M. 2004. Scaffolding of Keap1 to the actin cytoskeleton controls the function of Nrf2 as key regulator of cytoprotective phase 2 genes. *Proc Natl Acad Sci U S A,* 101**,** 2046-51.
KANTARJIAN, H., O'BRIEN, S., JABBOUR, E., GARCIA-MANERO, G., QUINTAS-CARDAMA, A., SHAN, J., RIOS, M. B., RAVANDI, F., FADERL, S., KADIA, T., BORTHAKUR, G., HUANG, X., CHAMPLIN, R., TALPAZ, M. & CORTES, J. 2012. Improved survival in chronic myeloid leukemia since the introduction of imatinib therapy: a single-institution historical experience. *Blood,* 119**,** 1981-7.
KEENEY, S., GIROUX, C. N. & KLECKNER, N. 1997. Meiosis-specific DNA double-strand breaks are catalyzed by Spo11, a member of a widely conserved protein family. *Cell,* 88**,** 375-84.
KELLY, L. M. & GILLILAND, D. G. 2002. Genetics of myeloid leukemias. *Annu Rev Genomics Hum Genet,* 3**,** 179-98.

KIM, J. & KEUM, Y. S. 2016. NRF2, a Key Regulator of Antioxidants with Two Faces towards Cancer. *Oxid Med Cell Longev,* 2016**,** 2746457.

KIM, Y. B., KOMOR, A. C., LEVY, J. M., PACKER, M. S., ZHAO, K. T. & LIU, D. R. 2017. Increasing the genome-targeting scope and precision of base editing with engineered Cas9-cytidine deaminase fusions. *Nat Biotechnol,* 35**,** 371-376.

KIM, Y. R., OH, J. E., KIM, M. S., KANG, M. R., PARK, S. W., HAN, J. Y., EOM, H. S., YOO, N. J. & LEE, S. H. 2010. Oncogenic NRF2 mutations in squamous cell carcinomas of oesophagus and skin. *J Pathol,* 220**,** 446-51.

KLEINSTIVER, B. P., PATTANAYAK, V., PREW, M. S., TSAI, S. Q., NGUYEN, N. T., ZHENG, Z. & JOUNG, J. K. 2016. High-fidelity CRISPR-Cas9 nucleases with no detectable genome-wide off-target effects. *Nature,* 529**,** 490-5.

KLEINSTIVER, B. P., PREW, M. S., TSAI, S. Q., TOPKAR, V. V., NGUYEN, N. T., ZHENG, Z., GONZALES, A. P., LI, Z., PETERSON, R. T., YEH, J. R., ARYEE, M. J. & JOUNG, J. K. 2015. Engineered CRISPR-Cas9 nucleases with altered PAM specificities. *Nature,* 523**,** 481-5.

KOMOR, A. C., KIM, Y. B., PACKER, M. S., ZURIS, J. A. & LIU, D. R. 2016. Programmable editing of a target base in genomic DNA without double-stranded DNA cleavage. *Nature,* 533**,** 420-4.

KONDO, M. 2010. Lymphoid and myeloid lineage commitment in multipotent hematopoietic progenitors. *Immunol Rev,* 238**,** 37-46.

KONG, X., LIU, F. & GAO, J. 2016. MiR-155 promotes epithelial-mesenchymal transition in hepatocellular carcinoma cells through the activation of PI3K/SGK3/β-catenin signaling pathways. *Oncotarget,* 7**,** 66051-66060.

KOONIN, E. V. & WOLF, Y. I. 2015. Evolution of the CRISPR-Cas adaptive immunity systems in prokaryotes: models and observations on virus-host coevolution. *Mol Biosyst,* 11**,** 20-7.

KORALOV, S. B., MULJO, S. A., GALLER, G. R., KREK, A., CHAKRABORTY, T., KANELLOPOULOU, C., JENSEN, K., COBB, B. S., MERKENSCHLAGER, M., RAJEWSKY, N. & RAJEWSKY, K. 2008. Dicer ablation affects antibody diversity and cell survival in the B lymphocyte lineage. *Cell,* 132**,** 860-74.

KRIEGEL, A. J., LIU, Y., FANG, Y., DING, X. & LIANG, M. 2012. The miR-29 family: genomics, cell biology, and relevance to renal and cardiovascular injury. *Physiol Genomics,* 44**,** 237-44.

KROEGER, H., JELINEK, J., ESTÉCIO, M. R., HE, R., KONDO, K., CHUNG, W., ZHANG, L., SHEN, L., KANTARJIAN, H. M., BUESO-RAMOS, C. E. & ISSA, J. P. 2008. Aberrant CpG island methylation in acute myeloid leukemia is accentuated at relapse. *Blood,* 112**,** 1366-73.

KUMAR, C. C. 2011. Genetic abnormalities and challenges in the treatment of acute myeloid leukemia. *Genes Cancer,* 2**,** 95-107.

KUNDU, M. & LIU, P. P. 2001. Function of the inv(16) fusion gene CBFB-MYH11. *Curr Opin Hematol,* 8**,** 201-5.

KVINLAUG, B. T., CHAN, W. I., BULLINGER, L., RAMASWAMI, M., SEARS, C., FOSTER, D., LAZIC, S. E., OKABE, R., BENNER, A., LEE, B. H., DE SILVA, I., VALK, P. J., DELWEL, R., ARMSTRONG, S. A.,

DOHNER, H., GILLILAND, D. G. & HUNTLY, B. J. 2011. Common and overlapping oncogenic pathways contribute to the evolution of acute myeloid leukemias. *Cancer Res,* 71**,** 4117-29.

LAI, A. Y. & KONDO, M. 2008. T and B lymphocyte differentiation from hematopoietic stem cell. *Semin Immunol,* 20**,** 207-12.

LE BEAU, M. M., LARSON, R. A., BITTER, M. A., VARDIMAN, J. W., GOLOMB, H. M. & ROWLEY, J. D. 1983. Association of an inversion of chromosome 16 with abnormal marrow eosinophils in acute myelomonocytic leukemia. A unique cytogenetic-clinicopathological association. *N Engl J Med,* 309**,** 630-6.

LEE, Y., KIM, M., HAN, J., YEOM, K. H., LEE, S., BAEK, S. H. & KIM, V. N. 2004. MicroRNA genes are transcribed by RNA polymerase II. *EMBO J,* 23**,** 4051-60.

LEI, Z., LI, B., YANG, Z., FANG, H., ZHANG, G. M., FENG, Z. H. & HUANG, B. 2009. Regulation of HIF-1alpha and VEGF by miR-20b tunes tumor cells to adapt to the alteration of oxygen concentration. *PLoS One,* 4**,** e7629.

LEONG, S. M., TAN, B. X., BTE AHMAD, B., YAN, T., CHEE, L. Y., ANG, S. T., TAY, K. G., KOH, L. P., YEOH, A. E., KOAY, E. S., MOK, Y. K. & LIM, T. M. 2010. Mutant nucleophosmin deregulates cell death and myeloid differentiation through excessive caspase-6 and -8 inhibition. *Blood,* 116**,** 3286-96.

LEVIS, M. 2017. Midostaurin approved for FLT3-mutated AML. *Blood,* 129**,** 3403-3406.

LEVIS, M. & SMALL, D. 2003. FLT3: ITDoes matter in leukemia. *Leukemia,* 17**,** 1738-52.

LEY, T. J., DING, L., WALTER, M. J., MCLELLAN, M. D., LAMPRECHT, T., LARSON, D. E., KANDOTH, C., PAYTON, J. E., BATY, J., WELCH, J., HARRIS, C. C., LICHTI, C. F., TOWNSEND, R. R., FULTON, R. S., DOOLING, D. J., KOBOLDT, D. C., SCHMIDT, H., ZHANG, Q., OSBORNE, J. R., LIN, L., O'LAUGHLIN, M., MCMICHAEL, J. F., DELEHAUNTY, K. D., MCGRATH, S. D., FULTON, L. A., MAGRINI, V. J., VICKERY, T. L., HUNDAL, J., COOK, L. L., CONYERS, J. J., SWIFT, G. W., REED, J. P., ALLDREDGE, P. A., WYLIE, T., WALKER, J., KALICKI, J., WATSON, M. A., HEATH, S., SHANNON, W. D., VARGHESE, N., NAGARAJAN, R., WESTERVELT, P., TOMASSON, M. H., LINK, D. C., GRAUBERT, T. A., DIPERSIO, J. F., MARDIS, E. R. & WILSON, R. K. 2010. DNMT3A mutations in acute myeloid leukemia. *N Engl J Med,* 363**,** 2424-33.

LIANG, L., WONG, C. M., YING, Q., FAN, D. N., HUANG, S., DING, J., YAO, J., YAN, M., LI, J., YAO, M., NG, I. O. & HE, X. 2010. MicroRNA-125b suppressesed human liver cancer cell proliferation and metastasis by directly targeting oncogene LIN28B2. *Hepatology,* 52**,** 1731-40.

LIEBER, M. R. 2010. The mechanism of double-strand DNA break repair by the nonhomologous DNA end-joining pathway. *Annu Rev Biochem,* 79**,** 181-211.

LIU, S., WU, L. C., PANG, J., SANTHANAM, R., SCHWIND, S., WU, Y. Z., HICKEY, C. J., YU, J., BECKER, H., MAHARRY, K., RADMACHER,

M. D., LI, C., WHITMAN, S. P., MISHRA, A., STAUFFER, N., EIRING, A. M., BRIESEWITZ, R., BAIOCCHI, R. A., CHAN, K. K., PASCHKA, P., CALIGIURI, M. A., BYRD, J. C., CROCE, C. M., BLOOMFIELD, C. D., PERROTTI, D., GARZON, R. & MARCUCCI, G. 2010a. Sp1/NFkappaB/HDAC/miR-29b regulatory network in KIT-driven myeloid leukemia. *Cancer Cell,* 17**,** 333-347.

LIU, S., WU, L. C., PANG, J., SANTHANAM, R., SCHWIND, S., WU, Y. Z., HICKEY, C. J., YU, J., BECKER, H., MAHARRY, K., RADMACHER, M. D., LI, C., WHITMAN, S. P., MISHRA, A., STAUFFER, N., EIRING, A. M., BRIESEWITZ, R., BAIOCCHI, R. A., CHAN, K. K., PASCHKA, P., CALIGIURI, M. A., BYRD, J. C., CROCE, C. M., BLOOMFIELD, C. D., PERROTTI, D., GARZON, R. & MARCUCCI, G. 2010b. Sp1/NFkappaB/HDAC/miR-29b regulatory network in KIT-driven myeloid leukemia. *Cancer Cell,* 17**,** 333-47.

LU, J., GETZ, G., MISKA, E. A., ALVAREZ-SAAVEDRA, E., LAMB, J., PECK, D., SWEET-CORDERO, A., EBERT, B. L., MAK, R. H., FERRANDO, A. A., DOWNING, J. R., JACKS, T., HORVITZ, H. R. & GOLUB, T. R. 2005. MicroRNA expression profiles classify human cancers. *Nature,* 435**,** 834-8.

LUO, J., SU, F., CHEN, D., SHILOH, A. & GU, W. 2000. Deacetylation of p53 modulates its effect on cell growth and apoptosis. *Nature,* 408**,** 377-81.

LUX, C. T., YOSHIMOTO, M., MCGRATH, K., CONWAY, S. J., PALIS, J. & YODER, M. C. 2008. All primitive and definitive hematopoietic progenitor cells emerging before E10 in the mouse embryo are products of the yolk sac. *Blood,* 111**,** 3435-8.

MACKAREHTSCHIAN, K., HARDIN, J. D., MOORE, K. A., BOAST, S., GOFF, S. P. & LEMISCHKA, I. R. 1995. Targeted disruption of the flk2/flt3 gene leads to deficiencies in primitive hematopoietic progenitors. *Immunity,* 3**,** 147-61.

MAKAROVA, K. S., WOLF, Y. I., ALKHNBASHI, O. S., COSTA, F., SHAH, S. A., SAUNDERS, S. J., BARRANGOU, R., BROUNS, S. J., CHARPENTIER, E., HAFT, D. H., HORVATH, P., MOINEAU, S., MOJICA, F. J., TERNS, R. M., TERNS, M. P., WHITE, M. F., YAKUNIN, A. F., GARRETT, R. A., VAN DER OOST, J., BACKOFEN, R. & KOONIN, E. V. 2015. An updated evolutionary classification of CRISPR-Cas systems. *Nat Rev Microbiol,* 13**,** 722-36.

MARCUCCI, G., MRÓZEK, K., RADMACHER, M. D., BLOOMFIELD, C. D. & CROCE, C. M. 2009. MicroRNA expression profiling in acute myeloid and chronic lymphocytic leukaemias. *Best Pract Res Clin Haematol,* 22**,** 239-48.

MARI, P. O., FLOREA, B. I., PERSENGIEV, S. P., VERKAIK, N. S., BRÜGGENWIRTH, H. T., MODESTI, M., GIGLIA-MARI, G., BEZSTAROSTI, K., DEMMERS, J. A., LUIDER, T. M., HOUTSMULLER, A. B. & VAN GENT, D. C. 2006. Dynamic assembly of end-joining complexes requires interaction between Ku70/80 and XRCC4. *Proc Natl Acad Sci U S A,* 103**,** 18597-602.

MARTINEZ-NUNEZ, R. T., LOUAFI, F. & SANCHEZ-ELSNER, T. 2011. The interleukin 13 (IL-13) pathway in human macrophages is modulated by

microRNA-155 via direct targeting of interleukin 13 receptor alpha1 (IL13Ralpha1). *J Biol Chem,* 286**,** 1786-94.

MARZEC, J. M., CHRISTIE, J. D., REDDY, S. P., JEDLICKA, A. E., VUONG, H., LANKEN, P. N., APLENC, R., YAMAMOTO, T., YAMAMOTO, M., CHO, H. Y. & KLEEBERGER, S. R. 2007. Functional polymorphisms in the transcription factor NRF2 in humans increase the risk of acute lung injury. *FASEB J,* 21**,** 2237-46.

MASTON, G. A., EVANS, S. K. & GREEN, M. R. 2006. Transcriptional regulatory elements in the human genome. *Annu Rev Genomics Hum Genet,* 7**,** 29-59.

MCMAHON, M., THOMAS, N., ITOH, K., YAMAMOTO, M. & HAYES, J. D. 2004. Redox-regulated turnover of Nrf2 is determined by at least two separate protein domains, the redox-sensitive Neh2 degron and the redox-insensitive Neh6 degron. *J Biol Chem,* 279**,** 31556-67.

MEDBERRY, S. L., DALE, E., QIN, M. & OW, D. W. 1995. Intra-chromosomal rearrangements generated by Cre-lox site-specific recombination. *Nucleic Acids Res,* 23**,** 485-90.

MENZIN, J., LANG, K., EARLE, C. C., KERNEY, D. & MALLICK, R. 2002. The outcomes and costs of acute myeloid leukemia among the elderly. *Arch Intern Med,* 162**,** 1597-603.

MEYERS, J., YU, Y., KAYE, J. A. & DAVIS, K. L. 2013. Medicare fee-for-service enrollees with primary acute myeloid leukemia: an analysis of treatment patterns, survival, and healthcare resource utilization and costs. *Appl Health Econ Health Policy,* 11**,** 275-86.

MILLER, J. C., HOLMES, M. C., WANG, J., GUSCHIN, D. Y., LEE, Y. L., RUPNIEWSKI, I., BEAUSEJOUR, C. M., WAITE, A. J., WANG, N. S., KIM, K. A., GREGORY, P. D., PABO, C. O. & REBAR, E. J. 2007. An improved zinc-finger nuclease architecture for highly specific genome editing. *Nat Biotechnol,* 25**,** 778-85.

MILLER, J. C., TAN, S., QIAO, G., BARLOW, K. A., WANG, J., XIA, D. F., MENG, X., PASCHON, D. E., LEUNG, E., HINKLEY, S. J., DULAY, G. P., HUA, K. L., ANKOUDINOVA, I., COST, G. J., URNOV, F. D., ZHANG, H. S., HOLMES, M. C., ZHANG, L., GREGORY, P. D. & REBAR, E. J. 2011. A TALE nuclease architecture for efficient genome editing. *Nat Biotechnol,* 29**,** 143-8.

MITSUISHI, Y., MOTOHASHI, H. & YAMAMOTO, M. 2012a. The Keap1-Nrf2 system in cancers: stress response and anabolic metabolism. *Front Oncol,* 2**,** 200.

MITSUISHI, Y., TAGUCHI, K., KAWATANI, Y., SHIBATA, T., NUKIWA, T., ABURATANI, H., YAMAMOTO, M. & MOTOHASHI, H. 2012b. Nrf2 redirects glucose and glutamine into anabolic pathways in metabolic reprogramming. *Cancer Cell,* 22**,** 66-79.

MOI, P., CHAN, K., ASUNIS, I., CAO, A. & KAN, Y. W. 1994. Isolation of NF-E2-related factor 2 (Nrf2), a NF-E2-like basic leucine zipper transcriptional activator that binds to the tandem NF-E2/AP1 repeat of the beta-globin locus control region. *Proc Natl Acad Sci U S A,* 91**,** 9926-30.

MONTAGUE, T. G., CRUZ, J. M., GAGNON, J. A., CHURCH, G. M. & VALEN, E. 2014. CHOPCHOP: a CRISPR/Cas9 and TALEN web tool for genome editing. *Nucleic Acids Res,* 42**,** W401-7.

MOORE, M. A. & METCALF, D. 1970. Ontogeny of the haemopoietic system: yolk sac origin of in vivo and in vitro colony forming cells in the developing mouse embryo. *Br J Haematol,* 18**,** 279-96.

MRÓZEK, K., HEEREMA, N. A. & BLOOMFIELD, C. D. 2004. Cytogenetics in acute leukemia. *Blood Rev,* 18**,** 115-36.

MU, J., ZHU, D., SHEN, Z., NING, S., LIU, Y., CHEN, J., LI, Y. & LI, Z. 2017. The repressive effect of miR-148a on Wnt/β-catenin signaling involved in Glabridin-induced anti-angiogenesis in human breast cancer cells. *BMC Cancer,* 17**,** 307.

MULJO, S. A., ANSEL, K. M., KANELLOPOULOU, C., LIVINGSTON, D. M., RAO, A. & RAJEWSKY, K. 2005. Aberrant T cell differentiation in the absence of Dicer. *J Exp Med,* 202**,** 261-9.

MURPHY, A. J., GUYRE, P. M. & PIOLI, P. A. 2010. Estradiol suppresses NF-kappa B activation through coordinated regulation of let-7a and miR-125b in primary human macrophages. *J Immunol,* 184**,** 5029-37.

MÅLØY, M., MÅLØY, F., JAKOBSEN, P. & OLAV BRANDSDAL, B. 2017. Dynamic self-organisation of haematopoiesis and (a)symmetric cell division. *J Theor Biol,* 414**,** 147-164.

NAGY, A. 2000. Cre recombinase: the universal reagent for genome tailoring. *Genesis,* 26**,** 99-109.

NAMKUNG, J., KWON, W., CHOI, Y., YI, S. G., HAN, S., KANG, M. J., KIM, S. W., PARK, T. & JANG, J. Y. 2016. Molecular subtypes of pancreatic cancer based on miRNA expression profiles have independent prognostic value. *J Gastroenterol Hepatol,* 31**,** 1160-7.

NATHAN, C. 2003. Specificity of a third kind: reactive oxygen and nitrogen intermediates in cell signaling. *J Clin Invest,* 111**,** 769-78.

NEGI, G., KUMAR, A. & SHARMA, S. S. 2011. Nrf2 and NF-κB modulation by sulforaphane counteracts multiple manifestations of diabetic neuropathy in rats and high glucose-induced changes. *Curr Neurovasc Res,* 8**,** 294-304.

NEMUDRYI, A. A., VALETDINOVA, K. R., MEDVEDEV, S. P. & ZAKIAN, S. M. 2014. TALEN and CRISPR/Cas Genome Editing Systems: Tools of Discovery. *Acta Naturae,* 6**,** 19-40.

NICK MCELHINNY, S. A., HAVENER, J. M., GARCIA-DIAZ, M., JUÁREZ, R., BEBENEK, K., KEE, B. L., BLANCO, L., KUNKEL, T. A. & RAMSDEN, D. A. 2005. A gradient of template dependence defines distinct biological roles for family X polymerases in nonhomologous end joining. *Mol Cell,* 19**,** 357-66.

NIOI, P. & NGUYEN, T. 2007. A mutation of Keap1 found in breast cancer impairs its ability to repress Nrf2 activity. *Biochem Biophys Res Commun,* 362**,** 816-21.

NISHIDA, K., ARAZOE, T., YACHIE, N., BANNO, S., KAKIMOTO, M., TABATA, M., MOCHIZUKI, M., MIYABE, A., ARAKI, M., HARA, K. Y., SHIMATANI, Z. & KONDO, A. 2016. Targeted nucleotide editing using hybrid prokaryotic and vertebrate adaptive immune systems. *Science,* 353.

NISHIDA, N., YOKOBORI, T., MIMORI, K., SUDO, T., TANAKA, F., SHIBATA, K., ISHII, H., DOKI, Y., KUWANO, H. & MORI, M. 2011. MicroRNA miR-125b is a prognostic marker in human colorectal cancer. *Int J Oncol,* 38**,** 1437-43.

O'CONNELL, R. M., CHAUDHURI, A. A., RAO, D. S., GIBSON, W. S., BALAZS, A. B. & BALTIMORE, D. 2010. MicroRNAs enriched in hematopoietic stem cells differentially regulate long-term hematopoietic output. *Proc Natl Acad Sci U S A,* 107**,** 14235-40.

OECKINGHAUS, A. & GHOSH, S. 2009. The NF-kappaB family of transcription factors and its regulation. *Cold Spring Harb Perspect Biol,* 1**,** a000034.

OOI, A., DYKEMA, K., ANSARI, A., PETILLO, D., SNIDER, J., KAHNOSKI, R., ANEMA, J., CRAIG, D., CARPTEN, J., TEH, B. T. & FURGE, K. A. 2013. CUL3 and NRF2 mutations confer an NRF2 activation phenotype in a sporadic form of papillary renal cell carcinoma. *Cancer Res,* 73**,** 2044-51.

OOI, A. G., SAHOO, D., ADORNO, M., WANG, Y., WEISSMAN, I. L. & PARK, C. Y. 2010. MicroRNA-125b expands hematopoietic stem cells and enriches for the lymphoid-balanced and lymphoid-biased subsets. *Proc Natl Acad Sci U S A,* 107**,** 21505-10.

ORKIN, S. H. & ZON, L. I. 2008. Hematopoiesis: An evolving paradigm for stem cell biology. *Cell,* 132**,** 631-644.

PALII, S. S., VAN EMBURGH, B. O., SANKPAL, U. T., BROWN, K. D. & ROBERTSON, K. D. 2008. DNA methylation inhibitor 5-Aza-2'-deoxycytidine induces reversible genome-wide DNA damage that is distinctly influenced by DNA methyltransferases 1 and 3B. *Mol Cell Biol,* 28**,** 752-71.

PAYNE, K. J. & DOVAT, S. 2011. Ikaros and tumor suppression in acute lymphoblastic leukemia. *Crit Rev Oncog,* 16**,** 3-12.

PEKARSKY, Y. & CROCE, C. M. 2015. Role of miR-15/16 in CLL. *Cell Death Differ,* 22**,** 6-11.

PENG, Y. & CROCE, C. M. 2016. The role of MicroRNAs in human cancer. *Signal Transduct Target Ther,* 1**,** 15004.

PETERSON, L. F., BOYAPATI, A., AHN, E. Y., BIGGS, J. R., OKUMURA, A. J., LO, M. C., YAN, M. & ZHANG, D. E. 2007. Acute myeloid leukemia with the 8q22;21q22 translocation: secondary mutational events and alternative t(8;21) transcripts. *Blood,* 110**,** 799-805.

PETERSON, L. F. & ZHANG, D. E. 2004. The 8;21 translocation in leukemogenesis. *Oncogene,* 23**,** 4255-62.

PETRIV, O. I., KUCHENBAUER, F., DELANEY, A. D., LECAULT, V., WHITE, A., KENT, D., MARMOLEJO, L., HEUSER, M., BERG, T., COPLEY, M., RUSCHMANN, J., SEKULOVIC, S., BENZ, C., KURODA, E., HO, V., ANTIGNANO, F., HALIM, T., GIAMBRA, V., KRYSTAL, G., TAKEI, C. J., WENG, A. P., PIRET, J., EAVES, C., MARRA, M. A., HUMPHRIES, R. K. & HANSEN, C. L. 2010. Comprehensive microRNA expression profiling of the hematopoietic hierarchy. *Proc Natl Acad Sci U S A,* 107**,** 15443-8.

PICHIORRI, F., SUH, S. S., ROCCI, A., DE LUCA, L., TACCIOLI, C., SANTHANAM, R., ZHOU, W., BENSON, D. M., HOFMAINSTER, C., ALDER, H., GAROFALO, M., DI LEVA, G., VOLINIA, S., LIN, H. J., PERROTTI, D., KUEHL, M., AQEILAN, R. I., PALUMBO, A. & CROCE, C. M. 2010. Downregulation of p53-inducible microRNAs 192, 194, and 215 impairs the p53/MDM2 autoregulatory loop in multiple myeloma development. *Cancer Cell,* 18**,** 367-81.

QASIM, W., ZHAN, H., SAMARASINGHE, S., ADAMS, S., AMROLIA, P., STAFFORD, S., BUTLER, K., RIVAT, C., WRIGHT, G., SOMANA, K., GHORASHIAN, S., PINNER, D., AHSAN, G., GILMOUR, K., LUCCHINI, G., INGLOTT, S., MIFSUD, W., CHIESA, R., PEGGS, K. S., CHAN, L., FARZENEH, F., THRASHER, A. J., VORA, A., PULE, M. & VEYS, P. 2017. Molecular remission of infant B-ALL after infusion of universal TALEN gene-edited CAR T cells. *Sci Transl Med,* 9.

RADICH, J. P. 2007. The Biology of CML blast crisis. *Hematology Am Soc Hematol Educ Program***,** 384-91.

RAELSON, J. V., NERVI, C., ROSENAUER, A., BENEDETTI, L., MONCZAK, Y., PEARSON, M., PELICCI, P. G. & MILLER, W. H. 1996. The PML/RAR alpha oncoprotein is a direct molecular target of retinoic acid in acute promyelocytic leukemia cells. *Blood,* 88**,** 2826-32.

RAJABI, H., JIN, C., AHMAD, R., MCCLARY, C., JOSHI, M. D. & KUFE, D. 2010. MUCIN 1 ONCOPROTEIN EXPRESSION IS SUPPRESSED BY THE miR-125b ONCOMIR. *Genes Cancer,* 1**,** 62-68.

RAMADAN, K., SHEVELEV, I. V., MAGA, G. & HÜBSCHER, U. 2004. De novo DNA synthesis by human DNA polymerase lambda, DNA polymerase mu and terminal deoxyribonucleotidyl transferase. *J Mol Biol,* 339**,** 395-404.

RAMOS-GOMEZ, M., KWAK, M. K., DOLAN, P. M., ITOH, K., YAMAMOTO, M., TALALAY, P. & KENSLER, T. W. 2001. Sensitivity to carcinogenesis is increased and chemoprotective efficacy of enzyme inducers is lost in nrf2 transcription factor-deficient mice. *Proc Natl Acad Sci U S A,* 98**,** 3410-5.

RAMSAY, R. G. & GONDA, T. J. 2008. MYB function in normal and cancer cells. *Nat Rev Cancer,* 8**,** 523-34.

RAN, F. A., CONG, L., YAN, W. X., SCOTT, D. A., GOOTENBERG, J. S., KRIZ, A. J., ZETSCHE, B., SHALEM, O., WU, X., MAKAROVA, K. S., KOONIN, E. V., SHARP, P. A. & ZHANG, F. 2015. In vivo genome editing using Staphylococcus aureus Cas9. *Nature,* 520**,** 186-91.

RAN, F. A., HSU, P. D., LIN, C. Y., GOOTENBERG, J. S., KONERMANN, S., TREVINO, A. E., SCOTT, D. A., INOUE, A., MATOBA, S., ZHANG, Y. & ZHANG, F. 2013a. Double nicking by RNA-guided CRISPR Cas9 for enhanced genome editing specificity. *Cell,* 154**,** 1380-9.

RAN, F. A., HSU, P. D., WRIGHT, J., AGARWALA, V., SCOTT, D. A. & ZHANG, F. 2013b. Genome engineering using the CRISPR-Cas9 system. *Nat Protoc,* 8**,** 2281-308.

RATH, D., AMLINGER, L., RATH, A. & LUNDGREN, M. 2015. The CRISPR-Cas immune system: biology, mechanisms and applications. *Biochimie,* 117**,** 119-28.

RAVER-SHAPIRA, N., MARCIANO, E., MEIRI, E., SPECTOR, Y., ROSENFELD, N., MOSKOVITS, N., BENTWICH, Z. & OREN, M. 2007. Transcriptional activation of miR-34a contributes to p53-mediated apoptosis. *Mol Cell,* 26**,** 731-43.

REILLY, J. T. 2005. Pathogenesis of acute myeloid leukaemia and inv(16)(p13;q22): a paradigm for understanding leukaemogenesis? *Br J Haematol,* 128**,** 18-34.

ROBERTS, A. W., DAVIDS, M. S., PAGEL, J. M., KAHL, B. S., PUVVADA, S. D., GERECITANO, J. F., KIPPS, T. J., ANDERSON, M. A., BROWN, J. R., GRESSICK, L., WONG, S., DUNBAR, M., ZHU, M., DESAI, M. B., CERRI, E., HEITNER ENSCHEDE, S., HUMERICKHOUSE, R. A., WIERDA, W. G. & SEYMOUR, J. F. 2016. Targeting BCL2 with Venetoclax in Relapsed Chronic Lymphocytic Leukemia. *N Engl J Med,* 374**,** 311-22.

RODGERS, K. & MCVEY, M. 2016. Error-Prone Repair of DNA Double-Strand Breaks. *J Cell Physiol,* 231**,** 15-24.

ROLDO, C., MISSIAGLIA, E., HAGAN, J. P., FALCONI, M., CAPELLI, P., BERSANI, S., CALIN, G. A., VOLINIA, S., LIU, C. G., SCARPA, A. & CROCE, C. M. 2006. MicroRNA expression abnormalities in pancreatic endocrine and acinar tumors are associated with distinctive pathologic features and clinical behavior. *J Clin Oncol,* 24**,** 4677-84.

RUSHWORTH, S. A., BOWLES, K. M. & MACEWAN, D. J. 2011a. High basal nuclear levels of Nrf2 in acute myeloid leukemia reduces sensitivity to proteasome inhibitors. *Cancer Res,* 71**,** 1999-2009.

RUSHWORTH, S. A., BOWLES, K. M. & MACEWAN, D. J. 2011b. High Basal Nuclear Levels of Nrf2 in Acute Myeloid Leukemia Reduces Sensitivity to Proteasome Inhibitors. *Cancer Research,* 71**,** 1999-2009.

RUSHWORTH, S. A., BOWLES, K. M., RANINGA, P. & MACEWAN, D. J. 2010. NF-kappaB-inhibited acute myeloid leukemia cells are rescued from apoptosis by heme oxygenase-1 induction. *Cancer Res,* 70**,** 2973-83.

RUSHWORTH, S. A. & MACEWAN, D. J. 2008. HO-1 underlies resistance of AML cells to TNF-induced apoptosis. *Blood,* 111**,** 3793-801.

RUSHWORTH, S. A., MACEWAN, D. J. & O'CONNELL, M. A. 2008. Lipopolysaccharide-induced expression of NAD(P)H:quinone oxidoreductase 1 and heme oxygenase-1 protects against excessive inflammatory responses in human monocytes. *J Immunol,* 181**,** 6730-7.

RUSHWORTH, S. A., ZAITSEVA, L., MURRAY, M. Y., SHAH, N. M., BOWLES, K. M. & MACEWAN, D. J. 2012. The high Nrf2 expression in human acute myeloid leukemia is driven by NF-κB and underlies its chemo-resistance. *Blood,* 120**,** 5188-98.

SAITO, Y., LIANG, G., EGGER, G., FRIEDMAN, J. M., CHUANG, J. C., COETZEE, G. A. & JONES, P. A. 2006. Specific activation of microRNA-127 with downregulation of the proto-oncogene BCL6 by chromatin-modifying drugs in human cancer cells. *Cancer Cell,* 9**,** 435-43.

SANGOKOYA, C., TELEN, M. J. & CHI, J. T. 2010. microRNA miR-144 modulates oxidative stress tolerance and associates with anemia severity in sickle cell disease. *Blood,* 116**,** 4338-4348.

SANJANA, N. E., SHALEM, O. & ZHANG, F. 2014. Improved vectors and genome-wide libraries for CRISPR screening. *Nat Methods,* 11**,** 783-4.

SATOH, H., MORIGUCHI, T., TAGUCHI, K., TAKAI, J., MAHER, J. M., SUZUKI, T., WINNARD, P. T., RAMAN, V., EBINA, M., NUKIWA, T. & YAMAMOTO, M. 2010. Nrf2-deficiency creates a responsive microenvironment for metastasis to the lung. *Carcinogenesis,* 31**,** 1833-43.

SATOH, H., MORIGUCHI, T., TAKAI, J., EBINA, M. & YAMAMOTO, M. 2013. Nrf2 prevents initiation but accelerates progression through the Kras signaling pathway during lung carcinogenesis. *Cancer Res,* 73**,** 4158-68.

SCHNITTGER, S., SCHOCH, C., DUGAS, M., KERN, W., STAIB, P., WUCHTER, C., LÖFFLER, H., SAUERLAND, C. M., SERVE, H., BÜCHNER, T., HAFERLACH, T. & HIDDEMANN, W. 2002. Analysis of FLT3 length mutations in 1003 patients with acute myeloid leukemia: correlation to cytogenetics, FAB subtype, and prognosis in the AMLCG study and usefulness as a marker for the detection of minimal residual disease. *Blood,* 100**,** 59-66.

SCHULZE, K., IMBEAUD, S., LETOUZÉ, E., ALEXANDROV, L. B., CALDERARO, J., REBOUISSOU, S., COUCHY, G., MEILLER, C., SHINDE, J., SOYSOUVANH, F., CALATAYUD, A. L., PINYOL, R., PELLETIER, L., BALABAUD, C., LAURENT, A., BLANC, J. F., MAZZAFERRO, V., CALVO, F., VILLANUEVA, A., NAULT, J. C., BIOULAC-SAGE, P., STRATTON, M. R., LLOVET, J. M. & ZUCMAN-ROSSI, J. 2015. Exome sequencing of hepatocellular carcinomas identifies new mutational signatures and potential therapeutic targets. *Nat Genet,* 47**,** 505-511.

SCHUNDER, E., RYDZEWSKI, K., GRUNOW, R. & HEUNER, K. 2013. First indication for a functional CRISPR/Cas system in Francisella tularensis. *Int J Med Microbiol,* 303**,** 51-60.

SCOTT, G. K., GOGA, A., BHAUMIK, D., BERGER, C. E., SULLIVAN, C. S. & BENZ, C. C. 2007. Coordinate suppression of ERBB2 and ERBB3 by enforced expression of micro-RNA miR-125a or miR-125b. *J Biol Chem,* 282**,** 1479-86.

SEVAL, G. C. & OZCAN, M. 2015. Treatment of Acute Myeloid Leukemia in Adolescent and Young Adult Patients. *J Clin Med,* 4**,** 441-59.

SHAH, N. M., RUSHWORTH, S. A., MURRAY, M. Y., BOWLES, K. M. & MACEWAN, D. J. 2013. Understanding the role of NRF2-regulated miRNAs in human malignancies. *Oncotarget,* 4**,** 1130-42.

SHEN, H. & ANASTASIO, C. 2012. A Comparison of Hydroxyl Radical and Hydrogen Peroxide Generation in Ambient Particle Extracts and Laboratory Metal Solutions. *Atmos Environ (1994),* 46**,** 665-668.

SHIBATA, T., OHTA, T., TONG, K. I., KOKUBU, A., ODOGAWA, R., TSUTA, K., ASAMURA, H., YAMAMOTO, M. & HIROHASHI, S. 2008. Cancer related mutations in NRF2 impair its recognition by Keap1-Cul3 E3 ligase and promote malignancy. *Proc Natl Acad Sci U S A,* 105**,** 13568-73.

SHIH, A. H., ABDEL-WAHAB, O., PATEL, J. P. & LEVINE, R. L. 2012. The role of mutations in epigenetic regulators in myeloid malignancies. *Nat Rev Cancer,* 12**,** 599-612.

SHINNERS, N. P., CARLESSO, G., CASTRO, I., HOEK, K. L., CORN, R. A., WOODLAND, R. T., WOODLAND, R. L., SCOTT, M. L., WANG, D. & KHAN, W. N. 2007. Bruton's tyrosine kinase mediates NF-kappa B activation and B cell survival by B cell-activating factor receptor of the TNF-R family. *J Immunol,* 179**,** 3872-80.

SHOWEL, M. M. & LEVIS, M. 2014. Advances in treating acute myeloid leukemia. *F1000Prime Rep,* 6**,** 96.

SINGH, A., HAPPEL, C., MANNA, S. K., ACQUAAH-MENSAH, G., CARRERERO, J., KUMAR, S., NASIPURI, P., KRAUSZ, K. W., WAKABAYASHI, N., DEWI, R., BOROS, L. G., GONZALEZ, F. J., GABRIELSON, E., WONG, K. K., GIRNUN, G. & BISWAL, S. 2013a. Transcription factor NRF2 regulates miR-1 and miR-206 to drive tumorigenesis. *J Clin Invest,* 123**,** 2921-34.

SINGH, A., MISRA, V., THIMMULAPPA, R. K., LEE, H., AMES, S., HOQUE, M. O., HERMAN, J. G., BAYLIN, S. B., SIDRANSKY, D., GABRIELSON, E., BROCK, M. V. & BISWAL, S. 2006. Dysfunctional KEAP1-NRF2 interaction in non-small-cell lung cancer. *PLoS Med,* 3**,** e420.

SINGH, B., RONGHE, A. M., CHATTERJEE, A., BHAT, N. K. & BHAT, H. K. 2013b. MicroRNA-93 regulates NRF2 expression and is associated with breast carcinogenesis. *Carcinogenesis,* 34**,** 1165-72.

SLAYMAKER, I. M., GAO, L., ZETSCHE, B., SCOTT, D. A., YAN, W. X. & ZHANG, F. 2016. Rationally engineered Cas9 nucleases with improved specificity. *Science,* 351**,** 84-8.

SOLIS, L. M., BEHRENS, C., DONG, W., SURAOKAR, M., OZBURN, N. C., MORAN, C. A., CORVALAN, A. H., BISWAL, S., SWISHER, S. G., BEKELE, B. N., MINNA, J. D., STEWART, D. J. & WISTUBA, I. I. 2010. Nrf2 and Keap1 abnormalities in non-small cell lung carcinoma and association with clinicopathologic features. *Clin Cancer Res,* 16**,** 3743-53.

SPANGRUDE, G. J., HEIMFELD, S. & WEISSMAN, I. L. 1988. Purification and characterization of mouse hematopoietic stem cells. *Science,* 241**,** 58-62.

SPORN, M. B. & LIBY, K. T. 2012. NRF2 and cancer: the good, the bad and the importance of context. *Nat Rev Cancer,* 12**,** 564-71.

STERNBERG, S. H., LAFRANCE, B., KAPLAN, M. & DOUDNA, J. A. 2015. Conformational control of DNA target cleavage by CRISPR-Cas9. *Nature,* 527**,** 110-3.

STONE, R. M., MANLEY, P. W., LARSON, R. A. & CAPDEVILLE, R. 2018. Midostaurin: its odyssey from discovery to approval for treating acute myeloid leukemia and advanced systemic mastocytosis. *Blood Adv,* 2**,** 444-453.

STĘPKOWSKI, T. M. & KRUSZEWSKI, M. K. 2011. Molecular cross-talk between the NRF2/KEAP1 signaling pathway, autophagy, and apoptosis. *Free Radic Biol Med,* 50**,** 1186-95.

SUN, Y. M., LIN, K. Y. & CHEN, Y. Q. 2013. Diverse functions of miR-125 family in different cell contexts. *J Hematol Oncol,* 6**,** 6.

SURDZIEL, E., CABANSKI, M., DALLMANN, I., LYSZKIEWICZ, M., KRUEGER, A., GANSER, A., SCHERR, M. & EDER, M. 2011.

Enforced expression of miR-125b affects myelopoiesis by targeting multiple signaling pathways. *Blood,* 117**,** 4338-48.

SUZUKI, M., BETSUYAKU, T., ITO, Y., NAGAI, K., NASUHARA, Y., KAGA, K., KONDO, S. & NISHIMURA, M. 2008. Down-regulated NF-E2-related factor 2 in pulmonary macrophages of aged smokers and patients with chronic obstructive pulmonary disease. *Am J Respir Cell Mol Biol,* 39**,** 673-82.

SUZUKI, T., MOTOHASHI, H. & YAMAMOTO, M. 2013a. Toward clinical application of the Keap1-Nrf2 pathway. *Trends Pharmacol Sci,* 34**,** 340-6.

SUZUKI, T., SHIBATA, T., TAKAYA, K., SHIRAISHI, K., KOHNO, T., KUNITOH, H., TSUTA, K., FURUTA, K., GOTO, K., HOSODA, F., SAKAMOTO, H., MOTOHASHI, H. & YAMAMOTO, M. 2013b. Regulatory nexus of synthesis and degradation deciphers cellular Nrf2 expression levels. *Mol Cell Biol,* 33**,** 2402-12.

SVORONOS, A. A., ENGELMAN, D. M. & SLACK, F. J. 2016. OncomiR or Tumor Suppressor? The Duplicity of MicroRNAs in Cancer. *Cancer Res,* 76**,** 3666-70.

TAGUCHI, K., MOTOHASHI, H. & YAMAMOTO, M. 2011. Molecular mechanisms of the Keap1–Nrf2 pathway in stress response and cancer evolution. *Genes Cells,* 16**,** 123-40.

TAGUCHI, K. & YAMAMOTO, M. 2017. The KEAP1-NRF2 System in Cancer. *Front Oncol,* 7**,** 85.

TAMAMYAN, G., KADIA, T., RAVANDI, F., BORTHAKUR, G., CORTES, J., JABBOUR, E., DAVER, N., OHANIAN, M., KANTARJIAN, H. & KONOPLEVA, M. 2017. Frontline treatment of acute myeloid leukemia in adults. *Crit Rev Oncol Hematol,* 110**,** 20-34.

TANAKA, R., TOMOSUGI, M., HORINAKA, M., SOWA, Y. & SAKAI, T. 2015. Metformin Causes G1-Phase Arrest via Down-Regulation of MiR-221 and Enhances TRAIL Sensitivity through DR5 Up-Regulation in Pancreatic Cancer Cells. *PLoS One,* 10**,** e0125779.

TANAKA, Y., HAYASHI, M., KUBOTA, Y., NAGAI, H., SHENG, G., NISHIKAWA, S. & SAMOKHVALOV, I. M. 2012. Early ontogenic origin of the hematopoietic stem cell lineage. *Proc Natl Acad Sci U S A,* 109**,** 4515-20.

TEBAS, P., STEIN, D., TANG, W. W., FRANK, I., WANG, S. Q., LEE, G., SPRATT, S. K., SUROSKY, R. T., GIEDLIN, M. A., NICHOL, G., HOLMES, M. C., GREGORY, P. D., ANDO, D. G., KALOS, M., COLLMAN, R. G., BINDER-SCHOLL, G., PLESA, G., HWANG, W. T., LEVINE, B. L. & JUNE, C. H. 2014. Gene editing of CCR5 in autologous CD4 T cells of persons infected with HIV. *N Engl J Med,* 370**,** 901-10.

TENG, Y., ZHANG, Y., QU, K., YANG, X., FU, J., CHEN, W. & LI, X. 2015. MicroRNA-29B (mir-29b) regulates the Warburg effect in ovarian cancer by targeting AKT2 and AKT3. *Oncotarget,* 6**,** 40799-814.

TILI, E., MICHAILLE, J. J., CIMINO, A., COSTINEAN, S., DUMITRU, C. D., ADAIR, B., FABBRI, M., ALDER, H., LIU, C. G., CALIN, G. A. & CROCE, C. M. 2007. Modulation of miR-155 and miR-125b levels following lipopolysaccharide/TNF-alpha stimulation and their possible

roles in regulating the response to endotoxin shock. *J Immunol,* 179**,** 5082-9.

TOMITA, A., KIYOI, H. & NAOE, T. 2013. Mechanisms of action and resistance to all-trans retinoic acid (ATRA) and arsenic trioxide (As2O 3) in acute promyelocytic leukemia. *Int J Hematol,* 97**,** 717-25.

TONG, K. I., KATOH, Y., KUSUNOKI, H., ITOH, K., TANAKA, T. & YAMAMOTO, M. 2006. Keap1 recruits Neh2 through binding to ETGE and DLG motifs: characterization of the two-site molecular recognition model. *Mol Cell Biol,* 26**,** 2887-900.

TSAI, S. Q. & JOUNG, J. K. 2016. Defining and improving the genome-wide specificities of CRISPR-Cas9 nucleases. *Nat Rev Genet,* 17**,** 300-12.

TURRENS, J. F. 2003. Mitochondrial formation of reactive oxygen species. *J Physiol,* 552**,** 335-44.

VALTON, J., DUPUY, A., DABOUSSI, F., THOMAS, S., MARÉCHAL, A., MACMASTER, R., MELLIAND, K., JUILLERAT, A. & DUCHATEAU, P. 2012. Overcoming transcription activator-like effector (TALE) DNA binding domain sensitivity to cytosine methylation. *J Biol Chem,* 287**,** 38427-32.

VARGAS ROMERO, P., CIALFI, S., PALERMO, R., DE BLASIO, C., CHECQUOLO, S., BELLAVIA, D., CHIARETTI, S., FOÀ, R., AMADORI, A., GULINO, A., ZARDO, G., TALORA, C. & SCREPANTI, I. 2015. The deregulated expression of miR-125b in acute myeloid leukemia is dependent on the transcription factor C/EBPα. *Leukemia,* 29**,** 2442-5.

VENUGOPAL, R. & JAISWAL, A. K. 1996. Nrf1 and Nrf2 positively and c-Fos and Fra1 negatively regulate the human antioxidant response element-mediated expression of NAD(P)H:quinone oxidoreductase1 gene. *Proc Natl Acad Sci U S A,* 93**,** 14960-5.

VISCONTI, R. & GRIECO, D. 2009. New insights on oxidative stress in cancer. *Curr Opin Drug Discov Devel,* 12**,** 240-5.

WANG, B., HSU, S. H., WANG, X., KUTAY, H., BID, H. K., YU, J., GANJU, R. K., JACOB, S. T., YUNEVA, M. & GHOSHAL, K. 2014a. Reciprocal regulation of microRNA-122 and c-Myc in hepatocellular cancer: role of E2F1 and transcription factor dimerization partner 2. *Hepatology,* 59**,** 555-66.

WANG, B., ZHU, X., KIM, Y., LI, J., HUANG, S., SALEEM, S., LI, R. C., XU, Y., DORE, S. & CAO, W. 2012. Histone deacetylase inhibition activates transcription factor Nrf2 and protects against cerebral ischemic damage. *Free Radic Biol Med,* 52**,** 928-36.

WANG, J., CHU, E. S., CHEN, H. Y., MAN, K., GO, M. Y., HUANG, X. R., LAN, H. Y., SUNG, J. J. & YU, J. 2015a. microRNA-29b prevents liver fibrosis by attenuating hepatic stellate cell activation and inducing apoptosis through targeting PI3K/AKT pathway. *Oncotarget,* 6**,** 7325-38.

WANG, J., HAUBROCK, M., CAO, K. M., HUA, X., ZHANG, C. Y., WINGENDER, E. & LI, J. 2011. Regulatory coordination of clustered microRNAs based on microRNA-transcription factor regulatory network. *BMC Syst Biol,* 5**,** 199.

WANG, L., LIU, C., LI, C., XUE, J., ZHAO, S., ZHAN, P., LIN, Y., ZHANG, P., JIANG, A. & CHEN, W. 2015b. Effects of microRNA-221/222 on cell proliferation and apoptosis in prostate cancer cells. *Gene,* 572**,** 252-8.

WANG, T., WEI, J. J., SABATINI, D. M. & LANDER, E. S. 2014b. Genetic screens in human cells using the CRISPR-Cas9 system. *Science,* 343**,** 80-4.

WANG, X. J., HAYES, J. D., HENDERSON, C. J. & WOLF, C. R. 2007. Identification of retinoic acid as an inhibitor of transcription factor Nrf2 through activation of retinoic acid receptor alpha. *Proc Natl Acad Sci U S A,* 104**,** 19589-94.

WANG, Z. Y. & CHEN, Z. 2008. Acute promyelocytic leukemia: from highly fatal to highly curable. *Blood,* 111**,** 2505-15.

WARDYN, J. D., PONSFORD, A. H. & SANDERSON, C. M. 2015. Dissecting molecular cross-talk between Nrf2 and NF-κB response pathways. *Biochem Soc Trans,* 43**,** 621-6.

WINTER, J., JUNG, S., KELLER, S., GREGORY, R. I. & DIEDERICHS, S. 2009. Many roads to maturity: microRNA biogenesis pathways and their regulation. *Nature Cell Biology,* 11**,** 228-234.

WONG, T. F., YOSHINAGA, K., MONMA, Y., ITO, K., NIIKURA, H., NAGASE, S., YAMAMOTO, M. & YAEGASHI, N. 2011. Association of keap1 and nrf2 genetic mutations and polymorphisms with endometrioid endometrial adenocarcinoma survival. *Int J Gynecol Cancer,* 21**,** 1428-35.

WU, N., LIN, X., ZHAO, X., ZHENG, L., XIAO, L., LIU, J., GE, L. & CAO, S. 2013. MiR-125b acts as an oncogene in glioblastoma cells and inhibits cell apoptosis through p53 and p38MAPK-independent pathways. *Br J Cancer,* 109**,** 2853-63.

WU, Q. & NI, X. 2015. ROS-mediated DNA methylation pattern alterations in carcinogenesis. *Curr Drug Targets,* 16**,** 13-9.

XU, L., XU, Y., JING, Z., WANG, X., ZHA, X., ZENG, C., CHEN, S., YANG, L., LUO, G., LI, B. & LI, Y. 2014. Altered expression pattern of miR-29a, miR-29b and the target genes in myeloid leukemia. *Exp Hematol Oncol,* 3**,** 17.

YAMAKUCHI, M. & LOWENSTEIN, C. J. 2009. MiR-34, SIRT1 and p53: the feedback loop. *Cell Cycle,* 8**,** 712-5.

YAN, B., GUO, Q., FU, F. J., WANG, Z., YIN, Z., WEI, Y. B. & YANG, J. R. 2015. The role of miR-29b in cancer: regulation, function, and signaling. *Onco Targets Ther,* 8**,** 539-48.

YAN, L. X., HUANG, X. F., SHAO, Q., HUANG, M. Y., DENG, L., WU, Q. L., ZENG, Y. X. & SHAO, J. Y. 2008. MicroRNA miR-21 overexpression in human breast cancer is associated with advanced clinical stage, lymph node metastasis and patient poor prognosis. *RNA,* 14**,** 2348-60.

YI, R., QIN, Y., MACARA, I. G. & CULLEN, B. R. 2003. Exportin-5 mediates the nuclear export of pre-microRNAs and short hairpin RNAs. *Genes Dev,* 17**,** 3011-6.

YOH, K., ITOH, K., ENOMOTO, A., HIRAYAMA, A., YAMAGUCHI, N., KOBAYASHI, M., MORITO, N., KOYAMA, A., YAMAMOTO, M. & TAKAHASHI, S. 2001. Nrf2-deficient female mice develop lupus-like autoimmune nephritis. *Kidney Int,* 60**,** 1343-53.

YOO, N. J., KIM, H. R., KIM, Y. R., AN, C. H. & LEE, S. H. 2012. Somatic mutations of the KEAP1 gene in common solid cancers. *Histopathology,* 60**,** 943-52.

YU, J., LI, Q., XU, Q., LIU, L. & JIANG, B. 2011. MiR-148a inhibits angiogenesis by targeting ERBB3. *J Biomed Res,* 25**,** 170-7.

YUXIA, M., ZHENNAN, T. & WEI, Z. 2012. Circulating miR-125b is a novel biomarker for screening non-small-cell lung cancer and predicts poor prognosis. *J Cancer Res Clin Oncol,* 138**,** 2045-50.

ZABOIKIN, M., ZABOIKINA, T., FRETER, C. & SRINIVASAKUMAR, N. 2017. Non-Homologous End Joining and Homology Directed DNA Repair Frequency of Double-Stranded Breaks Introduced by Genome Editing Reagents. *PLoS One,* 12**,** e0169931.

ZAGHLOUL, E. M., GISSBERG, O., MORENO, P. M. D., SIGGENS, L., HÄLLBRINK, M., JØRGENSEN, A. S., EKWALL, K., ZAIN, R., WENGEL, J., LUNDIN, K. E. & SMITH, C. I. E. 2017. CTG repeat-targeting oligonucleotides for down-regulating Huntingtin expression. *Nucleic Acids Res,* 45**,** 5153-5169.

ZAIDI, S. K., PEREZ, A. W., WHITE, E. S., LIAN, J. B., STEIN, J. L. & STEIN, G. S. 2017. An AML1-ETO/miR-29b-1 regulatory circuit modulates phenotypic properties of acute myeloid leukemia cells. *Oncotarget,* 8**,** 39994-40005.

ZETSCHE, B., GOOTENBERG, J. S., ABUDAYYEH, O. O., SLAYMAKER, I. M., MAKAROVA, K. S., ESSLETZBICHLER, P., VOLZ, S. E., JOUNG, J., VAN DER OOST, J., REGEV, A., KOONIN, E. V. & ZHANG, F. 2015a. Cpf1 is a single RNA-guided endonuclease of a class 2 CRISPR-Cas system. *Cell,* 163**,** 759-71.

ZETSCHE, B., HEIDENREICH, M., MOHANRAJU, P., FEDOROVA, I., KNEPPERS, J., DEGENNARO, E. M., WINBLAD, N., CHOUDHURY, S. R., ABUDAYYEH, O. O., GOOTENBERG, J. S., WU, W. Y., SCOTT, D. A., SEVERINOV, K., VAN DER OOST, J. & ZHANG, F. 2017. Multiplex gene editing by CRISPR-Cpf1 using a single crRNA array. *Nat Biotechnol,* 35**,** 31-34.

ZETSCHE, B., VOLZ, S. E. & ZHANG, F. 2015b. A split-Cas9 architecture for inducible genome editing and transcription modulation. *Nat Biotechnol,* 33**,** 139-42.

ZHANG, C., WANG, H. J., BAO, Q. C., WANG, L., GUO, T. K., CHEN, W. L., XU, L. L., ZHOU, H. S., BIAN, J. L., YANG, Y. R., SUN, H. P., XU, X. L. & YOU, Q. D. 2016. NRF2 promotes breast cancer cell proliferation and metastasis by increasing RhoA/ROCK pathway signal transduction. *Oncotarget,* 7**,** 73593-73606.

ZHANG, D. D. & HANNINK, M. 2003. Distinct cysteine residues in Keap1 are required for Keap1-dependent ubiquitination of Nrf2 and for stabilization of Nrf2 by chemopreventive agents and oxidative stress. *Mol Cell Biol,* 23**,** 8137-51.

ZHANG, H., LUO, X.-Q., FENG, D.-D., ZHANG, X.-J., WU, J., ZHENG, Y.-S., CHEN, X., XU, L. & CHEN, Y.-Q. 2011a. Upregulation of microRNA-125b contributes to leukemogenesis and increases drug resistance in pediatric acute promyelocytic leukemia. *Molecular Cancer,* 10.

ZHANG, L., GE, Y. & FUCHS, E. 2014. miR-125b can enhance skin tumor initiation and promote malignant progression by repressing differentiation and prolonging cell survival. *Genes Dev,* 28**,** 2532-46.

ZHANG, P., SINGH, A., YEGNASUBRAMANIAN, S., ESOPI, D., KOMBAIRAJU, P., BODAS, M., WU, H., BOVA, S. G. & BISWAL, S. 2010. Loss of Kelch-like ECH-associated protein 1 function in prostate cancer cells causes chemoresistance and radioresistance and promotes tumor growth. *Mol Cancer Ther,* 9**,** 336-46.

ZHANG, Y., YAN, L. X., WU, Q. N., DU, Z. M., CHEN, J., LIAO, D. Z., HUANG, M. Y., HOU, J. H., WU, Q. L., ZENG, M. S., HUANG, W. L., ZENG, Y. X. & SHAO, J. Y. 2011b. miR-125b is methylated and functions as a tumor suppressor by regulating the ETS1 proto-oncogene in human invasive breast cancer. *Cancer Res,* 71**,** 3552-62.

ZHAO, A., ZENG, Q., XIE, X., ZHOU, J., YUE, W., LI, Y. & PEI, X. 2012. MicroRNA-125b induces cancer cell apoptosis through suppression of Bcl-2 expression. *J Genet Genomics,* 39**,** 29-35.

ZHOU, M., LIU, Z., ZHAO, Y., DING, Y., LIU, H., XI, Y., XIONG, W., LI, G., LU, J., FODSTAD, O., RIKER, A. I. & TAN, M. 2010. MicroRNA-125b confers the resistance of breast cancer cells to paclitaxel through suppression of pro-apoptotic Bcl-2 antagonist killer 1 (Bak1) expression. *J Biol Chem,* 285**,** 21496-507.

ZHU, J., GIANNI, M., KOPF, E., HONORÉ, N., CHELBI-ALIX, M., KOKEN, M., QUIGNON, F., ROCHETTE-EGLY, C. & DE THÉ, H. 1999. Retinoic acid induces proteasome-dependent degradation of retinoic acid receptor alpha (RARalpha) and oncogenic RARalpha fusion proteins. *Proc Natl Acad Sci U S A,* 96**,** 14807-12.

ZHU, K., LIU, L., ZHANG, J., WANG, Y., LIANG, H., FAN, G., JIANG, Z., ZHANG, C. Y., CHEN, X. & ZHOU, G. 2016. MiR-29b suppresses the proliferation and migration of osteosarcoma cells by targeting CDK6. *Protein Cell,* 7**,** 434-44.

ZHU, S., WU, H., WU, F., NIE, D., SHENG, S. & MO, Y. Y. 2008. MicroRNA-21 targets tumor suppressor genes in invasion and metastasis. *Cell Res,* 18**,** 350-9.

ZIPPER, L. M. & MULCAHY, R. T. 2000. Inhibition of ERK and p38 MAP kinases inhibits binding of Nrf2 and induction of GCS genes. *Biochem Biophys Res Commun,* 278**,** 484-92.

Appendix

Cell Death and Differentiation (2015) 22, 654–664

www.nature.com/cdd

NRF2-driven miR-125B1 and miR-29B1 transcriptional regulation controls a novel anti-apoptotic miRNA regulatory network for AML survival

NM Shah[1,2], L Zaitseva[1], KM Bowles[1,3], DJ MacEwan[2,4] and SA Rushworth*[,1,4]

Transcription factor NRF2 is an important regulator of oxidative stress. It is involved in cancer progression, and has abnormal constitutive expression in acute myeloid leukaemia (AML). Posttranscriptional regulation by microRNAs (miRNAs) can affect the malignant phenotype of AML cells. In this study, we identified and characterised NRF2-regulated miRNAs in AML. An miRNA array identified miRNA expression level changes in response to NRF2 knockdown in AML cells. Further analysis of miRNAs concomitantly regulated by knockdown of the NRF2 inhibitor KEAP1 revealed the major candidate NRF2-mediated miRNAs in AML. We identified miR-125B to be upregulated and miR-29B to be downregulated by NRF2 in AML. Subsequent bioinformatic analysis identified putative NRF2 binding sites upstream of the miR-125B1 coding region and downstream of the mir-29B1 coding region. Chromatin immunoprecipitation analyses showed that NRF2 binds to these antioxidant response elements (AREs) located in the 5′ untranslated regions of miR-125B and miR-29B. Finally, primary AML samples transfected with anti-miR-125B antagomiR or miR-29B mimic showed increased cell death responsiveness either alone or co-treated with standard AML chemotherapy. In summary, we find that NRF2 regulation of miR-125B and miR-29B acts to promote leukaemic cell survival, and their manipulation enhances AML responsiveness towards cytotoxic chemotherapeutics.
Cell Death and Differentiation (2015) **22,** 654–664; doi:10.1038/cdd.2014.152; published online 17 October 2014

Acute myeloid leukaemia (AML) is a biologically heterogenous disorder that occurs as a consequence of a wide variety of genetic abnormalities in haematopoietic progenitors that are derived from the bone marrow.[1] However, it is likely that AML share various survival pathways downstream of the driver mutations, making the existence of common survival pathways and therapeutic targets likely.[2]

Nuclear factor (erythroid-derived 2)-like 2 (NRF2) is a member of the Cap 'n' Collar basic leucine zipper transcription factor family that protects cells from reactive oxygen species through the regulation of a number of cytoprotective genes including heme oxygenase-1 (HO-1) and NAD(P)H dehydrogenase quinone 1 (NQO1).[3–5] In cancer, NRF2 activation is pro-tumoural in a spectrum of malignancies through mutations in NRF2 or its cytosolic inhibitor KEAP1.[6–9] However, we have previously shown that in human AML constitutive activation of the NRF2 signalling pathway is not through somatic mutations of NRF2/Keap1 but as a consequence of upstream constitutive activation by NF-κB.[10,11] In addition to contributing to the malignant phenotype of AML, we also found that NRF2 contributes to intrinsic leukaemia cell resistance to standard front-line chemotherapy agents.[12,10]

microRNAs (miRNAs) are short non-coding RNA molecules, approximately 20–30 nucleotides in length, that can posttranscriptionally regulate gene expression by binding to the 3′ UTR of their target mRNA, thereby repressing gene transcription.[13] miRNA expression has shown to be dysregulated in a range of cancers, and can act as tumour suppressor miRs (by downregulating oncogenes) or oncomiRs (by targeting tumour suppressors).[14] miRNAs are being increasingly studied with the expectation that modulation of their expression can be harnessed to improve cancer therapy. A recent study using chromatin immunoprecipitation sequencing (ChIP-Seq) identified high-confidence ChIP-Seq peaks for NRF2 binding in the vicinity of several miRNAs, suggesting they could be regulated by NRF2.[15]

In the present study, we look to identify whether NRF2 regulates miRNA in human AML. Furthermore, we evaluate whether NRF2-regulated miRNAs have functional importance not only on the biology of the disease but also in the leukaemia cell death to chemotherapy treatment.

Results

Lentiviral NRF2 knockdown alters miRNA expression. NRF2 can regulate drug resistance in AML via the induction of cytoprotective and detoxification genes.[10,12] To assess whether NRF2 regulates miRNA expression in AML, we used

[1]Department of Molecular Haematology, Norwich Medical School, University of East Anglia, Norwich Research Park, Norwich, UK; [2]Department of Molecular and Clinical Pharmacology, Institute of Translational Medicine, University of Liverpool, Liverpool, UK and [3]Department of Haematology, Norfolk and Norwich University Hospitals NHS Trust, Colney Lane, Norwich, UK
*Corresponding author: SA Rushworth, Department of Molecular Haematology, Norwich Medical School, Norwich Research Park, Norwich, NR4 7TJ, UK. Tel: +44 (0)1603 591802; Fax: +44 (0)1603 591750; E-mail: s.rushworth@uea.ac.uk
[4]These authors contributed equally to this work.
Abbreviations: AML, Acute myeloid leukaemia; NRF2, Nuclear factor (erythroid-derived 2)-like 2; HO-1, heme oxygenase-1; NQO1, NAD(P)H dehydrogenase quinone 1; NRF2-KD, NRF2 lentiviral knockdown; NEG-KD, negative control knockdown; ChIP, chromatin immunoprecipitation assay; miRNAs, microRNAs
Received 25.2.14; revised 23.8.14; accepted 25.8.14; Edited by A Villunger; published online 17.10.14

a commercially available OncomiR Cancer miRNA qRT-PCR Array on THP-1 cells infected with an NRF2 lentiviral knockdown (NRF2-KD) and a negative control knockdown (NEG-KD). Figure 1a shows the change in expression of miRNA in response to NRF2-KD compared with the control infected with NEG-KD. We then treated THP-1 cells with the NRF2 activator sulforaphane for 6 h for comparison. Supplementary Table 1 shows the fold increase of miRNA in response to both NRF-KD and sulforaphane treatment. From these experiments, we identified miR-125B, miR-222, miR-221 and miR-223 as potential miRNAs upregulated by NRF2 and miR-29B and miR-154 as potential miRNAs downregulated by NRF2. Figure 1c shows western blot analysis of NRF2 and KEAP1 protein expression in THP-1 cells in response to NRF2-KD, KEAP1-KD and NEG-KD.

Increased NRF2 activity increases miR-125B and decreases miR-29B expression in AML. We used a qRT-PCR approach to validate the data from the lentiviral array experiments.[10] NRF2-KD results in THP-1 cells showing a consistent decrease in miR-125B expression and increasing miR-29B expression as well as smaller but not significant fluctuations in miR-221, miR-222, miR-223 and miR-154 expression (Figure 1b). To further assess the role of NRF2 in regulating miRNA, we increased the activity of NRF2 in THP-1 cells by knockdown of the NRF2 inhibitor KEAP1.[16] THP-1 were infected with KEAP1 lentiviral knockdown (KEAP1-KD). QRT-PCR confirmed the downregulation of KEAP1 and as a positive control, we showed that KEAP-KD upregulated the NRF2 target gene HO-1. Moreover, miR-125B expression showed a similar increase to HO-1 and miR-29B showed a significant decrease in response to KEAP1-KD (Figure 1b). The expression of miR-221, miR--222, miR223 and miR-154 were not significantly changed in response in NRF2-KD or KEAP1-KD to warrant its inclusion in further experiments.

NRF2 regulates homologues miR-125B1 and miR-29B1 and miR-29A in human AML. Both miR-125B and miR-29B exist as two homologues (Figure 2a). miR-125B1 (located on chromosome 11) and miR-125B2 (located on chromosome 21), both contain identical seed sequences. Both homologues lie in the region of regulatory miRNA clusters, miR-100-let-7-a-2 and LINC00478, respectively. miR-29B also exists as two homologues, miR-29B1 (located on chromosome 7) and miR-29B2 (located on chromosome 1) (Figure 2a).

The sequence of the miRNA seed region of both miR-125B1 and 2 is identical. Similarly, the seed sequence of miR-29B1 is identical to that of miR-29B2. Therefore, we used primers designed specifically for the immature miRNA sequences (which does differ between the miRNA homologues) to identify which miR-125B and miR-29B homologues were being regulated by NRF2. QRT-PCR on lentiviral NRF2-KD THP-1 cells identified reduced expression of the immature miR-125B1 and increased expression of the immature miR--29B1, but no change in the expression of immature miR-125B2 and miR-29B2 sequence (Figures 2b and c). This suggests that miR-125B1 and miR-29B1, but not miR-125B2 or miR-29B2, are regulated by NRF2.

To determine whether NRF2 specifically regulated miR-125B1 and miR-29B1 or had a more general regulatory effect on their clusters, we looked for a differential expression on other miRNAs in each of the homologue regions in response to NRF2-KD. Following NRF2 knockdown, however, there was no difference in the expression of miR-100 and let-7a-2 (miR-125B1 cluster; chromosome 11) or miR-99a and let7c (miR-125B2 cluster; chromosome 21) (Figure 2b). This implies that NRF2 does not regulate these clusters to control miR-125B expression but instead binds to a miR-125B1-specific regulatory region. Conversely, knockdown of NRF2 elevated miR-29B1 and miR-29A but had no effect on miR-29B2 and miR-29C (Figure 2c). NRF2 therefore regulates

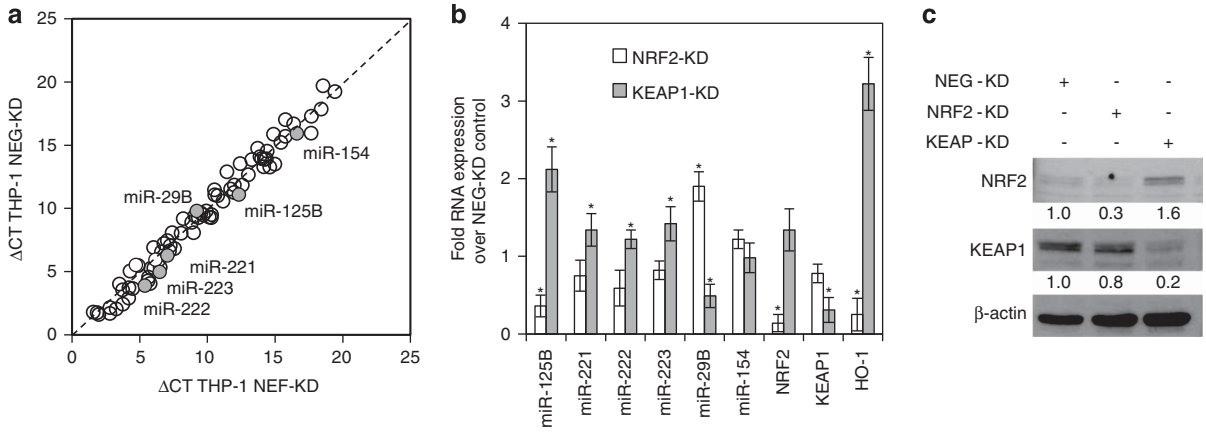

Figure 1 miRNA profiling of AML cells in response lentiviral NRF2 knockdown. (**a**) THP-1 cells were transduced with NEG (NEG-KD)- and NRF2 (NRF2-KD)-targeted miRNA lentiviral constructs. QRT-PCR analysis of 92 cancer-associated miRNAs in NRF2-KD THP-1 cells. Values represent change in qRT-PCR cycle threshold normalised to RNU6B (ΔCT). Dashed line indicates no change in expression. A red circle indicates miR-125B, miR221, miR-223, miR222, miR29B and miR154. (**b**) QRT-PCR of miR-125B, miR221, miR-223, miR222, miR29B, miR154, NRF2, KEAP1 and HO1 in THP-1 cells transduced with NEG-KD, NRF2-KD or KEAP1-KD. Values represent fold change in RNA expression over NEG-KD control. (**c**) THP-1 were transduced with NEG-KD, NRF2-KD or KEAP1-KD before cells were analysed for NRF2 and KEAP1 using western blotting. Blots were reprobed for β-actin to show sample loading. The numbers under the blots indicate densitometry analysis of the blots using Image J software, and the results are expressed as fold change relative to the NEG-KD control

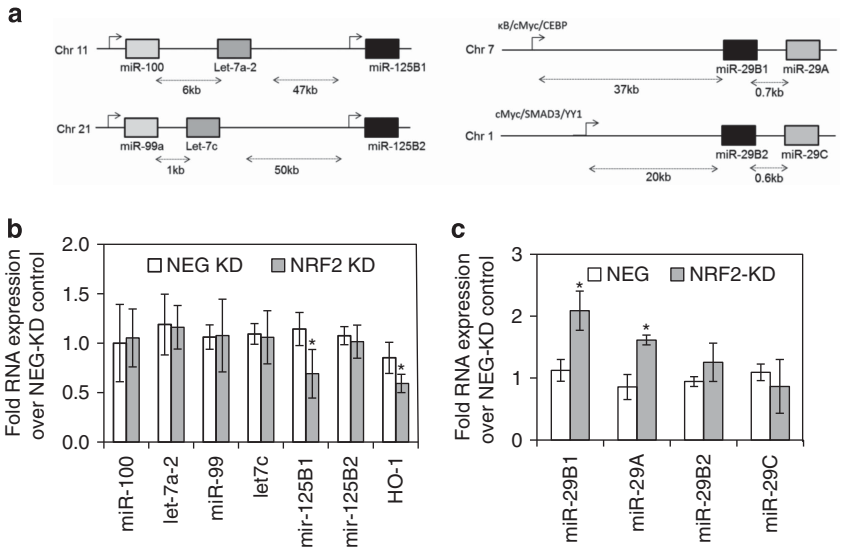

Figure 2 NRF2 regulates homologues miR-125B1 and miR-29B1 and miR-29A in human AML. (**a**) Schematic representation of the miRNA chromosomal positioning of miR-125B (1 and 2) and miR-29B (1 and 2). (**b**) Total RNA was extracted from THP-1 transduced with NEG-KD and NRF2-KD and examined for miRNA expression including immature miR-125B1, miR-125B2 RNA and HO-1 mRNA expression. (**c**) Total RNA was extracted from THP-1 transduced with NEG-KD and NRF2-KD and examined for miR-29A and miR-29C expression including immature miR-29B1, miR-29B2 RNA and HO-1 mRNA expression

a defined pattern of expression of the miR-125B1 and miR-29B1 cluster in human AML. Moreover, results from Figure 1b and Figures 2b and c show that changes in total levels of miR-125B and miR-29B are similar to changes in miR-125B1 and miR-29B1. The main reason for this similarity is that constitutive levels of miR-125B2 and miR-29B2 are much lower in AML than that of their homologue, thus changes observed in total miR-125B and miR-29B reflect changes observed in miR-125B1 and miR-29B1 levels.

NRF2 binds to ARE sites in the promoters of miR-125B1 and miR-29B1. NRF2 acts as a transcription factor by binding to the antioxidant response element (ARE) region in the promoter regions of its target genes.[17] To analyse the 5′ miR-125B1 and miR-29B1 promoter sequence, we used transcription factor analysis programmes (http://www.gene-regulation.com/cgi-bin/pub/programs/pmatch/bin/p-match.cgi and www.genomatix.de/matinspector.html). These analyses identified three potential ARE sites within the miR-125B1 promoter and two in the miR-29B1 promoter (Figure 3a).

To confirm whether NRF2 bound to ARE binding sites in the miR-29B1 or the miR-125B1 promoter, a ChIP assay was undertaken. Figure 3b shows the analysis using antibodies for NRF2 and quantified against control IgG with specific primers for ARE1-3 (promoter region of miR-125B1; chromosome 11) and ARE4 and ARE5 (promoter region of miR-29B1; chromosome 7). Recruitment of NRF2 was markedly enhanced to ARE5 in the miR-29B1 promoter and ARE3 in the miR-125B1 promoter. Next, we evaluated the recruitment of NRF2 to ARE1-5 sites in THP-1 cells transfected with KEAP1 siRNA. Figure 3c shows that there was increased recruitment of NRF2 to the ARE3 and ARE5 site, but not the other potential ARE sites in THP-1 cells transfected with KEAP siRNA over control siRNA. These observations confirmed that NRF2 specifically binds the miR-29B1 ARE5 site and the miR-125B1 ARE3 site.

To establish whether NRF2 functionally controls miR-125B1 expression, the miR-125B1 promoter was cloned into a PGL4 luciferase plasmid and the putative ARE3 site was mutated (Figure 3d). AML is a disease characterised by constitutive activation of NRF2, therefore the luciferase vector PGL4 and PGL4/p125B were transfected into THP-1 cells without prior treatment of an NRF2 activator or repressor. We observed an approximate eightfold increase in luciferase activity in the PGL4/p125B plasmid in comparison with the control (Figure 3e). Site-directed mutagenesis of the ARE3 site in the miR-125B1 promoter corresponded with a significant decrease in miR-125B1 promoter activity (Figure 3e). Moreover, when we co-transfected KEAP1 and NRF2 siRNA with the p125B and p125BNRF2Mut plasmids, KEAP1 siRNA induced significant increase in p125B promoter activity and NRF2 siRNA inhibited p125B promoter activity. KEAP1 siRNA and NRF2 siRNA had no effect on p125BNRF2Mut promoter activity (Figure 3f). Similar experiments on the miR-29B1 promoter were technically not possible as the construct was too big and would not clone into a luciferase reporter vector. These results demonstrate that the ARE3 site in the promoter of mir-125B1 is regulated by NRF2.

NRF2 regulates the expression of miR-125B1 and miR-29B1 in primary human AML. As we have established in AML that high NRF2 mRNA expression causes an increase in NRF2 activity,[10] and that miR-125B1 and miR-29B1 are regulated by NRF2 in AML cell lines, we next examined the expression of NRF2, mir-125B1 and miR-29B1 in primary human AML cells. NRF2 and miR-125B1 is increased in AML compared with normal CD34+ haematopoietic stem cells (HSC), whereas miR-29B1 is decreased in AML compared with normal CD34+ HSC (Figure 4a). As total levels of miR-125B and miR-29B most likely determine their biological function, we analysed total levels of miR-125B and

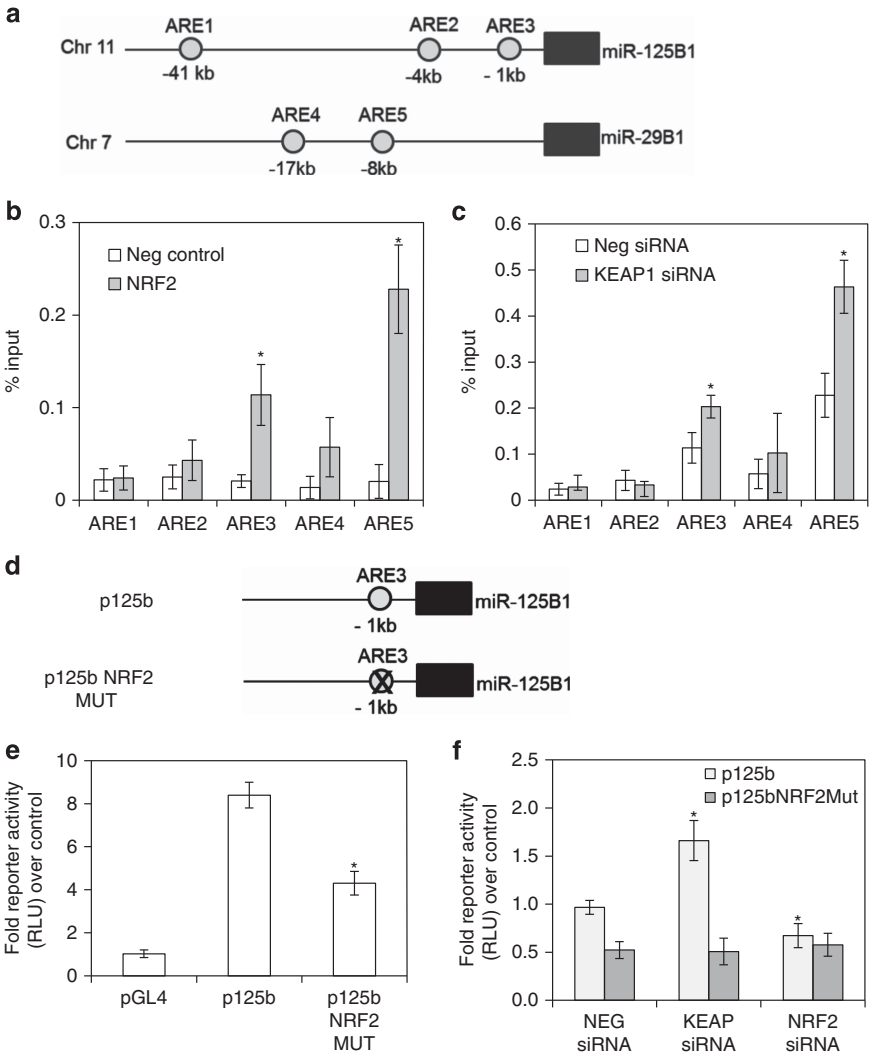

Figure 3 NRF2 binds to ARE sites in the promoters of miR-125B1 and miR-29B1. (**a**) Schematic presentation of ARE binding sequences in the 5′ region of miR-29B1 on chromosome 7 and miR-125B1 on chromosome 11. (**b**) Chromatin immunoprecipitation (ChIP) analysis of the miR-29B1 and miR-125B1 promoter using antibodies against NRF2 and normal rabbit IgG was used as a control. QRT-PCR was performed in triplicate on immunoprecipitated DNA and input DNA. Data presented as percent of input. * indicates $P<0.05$ between the different treatment groups. (**c**) THP-1 cells were transfected with control siRNA and KEAP1 siRNA for 24 h and ChIP was performed. Real-time PCR was performed in triplicate on immunoprecipitated DNA and input DNA. Data presented as percent of input. * indicates $P<0.05$ between the different treatment groups. (**d**) Schematic representation of mutated miR-125B promoter sequence. (**e**) THP-1 cells were transiently transfected with 0.5 μg of each promoter construct including control plasmid and pRL-TK for normalisation of transfection efficiency. Cell extracts were harvested and luciferase assays were performed. Values are the means $\pm$ S.D., $n=4$. * indicates $P<0.01$ of deleted ARE against PGL4 control. (**f**) Control, KEAP1 and NRF2 siRNA were transfected at the same time as p125b and p125bNRF2 MUT and incubated for 48 h. Cell extracts were harvested and luciferase assays were performed. Values are the means $\pm$ S.D., $n=4$. * indicates $P<0.01$ of KEAP1 siRNA and NRF2 siRNA against NEG siRNA control

miR-29B in AML. Supplementary Figure 2 shows that total miR-125B is increased in AML compared with normal CD34+ HSC, whereas miR-29B is decreased in AML compared with normal CD34+ HSC. Furthermore, there is a positive correlation between NRF2 RNA expression and mir-125B1 RNA expression, with an inverse correlation between NRF2 RNA expression and miR-29B1 RNA expression in primary AML cells (Figure 4b). To confirm that NRF2 regulates miR-125B1 and miR-29B1 expression in primary human AML cells, we used NRF2 siRNA to silence NRF2 RNA expression in eight AML patient samples. NRF2 mRNA is significantly knocked down in seven out of the eight AML samples of which the majority also had significantly lower miR-125B1 expression (Figure 4c). Moreover, NRF2 siRNA in the AML samples increased miR-29B1 expression (Figure 4c). Together, these results show that knockdown of NRF2 regulates the expression of miR-125B1 and miR-29B1 in primary human AML.

miR-125B antagomiR and miR-29B mimic increases AML apoptosis and sensitivity to frontline chemotherapy agents. Previous studies in AML have suggested that the overexpression of miR-125B plays an oncogenic role by repressing apoptosis and the reduction of miR-29B increases

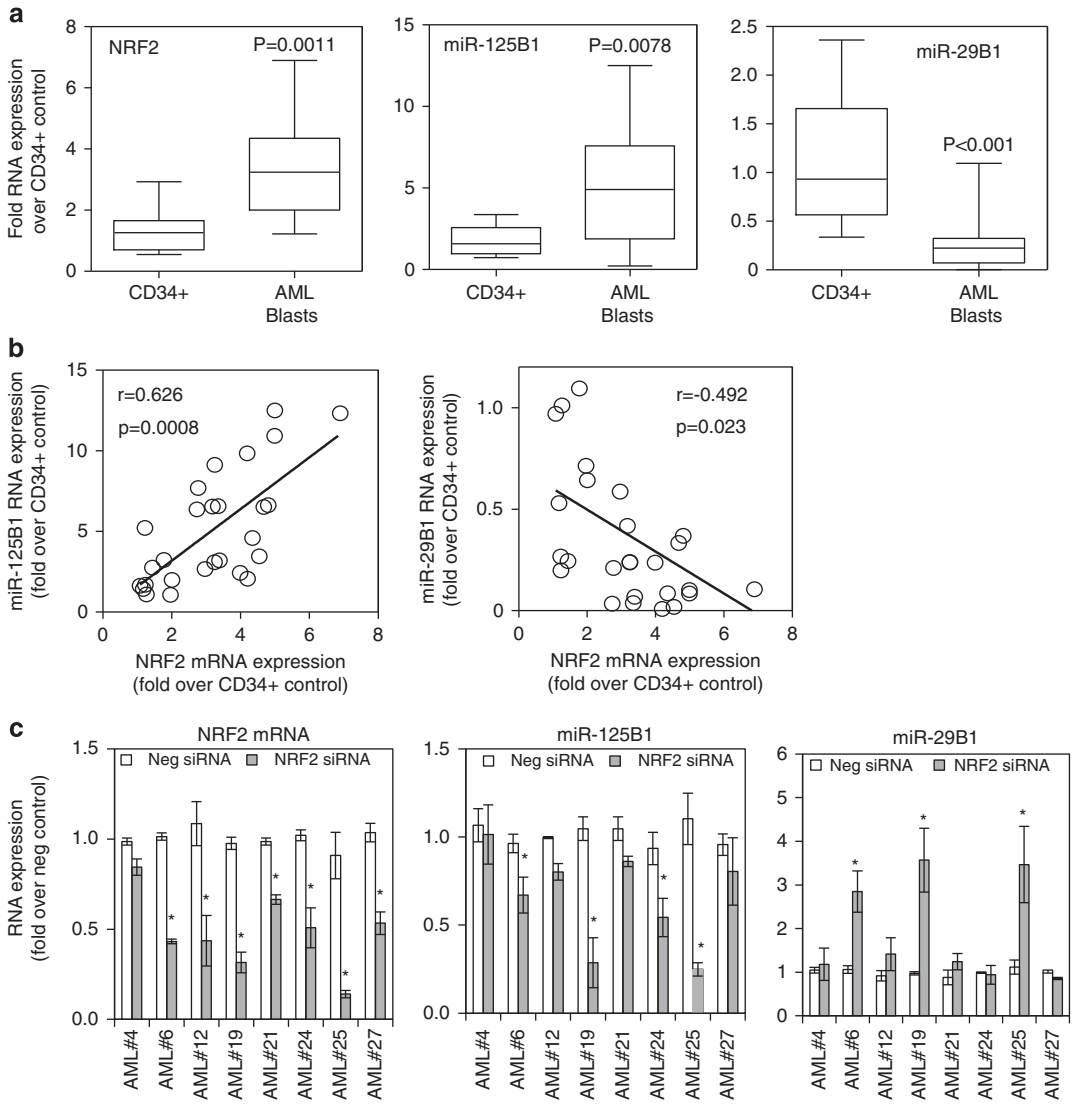

Figure 4 NRF2 regulates miR-29B1 and miR-125B1 in primary AML. (**a**) Total RNA was extracted from patient AML blasts ($n=18$) and CD34+ HSC ($n=8$). NRF2, miR-29B1 and miR-125B1 RNA expression levels were measured using QRT-PCR. (**b**) Pearson's correlation analysis between miR-125B1 or miR-29B1 and NRF2 mRNA expression in human primary AML cells. (**c**) Control and NRF2 siRNA were transfected into primary blasts ($n=7$) for 48 h and RNA extracted. RNA was analysed for NRF2, miR-125B1 and miR-29B RNA expression. Values are the means ± S.D., $n=3$

proliferation and represses apoptosis.[18,19] To determine the functional role of inhibiting miR-125B and overexpressing miR-29B both alone and in-combination, we transfected miR-125B antagomiR and miR-29B mimic into THP-1 cells and analysed cells for apoptosis by annexin V/PI staining. However, before we did this, we showed that the concentrations of transfected miR-125B antagomiR and miR-29B mimic used manipulated the miRNA levels comparable with that observed in the NRF2-KD and KEAP1-KD THP-1 cells (Supplementary Figure 1). THP-1 cells transfected with the miR-125B antagomiR or miR-29B mimic showed a small but significant increase in annexin V/PI staining in comparison with the control transfection (Figure 5a). Moreover, when we co-transfected miR-125B antagomir and miR-29B mimic, we observed a synergistic increase in annexin V/PI staining in comparison with the control (Figure 5a). Transfection of miR-125B antagomir and miR29B mimic into THP-1 and Kasumi-1 cells potentiated the cytotoxic effect of the frontline AML chemotherapy agent daunorubicin (Supplementary Table 2).

Next, we examined the effects of inhibiting miR-125B and increasing miR-29B expression in primary AML cells in comparison with non-malignant primary CD34+ HSC. In six primary AML patient samples, inhibition of miR-125B or increasing miR-29B showed a significant decrease in cell viability (Figure 5b). Finally, we compared the viability of primary AML patient cells that had normal NRF2 expression (and thus normal miR-125B and miR-29B expression) with an AML patient sample that had high NRF2 expression (and thus high miR-125B and low miR-29B expression) after treatment with daunorubicin (Figure 5c and Table 1 and Supplementary Table 2). AML with normal NRF2 and normal miR-125B and

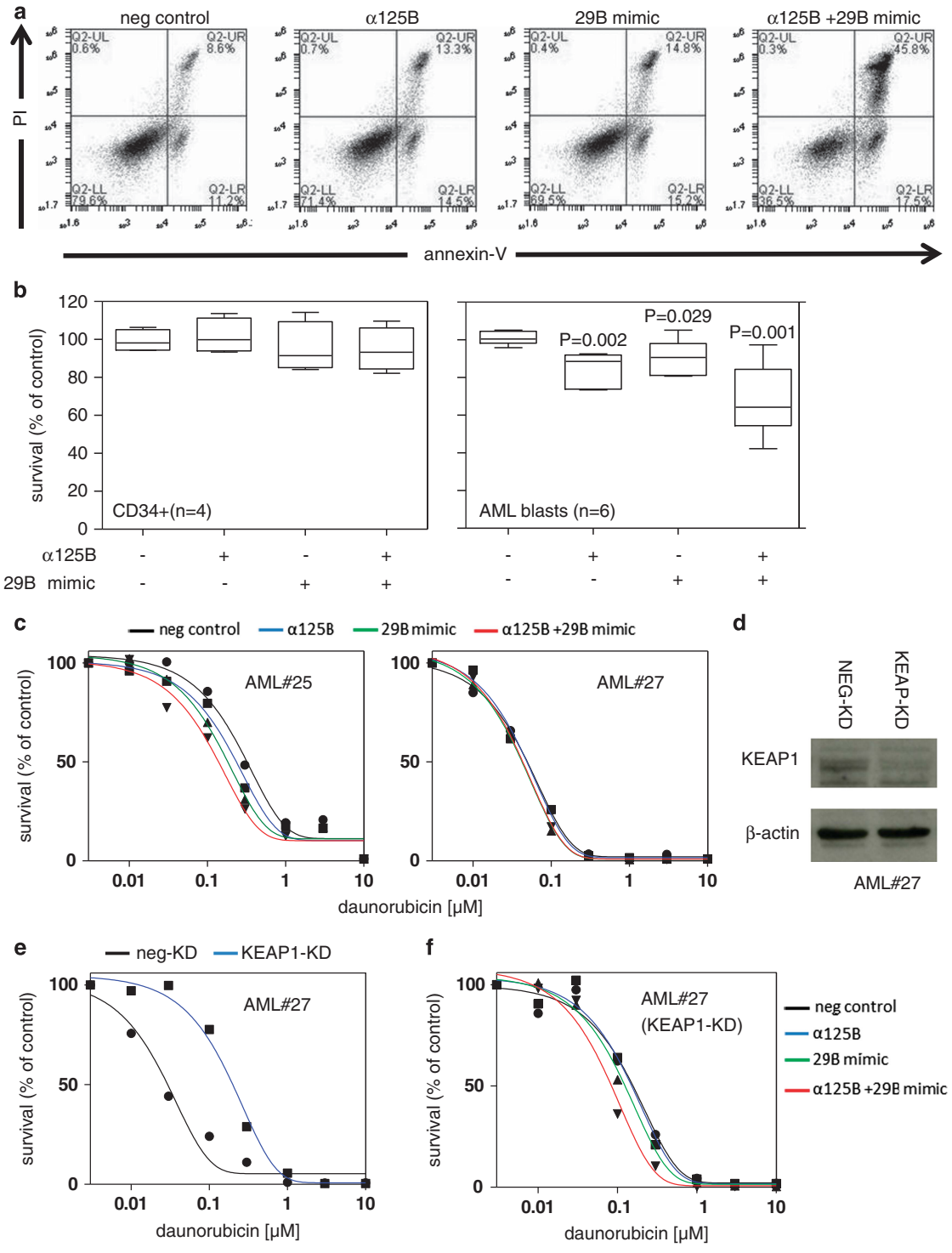

Figure 5 miR-125B antagomiR and miR-29B mimic induce apoptosis of AML cells and increases there sensitivity to AML chemotherapy. (**a**) THP-1 were transfected with control miRNA, miR-125B antagomiR (α125B), miR-29B mimic (29B mimic) and miR-125B antagomiR in combination with miR-29B mimic for 48 h before cells were analysed for apoptosis by PI/Annexin V staining. (**b**) AML blasts ($n=6$) and CD34+ ($n=4$) were transfected with control miRNA, miR-125B antagomiR and miR-29B mimic and miR-125B antagomiR in combination with miR-29B mimic for 24 h and then assessed for cell viability by Cell Titer-GLO. (**c**) AML blasts and CD34+ cells were transfected with control miRNA (miR-mimic negative control and the anti-miR miRNA inhibitor negative control for single experiments and combined miR-mimic negative control and the anti-miR miRNA inhibitor negative control in combined experiments), miR-125B antagomiR, miR-29B mimic and miR-125B antagomiR in combination with miR-29B mimic for 24 h before the addition of increasing doses of daunorubicin for 48 h. Cells assessed for viability by Cell Titer-GLO. (**d**) AML#27 was transduced with NEG-KD and KEAP1-KD for 48 h before cells before the addition of increasing doses of daunorubicin for 48 h before cells were analysed for KEAP1 using western blotting. Blots were reprobed for β-actin to show sample loading. (**e**) AML#27 was transduced with NEG-KD and KEAP1-KD for 48 h before the addition of increasing doses of daunorubicin for 48 h. Cells were assessed for viability by Cell Titer-GLO. (**f**) AML#27 was transduced with KEAP1-KD for 48 h before cells were transfected with control miRNA, miR-125B antagomiR, miR-29B mimic and miR-125B antagomiR in combination with miR-29B mimic for 24 h followed by the addition of increasing doses of daunorubicin for 48 h. Cells were assessed for viability by Cell Titer-GLO

Table 1 AML patient sample information, NRF2 RNA expression and relative miR-125B1 and miR-29B1 RNA expression levels

Number	Age	Gender	WHO diagnosis	Cytogenetics	% Blasts	Fold NRF2 mRNA over CD34+	Fold RNA over CD34+	
							miR-125B1	miR-29B1
AML#1	49	M	AML with maturation	Normal	80	3.35	6.57	0.04
AML#2	39	M	AML with maturation	Normal	65*	6.89	12.33	0.11
AML#3	64	M	AML with RUNX1-RUNX1T1	t(8;21)	85	1.26	1.09	1.01
AML#4	92	F	AML with myelodysplasia related changes	Not available	70*	1.23	1.70	0.20
AML#5	82	F	AML with MDSrelated changes	Deletion 13	85	3.39	3.20	0.07
AML#6	46	F	AML with maturation	+4,+8, t(9;22)	70*	4.99	12.51	0.10
AML#7	66	F	AML with maturation	t(2;12)	65*	1.23	5.22	0.27
AML#8	78	M	AML with MDS related changes	Not available	85	4.19	9.85	0.01
AML#9	57	M	AML without maturation	Not available	95	4.35	4.59	0.09
AML#10	27	M	AML with RUNX1-RUNX1T1	t(8;21)	60*	4.99	10.93	0.08
AML#11	25	M	AML with maturation	Normal	50*	4.81	6.63	0.37
AML#12	61	M	Relapsed AML without maturation	Not available	95	1.96	1.07	0.71
AML#13	28	F	Acute Monoblastic and Monocytic Leukaemia	Normal	90	4.68	6.52	0.33
AML#14	31	F	AML without maturation	Trisomy 8	75*	2.73	6.37	0.03
AML#15	84	M	Acute meyloid leukaemia, NOS	Not available	70*	3.99	2.43	0.24
AML#16	53	M	AML with t(6;9)(p23;q34);*DEK-NUP214*	t(6;9)	65*	3.25	9.13	0.24
AML#17	51	F	AML with maturation	Normal	40*	4.54	3.45	0.02
AML#18	47	M	Acute myeloid leukaemia without maturation	Not available	90	4.20	2.07	1.33
AML#19	77	F	AML with maturation	Normal	70*	2.78	7.70	0.21
AML#20	62	M	AML with maturation	Complex	55*	2.96	2.67	0.59
AML#21	70	M	AML with minimal differentiation	Normal	95	2.01	1.98	0.64
AML#22	65	F	AML with maturation	Normal	40*	1.44	2.75	0.24
AML#23	77	M	Therapy related AML	Complex	70*	3.24	3.10	0.24
AML#24	40	F	AML with minimal differentiation	Normal	90	1.77	3.23	1.09
AML#25	70	M	AML without maturation	Complex	95	3.18	6.54	0.42
AML#26	91	F	AML NOS	Not available	75*	1.08	1.63	0.97
AML#27	59	F	AML with t(8;21)(q22;q22); RUNX1-RUNX1T1	t(8;21)	85	1.17	1.44	0.53

This table defines the nature of the AML disease including WHO diagnosis and cytogenetics. NRF2, miR125B1 and miR-29B1 RNA expression levels over CD34+ control cells

miR-29B expression were much more sensitive to daunorubicin than AML patient samples that had high NRF2 expression and thus high miR-125B and low miR-29B expression. Moreover, when we transfected the primary AML that had high NRF2 and high mir-125B and low miR29B with miR-125B antagomiR together with miR-29B mimic, the result was that sensitivity of these AML cells to daunorubicin was increased to a level comparable with AML with normal NRF2 expression. Because AML#27 has low NRF2 expression over normal CD34+ HSC (Table 1), which is more sensitive to daunorubicin (Figure 5c), and miR-125B antagomiR together with miR-29B mimic had no effect on resistance to daunorubicin (Figure 5c), we examined the effect of KEAP1-KD on AML#27 to determine if we could increase the activity of NRF2 and increase the chemoresistance of this sample. Figure 5d shows KEAP1-KD in AML#27. Figure 5e shows that KEAP1-KD AML#27 is more resistant to daunorubicin compared with NEG-KD. However, when we transfected AML#27 KEAP1-KD cells with control miRNA, miR-125B antagomiR, miR-29B mimic and miR-125B antagomiR in combination with miR-29B mimic, only the combination decreased resistance to daunorubicin (Figure 5f). These results demonstrate that inhibiting miR-125B and overexpressing miR-29B in combination increases apoptosis of primary AML and also increases sensitivity of AML cells to current frontline chemotherapy.

miR-29B and miR-125B gene targets in human AML. Studies have shown that a number of different targets exist for both miR-29B and miR-125B in AML (Supplementary Table 3).[18,20–28] Here we examine the expression of genes listed in Supplementary Table 3 for their response to transfection of control miRNA, miR-125B antagomiR, miR-29B mimic and miR-125B antagomiR in combination with miR-29B mimic. Figure 6a shows that MYBL2, AKT2, CDK4 and SP1 are inhibited by miR-29B mimic in THP-1 cells; we also observe that AKT2 and CDK4 are further inhibited by the addition of miR-125B antagomiR. From the miR-125B targets, Figure 6a shows that MAPK14, STAT3 and BAK1 show an increase in mRNA in response to miR-125B antagomiR. Next, we examined the protein expression of AKT2, STAT3 and BAK1. Figure 6b shows a reduction in AKT2 protein expression in response to miR-29B mimic and miR-125B antagomiR in combination with miR-29B mimic. STAT3 showed a slight increase in response to miR-29B mimic and miR-125B antagomiR in combination with miR-29B mimic. BAK1 showed an increase in response to miR-125B antagomir and miR-125B antagomiR in combination with miR-29B mimic.

Finally, we wanted to determine whether NRF2 deregulation in AML affects miRNA levels to such an extent that expression of their target genes is changed as a consequence. Figure 6c shows a change in expression of AKT2, STAT3 and BAK1 but not MCL1 mRNA in response to NRF2-KD or KEAP1-KD compared with NEG-KD. Figure 6d shows changes in AKT2 and BAK1 protein expression in response to NRF2-KD and an increase in response to KEAP1-KD. Together, these results link the two major observations of this study; first, that NRF2

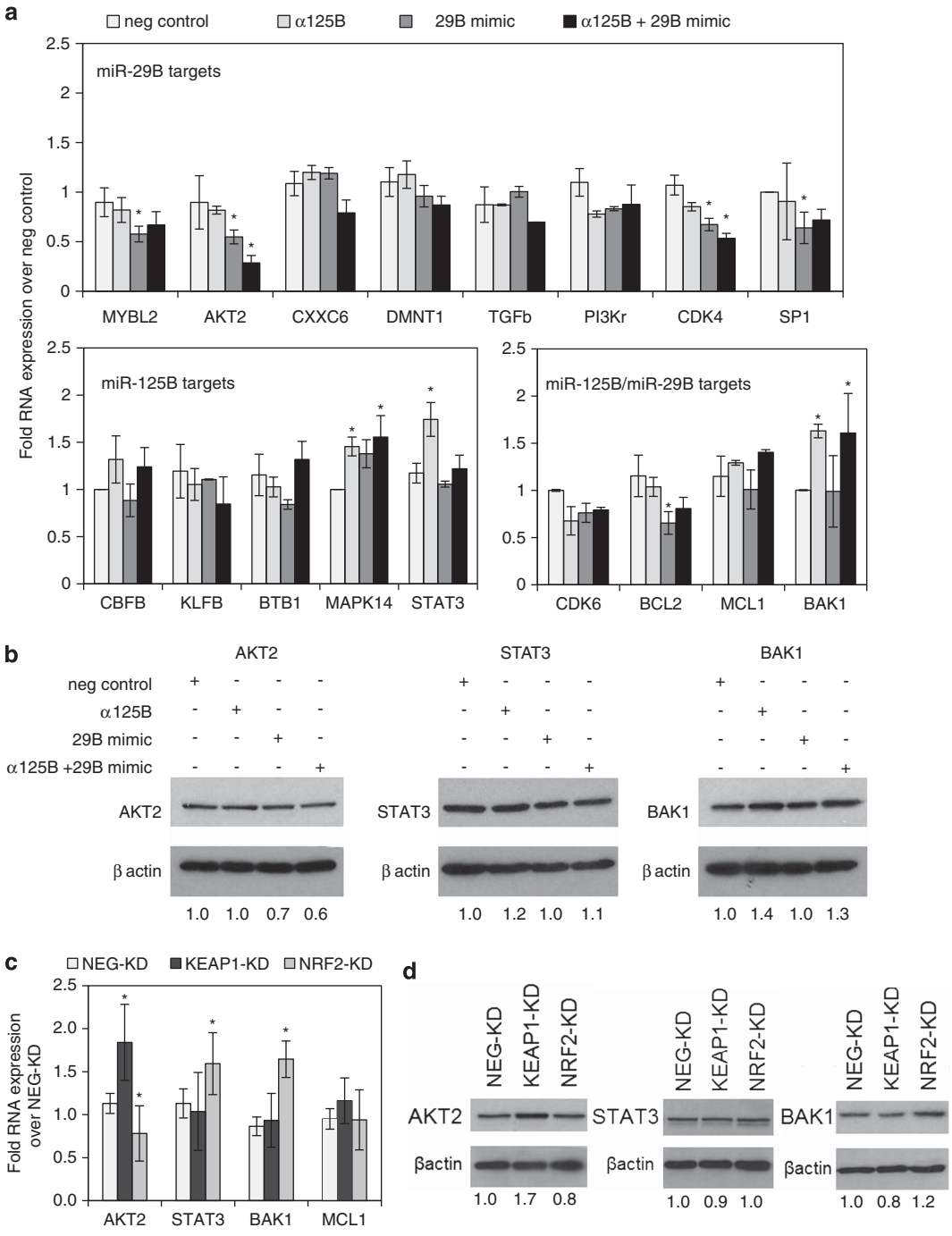

Figure 6 miR-125B antagomiR and miR-29B mimic gene targets in AML cells. (**a**) THP-1 were transfected with control miRNA, miR-125B antagomiR (α125B), miR-29B mimic (29B mimic) and miR-125B antagomiR in combination with miR-29B mimic for 48 h before cells were analysed for target gene expression using QRT-PCR. (**b**) THP-1 cells were transfected with control miRNA, miR-125B antagomiR (α125B), miR-29B mimic (29B mimic) and miR-125B antagomiR in combination with miR-29B mimic for 48 h before cells were analysed for AKT2, STAT3 and BAK1 using western blotting. Blots were reprobed for β-actin to show sample loading. (**c**) QRT-PCR of mRNA for AKT2, STAT3, BAK1 and MCL1 in THP-1 cells transduced with NEG-KD, NRF2-KD or KEAP1-KD. Values represent fold change in RNA expression over NEG-KD control. (**d**) THP-1 cells were transduced with NEG-KD, NRF2-KD or KEAP1-KD before cells were analysed for AKT2, STAT3 and BAK1 protein expression using western blotting. Blots were reprobed for β-actin to show sample loading. The numbers under the blots indicate densitometry analysis of the blots using Image J software, and the results are expressed as fold change relative to the negative control

directly regulates miR-125B and miR-29B expression. Second, that miR-125B and miR-29B synergistically influence AML survival and chemoresistance, possibly via deregulation of target genes such as AKT2, STAT3 or BAK1.

Discussion

Our understanding of the role of non-coding RNA molecules in diseases such as cancer is presently in its infancy. To date, miRNAs have been shown to have a significant role in cancer

biology through the regulation of both tumour suppressors and oncogenes. Less is known, however, about the upstream control of miRNA expression in cancer and the biological processes that control miRNA expression. In AML, the differential expression of a number of miRNAs has been reported to be associated with the malignant phenotype but as yet the upstream mechanisms by which this is controlled are yet to be described.[29–32] As we have previously identified NRF2 as an important regulator of cell survival in AML, the aim of the present study was to investigate the ability of NRF2 to affect miRNA expression and furthermore define the function of these miRNAs in human AML both in a resting state and in response to front-line chemotherapeutic agents.

Through gene expression data and multiple transcription factor binding assays, we found that NRF2 upregulates mir-125B1 and downregulates miR-29B1 though binding to specific ARE sites in the miR-125B1 and miR-29B1 regulatory regions. Furthermore, we observed that by decreasing the expression of miR-125B and increasing the expression of miR-29B, the cells become more sensitive to apoptotic stimuli. These findings are in keeping with previous observations that miR-29B and miR-125B regulate the expression of multiple survival pathways in AML. The global repression of miR-125B targets and elevation of miR-29B targets genes would aid the uncontrolled proliferative phenotype of AML. Therefore, in Figures 6a and b, we analyse the targets of miR-29B and miR-125B in AML cells transfected with corresponding mimic and antagomir, both alone and in combination. We observe changes in a number of genes including AKT2, CDK4, MAPK14, STAT3, BCL2 and BAK1. Interestingly, AKT2 and CDK4 are targets of miR-29B only; however, when we co-transfect miR-125B antagomir and miR-29B mimic, we do observe a further reduction over miR-29B mimic only. There are no miR-125B sites within these two genes suggesting that the combined observations are due to off-target effects. Together, the cumulative repression of miR-29B and the overexpression of miR-125B significantly contribute to leukaemia cell proliferation within the bone marrow niche.

Transcription factors are generally structured in context of networks. In AML, miR-29B downregulation has been found to be associated with high C-MYC levels as well as high SP1 and NF-κB.[33,34] Furthermore, NF-κB, JUN and C-MYC have been linked to increased NRF2 activity in human cancer (including AML)[10,35] and NRF2 has been shown to transcriptionally regulate miR-125B in kidney epithelia cells in response to cisplatin-induced toxicity.[36] Taken together, it is likely that NRF2 has a central role in the complex network regulating miR-29B and miR-125B in human AML.

We also highlight that other miRNAs may be regulated by NRF2. The array data shown as Supplementary Table 1 show that some miRNAs are downregulated in response to NRF2-KD and increased in response to sulforaphane. This list includes miR-222, miR221, miR-223 miR-23a, miR-195 and miR-196a. Of particular interest from this group is miR-222, miR-221 and miR223, which have been shown to be highly expressed in AML compared with other leukaemias.[37] Moreover, we also noted that high NRF2 activity caused a decrease in the expression of miRNAs, which includes miR-154, miR146a and miR-181B. All these miRNAs have been shown to be of interest in AML with miR-146a being shown to have low expression in AML, which correlates with high expression of its target gene CXCR4,[38] which in a separate study has been shown to be regulated by NRF2 in human HSC.[39] Consequently in human AML, NRF2 not only regulates key genes involved in the reaction to oxidative stress but also regulates miRNAs that appear to have a broader impact on gene expression and regulation.

In summary, here we report the first description of upstream miRNA regulation by NRF2 in a human cancer and its downstream cyto-protective consequences. In doing so, we not only provide novel mechanistic insight into the pro-tumoural consequences of the constitutive NRF2 expression in AML, but we also propose that targeting the NRF2 regulation of these miRNA (or the miRNA directly) would be a biologically plausible therapeutic strategy to increase the effectiveness of chemotherapy in human AML.

Materials and Methods

Materials. The AML-derived cell lines were obtained from the European Collection of Cell Cultures where they are authenticated by DNA fingerprinting. In the laboratory, they are used at low passage number for a maximum of 6 months post-resuscitation, testing regularly for Mycoplasma infection. All primers were purchased from Invitrogen (Paisley, UK). AKT2, STAT3 and BAK1 antibodies were purchased from Cell Signalling Technology (Cambridge, MA, USA). NRF2 and KEAP1 antibodies were purchased from Santa Cruz Biotechnology (Santa Cruz, CA, USA). All other reagents were obtained from Sigma-Aldrich (St. Louis, MO, USA), unless indicated. To assess whether NRF2 regulates miRNA expression in AML, we used commercially available OncomiR collection Cancer miRNA qRT-PCR Array (SBI, Mountain View, CA, USA).

Primary AML cell culture. AML cells were obtained from patients' bone marrow or blood following informed consent and under approval from the UK National Research Ethics Service (LRECref07/H0310/146). For primary cell isolation, heparinised blood was collected from volunteers and human peripheral blood mononuclear cells isolated by Histopaque (Sigma-Aldrich, Dorset, UK) density gradient centrifugation. AML samples that were less than 80% blasts were purified using the CD34-positive selection kit (Miltenyi Biotec, Auburn, CA, USA) (denoted by * in Table 1). Cell type was confirmed by microscopy and flow cytometry. We obtained haematopoietic CD34+ cells from two sources, Stem Cell Technologies (Manchester, UK) and volunteers. Positive selection of CD34+ cells were isolated from peripheral blood mononuclear cells using a CD34-positive selection kit (Miltenyi Biotec). For all CD34+ experiments, at least three different donors were used to obtain the results presented in this paper. Cell type was confirmed by microscopy and flow cytometry.

RNA extraction and real time PCR (RT-PCR). Total mRNA extraction was carried out using mirVana miRNA isolation kit (Ambion, Paisley, UK) and reverse transcribed using the miRscript II RT kit (Qiagen, Manchester, UK). All mature miRNA were normalised to RNU6B and immature miRNA and mRNA were normailsed to GAPDH for qRT-PCR as described previously.[40] qRT-PCR was carried out using SYBR green technology (Qiagen). The samples were preamplified at 95 °C for 2 min, after which was amplified for 45 cycles at 95 °C for 15 s, 60 °C for 10 s and 72 °C for 10 s. The qRT-PCR was performed on the LightCycler480 (Roche, Burgess Hill, UK).

Virus construction and infection. Lentiviruses containing miRNA sequence miRNA-Nrf2 (5′-TTAATGAGTTCACTGTCAACT-3′), miRNA-KEAP1 (5′-GTTTTGGCCACTGACTGAC-3′) and miR-NEG were constructed and produced as described previously.[41] For transduction, THP-1 cells and AML blasts cells were plated onto 12-well plates (5×10^4 cells/well) and infected with lentiviruses (multiplicity of infection of 15) with 8 μg/ml Polybrene (Sigma, Dorset, UK). Transduced cells were analyzed by flow cytometry (Accuri, BD Biosciences, Oxford, UK), real-time PCR (Roche) and western blotting.

Transfections. AML transfections were carried out with 2×10^6 cells using the Amaxa Nucleofactor Kit II (Cambridge, UK). Control miR, miR-29B mimic and miR-125B antagomiR, control siRNA, KEAP1 and NRF2 siRNA were purchased

from Invitrogen were transfected in at a concentration of 45 nm. For control miR, the miR-mimic negative control and the anti-miR miRNA inhibitor negative control for single experiments and combined miR-mimic negative control and the anti-miR miRNA inhibitor negative control in combined experiments were used. For all gene expression experiments, the cells were incubated for 24 h post transfection before RNA extraction. For the cell viability assays, AML cells were incubated for 48 h post transfection. For reporter assays, 0.5 μg of PGL4 reporter and pRL-TK control constructs were co-transfected into THP-1. Transfected cells were incubated for 24 h before the indicated treatments. For reporter assay, cells were treated with Dual-Luciferase reporter assay system (Promega, Southampton, UK).

Western blotting. Sodium dodecyl sulfate-polyacrylamide gel electrophoresis and western blot analyses were performed as described previously. Briefly, whole cell lysates as well as nuclear and cytosolic were extracted and sodium dodecyl sulfate-polyacrylamide gel electrophoresis separation was performed.[42] Protein was transferred to nitrocellulose and western blot analysis performed with the indicated antisera according to their manufacturer's guidelines.

Cloning of miR-125B promoter construct. To generate the p125B promoter construct containing ARE3, a DNA fragment containing 2.6 kb of the human 125b promoter region was amplified from genomic DNA with PCR and specific primers: 5′-TGAGAGGAGCGCAACAATG-3′ reverse primer and 5′-AGAAAGGCCACCAAGATTCAC-3′ forward primer. The fragment was cloned into the PGL4.11 basic plasmid (Promega). To generate mutated NRF2 construct (p125B NRF2 MUT) the sense PCR primer used was 5′-GCTGTG GCTGtTTTGTtATTCTCTTTGACTAG-3′. This mutation was introduced with the QuikChange XL Site-Directed Mutagenesis Kit (Agilent, Stockport, UK).

Cell viability and apoptosis assays. THP-1, Kasumi-1, primary CD34+ HSC and primary AML cells were transfected with control miR (miR-mimic negative control and the anti-miR miRNA inhibitor negative control for single experiments and combined miR-mimic negative control and the anti-miR miRNA inhibitor negative control in combined experiments), miR-29B mimic and miR-125B antagomiR and combined miR-29B mimic and miR-125B antagomiR for 24 h. THP-1 cells were analysed for apoptosis using PI/Annexin V staining. THP-1, Kasumi-1, primary CD34+ HSC and primary AML transfected cells were treated with different concentrations of chemotherapy agents and incubated for 48 h; then, viable cells were measured with Cell-Titre GLO (Promega).

Chromatin immunoprecipitation assay. THP-1 cells were transfected with control siRNA or KEAP1 siRNA 24 h before the cells were fixed with 1% formaldehyde in medium for 10 min at room temperature. The sonication conditions were optimised to determine generation of DNA fragments between 300 and 600 base pairs in length. Chromatin was immunoprecipitated with IgG, anti-NRF2 (Cell Signalling). The association of NRF2 was measured by RT-PCR on immunoprecipitated chromatin using primers spanning the ARE sites described in Figure 3a and Supplementary Table 4.

Statistical analyses. Student's *t* test was performed to assess statistical significance from controls. Results with $P<0.05$ were considered statistically significant (*). Results represent the mean $\pm$ S.D. of three independent experiments.

Conflict of Interest

The authors declare no conflict of interest.

Acknowledgements. We wish to thank the World Cancer Research, National Institutes for Health Research (Flexibility and Sustainability Funding) and The Big C. We thank Professor Richard Ball at the Norfolk and Norwich University Hospital tissue bank for assistance with primary tissue collection.

1. Estey E, Dohner H. Acute myeloid leukaemia. *Lancet* 2006; **368**: 1894–1907.
2. Kvinlaug BT, Chan WI, Bullinger L, Ramaswami M, Sears C, Foster D *et al.* Common and overlapping oncogenic pathways contribute to the evolution of acute myeloid leukemias. *Cancer Res* 2011; **71**: 4117–4129.
3. Moi P, Chan K, Asunis I, Cao A, Kan YW. Isolation of NF-E2-related factor 2 (Nrf2), a NF-E2-like basic leucine zipper transcriptional activator that binds to the tandem NF-E2/AP1 repeat of the beta-globin locus control region. *Proc Natl Acad Sci USA* 1994; **91**: 9926–9930.
4. Alam J, Stewart D, Touchard C, Boinapally S, Choi AMK, Cook JL. Nrf2, a Cap'n'Collar transcription factor, regulates induction of the heme oxygenase-1 gene. *J Biol Chem* 1999; **274**: 26071–26078.
5. Venugopal R, Jaiswal AK. Nrf1 and Nrf2 positively and c-Fos and Fra1 negatively regulate the human antioxidant response element-mediated expression of NAD(P)H:quinone oxidoreductase1 gene. *Proc Natl Acad Sci USA* 1996; **93**: 14960–14965.
6. Ooi A, Dykema K, Ansari A, Petillo D, Snider J, Kahnoski R *et al.* CUL3 and NRF2 mutations confer an NRF2 activation phenotype in a sporadic form of papillary renal cell carcinoma. *Cancer Res* 2013; **73**: 2044–2051.
7. Hanada N, Takahata T, Zhou Q, Ye X, Sun R, Itoh J *et al.* Methylation of the KEAP1 gene promoter region in human colorectal cancer. *BMC Cancer* 2012; **12**: 66.
8. Kim YR, Oh JE, Kim MS, Kang MR, Park SW, Han JY *et al.* Oncogenic NRF2 mutations in squamous cell carcinomas of oesophagus and skin. *J Pathol* 2011; **220**: 446–451.
9. Konstantinopoulos PA, Spentzos D, Fountzilas E, Francoeur N, Sanisetty S, Grammatikos AP *et al.* Keap1 mutations and Nrf2 pathway activation in epithelial ovarian cancer. *Cancer Res* 2011; **71**: 5081–5089.
10. Rushworth SA, Zaitseva L, Murray MY, Shah NM, Bowles KM, MacEwan DJ. The high Nrf2 expression in human acute myeloid leukemia is driven by NF-κB and underlies its chemo-resistance. *Blood* 2012; **120**: 5188–5198.
11. Sporn MB, Liby KT. NRF2 and cancer: the good, the bad and the importance of context. *Nat Rev Cancer* 2012; **12**: 564–571.
12. Rushworth SA, Bowles KM, MacEwan DJ. High basal nuclear levels of Nrf2 in acute myeloid leukemia reduces sensitivity to proteasome inhibitors. *Cancer Res* 2011; **71**: 1999–2009.
13. Winter J, Jung S, Keller S, Gregory RI, Diederichs S. Many roads to maturity: microRNA biogenesis pathways and their regulation. *Nat Cell Biol* 2009; **11**: 228–234.
14. Garzon R, Marcucci G, Croce CM. Targeting microRNAs in cancer: rationale, strategies and challenges. *Nat Rev Drug Discovery* 2010; **9**: 775–789.
15. Chorley BN, Campbell MR, Wang X, Karaca M, Sambandan D, Bangura F *et al.* Identification of novel NRF2-regulated genes by ChIP-Seq: influence on retinoid X receptor alpha. *Nucleic Acids Res* 2012; **40**: 7416–7429.
16. Devling TWP, Lindsay CD, McLellan LI, McMahon M, Hayes JD. Utility of siRNA against Keap1 as a strategy to stimulate a cancer chemopreventive phenotype. *Proc Natl Acad Sci USA* 2005; **102**: 7280–7285.
17. Zhao CR, Gao ZH, Qu XJ. Nrf2-ARE signaling pathway and natural products for cancer chemoprevention. *Cancer Epidemiol* 2010; **34**: 523–533.
18. Garzon R, Heaphy CE, Havelange V, Fabbri M, Volinia S, Tsao T *et al.* MicroRNA 29b functions in acute myeloid leukemia. *Blood* 2009; **114**: 5331–5341.
19. Bousquet M, Harris MH, Zhou B, Lodish HF. MicroRNA miR-125b causes leukemia. *Proc Natl Acad Sci USA* 2010; **107**: 21558–21563.
20. Gong J, Zhang JP, Li B, Zeng C, You K, Chen MX *et al.* MicroRNA-125b promotes apoptosis by regulating the expression of Mcl-1, Bcl-w and IL-6R. *Oncogene* 2013; **32**: 3071–3079.
21. Zhang H, Luo XQ, Feng DD, Zhang XJ, Wu J, Zheng YS *et al.* Upregulation of microRNA-125b contributes to leukemogenesis and increases drug resistance in pediatric acute promyelocytic leukemia. *Mol Cancer* 2011; **10**: 108.
22. Garzon R, Liu S, Fabbri M, Liu Z, Heaphy CE, Callegari E *et al.* MicroRNA-29b induces global DNA hypomethylation and tumor suppressor gene reexpression in acute myeloid leukemia by targeting directly DNMT3A and 3B and indirectly DNMT1. *Blood* 2009; **113**: 6411–6418.
23. Zhao JJ, Lin J, Lwin T, Yang H, Guo J, Kong W *et al.* microRNA expression profile and identification of miR-29 as a prognostic marker and pathogenetic factor by targeting CDK6 in mantle cell lymphoma. *Blood* 2010; **115**: 2630–2639.
24. Bousquet M, Nguyen D, Chen C, Shields L, Lodish HF. MicroRNA-125b transforms myeloid cell lines by repressing multiple mRNA. *Haematologica* 2012; **97**: 1713–1721.
25. Ooi AG, Sahoo D, Adorno M, Wang Y, Weissman IL, Park CY. MicroRNA-125b expands hematopoietic stem cells and enriches for the lymphoid-balanced and lymphoid-biased subsets. *Proc Natl Acad Sci USA* 2010; **107**: 21505–21510.
26. Tan G, Niu J, Shi Y, Ouyang H, Wu ZH. NF-kappaB-dependent microRNA-125b up-regulation promotes cell survival by targeting p38alpha upon ultraviolet radiation. *J Biol Chem* 2012; **287**: 33036–33047.
27. Surdziel E, Cabanski M, Dallmann I, Lyszkiewicz M, Krueger A, Ganser A *et al.* Enforced expression of miR-125b affects myelopoiesis by targeting multiple signaling pathways. *Blood* 2011; **117**: 4338–4348.
28. Luna C, Li G, Qiu J, Epstein DL, Gonzalez P. Cross-talk between miR-29 and transforming growth factor-betas in trabecular meshwork cells. *Invest Ophthalmol Vis Sci* 2011; **52**: 3567–3572.
29. Anderson JE, Kopecky KJ, Willman CL, Head D, O'Donnell MR, Luthardt FW *et al.* Outcome after induction chemotherapy for older patients with acute myeloid leukemia is not improved with mitoxantrone and etoposide compared to cytarabine and daunorubicin: a Southwest Oncology Group study. *Blood* 2002; **100**: 3869–3876.
30. Wang H, Tan G, Dong L, Cheng L, Li K, Wang Z *et al.* Circulating MiR-125b as a Marker Predicting Chemoresistance in Breast Cancer. *PLoS One* 2012; **7**: e34210.
31. Okamoto K, Miyoshi K, Murawaki Y. miR-29b, miR-205 and miR-221 Enhance Chemosensitivity to Gemcitabine in HuH28 Human Cholangiocarcinoma Cells. *PLoS One* 2013; **8**: e77623.

32. Blum W, Garzon R, Klisovic RB, Schwind S, Walker A, Geyer S *et al.* Clinical response and miR-29b predictive significance in older AML patients treated with a 10-day schedule of decitabine. *Proc Natl Acad Sci USA* 2010; **107**: 7473–7478.
33. Liu S, Wu LC, Pang J, Santhanam R, Schwind S, Wu YZ *et al.* Sp1/NFkappaB/HDAC/miR-29b regulatory network in KIT-driven myeloid leukemia. *Cancer Cell* 2010; **17**: 333–347.
34. Gong JN, Yu J, Lin HS, Zhang XH, Yin XL, Xiao Z *et al.* The role, mechanism and potentially therapeutic application of microRNA-29 family in acute myeloid leukemia. *Cell Death Differ* 2014; **21**: 100–112.
35. DeNicola GM, Karreth FA, Humpton TJ, Gopinathan A, Wei C, Frese K *et al.* Oncogene-induced Nrf2 transcription promotes ROS detoxification and tumorigenesis. *Nature* 2011; **475**: 106–109.
36. Kong F, Sun C, Wang Z, Han L, Weng D, Lu Y *et al.* miR-125b confers resistance of ovarian cancer cells to cisplatin by targeting pro-apoptotic Bcl-2 antagonist killer 1. *J Huazhong Univ Sci Technolog Med Sci* 2011; **31**: 543–549.
37. Wang Y, Li Z, He C, Wang D, Yuan X, Chen J *et al.* MicroRNAs expression signatures are associated with lineage and survival in acute leukemias. *Blood Cells Mol Dis* 2010; **44**: 191–197.
38. Spinello I, Quaranta MT, Riccioni R, Riti V, Pasquini L, Boe A *et al.* MicroRNA-146a and AMD3100, two ways to control CXCR4 expression in acute myeloid leukemias. *Blood Cancer J* 2011; **1**: e26.
39. Tsai JJ, Dudakov JA, Takahashi K, Shieh J-H, Velardi E, Holland AM *et al.* Nrf2 regulates haematopoietic stem cell function. *Nat Cell Biol* 2013; **15**: 309–316.
40. Murray MY, Rushworth SA, Zaitseva L, Bowles KM, MacEwan DJ. Attenuation of dexamethasone-induced cell death in multiple myeloma is mediated by miR-125b expression. *Cell Cycle* 2013; **12**: 2144–2153.
41. Zaitseva L, Rushworth SA, MacEwan DJ. Silencing FLIPL modifies TNF-induced apoptotic protein expression. *Cell Cycle* 2011; **10**: 1067–72.
42. Rushworth SA, MacEwan DJ. HO-1 underlies resistance of AML cells to TNF-induced apoptosis. *Blood* 2008; **111**: 3793–3801.

Supplementary Information accompanies this paper on Cell Death and Differentiation website (http://www.nature.com/cdd)

Supplementary Table 1 - Shah et al

miRNA	Sequence (5' to 3')	miRNA fold expression in NRF2-KD compared to NEG-KD)	miRNA fold expression in sulf 5μM treated compared to untreated
miR-200b	TAATACTGCCTGGTAATGATGAC	0.2432	0.2031
miR-125b	TCCCTGAGACCCTAACTTGTGA	0.2912	3.6553
miR-222	AGCTACATCTGGCTACTGGGTCTC	0.2994	1.2386
miR-221	AGCTACATTGTCTGCTGGGTTTC	0.3896	0.9266
miR-15b	TAGCAGCACATCATGGTTTACA	0.3926	0.0487
miR-1224	GTGAGGACTCGGGAGGTGG	0.4005	0.8942
miR-30a	TGTAAACATCCTCGACTGGAAG	0.4175	0.8933
miR-25	CATTGCACTTGTCTCGGTCTGA	0.4204	1.6240
miR-223	TGTCAGTTTGTCAAATACCCC	0.4293	1.7291
miR-200c	TAATACTGCCGGGTAATGATGG	0.4353	0.5743
miR-18a	TAAGGTGCATCTAGTGCAGATA	0.4931	0.5946
miR-23a	ATCACATTGCCAGGGATTTCC	0.5035	1.2478
miR-27a+b	TTCACAGTGGCTAAGTTCCGC	0.5070	0.6969
mir-301	CAGTGCAATAGTATTGTCAAAGC	0.5249	0.1768
miR-24	TGGCTCAGTTCAGCAGGAACAG	0.5359	1.0404
miR-195	TAGCAGCACAGAAATATTGGC	0.6029	0.5471
miR-196a	TAGGTAGTTTCATGTTGTTGG	0.6242	1.3318
miR-20a	TAAAGTGCTTATAGTGCAGGTAG	0.6329	0.8645
miR-95	TTCAACGGGTATTTATTGAGCA	0.6462	0.9727
miR-30b	TGTAAACATCCTACACTCAGCT	0.6552	0.9794
miR-134	TGTGACTGGTTGACCAGAGGG	0.6643	1.1578
miR-17	CAAAGTGCTTACAGTGCAGGTAGT	0.7220	0.6783
miR-133a	TTGGTCCCCTTCAACCAGCTGT	0.7270	3.2193
miR-214	ACAGCAGGCACAGACAGGCAG	0.7631	0.6783
miR-183	TATGGCACTGGTAGAATTCACTG	0.7721	0.6507
miR-141	TAACACTGTCTGGTAAAGATGG	0.7792	0.6373
miR-185	TGGAGAGAAAGGCAGTTC	0.7871	1.1183
miR-103	AGCAGCATTGTACAGGGCTATGA	0.7900	2.0681
miR-34a	TGGCAGTGTCTTAGCTGGTTGT	0.7900	1.1385
miR-7	TGGAAGACTAGTGATTTTGTTG	0.8012	2.8879
miR-186	CAAAGAATTCTCCTTTTGGGCTT	0.8039	1.5911
miR-22	AAGCTGCCAGTTGAAGAACTGT	0.8293	1.1975
miR-203	GTGAAATGTTTAGGACCACTAG	0.8586	0.1331
miR-15a	TAGCAGCACATAATGGTTTGTG	0.8586	2.3134
miR-107	AGCAGCATTGTACAGGGCTATCA	0.8766	4.5948
let-7-family	TGAGGTAGTAGGTTGTATAGTT	0.9005	11.1579
miR-191	CAACGGAATCCCAAAAGCAGCT	0.9126	0.7684
miR-197	TTCACCACCTTCTCCACCCAGC	0.9330	1.9588
miR-21	TAGCTTATCAGACTGATGTTGA	0.9353	2.5669
miR-16	TAGCAGCACGTAAATATTGGCG	0.9395	1.1019
miR-125a-5p	TCCCTGAGACCCTTTAACCTGTG	0.9461	1.2592
miR-149	TCTGGCTCCGTGTCTTCACTCC	0.9466	0.4931
miR-106b	TAAAGTGCTGACAGTGCAGAT	0.9495	0.8888
miR-219	TGATTGTCCAAACGCAATTCT	0.9526	0.4863
miR-150	TCTCCCAACCCTTGTACCAGTG	0.9527	0.3737
miR-194	TGTAACAGCAACTCCATGTGGA	0.9659	0.9395
miR-17*	ACTGCAGTGAAGGCACTTGT	0.9859	0.9727

Supplementary table 1 (continued) - Shah et al

miRNA	Sequence (5' to 3')	miRNA fold expression in NRF2-KD compared to NEG-KD	miRNA fold expression in sulf 5μM treated compared to untreated
miR-34b	CAATCACTAACTCCACTGCCAT	1.0129	0.2872
miR-181a	AACATTCAACGCTGTCGGTGAGT	1.0329	0.3463
miR-151	ACTAGACTGAAGCTCCTTGAGG	1.0353	0.4444
miR-205	TCCTTCATTCCACCGGAGTCTG	1.0535	0.6878
miR-101	TACAGTACTGTGATAACTGAAG	1.0674	0.2774
miR-188-5p	CATCCCTTGCATGGTGGAGGG	1.0709	1.3755
miR-181c	AACATTCAACCTGTCGGTGAGT	1.0727	1.1975
miR-142-3p	TGTAGTGTTTCCTACTTTATGGA	1.0732	0.2045
miR-122	TGGAGTGTGACAATGGTGTTTGT	1.0792	0.0802
miR-373	GAAGTGCTTCGATTTTGGGGTGT	1.0831	1.3219
miR-140	AGTGGTTTTACCCTATGGTAG	1.0958	0.1250
miR-9	TCTTTGGTTATCTAGCTGTATGA	1.1383	1.1810
miR-128	TCACAGTGAACCGGTCTCTTTC	1.1487	0.9303
miR-296	AGGGCCCCCCCTCAATCCTGT	1.1810	0.9395
miR-26a	TTCAAGTAATCCAGGATAGGC	1.1892	1.0987
miR-192	CTGACCTATGAATTGACAGCC	1.2086	1.5801
miR-144	TACAGTATAGATGATGTACT	1.2544	1.0987
miR-143	TGAGATGAAGCACTGTAGCTCA	1.2570	0.0708
miR-193b	AACTGGCCCTCAAAGTCCCGCT	1.2689	0.4617
miR-19a+b	TGTGCAAATCTATGCAAAACTGA	1.2863	0.4133
miR-106a	AAAAGTGCTTACAGTGCAGGTAGC	1.3021	0.5946
miR-92a	TATTGCACTTGTCCCGGCCTG	1.3287	1.9810
miR-181d	AACATTCATTGTTGTCGGTGGGTT	1.3471	1.6021
miR-155	TTAATGCTAATCGTGATAGGGG	1.3660	0.4730
miR-29a	TAGCACCATCTGAAATCGGTTA	1.4142	0.3415
miR-93	AAAGTGCTGTTCGTGCAGGTAG	1.4271	0.8645
miR-202	AGAGGTATAGGGCATGGGAAAA	1.4641	0.7120
miR-181b	AACATTCATTGCTGTCGGTGGG	1.4641	0.7919
miR-146a	TGAGAACTGAATTCCATGGGTT	1.4871	0.5548
miR-372	AAAGTGCTGCGACATTTGAGCGT	1.5602	1.4241
miR-200a	TAACACTGTCTGGTAACGATGT	1.7532	2.4453
miR-154	TAGGTTATCCGTGTTGCCTTCG	1.7570	0.6690
miR-132	TAACAGTCTACAGCCATGGTCG	1.8921	1.9811
miR-29b	TAGCACCATTTGAAATCAGTGTT	2.1435	0.3660

Supplementary Table 1. miRNA profiling of AML cells in response lentiviral NRF2 knockdown and treatment with the NRF2 activator sulforaphane. THP-1 cells were either transduced with NEG (NEG-KD) and NRF2 (NRF2-KD) targeted miRNA lentiviral constructs or with sulforaphane (5μM) for 8 hours. QRTPCR analysis of 92 cancer-associated miRNAs in treated cells were evaluated. Values represent fold increase over control conditions normalized to RNU6B (ΔCT).

Supplementary Table 2 - Shah et al

	IC50 daunorubicin [μM]				
	THP-1	Kasumi1	CD34+	AML#25	AML#27
negative control	0.276	0.092	0.207	0.293	0.037
α125B	0.221	0.077	0.186	0.219	0.036
29B mimic	0.153	0.085	0.187	0.152	0.034
α125B + 29B mimic	0.123	0.066	0.157	0.106	0.033

Supplementary Table 2. miR-125B antagomiR and miR-29B mimic increases AML sensitivity to chemotherapy. THP-1, Kasumi-1, primary CD34+ HSC, AML#25 and AML#27 were transfected with control miRNA, miR-125B antagomiR, miR-29B mimic and miR-125B antagomiR in combination with miR-29B mimic for 24 h before the addition of increasing doses of daunorubicin for 48 h. Cells assessed for viability by Cell Titer-GLO. Table shows the IC50 values for all cells types in response to daunorubicin

Supplementary Table 3 - Shah et al

Gene name	Function/disease	Reference
miR-29B targets		
MYBL2	AML	18
AKT2	AML	23
Cxxc6	AML	18
DNMT1	AML	38
TGFB1	Trabecular meshwork	42
PIK3R1	Cholangiocarcinoma	28
CDK4	Mantle cell lymphoma	25
SP1	AML	24
miR-125B targets		
CBFβ	AML subtype-APL	39
KLF13	Haematopoietic stem cells	22
ABTB1	AML subtype-APL	39
MAPK14	Kidney/Fibroblast/Colon cancer/osteocarcinoma	40
STAT3	Myelopoiesis	41
miR-125B/mIR-29B targets		
CDK6	Mantle cell lymphoma	25
BCL2	Hepatacellular carcinoma	20
MCL1	Hepatacellular carcinoma	20
BAK1	AML/Breast Cancer	21

Supplementary Figure 3. Targets for miR-29B and miR-125B

Supplementary Table 4 - Shah et al

miRNA	Sites	position	ARE sequence	5'-3' oligos for ChIP analysis
miR-125B1	ARE1	40923-40933	ATGACTCAGTG	For - ATGTTTCCAAACCAGGCTGA Rev - CTAACACTGCAGGCTCACCA
miR-125B1	ARE2	4537-4548	TGATCTCAGCA	For - CAGAGCCAGCTGTCAATGAA Rev - CCAGAATGGGAGAAATGGAG
miR-125B1	ARE3	1357-1368	GCTTTGTCATT	For - GTTGAGGCCTCTCCAGTGTC Rev - GCCACCAAAAATGAAAGGAA
miR-29B1	ARE4	16788-16799	AGCTGAGTCAC	For - TCAAGGTGCAGGATCTTTCC Rev - GTCTACCTTGGATGGCCTCA
miR-29B1	ARE5	7647-7658	TGCTGAGTCAT	For - CACATCTGGGCAACATCATC Rev - CTCCAAGGGGGTGTCCTTAT

Supplementary Figure 4. Locations and sequences of putative ARE elements. Primers used in ChIP analysis.

Supplementary Figure 1 - Shah et al

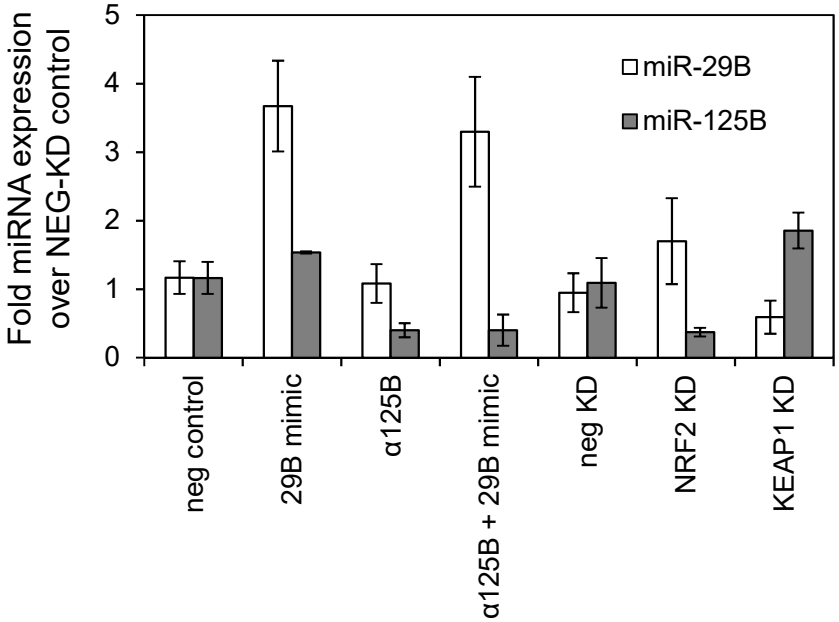

Supplementary Figure 1. Expression analysis of miRNA levels after transfection with miR-29B mimic and miR-125B antagomir. THP-1 were transfected with control miRNA, miR-125B antagomiR (α125B), miR-29B mimic (29B mimic) and miR-125B antagomiR in combination with miR-29B mimic for 48 h. Also THP-1 cells were transduced with NEG (NEG-KD) and NRF2 (NRF2-KD) targeted miRNA lentiviral constructs for 72 hours. QRTPCR analysis of miR-29B and miR-125B was carried out on all transfected and transduced cells.

Supplementary Figure 2 - Shah et al

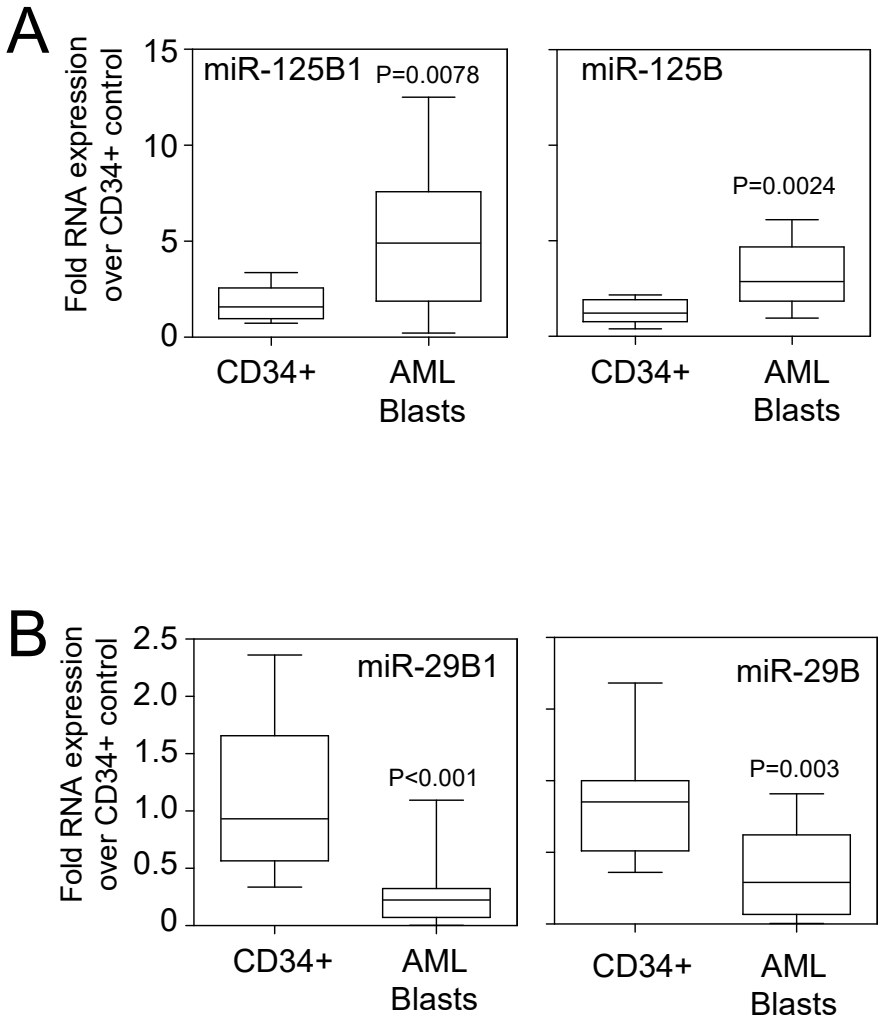

Supplementary Figure 2. miR-29B and miR-125B in primary AML. Total RNA was extracted from patient AML blasts (n=18) and CD34+ HSC (n=8), miR-125B (A) and miR-29B (B) RNA expression levels were measured using QRTPCR and compared to miR-125B1 and miR-29B respectively from figure 4 A.